

Investigation of Selective Targeting of Lumbar Spinal Structures  
with Spinal Manipulative Therapy

by

Martha Funabashi

A thesis submitted in partial fulfillment of the requirements for the degree of

Doctor of Philosophy

in

Rehabilitation Science

Faculty of Rehabilitation Medicine  
University of Alberta

© Martha Funabashi, 2016

## **ABSTRACT**

### **Background**

Low back pain is a prevalent condition commonly treated with conservative care, including spinal manipulative therapy (SMT). It is well known that forces applied by SMT are transferred to spinal tissues and that these forces initiate SMT's beneficial (or possibly harmful) health outcomes. Importantly, the distribution of these forces within spinal tissues and how it compares to forces arising from daily activities remains unclear. By identifying the distribution of these forces, it may be possible to design treatments that can specifically target, or avoid particular spinal tissues thereby making SMT intervention more effective, efficient and safe.

### **Objective**

The overall objective of this dissertation was to biomechanically investigate how forces and moments arising from SMT application were distributed within spinal structures when using varied SMT input parameters and how these forces and moments compared to the ones arising from passive movements. Specifically, this dissertation had four definite objectives: 1) to verify the application of the principle of superposition when testing biomechanical structures with time-dependent non-linear behavior; 2) to identify the loading characteristics of spinal tissues during SMT with different parameters of application (force magnitude and application site); 3) to investigate spinal tissues' loading characteristics when SMT is delivered using different methods of application; and 4) to describe the loads arising from manual SMT application in comparison to passive physiological movements of the lumbar spine.

## Methods

To address the first objective, a stable robotic platform was used to evaluate 3D print models having time-dependent non-linear material properties. To address objectives 2-4, the following general methodology was implemented. Vertebral movement arising from SMT application with varied input parameters as well as during passive physiological movements was quantified by optical tracking of indwelling vertebral bone pins from a cadaveric pig model. Vertebral segments were harvested *en bloc* and mounted in a parallel robot equipped with a 6 degree-of-freedom load cell. The parallel robot replicated the exact vertebral displacements arising from SMT applications and physiological movements while the load cell measured and recorded the loads experienced by the motion segment. By combining kinematics replication with serial dissection, loads experienced by spinal structures were measured and analysed. The four experiments that addressed objectives 2-4 applied SMT varying in force magnitude, application site and method of application, and the resulting motion segment forces and moments along and around the three Cartesian axes were then compared. Finally, motion segments' loads arising from SMT were compared with ones from passive spinal movements to provide a framework for understanding the magnitude of tissue response created by SMT.

## Results

The results of the first experiment suggest that even in an optimized environment with identical testing objects, the principle of superposition could not be observed: removal order and/or unique testing circumstances influence structure loading characteristics. The experiments investigating the influence of SMT input parameters on the loading characteristics of the intact specimen and spinal structures revealed that SMT input parameters of peak force magnitude and application

site significantly affect SMT load distribution within spinal structures and specific spinal structures will experience unique loads as a function of the SMT input parameters of peak force magnitude and application site. Similarly, the experiment in which three different methods of SMT application were investigated revealed that the method in which SMT is applied also influenced SMT loading distribution within spinal structures and, consequently, the loading characteristics of the intact specimen and spinal structures. Finally, the comparison between the loads experienced by the intact specimen and spinal structures during SMT and passive physiological movements revealed that although loading distribution within spinal structures varied as a function of the motion applied to the spine, the forces and moments experienced during SMT were comparable to those experienced during passive physiological movements, with notable exceptions.

## **Conclusion**

Although the results reported here are specific to the order of spinal structure removal, these results provide novel evidence that it may possible to alter SMT input parameters, or use specific methods of SMT application, to specifically target particular spinal structures. Additionally, loading rate, forces and moments created by manual SMT are below previously reported injury values. The unique loading profile created by SMT may be the mechanism that confers SMT's therapeutic effect in comparison to the loading created during daily activities. This work provides important information for clinicians about the potential impact of SMT parameters as well as a foundation for future investigations of SMT biomechanics and underlying therapeutic mechanisms.



## **PREFACE**

This dissertation is an original work by Martha Funabashi. The research projects in this dissertation received research ethics approval from the University of Alberta Health Research Ethics Board. Project Name “Effects of SMT parameters on spinal tissue forces”, Project ID RES0009942, DATE: 25 September 2013. Findings from the current doctoral research have been published in peer review journal.

Chapter 3 of this dissertation has been published as Funabashi M, El-Rich M, Prasad N, Kawchuk G. Quantification of loading in biomechanical testing: the influence of dissection sequence. *Journal of biomechanics* 2015 48(12):3522-6. M. Funabashi was responsible for concept formation, 3D print models design, data collection and analysis, as well as manuscript composition and revision. M. El-Rich and G. Kawchuk were the supervisory authors and were involved with concept formation and manuscript edits. N. Prasad supervised statistical analysis and contributed to manuscript edits.

I would like to dedicate this dissertation to my parents *Suely and Edson*, who are my role models of strength, understanding, dedication and love. My parents, who have always supported and encouraged all my choices in life, even when these choices broke their hearts.

I would also like to dedicate this work to my beloved uncle *Helio*, to whom I could not say goodbye in person. Uncle Helio, sorry for not being there - I miss you.

Finally, I would also like to dedicate it to my boyfriend *Tiago* who supported me in the hardest times of this work, who every day showed me his unconditional support and patience, who has always believed in me, and who did not let me fall in many circumstances.

## ACKNOWLEDGEMENTS

As this work is the result of a journey that did not start only 5 years ago, I would like to thank everyone who has passed through my life and somehow contributed to shaping me into who I am today. I also would like to thank some people who specifically supported me throughout this PhD adventure:

I would like to express my deepest gratitude to my supervisor Dr. Greg Kawchuk. Greg has not only awoken my interest in SMT biomechanics (the area I found out to be my great passion), but also has believed in me, kindly challenged me, and patiently taught me things I didn't believe I could learn. Without his commitment, support, guidance, patience and enthusiasm for knowledge, this work would have not been possible. He is one of my great examples of human being and professional. Having him as my mentor has taught me so much not only about research and biomechanics, but also about communication, networking and, above all, about Canadian life and culture. Greg, I am honoured I could be your trainee - thank you so much for everything, this experience has changed my life.

I would also like to thank Dr. Narasimha Prasad, for sharing his amazing knowledge, for guiding me through my statistical analysis, for his patience, availability and commitment. I would like to thank Dr. Eric Parent for his honest, challenging, insightful and stimulating feedback through this process and for always being available to assist me whenever I needed. I am also grateful to Dr. Marwan El-Rich for his great knowledge, patience and for not only teaching me engineering concepts and application to spinal biomechanics, but also for his always instructive and insightful feedback. Thank you to my external examiners, Dr. Martin Descarreaux (who allowed me to use his "Le Robot", significantly contributing to this work) and Dr. Jason Carey for their time and their willingness to support this important step of my process and their commitment to the education of future researchers.

A very special thank you James Willis, Janes Goller, Sheila Schaller and all the staff from the University of Alberta's Swine Research and Technology Centre (SRTC) for their fundamental

assistance during the process of data collection. Their help, understanding, professionalism and enthusiasm greatly assisted me not only with the practical procedures of data collection, but also with my emotional struggles throughout this process. I would also like to thank Angela Libutti, who is always taking care of all Rehabilitation Sciences' graduate student, for all her assistance and for making some processes easier during the PhD life.

My gratitude also goes to my friends Liliana and Brea for being my partners in this PhD adventure, for always rescuing me when I was having melt downs and for their support, advice, ears and shoulders. A special thank you to all my Brazilian friends Carol, Alvaro, Guri, Fernanda, Lari, Ane, Mari, Lu, Le, Bia, Lu Nigro, Thais, Bru, Paulao, Machado, Tiagos, Ivan, Gabi, Stephan, Cibebe, Elisa, Claudia, Marcela, Spaka, Digui, Flavinha, Ariba, Erikinha, Bruninha and Re for their fundamental support, encouragement from wherever they were and for making me smile and laugh at least once every day. My great gratitude to my friends Denise and Paula and their mothers Sizue and Nadir for taking care and supporting my parents when they needed and I couldn't be there for them. Thank you to Susan, Darrel, François, Alex, Katie who have taken the time to support and assist me as well as to share their amazing knowledge with me. I also want to thank my lab mates Arnold, Anthony, Ashley, Maryse, Maxi, Kyria, Yolanda, Peter, Maliheh and Zohreh for the supportive, cheerful and friendly work environment.

I also would like to thank the funding agencies for their financial support during my PhD program: Canadian Institute for Health Research (STAIR grant), College of Physical Therapists of Alberta and University of Alberta.

Finally, I would like to thank the loves of my life: my parents Suely and Edson, my brother Eric, my grandparents Ytsue and Yasuhiro, my uncles and aunts Helio, Marcia, Jones and Mary, my cousins Paula, Deborah, Vanessa and Camila, my dear boyfriend Tiago, my mother in law Terezinha and my step kids Lucas and Nicolas. For their encouragement and support to pursue my dreams, even though it would mean that I would be away from them, would miss family celebrations and would imply in sacrifices made by them. Thank you so much for all your love, patience, efforts, understanding and support. For always believing in me and giving me strength and motivation to keep trying to be a better person and professional.

## TABLE OF CONTENTS

### Chapter 1.

<b>Introduction .....</b>	<b>1</b>
<b>1.1 Spinal manipulative therapy load distribution .....</b>	<b>2</b>
1.1.1 Significance.....	3
<b>1.2 Current evidence on spinal manipulative therapy parameters .....</b>	<b>3</b>
1.2.1 Peak Force Magnitude .....	3
1.2.2 Application site .....	5
<b>1.3 Clinical application .....</b>	<b>6</b>
Summary .....	7
<b>1.2 Dissertation Objectives .....</b>	<b>8</b>

### Chapter 2.

<b>Literature Review .....</b>	<b>12</b>
<b>2.1 Introduction.....</b>	<b>12</b>
<b>2.2 Lumbar Spine Biomechanics .....</b>	<b>13</b>
2.2.1 Bony structures .....	13
2.2.1.1 Vertebral body.....	13
2.2.1.2 Vertebral arch.....	14
2.2.2 Intervertebral disc .....	15
2.2.3 Ligaments.....	16
2.2.3.1 Supra- and interspinous ligaments .....	16
2.2.3.2 Ligamentum flavum .....	16
2.2.3.3 Intertransverse ligament .....	16
2.2.3.4 Anterior and posterior longitudinal ligaments .....	17
2.2.4 Biomechanical function .....	17
2.2.5 Lumbar coupled motion.....	18
2.2.6 Biomechanical characteristics.....	19
<b>2.3 Spinal Manipulative Therapy .....</b>	<b>20</b>
2.3.1 Spinal manipulative therapy techniques.....	21
<b>2.4 Spinal Manipulative Therapy Outcomes .....</b>	<b>22</b>
2.4.1 Biomechanical outcomes .....	22
2.4.2 Neurophysiological Outcomes .....	24
<b>2.5 Spinal manipulative therapy input parameters and specific responses .....</b>	<b>25</b>
2.5.1 Preload force .....	28
2.5.2 Peak force magnitude.....	28
2.5.3 Method of application .....	29
2.5.4 Thrust duration.....	30
2.5.5 Loading rate .....	31
2.5.6 Application site .....	31

<b>2.6 Animal Models .....</b>	<b>32</b>
2.6.1 Specific differences between porcine and human lumbar spines .....	34
2.6.1.1 Anatomical differences .....	34
2.6.1.2 Biomechanical differences .....	36
<b>2.7 Robotic Biomechanical Testing.....</b>	<b>36</b>
<b>2.8 Robotic Biomechanical Testing of the Lumbar Spine .....</b>	<b>40</b>
<b>2.9 Robotic Biomechanical Testing and Spinal Manipulative Therapy .....</b>	<b>42</b>

## **Chapter 3.**

### **Quantification of loading in biomechanical testing: the influence of dissection**

<b>sequence .....</b>	<b>43</b>
<b>3.1 Introduction.....</b>	<b>43</b>
<b>3.2 Materials and Methods.....</b>	<b>44</b>
3.2.1 Model design and fabrication.....	44
3.2.2 Model preparation and mounting .....	45
3.2.3 Testing protocol .....	46
3.2.3.1 Sequential connector removal .....	47
3.2.4 Statistical Analysis.....	47
<b>3.3 Results .....</b>	<b>48</b>
<b>3.4 Discussion.....</b>	<b>55</b>
3.4.1 Limitations .....	57
<b>3.5 Acknowledgements .....</b>	<b>57</b>

## **Chapter 4.**

### **Spinal tissues loaded by spinal manipulative therapy (SMT)**

<b>Part I: the influence of SMT force magnitude and application site .....</b>	<b>58</b>
<b>4.1 Introduction.....</b>	<b>58</b>
<b>4.2 Methods.....</b>	<b>60</b>
4.2.1 Overview .....	60
4.2.2 Sample Size Calculation .....	61
4.2.3 Specimen Preparation .....	62
4.2.4 Spinal Manipulation and Kinematic Recording.....	64
4.2.5 Potting Procedure.....	65
4.2.6 Robotic Testing.....	67
4.2.7 Statistical Analysis.....	69
4.2.7.1 Variables .....	69
4.2.7.2 Statistical Tests .....	70
<b>4.3 Results .....</b>	<b>71</b>
4.3.1 Overview .....	71
4.3.2 Vertebral Displacements .....	74
4.3.3 Intact Specimen.....	76
4.3.3.1 Interaction effect .....	76

4.3.3.2 Force magnitude main effect.....	79
4.3.3.3 Application site main effect.....	79
4.3.4 Cut 1: Supra- and interspinous ligaments (SL).....	80
4.3.4.1 Interaction effect.....	80
4.3.4.2 Force magnitude main effect.....	80
4.3.4.3 Application site main effect.....	80
4.3.5 Cut 2: Bilateral facet joints, capsules and ligamentum flavum (PJ).....	83
4.3.5.1 Interaction effects.....	83
4.3.5.2 Force magnitude main effect.....	84
4.3.5.3 Application site main effect.....	84
4.3.6 Cut 3: Intervertebral disc and anterior and posterior longitudinal ligaments (IVD).....	87
4.3.6.1 Interaction effects.....	88
4.3.6.2 Force magnitude main effect.....	88
4.3.6.3 Application site main effect.....	88
<b>4.4 Discussion.....</b>	<b>91</b>
4.4.1 Methodological choices.....	92
4.4.2 Interpretation of Results.....	93
4.4.2.1 Vertebral displacements and rotations.....	93
4.4.2.2 Intact Specimen.....	94
4.4.2.3 Cut 1: Supra- and interspinous ligaments (SL).....	98
4.4.2.4 Cut 2: Bilateral facet joints, capsules and ligamentum flavum (PJ).....	98
4.4.2.5 Cut 3: Intervertebral disc, anterior and posterior longitudinal ligaments (IVD).....	101
4.4.2.6 General Discussion.....	101
4.4.2.5 Clinical implications.....	105
4.4.3 Limitations.....	108
<b>4.5 Conclusion.....</b>	<b>108</b>

## Chapter 5.

### Spinal tissues loaded by spinal manipulative therapy (SMT)

#### Part II: the influence of application site..... 109

##### 5.1 Introduction..... 109

##### 5.2 Methods..... 111

###### 5.2.1 Overview..... 111

###### 5.2.2 Sample Size Calculation..... 111

###### 5.2.3 Specimen Preparation..... 112

###### 5.2.4 Spinal Manipulation..... 113

###### 5.2.5 Kinematic Recording..... 113

###### 5.2.6 Potting Procedure..... 114

###### 5.2.7 Robotic Testing..... 114

###### 5.2.8 Data Analysis..... 116

###### 5.2.8.1 Overview..... 116

###### 5.2.8.2. Data Processing..... 116

###### 5.2.8.3 Statistical Tests..... 117

<b>5.3 Results .....</b>	<b>118</b>
5.3.1 Overview .....	118
5.3.2 General descriptive statistics .....	118
5.3.2.1 Vertebral displacements and rotations .....	127
5.3.3 Intact Specimen .....	128
5.3.4 Cut 1: Supra- and interspinous ligaments (SL) .....	130
5.3.5 Cut 2: Facet capsules, facet joints and ligamentum flavum (PJ) .....	132
5.3.6 Cut 3: Intervertebral disc and anterior and posterior longitudinal ligaments (IVD) .....	135
<b>5.4 Discussion.....</b>	<b>138</b>
5.4.1 Vertebral displacements and rotations .....	139
5.4.2 Interpretation of Results.....	142
5.4.2.1 Forces and moments in the intact specimen.....	142
5.4.2.2 Cut 1: Supra- and interspinous ligaments (SL) .....	146
5.4.2.3 Cut 2: Bilateral facet joints, capsules and ligamentum flavum (PJ) .....	148
5.4.2.4 Cut 3: Intervertebral disc, anterior and posterior longitudinal ligaments (IVD).....	152
5.4.2.5 General discussion .....	156
5.4.2.6 Clinical implications .....	158
5.4.3 Limitations .....	162
<b>5.5 Conclusion .....</b>	<b>163</b>

## Chapter 6.

### Spinal tissue loading as a function of the method of spinal manipulative therapy

<b>application .....</b>	<b>164</b>
<b>6.1 Introduction.....</b>	<b>164</b>
<b>6.2 Methods.....</b>	<b>166</b>
6.2.1 Overview .....	166
6.2.2 Sample Size Calculation .....	167
6.2.3 Specimen Preparation .....	167
6.2.4 Spinal manipulation .....	168
6.2.5 Kinematic Recording .....	169
6.2.6 Potting Procedure.....	170
6.2.7 Robotic Testing .....	170
6.2.8 Data Analysis .....	172
6.2.8.1 Overview .....	172
6.2.8.2 Data Processing.....	173
6.2.8.3 Statistical Tests .....	174
<b>6.3 Results .....</b>	<b>175</b>
6.3.1 Overview .....	175
6.3.2 General descriptive statistics.....	175
6.3.2.1 Spinal manipulative therapy characteristics.....	175
6.3.2.2 Vertebral Displacements .....	177
6.3.2.3 General forces and moments .....	178
6.3.3 Intact Specimen.....	182



6.3.4 Cut 1: Supra- and interspinous ligaments (SL).....	184
6.3.5 Cut 2: Bilateral facet joints, capsules and ligamentum flavum (PJ) .....	187
6.3.6 Cut 3: Intervertebral disc, anterior and posterior longitudinal ligaments (IVD).....	190
<b>6.4 Discussion.....</b>	<b>193</b>
6.4.1 Spinal manipulative therapy characteristics - Comparison with previous studies .....	195
6.4.2 Vertebral displacements and rotations - Comparison with previous studies.....	195
6.4.3 Interpretation of Results.....	198
6.4.3.1 Intact Specimen.....	198
6.4.3.2 Cut 1: Supra- and interspinous ligaments (SL).....	200
6.4.3.3 Cut 2: Bilateral facet joints, capsules and ligamentum flavum (PJ) .....	201
6.4.3.4 Cut 3: Intervertebral disc, anterior and posterior longitudinal ligaments (IVD).....	204
6.4.3.5 General discussion .....	207
6.4.3.6 Clinical implications .....	210
6.4.4 Limitations .....	211
<b>6.5 Conclusion .....</b>	<b>212</b>

## Chapter 7.

### **Quantification of spinal tissues loading: a comparison between spinal manipulative therapy (SMT) and passive lumbar movements..... 213**

<b>7.1 Introduction.....</b>	<b>213</b>
<b>7.2 Methods.....</b>	<b>215</b>
7.2.1 Overview .....	215
7.2.2 Sample Size Calculation .....	216
7.2.3 Specimen Preparation .....	216
7.2.4 Passive Lumbar Movements .....	218
7.2.5 Spinal Manipulation.....	219
7.2.6 Kinematic Recording .....	220
7.2.7 Potting Procedure.....	220
7.2.8 Robotic Testing.....	221
7.2.9 Data Analysis .....	222
7.2.9.1 Overview.....	222
7.2.9.2 Data Processing.....	223
7.2.9.3 Statistical Tests .....	224
<b>7.3 Results .....</b>	<b>225</b>
7.3.1 Overview .....	225
7.3.2 Spinal manipulative therapy characteristics.....	225
7.3.3 Vertebral displacements and rotations .....	225
7.3.4 Forces and Moments .....	226
7.3.4.1 General descriptive statistics.....	226
7.3.4.2 Intact Specimen.....	229
7.3.4.3 Cut 1: Supra- and interspinous ligaments (SL).....	232
7.3.4.4 Cut 2: Bilateral facet joints, capsules and ligamentum flavum (PJ) .....	237
7.3.4.5 Cut 3: Intervertebral disc, anterior and posterior longitudinal ligaments (IVD).....	241

<b>7.4 Discussion.....</b>	<b>245</b>
7.4.1 Spinal manipulative therapy characteristics - Comparison with previous studies .....	247
7.4.2 Vertebral motion during lumbar movements - Comparison with previous studies .....	248
7.4.3 Interpretation of Results.....	250
7.4.3.1 Intact specimen .....	250
7.4.3.2 Cut 1: Supra- and interspinous ligaments (SL) .....	252
7.4.3.3 Cut 2: Bilateral facet joints, capsules and ligamentum flavum (PJ) .....	254
7.4.3.4 Cut 3: Intervertebral disc, anterior and posterior longitudinal ligaments (IVD).....	258
7.4.3.5 General discussion .....	261
7.4.3.6 Clinical implications .....	266
7.4.4 Limitations .....	267
<b>7.5 Conclusion .....</b>	<b>268</b>
 <b>Chapter 8.</b>	
<b>General discussion and conclusion.....</b>	<b>269</b>
<b>8.1 Introduction.....</b>	<b>269</b>
<b>8.2 Summary of experimental findings .....</b>	<b>269</b>
8.2.1 The principle of superposition .....	273
8.2.2 Spinal manipulative therapy input parameters - Peak force magnitude and application site .....	273
8.2.2.1 Interaction .....	273
8.2.2.2 Peak force magnitude.....	273
8.2.2.3 Application site .....	274
8.2.3 Spinal manipulative therapy input parameters - Application site .....	274
8.2.4 Spinal manipulative therapy input parameters - Method of SMT application .....	275
8.2.5 Spinal manipulative therapy and passive physiological movement load comparison .....	275
<b>8.3 Pilot studies and measurement errors.....</b>	<b>276</b>
<b>8.4 Synthesis of experimental data .....</b>	<b>276</b>
8.4.1 Principle of Superposition.....	276
8.4.2 Changing SMT input parameters can preferentially increase specific characteristics of spinal structure loading.....	277
8.4.3 Changing SMT input parameters alter specific spinal loads.....	278
<b>8.5 Implications .....</b>	<b>278</b>
8.5.1 Implications for biomechanical scientific research.....	279
8.5.1.1 Biomechanical testing.....	279
8.5.1.2 Underlying mechanism of SMT.....	279
8.5.2 Implications for clinicians.....	280
<b>8.6 Future research .....</b>	<b>281</b>
<b>8.7 Conclusion .....</b>	<b>284</b>
 <b>Bibliography.....</b>	<b>285</b>

## LIST OF TABLES

Table 2.1 Spinal manipulative therapy input parameters described in the literature.....	26
Table 2.2 Anatomical characteristics of porcine and human lumbar spines.....	35
Table 2.3 Biomechanical characteristics of porcine and human lumbar spines .....	36
Table 3.1 Sequence of connector removal for each 3D print model .....	47
Table 3.2 Area between curves of moment-displacement graph (Nm-deg) of each connector during rotations about all three axes. ....	50
Table 4.1 Description of conditions and variables used throughout the chapter .....	70
Table 4.2 Summary of significant interactions and main effects.....	72
Table 4.3 Maximal displacement and rotation (SD) created in the cadaveric specimens with the application of SMT (with different force magnitudes at different application sites) trajectories for all conditions.....	75
Table 4.4 Average (SD) maximum displacement and rotation of the current study and the previous study conducted by Kawchuk et al. (2010) .....	75
Table 4.5 Split plot ANOVA table for the intact condition.....	78
Table 4.6 Split plot ANOVA table for the supra- and interspinous ligaments.....	82
Table 4.7 Split plot ANOVA table for the bilateral facet joints, capsules and ligamentum flavum.....	86
Table 4.8. Split plot ANOVA table for the intervertebral disc and anterior and posterior longitudinal ligaments.....	90
Table 5.1. Description of conditions and variables used throughout the chapter .....	117
Table 5.2. Maximal displacement and rotation (SD) created in the cadaveric specimens with the application of SMT (at different application sites) trajectories.....	127
Table 5.3 Average (SD) maximum displacement and rotation of the current study, study described in Chapter 4 and the previous study conducted by Kawchuk et al. (2010)	128

Table 5.4. Median (IQR) forces and moments experienced by the intact specimen during the SMT application at each application site .....	129
Table 5.5. Median (IQR) normalized forces and moments (relative to the intact condition) experienced by the supra- and interspinous ligaments during the SMT application at each application site .....	131
Table 5.6. Median (IQR) normalized forces and moments (relative to the intact condition) experienced by the bilateral facet joints, capsules and ligamentum flavum during the SMT application at each application site .....	134
Table 5.7. Median (IQR) normalized forces and moments (relative to the intact condition) experienced by the intervertebral disc, anterior and posterior longitudinal ligaments during the SMT application at each application site .....	137
Table 6.1. Description of conditions and variables used throughout the chapter .....	173
Table 6.2 Average (SD) of spinal manipulative therapy characteristics of each method of application .....	175
Table 6.3 Spinal manipulative therapy maximum displacement and rotation (SD) created in the cadaveric specimen with the application of SMT (with different methods of application) trajectories .....	178
Table 6.4 Percentage of general forces and moments experienced by spinal structures during the SMT application with different methods in relation to the loads experienced by the intact specimen (100%) .....	187
Table 7.1. Description of conditions and variables used throughout the chapter .....	223
Table 7.2 Maximal displacement and rotation (SD) created in the cadaveric specimens with the application of manual SMT and passive lumbar movements trajectories .....	226
Table 7.4 Percentage of general forces and moments experienced by spinal structures during each applied motion (manual SMT and passive physiological movements) in relation to the loads experienced by the intact specimen (100%) .....	236

## LIST OF FIGURES

Figure 2.1 Spinal manipulative therapy input parameters. [Source: Adapted from Herzog, 2010.].....	25
Figure 3.1 Multi-material 3D print model and Cartesian axes. ....	45
Figure 3.2 Moment-rotation graph during positive and negative rotation around y-axis. ....	49
Figure 3.3 Bar chart showing the relative peak moments ( $\pm 2SE$ ) carried by each connector in different sequence of connector removal during positive rotation around y-axis. ....	52
Figure 3.4 Bar chart showing the relative mean moments ( $\pm 2SE$ ) carried by each connector in different sequence of connector removal during positive rotation around y-axis. ....	53
Figure 3.5 Bar chart showing the area under the curve ( $\pm 2SE$ ) of each connector in different sequence of connector removal during positive rotation around y-axis. ....	54
Figure 4.1 Potential relation between spinal tissue targeting and influence on physiological outcomes by adjusting SMT input parameters. ....	60
Figure 4.2 Summary of the overall methodology .....	61
Figure 4.3 Bone pin positioning. A. Intact cadaveric specimen. B. After spine was removed. ...	63
Figure 4.4 Rectangular flag with 4 infrared light-emitting diode markers. ....	64
Figure 4.5 Anchor screws placement on porcine lumbar segments. ....	65
Figure 4.6 Potting procedure of porcine lumbar spine specimens. A. Potting of L4 vertebra. B and C. Potting of L3 vertebra. ....	66
Figure 4.7 Robotic testing. A. Specimen fixed to the load cell. B. Parallel robot platform with load cell and specimen attached. ....	67
Figure 4.8 Combined loads of all conditions .....	73
Figure 4.9 Average and standard deviation of peak and mean forces and moments experienced by the intact specimen during the SMT application with each force magnitude (bottom of each graph) at each application site (bar colors). ....	77

Figure 4.10 Interaction between force magnitude and application site for peak (A) and mean (B) moment around x-axis (flexion extension moment) in the intact condition. FJ=Facet joint; TVP=Transverse process. ....	79
Figure 4.11 Average and standard deviation of normalized relative peak and mean forces and moments experienced by the supra- and interspinous ligaments during the SMT application with each force magnitude (bottom of each graph) at each application site (bar colors). ....	81
Figure 4.12 Force magnitude main effect of average (and standard deviation) mean force along x-axis (lateral force) and peak moment around y-axis (lateral bending) for supra- and interspinous ligaments. ....	83
Figure 4.13 Average and standard deviation of normalized relative peak and mean forces and moments experienced by the bilateral facet joints, capsules and ligamentum flavum during the SMT application with each force magnitude (bottom of each graph) at each application site (bar colors). ....	85
Figure 4.14 Force magnitude main effect of average (and standard deviation) mean moment around z-axis (axial rotation) for bilateral facet joints, capsules and ligamentum flavum. ....	87
Figure 4.15 Application site main effect of average (and standard deviation) peak force along x-axis (lateral force) and peak moment around y-axis (lateral bending moment) for bilateral facet joints, capsules and ligamentum flavum. ....	87
Figure 4.16 Average and standard deviation of normalized peak and mean forces and moments experienced by intervertebral disc and anterior and posterior longitudinal ligaments during the SMT application with different force magnitudes (bottom of each graph) at each application site (bar colors). ....	89
Figure 4.17 Summary of clinical implications. ....	107
Figure 5.1 Rectangular flags with 4 infrared light-emitting diode markers attached to bone pins drilled into L3 and L4 vertebrae. ....	112
Figure 5.2 Standardized potting procedure and L3/L4 spinal segment. ....	114

Figure 5.3 Median value of peak forces experienced by the intact specimen and median value of normalized peak forces experienced by spinal structures. ....	120
Figure 5.4 Median values of mean forces experienced by the intact specimen and median values of normalized mean forces experienced by spinal structures. ....	122
Figure 5.5 Median values of peak moments experienced by the intact specimen and median values of normalized peak moments experienced by spinal structures. ....	124
Figure 5.6 Median values of mean moments experienced by the intact specimen and median values of normalized mean moments experienced by spinal structures. ....	126
Figure 5.7 Summary of general findings of this study. ....	139
Figure 5.8 Posterior view of the L3-L4 motion segment. [Source: Netter FH. Atlas of human anatomy. 4th ed., 2006. Saunders Elsevier] .....	145
Figure 5.12 Summary of clinical implications. ....	162
Figure 6.1 Rectangular flags with 4 infrared light-emitting diode markers attached to bone pins drilled into L3 and L4 vertebrae. ....	168
Figure 6.2 Three methods used to apply SMT: A. mechanical force manually assisted instrument (Activator V-E); B. Manual SMT; C. linear actuator motor. ....	169
Figure 6.3 Standardized potting procedure and L3/L4 spinal segment. ....	170
Figure 6.4 Characteristic example of force- and moment-time plots of raw forces and moments experienced by the spinal segment in all three axes of movement during SMT application with all three methods (SMTact, SMTman and SMTmot). ....	176
Figure 6.5 Example of contact surface area at peak force magnitude during A. mechanical force manually assisted instrument (Activator V-E) and B. manual spinal manipulative therapy application. ....	177
Figure 6.6 Boxplots with median, interquartile range, distribution and outliers of peak and mean forces and moments experienced by the intact specimen and following each cut in the x-axis. ....	179

Figure 6.7 Boxplots with median, interquartile range, distribution and outliers of peak and mean forces and moments experienced by the intact specimen and following each cut in the y-axis. ....	180
Figure 6.8 Boxplots with median, interquartile range, distribution and outliers of peak and mean forces and moments experienced by the intact specimen and following each cut in the z-axis. ....	181
Figure 6.9 Average value of peak force, mean force, peak moment and mean moment experienced by the intact specimen during the application of SMT with different methods. ....	183
Figure 6.10 Average value of normalized peak force, mean force, peak moment and mean moment experienced by supra- and interspinous ligaments during the application of SMT with different methods. ....	186
Figure 6.11 Average value of normalized peak force, mean force, peak moment and mean moment experienced by bilateral facet joints, capsules and ligamentum flavum during the application of SMT with different methods. ....	188
Figure 6.12 Average value of normalized peak force, mean force, peak moment and mean moment experienced by intervertebral disc, anterior and posterior longitudinal ligaments during the application of SMT with different methods. ....	191
Figure 6.13 Summary of general findings of this study.....	194
Figure 6.14 Loading rate of different methods of SMT application.....	209
Figure 6.15 Summary of clinical implications.....	211
Figure 7.1 Rectangular flags with 4 infrared light-emitting diode markers attached to bone pins drilled into L3 and L4 vertebrae.....	217
Figure 7.2 Cadaveric porcine positioning on hinged hardwood board with L3 positioned above the hinge line and L4 bellow. ....	218
Figure 7.3 Passive extension movement.....	219
Figure 7.4 Passive left axial rotation movement.....	219



Figure 7.5 Standardized potting procedure and L3/L4 spinal segment. ....	220
Figure 7.6 Characteristic example of force- and moment-time plots of raw forces and moments experienced by the spinal segment in all three axes of movement during manual SMT and passive lumbar movements (left axial rotation, extension and flexion). ....	227
Figure 7.7 Boxplots with median, interquartile range, distribution and outliers of peak and mean forces and moments experienced by the intact specimen and following each cut. ....	228
Figure 7.8 Average value of peak force, mean force, peak moment and mean moment experienced by the intact specimen during the application of manual SMT and passive lumbar movements of flexion, extension and left axial rotation. ....	230
Figure 7.9 Three-dimensional plots of average values of peak force, mean force, peak moment and mean moment experienced by the intact specimen during the application of manual SMT and passive lumbar movements of flexion, extension and left axial rotation in each axis of movement. ....	231
Figure 7.10 Average value of normalized peak force, mean force, peak moment and mean moment experienced by the supra- and interspinous ligaments during the application of manual SMT and passive lumbar movements of flexion, extension and left axial rotation. ....	234
Figure 7.11 Three-dimensional plots of average values of normalized peak force, mean force, peak moment and mean moment experienced by the supra- and interspinous ligaments during the application of manual SMT and passive lumbar movements of flexion, extension and left axial rotation in each axis of movement. ....	235
Figure 7.12 Average value of normalized peak force, mean force, peak moment and mean moment experienced by the bilateral facet joint, capsules and ligamentum flavum during the application of manual SMT and passive lumbar movements of flexion, extension and left axial rotation. ....	238
Figure 7.13 Three-dimensional plots of average values of normalized peak force, mean force, peak moment and mean moment experienced by the facet joints, capsules and ligamentum flavum during the application of manual SMT and passive lumbar movements of flexion, extension and left axial rotation in each axis of movement. .	239

Figure 7.14 Average value of normalized peak force, mean force, peak moment and mean moment experienced by the intervertebral disc, anterior and posterior longitudinal ligaments during the application of manual SMT and passive lumbar movements of flexion, extension and left axial rotation. ....	242
Figure 7.15 Three-dimensional plots of average values of normalized peak force, mean force, peak moment and mean moment experienced by the intervertebral disc, anterior and posterior longitudinal ligaments during the application of manual SMT and passive lumbar movements of flexion, extension and left axial rotation in each axis of movement .....	243
Figure 7.16 Summary of the main findings of the current study. ....	246
Figure 7.17 Summary of clinical implications of the current study. ....	267
Figure 8.1 Summary of experimental results. ....	272
Figure 8.2 Overview of experimental findings. ....	272

## LIST OF APPENDICES

Appendix I. Linear Mixed Model ANOVA tables for relative mean and peak moments, and area between curves of the moment-displacement graph of Chapter 3 .....	311
Appendix II. Detailed description of spinal manipulative therapy simulator .....	312
Appendix III. Detailed description of optical tracking system .....	313
Appendix IV. Detailed description of calibration process .....	315

## **Chapter 1.**

### **Introduction**

Low back pain (LBP) is a very common condition with an estimated lifetime prevalence as high as 84% worldwide and 83.8% in Alberta, Canada [1–3]. It has been reported that globally, LBP is the primary cause of disability [4]. Consequently, LBP leads to important socioeconomic consequences involving not only the direct costs with health care, but also indirect costs related to missed working days and decrease of productivity [5–7]. The total costs of LBP direct expenses has been estimated at approximately US\$96 millions in 2008 in the USA and \$6-12 billions annually in Canada [8,9]. Although the majority of LBP cases recover within weeks with or without intervention, those patients who develop chronic LBP experience persistent symptoms, and are associated to most of the LBP-related expenses [10,11].

The majority of LBP cases are classified as non-specific LBP as they are not related to any specific known pathology, such as fracture, tumor, and structural deformity [1]. Studies have demonstrated that surgical interventions are not superior to conservative care in effectively treating chronic non-specific LBP patients [1,12,13]. Therefore several conservative interventions have been proposed to treat LBP patients including drug treatment, therapeutic exercise and spinal manipulative therapy [14–18].

Among the conservative interventions available for LBP patients, spinal manipulative therapy (SMT) has been described to be cost-effective either alone or combined with other interventions [19]. Spinal manipulative therapy is a mechanical intervention characterized by the application of a dynamic force with a high-velocity, low-amplitude thrust. This force is applied to a specific

location of the spine and causes a mechanical deformation of the specific spine region and surrounding tissues [20–22]. By mechanically loading spinal tissues, SMT triggers biomechanical and neurophysiological responses that contribute to the therapeutic effects of this popular intervention. However, how SMT forces are distributed within spinal tissues remains unclear. If SMT force distribution within spinal tissues were quantified, important advances could be realized not only scientifically by focusing mechanical investigations on the spinal tissues that are most affected by SMT parameters, but also clinically by allowing health care providers to adjust SMT parameters so that specific spinal tissues could be targeted, or avoided. Consequently, this could allow SMT to be tailored to each patient's specific condition contributing to the improvement of SMT's efficacy and safety.

### **1.1 Spinal manipulative therapy load distribution**

Previous studies have been conducted to investigate the forces applied during SMT and described the characteristics of the forces transmitted through the treated spinal region [23]. However, these studies did not quantify the distribution of SMT forces within spinal tissues. A recent study conducted by Kawchuk and colleagues (2010) [24] pioneered the investigation of the mechanical loading characteristics of spinal tissues during a general application of SMT. In this study, a clinical SMT was applied at the skin overlying the transverse process of L3 of a porcine cadaveric model and by using a novel methodology combining stable robotic biomechanical tests with serial dissection technique, they measured the forces and moments experienced by spinal tissues during the SMT application. Specifically, they found that the loading characteristics during SMT are not uniform among spinal tissues and the intervertebral disc is the spinal structure that experienced the greatest change in peak forces and moments in all

axes of movement [24]. Based on this finding, basic biomechanical theory suggests that altering the SMT force characteristics will also alter its distribution within spinal tissues.

### ***1.1.1 Significance***

Given that SMT interventions involve adapting the mechanical procedure (patient posture, preload amplitude, load direction, peak amplitude, impulse rate and load duration) to accommodate for each unique clinical presentation [25], previous investigations on SMT effectiveness have emphasized the importance of applying a patient-specific intervention to improve manual therapies' effectiveness [16,25]. Simultaneously, previous investigations have reported adverse event rate following a manual therapy intervention to be about 50% [26,27]. Therefore, if the distribution of SMT forces to spinal tissues could be changed by altering SMT application parameters, new therapeutic techniques could be developed to tailor specific SMT application to each individual's clinical presentation while optimizing SMT efficacy and safety.

## **1.2 Current evidence on spinal manipulative therapy parameters**

### ***1.2.1 Peak Force Magnitude***

The mechanical characteristics of SMT (e.g. force magnitude and direction) are usually adapted to the patient's clinical presentations [25]. Peak force magnitudes applied during SMT have been investigated and reported to vary depending on the region of the spine SMT is being applied [21]. The effects of using different peak force magnitudes on biological outcomes have also been investigated [28–31]. Clinical effects, such as increase in paraspinal muscle Electromyographic (EMG) responses, have been observed during the application of SMT with increased force magnitudes [28]. Spinal stiffness has also been demonstrated to be affected by the interaction

between force magnitude and duration: in a feline model, spinal stiffness was observed to increase with varied interactions: 1mm displacement force magnitude with 50ms to 100ms force durations; 2mm displacement force magnitude with 75, 200 and 250ms force durations; and 3mm displacement force magnitudes with 100 to 250ms force durations [29]. At a basic level, greater force magnitudes have been described to increase vertebral displacement and acceleration [32,33]. Related to this, vertebral displacements have been reported to change the neural responsiveness of muscle spindles [30,31]. Additionally, a minimal SMT amplitude has been reported to increase the response thresholds of nociceptive specific thalamic neurons [34]. Consequently, given that peak force magnitudes affect the biological responses of SMT, identifying the distribution of these forces within spinal tissues becomes fundamental to better understand the underlying mechanisms of SMT.

Nevertheless, previous studies have described significant variability in peak force magnitudes exerted during the application of clinical SMT, depending on the clinician and on the application site [20,21,35]. The peak force magnitude of SMT applied at the cervical region is greatly smaller than the ones applied at the thoracic and sacroiliac regions [20,21]. Additionally, previous studies have also shown that peak forces present great variability between clinicians [35,36]. Therefore, the standardization of SMT application is fundamental not only to homogenize the investigations of SMT underlying mechanisms, but also so that these effects can be translated into clinical practice. As a result of this necessity, devices have been developed and approaches have been suggested in order to standardize SMT application and minimize force variability. Mechanical force, manually assisted (MFMA) instruments have been developed to deliver a controlled force at osseous spinal structures and are being used in both research and

clinical settings [37,38]. Although the use of MFMA instruments are still subjected to variability, it has been demonstrated to reduce the SMT force magnitude and duration variability between clinicians [36]. Recently, a servo-controlled linear actuator motor device was developed to standardize the force-time profile of simulated SMT and reduce variability between SMT applications [39]. This device has been described to deliver repeatable, controlled and safe SMT forces with optimized precision (0.1 N) [39]. By using these devices and delivering a standardized SMT, clinical and mechanistic investigations can be advanced and better contribute to the current body of SMT intervention evidence.

### ***1.2.2 Application site***

Given that manual therapists usually identify spinal levels based on palpation technique and that previous findings have reported this technique to present limited accuracy and validity [40–43], the effects of applying SMT at different spinal levels becomes an important topic. Recent studies have investigated specific responses to the application of SMT at different application sites [44,45]. Different changes in muscle spindles' sensory input and spinal stiffness have been observed when SMT was applied at different application sites. This indicates that the location in which SMT is applied significantly affect both neurophysiological (muscle spindles sensory input) and biomechanical (spinal stiffness) responses. Therefore, if SMT application site can elicit different physiological outcomes, it is possible that other SMT parameters will also have a significant influence. Additionally, if the distribution of SMT forces within spinal tissues when SMT is applied at different locations of the spine were indentified, important elucidations regarding the effects of applying SMT forces at a spinal level above or below the target vertebra would be provided.



Generally, previous studies have shown that SMT thrusts displace not only the target vertebra, but also adjacent segments of the spine [46,47]. Significant increase in axial displacements of vertebrae distant to the SMT application site has been observed when SMT was applied with greater force magnitudes [47]. Also related to force magnitude, displacements of the local and remote regions of the spine are potential contributors to SMT responses evoked both locally and remotely from the SMT application site [32,48]. Specifically, EMG responses of muscles located beyond the immediate area of SMT force application have been observed [48,49]. While Colloca and Keller [49] elicited different EMG responses of erector spinae muscles at L3 and L5 levels when SMT was applied at the thoracic and lumbar levels, Herzog and colleagues [48] observed EMG responses of several muscles of the back, including splenius capitis, trapezius, latissimus dorsi and gluteus maximus, during a SMT application at L2-L4 vertebrae. Therefore, despite of the specific SMT application at one spinal level, physiological responses can also be observed at remote regions of the back. However, it remains unknown if these remote responses significantly contribute to the SMT-related clinical outcomes.

### **1.3 Clinical application**

Besides the elucidation of SMT load distribution within spinal tissues, verifying the clinical meaning of the loads arising from SMT and determining if whether SMT parameters is clinically relevant and is fundamental. In order to determine the clinical meaning of SMT force magnitude and application site parameters, the comparison with loading arising from physiological movements and daily activities is imperative. Lumbar spine biomechanics, including range of motion and spinal loading, has been investigated during physiological movements and daily

activities [50–55]. However, methodological differences, such as specimen characteristics, and testing protocol, make the comparison between studies improper, precluding the determination of the clinical meaning of SMT loads. Therefore, by unifying the investigation of spinal structures loading characteristics during SMT application and physiological movements in one study with comparable specimens and standardized testing protocol, the impact of SMT application parameters can be better understood.

### ***Summary***

Based on the recent finding by Kawchuk and colleagues [24] that the intervertebral disc experiences the greatest loads during a general SMT application, basic biomechanical theory can be incorporated and suggest that by altering SMT parameters, it is theoretically possible to change the force distribution within spinal tissues. Results from previous investigations describing various biomechanical and neurophysiological responses to SMT with specific parameters support this rationale [28,29,31,45,48,56]. Although it has been described that different SMT parameters evoke different biomechanical and neurophysiological responses [28,31,44,45,57], no study has been conducted to investigate if changes in SMT parameters would also change the load distribution within spinal tissues. Additionally, in order to fully understand the clinical meaning of the spinal tissues' loading characteristics during SMT with different parameters, the comparison of loads experienced during SMT with the ones experienced during physiological movements is fundamental.

By elucidating the distribution of SMT forces within spinal tissues, mechanical investigations can focus basic and clinical research on the response of those spinal tissues that experience the

greatest loads. Furthermore, being able to target or avoid specific spinal tissues will allow SMT application to be tailored to load specific spinal tissues based on each individual's condition. This way, the clinical efficacy of SMT will be properly investigated as well as the safety aspects of this popular intervention will be better understood.

## **1.2 Dissertation Objectives**

Given the above, the overall objective of this doctoral dissertation was to investigate how forces and moments arising from SMT application were distributed within spinal structures when using varied SMT input parameters and how these forces and moments compared to the ones arising from passive movements. Particularly, this dissertation had four specific objectives: 1) to investigate identical testing objects structural response to mechanical loading created through robotic testing when different sequence of structural removal is used; 2) to identify the forces and moments experienced by spinal tissues during SMT with different parameters of application (force magnitude and application site); 3) to investigate spinal tissues' loading characteristics when SMT is delivered using three different methods of application; and 4) to describe the loads arising from SMT application in comparison to passive physiological movements of flexion, extension and axial rotation of the lumbar spine.

To achieve these objectives, five biomechanical experiments were carefully designed and conducted. These experiments are detailed in 7 chapters of this dissertation: the first experiment (chapter 3) has been published as a short communication at the Journal of Biomechanics (doi: 10.1016/j.jbiomech.2015.06.020), the second to fourth experiments (chapters 4 to 7) are being formatted to the peer-reviewed journal specifications and will soon be submitted for publication.

Chapter 2 presents a review of what has been described in the scientific literature regarding relevant topics involved in this dissertation. Low back pain, spine biomechanics, SMT parameters and responses, animal models, and robotic biomechanical testing are some of the topics included in the literature review.

Chapter 3 describes the biomechanical experiment aiming to verify if the order in which structures presenting time-dependent and non-linear behavior are removed from the testing object influence the loads experienced by these structures during biomechanical testing. Although previous biomechanical studies have assumed that the sequence of tissue removal does not affect the loads experienced by biological tissues during biomechanical tests, it has not been demonstrated to date. Therefore, this study verified if structures would experience similar loads regardless of the order in which they were removed from the specimen. Based on the results of this experiment, the order in which structures were removed from cadaveric porcine lumbar spine segments in the following experiments of this dissertation was determined.

Chapter 4 reports the experiment aiming to identify the loading characteristics of spinal tissues when SMT is applied with varying force magnitudes and application site. This was an exploratory study to verify if interactions between force magnitude and application site would similarly load spinal structures. It was hypothesized that forces and moments experienced by spinal tissues would change with different combinations of SMT's force magnitude and application site. Based on the results of this study, the force magnitude that did not specifically

affect one particular spinal structure was selected to be used in the following experiments of this dissertation.

Chapter 5 describes the investigation of forces and moments experienced by porcine spinal tissues when SMT was applied at 6 distinct application sites: facet joints and transverse processes of L3 and L4 vertebrae and the interspace between those landmarks. Given that the location in which SMT force is applied will influence on the length of the moment arm created, it was speculated that SMT applied at different locations of the spine would load spinal tissues differently. Based on the results of this study, the application site that did not significantly loaded one specific spinal structure was selected to be used in the following experiments of this dissertation.

Chapter 6 presents the comparison of the forces and moments experienced by spinal tissues when SMT was provided at the back of a porcine cadaveric model using three different methods of application: a mechanical-force manually-assisted instrument (Activator), a clinical SMT and a standardized servo-controller motor. Given the difference in force magnitude and contact area surface, it was expected that different methods of SMT application would load the spinal tissues in different extents.

Chapter 7 describes the loading characteristics of cadaveric porcine lumbar spine tissues during a clinical SMT in comparison to the loads arising from passive physiological movements of flexion, extension and left axial rotation. Since SMT moves the target spinal motion segment beyond its normal physiologic range of motion into the parapysiological zone, it was

hypothesized that SMT would load spinal tissues in a greater extent when compared to physiological movements.

Chapter 8 combines the discussion and conclusion of this work. The discussion summarizes the findings and includes an extensive interpretation of them. It also describes the strengths, limitations and significance of these results. Future research directions are also suggested in this chapter.

This doctoral work characterized, for the first time, the loads experienced by porcine lumbar spine tissues during the application of SMT with different parameters. By elucidating the changes in the distribution of SMT loads with different characteristics within spinal tissues, researchers can concentrate their efforts and resources on the tissues that are most influenced by SMT parameters. Additionally, clinicians will have evidence of SMT parameters effects, which allows them to consciously adjust the mechanical characteristics of SMT to target or avoid a specific spinal tissue, according to each patient's condition. This work is also the pioneer in comparing the loads spinal tissues experienced during clinical SMT with the loads arising from physiological movements. This way, the current work greatly contributed to creating a framework for understanding the magnitude of spinal tissue loading and tissue response to SMT interventions.

## **Chapter 2.**

### **Literature Review**

#### **2.1 Introduction**

Low back pain (LBP) is defined as pain in the region between the 12<sup>th</sup> rib margins and the inferior gluteal folds, with or without leg pain [58]. Low back pain is an extremely common condition with an estimated lifetime prevalence of 84%, with 23% being chronic LBP and 11-12% of the population being disabled by LBP [1]. Low back pain has been reported as the leading cause of disability affecting about 630 million people globally and accounting for 70% of all years lived with disabilities due to musculoskeletal disorders [59–61]. The great socioeconomic burden caused by LBP involves mainly costs with health care resources, missed working days and decrease of productivity [2,5]. It has been estimated that in the USA, the total direct expenses of LBP-related wealth was approximately US\$96 million in 2008 [8]. Total health care costs for chronic LBP patients was estimated at £1074 per patient in 2009 in the UK [62], and €20,700 per patient in Sweden in 2002 [63].

The possible causes of low back pain has been widely investigated. However, about 85% of LBP cases are still considered non-specific LBP, as they are not resultant of any specific known pathology, such as vertebral fracture, spinal deformity and tumor [1,64,65]. Only approximately 15% of LBP patients who look for health care are diagnosed with specific LBP, such as infection, osteoporosis, vertebral fracture, tumor, radicular or cauda equina syndromes [1,64]. The majority of non-specific LBP cases are believed to emerge from any structure of the spine, including the intervertebral discs, facet joints, spinal ligaments, and paraspinal muscles [14,64,66]. Vertebral

motion and mechanical loads have also been reported to be important biomechanical factors associated with LBP and specifically, mechanical cumulative loads have been described as predictive for the occurrence of LBP [67,68].

## **2.2 Lumbar Spine Biomechanics**

The human spine presents complex anatomy with heterogeneous composition presenting time-dependent, non-linear behavior, that functions under dynamic loading conditions [69,70]. The function of the total spine is a result of the behavior of its individual regions (cervical, thoracic, and lumbar). Different regions of the spine behave differently in motion and have their unique dominant function in specific directions. Differences in motion capacity are largely attributed to differences in shape and orientation of the individual facet joints and to the influence of the intervertebral disc and spinal ligaments [69]. Specifically for the lumbar spine, the facet joint orientation allows great mobility on the sagittal axis, moving the upper-body in flexion-extension movement [71].

### ***2.2.1 Bony structures***

#### ***2.2.1.1 Vertebral body***

Lumbar vertebral bodies is a large kidney-shaped structure that is composed of a shell of cortical bone internally reinforced with trabeculae bones. With this architecture, the lumbar vertebral body has increased size in comparison to vertebral bodies from upper levels of the spine and is responsible for resisting most of the compressive (cranio-caudal) forces experienced by the spine [72]. Boundaries of vertebral bodies are characterized by the endplates, which are thin plates of cortical bones that assist the intervertebral disc nutrition by allowing metabolites permeability from



the vertebral body to the intervertebral disc nucleus. This permeability, however, weakens the endplates, becoming the most vulnerable structure of the vertebral body [73].

#### *2.2.1.2 Vertebral arch*

The vertebral arch of lumbar vertebrae involves bilateral pedicles and laminae posterior to the vertebral body, mainly composed of cortical bone. While the pedicles are the supporting structures of the posterior elements, they also transmit forces from and to the vertebral body. Several processes project from the vertebral arch (spinous and transverse processes and superior and inferior articular processes) serving as attachment sites for muscles and ligaments, and together with the vertebral arch, they compose the posterior elements of the lumbar vertebrae and control the position of the vertebral bodies [73].

While the superior articular processes present an articular facet on its medial surface, the inferior articular processes present this articular facet on their lateral surface. The superior articular process together with the inferior articular process of the immediately cranial vertebra form the zygapophyseal joints (facet joints). The facet joints are small synovial joints that restrict axial rotation, protecting the intervertebral disc from excessive torsion, and anterior and lateral translations of the lumbar vertebrae [73–75]. The orientation of articular surfaces have been described to vary within the lumbar spine and lower facet joints present an oblique surface in order to resist the compressive forces acting on the spine. While flexion movements reduce the loads borne by the vertebral arch and facet joints, extension movement causes the contact of the anterior inferior portion of articular surfaces, increasing the loads borne by facet joints [73,76].

### ***2.2.2 Intervertebral disc***

Intervertebral discs, located in between two adjacent lumbar vertebrae, involve the annulus fibrosus (consisting mainly of layers of collagen, named lamellae) and the nucleus pulposus (consisting of a hydrated gel of proteoglycans), allowing intervertebral movements. The direction of collagen fibers alternates in consecutive layers making the lamellae stiff and contributing to transferring compression loads from one vertebral body to the next [73]. The annulus fibrosus' function vary as a function of the region it is located and while the outer lamellae resist to excessive bending and twisting, the middle lamellae are more susceptible to deformation. On the other hand, while the nucleus pulposus presents high water content being highly deformable and equalizing the stresses, it presents a viscoelastic behavior when subjected to high loading rates [77].

Under compression forces, the hydrostatic pressure in the nucleus pulposus increases, stressing the annulus fibrosus, causing the disc to bulge reducing the intervertebral disc height. During flexion movement the anterior annulus are subjected to compression whereas the posterior annulus are subjected to tension which, in turn has been described to increase the hydrostatic pressure in the nucleus. Extension and lateral bending motions, on the other hand, leads to facet joint contact, which decreases the loads experienced by the intervertebral. During torsion movements, while half of the lamellae tend to become slack due to its collagen orientation, the other half are subjected to great tension, increasing the pressure within the nucleus [78].

### **2.2.3 Ligaments**

#### *2.2.3.1 Supra- and interspinous ligaments*

Supra- and interspinous ligaments are mainly constituted by collagen fibers connecting the tip of upper lumbar vertebral spinous processes and opposite edges of adjacent spinous processes, respectively [73,79]. While they do not significantly contribute to resist small degrees of flexion, supra- and interspinous ligaments have been reported to be great contributors to resisting full flexion movements. Tensile forces have been reported to range between 50 to 70N for supraspinous ligament and approximately 100N for interspinous ligament [79,80].

#### *2.2.3.2 Ligamentum flavum*

The ligamentum flavum is mainly composed of fibers of elastin with some disperse collagen fibers connecting the lower end of one lamina to the upper end of the caudal vertebral lamina, covering the space between laminae of adjacent vertebrae. Its high proportion of elastin not only allows the ligamentum flavum to be stretched and shortened without slacking or buckling, but also contributes to the vertebral positioning and prestresses the intervertebral disc in the upright posture [79]. These properties are important given its proximity with the spinal cord and its tensile strength has been reported to range between 250 to 350N [73].

#### *2.2.3.3 Intertransverse ligament*

Similar to interspinous ligament, intertransverse ligaments consist mainly of collagen fibers connecting two adjacent transverse process. Although it has been observed to stretch during lateral bending movement, its tensile strength has not been assessed and it is believed to be too fragile to function as a true ligament [73].

#### *2.2.3.4 Anterior and posterior longitudinal ligaments*

The anterior and posterior longitudinal ligaments contains crimped collagen fibers and are located in the anterior and posterior aspect of the vertebral bodies and intervertebral discs, respectively. Although the anterior longitudinal ligament has been described to assist the resistance to extension movements, the annulus fibrosus are stronger potentially being the main resistors to extension together with the vertebral arch contact. Posterior longitudinal ligaments, on the other hand, have been described to apply a small pretension to the intervertebral discs and protect the spinal cord from herniated disc material. Tensile strengths of approximately 330N and 180N have been reported for the anterior and posterior longitudinal ligaments, respectively [73,79,81].

#### **2.2.4 Biomechanical function**

Supporting body weight and providing flexibility for dynamic tasks are fundamental functions of the spine. The loads experienced by the spine during both static and dynamic activities are transferred from one vertebra to the adjacent one through the vertebral body/intervertebral disc complex as well as the facet joints at the posterior column [82]. Therefore, the integrity of the involved structures play an important role in how loads are shared within the spinal structures. Specifically, intervertebral disc degeneration has been shown to transfer loads from the anterior vertebral body to the neural arch in upright posture, causing the vertebral arch to stress-shield the anterior vertebral body [83,84]. Similarly, facet joint engagement has been described to act as a mechanical hinge resulting in stress shielding the intervertebral disc's posterior annulus fibrosus during extension [85]. Alapan and colleagues (2014) have also described changes in lumbar spine load sharing characteristics as a function of the centre of rotation location. By changing the centre

of rotation location, a change in motion path was observed and, consequently, changes in ligament stretch, moment arm and load sharing were also observed [86].

### ***2.2.5 Lumbar coupled motion***

Due to the time-dependent, non-linear behavior of spinal structures and the irregular geometry of facet joint surfaces, primary movements of the lumbar spine are accompanied by concomitant coupled motions in the other axes of movement in order to reduce the resistance to the primary movement [87]. *In vivo* coupled motions are influenced by posture and muscular contraction and specifically during active flexion-extension primary motion similar coupled translations in all three directions ranging from 0.7mm to 3.1mm has been reported as well as coupled rotations of lateral bending and axial rotation ranging from 1.7° to 2.9° [88,89]. Similarly, during active lateral bending motion, while coupled translations in all three have been described to range from 0.8mm to 2.1 mm, coupled flexion rotation ranged from 1.3° to 4.1° and coupled axial rotation from 2.2° to 4.6° [88–90]. Additionally, active axial rotation has been observed to present coupled anterior-posterior translations of 1.1-2.6mm, lateral translations of 0.5- 2.5mm and cranio-caudal translations of 0.3-1.1mm as well as coupled flexion movement ranging from 0.9° to 3.3° and coupled lateral bending ranging from 2.0° to 3.4° [88,89].

Despite the incontestable differences in methodological approaches between *in vivo* and *in vitro* investigations, they are complementary and each demonstrated coupled motions in unique conditions. In general, *in vitro* coupled motions are small in magnitude and may change as a function of specimen positioning and biomechanical testing. Specifically, previous intersegmental *in vitro* investigations observed coupled motions in all three axes of movement during all

primary movements of flexion-extension, lateral bending and axial rotation and maximum anterior posterior translation of approximately 3mm, lateral translation of 2.6mm and cranio-caudal translation of 1mm have been reported [74,91,92].

### **2.2.6 Biomechanical characteristics**

Previous studies have also investigated the biomechanical characteristics of the spine, such as range of motion, neutral zone and neutral zone stiffness [69,93,94]. Specifically for the lumbar spine, intersegmental range of motion has been widely investigated in both *in vivo* and *in vitro* conditions [69,89,95–97]. While biomechanical tests with *in vitro* specimens have observed the lumbar intersegmental to range from 5° to 7° in flexion-extension, 5.5° to 8° in lateral bending, and 2° to 3.5° in axial rotation [69,97,98], *in vivo* studies have reported rotations of approximately 5° during flexion extension and lateral bending and 4° during axial rotation [88,89,96].

The neutral zone, defined as the zone in between the points of the largest changes in stiffness of the load-displacement curve, with stiffness being defined as the slope of the tangent along the linear portion of the load-displacement curve. Specifically for the lumbar spine, neutral zone has been described to be about 2° for flexion-extension and lateral bending and 1° for axial rotation [69,93]. Neutral zone flexibility, calculated as the inverse of the slope of the load-displacement curve in the neutral zone, has been described to be about 0.6-0.8 Nm/deg for flexion-extension, 0.5-0.6 Nm/deg for lateral flexion and 2.5-2.7 Nm/deg for axial rotation [69,93].

### **2.3 Spinal Manipulative Therapy**

Among many conservative interventions available to treat LBP patients (such as exercise, massage therapy, nonsteroidal anti-inflammatory drugs, etc) [99,100], spinal manipulative therapy (SMT) has been described to be cost-effective either alone or combined with other interventions [19]. Spinal manipulative therapy is defined as the application of a high velocity low amplitude dynamic thrust to a specific location to the spine [20,22,101]. It is a popular intervention to treat both acute and chronic LBP and its usage has increased in the last few decades due to the increased utilization of complementary and alternative therapies by the public [99,102]. Previous studies revealed the rate of chiropractic services to be approximately 101.2 visits per 100 person-years in the USA and 140.9 visits per 100 person-years in Ontario, Canada [103].

Typically, the SMT application is composed of two phases: preload and thrust phases. While the target spinal segment is moved to the end of its range of motion during preload phase, the thrust phase is characterized by an impulsive force that moves the spinal segment beyond its normal range of motion into the parapsychological movement zone [21]. These forces are believed to cause a mechanical deformation of the target spinal segment and its surrounding spinal tissues eliciting the physiological outcomes (biomechanical and neurophysiological responses) observed following a SMT application [21,22,104].

The physiological effects elicited by SMT have been under investigation and while some randomized controlled trials have reported improvements in low back pain and spinal function following SMT interventions [101,105–107], others found SMT and other treatment interventions such as exercise and standard medical care to provide comparable improvements [108–110].

While this conflicting evidence can be associated with the heterogeneous nature of LBP itself, it can also be related to the recent finding from Wong and colleagues [111] who observed that SMT affects specific biomechanical characteristics present in some, but not all LBP patients. Consequently, the clarification of the underlying mechanisms in which SMT affects the human body becomes an important step towards elucidating indicators regarding SMT unique health outcomes. Specifically, physiological outcomes have been demonstrated following a SMT application being mainly categorized into biomechanical and neurophysiological responses [22,112,113].

### ***2.3.1 Spinal manipulative therapy techniques***

The SMT procedure selection is based on specific aspects presented by the patient (e.g. region of application, patient morphology and articular stiffness) [25,114] and despite the similarities between SMT techniques, they are believed to have specific goals on the target spine segment and are generally divided in two types: direct or indirect [115,116]. While the direct SMT technique applies direct pressure on the skin overlying the target spinal segment, the indirect SMT combines levers and rotational movements.

Among the common techniques used in SMT investigations, the prone unilateral hypothenar transverse push manipulation is a direct technique where the patient is in prone position, the clinician's pisiform bone is positioned on the skin overlying a specific spinal landmark (e.g. facet joint, mamillary process, transverse process) and a quick impulsive force vector with specific characteristics (i.e. input parameters, such as force magnitude, loading rate, direction, etc) is applied [23,114,117,118]. The supine thrust manipulation is an indirect technique performed in a



patient in the supine position with the fingers interlocked behind the head. The therapist adjusts the lever by moving the patient into side-bending and axial rotation, and then delivers a quick thrust to the patient's pelvis in a posterior and inferior direction [111,119,120]. In the side-posture manipulation, the patient is positioned in side-lying position with the upside inferior limb flexed and adducted, and the downside upper limb is moved in side-bending and axial rotation. The therapist supports the patient's inferior limbs with his/her thigh and the upper body with his/her cranial hand (relative to the patient) at the patient's upside shoulder. The therapist then positions the hypothenar region of his/her caudal hand on the skin overlying the mamillary process of a specific lumbar level and the thrust is applied by quickly rotating the patient (by pushing on the patient's shoulder) as well as applying an impulsive force vector on the lumbar mamillary process [120–122].

## **2.4 Spinal Manipulative Therapy Outcomes**

### ***2.4.1 Biomechanical outcomes***

The application of SMT thrusts have been observed to create specific biomechanical outcomes. Since sedentary lifestyle and specific occupational activities are believed to result in hypomobile joints which, in turn, culminates in adhesions within the spinal joints [123]. Spinal joint space separation has been demonstrated following SMT applications and is believed to affect segmental biomechanics by releasing intra-articular fibrous adhesion and entrapped meniscoids, restituting buckled segments, restoring normal behavior and, consequently, improving segmental hypomobility and reducing the mechanical stresses on adjacent spinal tissues [104,124].

Vertebral motions caused by SMT applications have been previously investigated [32,33,104]. Three dimensional displacements and accelerations of the target and adjacent spinal segments have been described during SMT and greater posterior to anterior displacements and flexion extension rotations have been consistently observed [32,33,125,126]. Although vertebral accelerations have also been measured during SMT applications, the direction of greater accelerations is less consistent between studies and are related to the SMT force-time characteristics [32,33,125]. These vertebral motions are likely related to the location where SMT is applied and potentially affect the SMT loading characteristics by loading different spinal structures [104,127]. In addition, given the spine's complex biomechanics and anatomy, adjacent vertebrae coupled motions during SMT application potentially change as a function of the spinal geometry, tissue viscoelastic behavior and the resultant applied force vector [127].

Additionally, significant changes in intradiscal pressure and disc diffusion have also been reported following a SMT application [111,128–130]. Specifically, at the beginning of the thrust phase, an increase in intradiscal pressure values during SMT application has been observed followed by a discrete decrease in these values at later stages of the thrust phase of SMT [128,129]. Additionally, increase in diffusion of water within lumbar intervertebral discs have been observed in nonspecific LBP patients who reported reduction of pain intensity following a SMT application potentially improving intervertebral disc health [111,130].

Furthermore, spinal stiffness has also been observed to significantly change following a SMT application [45,111,131]. Particularly, spinal stiffness has been demonstrated to significantly decrease after SMT applications and this reduction was observed to be sustained for at least 7 days

[111,131]. Interestingly, the location in which SMT was applied has been demonstrated to significantly influence spinal stiffness change following a SMT application suggesting that not only SMT force-time profile, but also the application site influence the biomechanical outcomes elicited by SMT [45].

#### ***2.4.2 Neurophysiological Outcomes***

In addition to the biomechanical outcomes, SMT has also been demonstrated to elicit neurophysiological responses by influencing on the sensory inflow to the central nervous system [47,112]. High frequency properties of primary afferents and post-synaptic neurons response are characteristics described to arise from SMT [22]. By releasing fibrous adhesions, entrapped meniscoids, and restoring buckled segments, the SMT mechanical input is believed to decrease nociceptive input originating at receptive nerve endings in paraspinal tissues [112]. Specifically, the SMT impulsive thrust increases the discharge rate of muscle spindles and Golgi tendon organs in deep lumbar paraspinal muscles [132]. Generally, group Ia afferents evoke a greater response to SMT than group II spindle afferents, and some afferents show a greater response only at specific thrust durations [133].

It has been shown that SMT not only elicits paraspinal muscle reflexes, but also alters motoneuron excitability [48,134]. Electromyographic (EMG) reflex responses (50-100 ms) have been described to be evoked during high, but not during low loading rate SMT force applications and to change as a function of the SMT force-time characteristics (which will be detailed later in this chapter) [28,32,48,56,57,135]. Additionally, SMT has also been reported to produce temporary but significant inhibition of motoneuron activity [134,136]. By evoking afferent discharges from free

nerve endings and mechanoreceptors in the annulus fibrosus, facet joint capsules and ligaments of the spine, SMT potentially suppresses motoneurons excitability via afferent synapses with inhibitory interneurons [134,136–138].

## 2.5 Spinal manipulative therapy input parameters and specific responses

Spinal manipulative therapy input parameters, such as preload and peak forces, thrust duration, loading rate and application site (Figure 2.1), have been described as important characteristics of SMT as they influence both neurophysiological and biomechanical responses elicited by SMT [28,32,56,57,133,139,140]. Table 2.1 summarizes the SMT input parameters previously described in the literature.

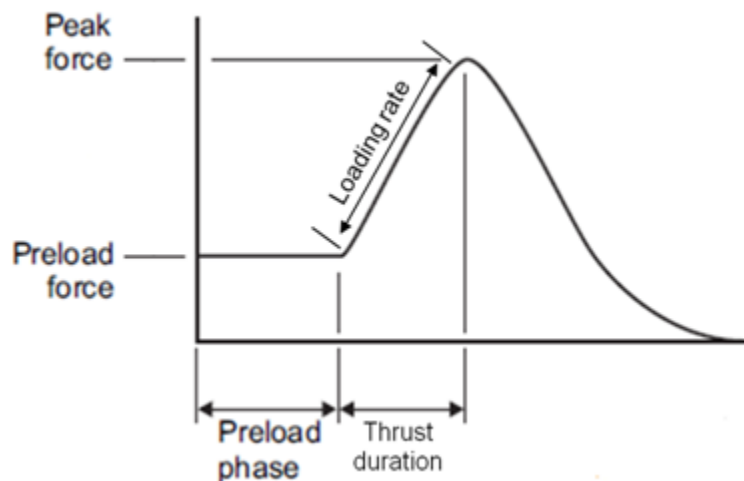


Figure 2.1 Spinal manipulative therapy input parameters. [Source: Adapted from Herzog, 2010.]

**Table 2.1 Spinal manipulative therapy input parameters described in the literature**

Spine region	Year	Author	Patient position, method of SMT application	Method of measurement	Note	Mean preload force (N)	Mean peak force (N)	Mean time to peak (ms)	Mean loading rate (N/s)	Comment
Thoracic and Lumbopelvic	1993	Herzog et al.	Prone, T4 TVP and posterior superior iliac spine	Pressure pad	T4 Sacroiliac joint	139 88	399 328	150		
Lumbopelvic	1997	Triano & Schultz	Side posture, manual SMT	Table-mounted load cell	L5 mammillary push L5 long lever Sacroiliac push		495 384.7 515.5		2176.6 1806.7 2483.4	
Thoracic	1999	Kirstukas & Backman	Prone	Pressure pad and table-mounted load cell		310	1044	96	15592	
Thoracic spine	2001	Herzog et al.	Prone, T3 and T10 TVP	Pressure pad		23.8	238.2	160	1368	
Thoracic and lumbopelvic	2003	Van Zoest et al.	T4 and T8 in prone position; sacroiliac in side posture	Handheld sensor	T4 T8 Sacroiliac	227 226 83	561 518 241	123 140 166		
Thoracic	2004	Forand et al.	Prone, T4 and T9 TVP	Pressure pad	Male Female	137 138	462 482	120 132	2.6 (N/ms) 2.7 (N/ms)	
Lumbopelvic	2004	Triano et al.	Side posture, L4 mammillary push	Table-mounted load cell	Inexperienced students Experienced students Experts		210.2 321.4 488.3	0.49(s) 0.41(s) 0.32(s)	840.7 2223.1 3812.6	

Thoracic	2005	Descarreaux et al.	Prone, pure posterior to anterior thrust	Instrumented manikin and force plate under therapist	2nd and 4th year students	36.3	569.5	166	3589	
						67.2	569.4	139	4217	
					5th year students and chiropractors					
Thoracic	2006	Descarreaux et al.	Prone, pure posterior to anterior thrust	Instrumented manikin and force plate under therapist	Pre-feedback training	66.1	630.9	155		
					Post-feedback training	176.7	538.4	147		
					Standard training	90.9	603.4	203		
Thoracic	2010	Descarreaux et al.	Prone, pure posterior to anterior thrust	Instrumented manikin and force plate under therapist	1st year	88	404.4	266	2557	Longitudinal study: data collected from the same students over 5 years.
					2nd year	32.8	460.2	168	3176	
					3rd year	124.1	508.8	134	4164	
					4th year	131.1	497.9	119	4271	
					5th year	116.1	450.0	122	3859	
Thoracic and lumbar	2014	Gudavalli	Side posture for lumbar spine SMT	Force transducer	Thoracic	98.69	369.67	215.83	2512.54	
					Lumbar	101.57	336.08	281.14	1742.97	
SMT=spinal manipulative therapy; TVP=transverse process										

### ***2.5.1 Preload force***

The preload phase precedes the SMT thrust phase and is characterized by a progressive loading of spinal tissues where the targeted spinal segment is positioned near the end of its physiological range of motion [21]. The relation between preload and the corresponding peak force magnitudes has been previously described [20]. This relation suggests that the preload forces may influence on the peak force magnitudes applied during the impulsive thrust application of SMT [20]. Recent studies have been investigating the particular effects of the preload force [57,141]. Specifically, Nougrou and colleagues [57] showed an increase in sagittal vertebral displacement during preload phase as a consequence of increased preload forces. Neurophysiologically, smaller preload force magnitudes produced larger increases in paraspinal muscle spindle discharge during SMT thrust application [141]. Additionally, increases in paraspinal electromyographic muscle activity was also observed during the preload phase with increased preload forces [57].

### ***2.5.2 Peak force magnitude***

Peak force magnitudes applied during SMT have been investigated and reported to greatly vary depending on the spinal level SMT is being applied to [20,21]. Peak force magnitudes applied to the cervical region were observed to be substantially reduced when compared to the forces applied to the thoracic and sacroiliac regions [20]. The effects of using different peak force magnitudes on biomechanical and neurophysiological outcomes has also been investigated. Vertebral displacements and acceleration have been demonstrated to increase as SMT applied forces increases [32,33,125]. Vaillant et al. [29] have shown that the interaction between SMT's force magnitude and force duration changes spinal stiffness of anesthetized cats. Additionally, SMT force magnitude has been demonstrated to affect electromyographic responses in both sheep and

humans [28,32]. Neurophysiologically, although it has been shown that SMT thrust displacement amplitude has an effect on lumbar muscle spindle neural responsiveness [30,31], the same was not as clearly produced when changing SMT force magnitudes [31].

### ***2.5.3 Method of application***

Due to the great variability of clinical SMT forces, mechanical force manually assisted (MFMA) instruments were developed and are being used in both research and clinical practice [37,38]. These instruments deliver an impulsive force that has a relatively large magnitude and act for a very short period of time [33]. The impulsive forces cause a sudden alteration in velocity producing oscillation and vibration on the spine [32]. Mechanical force manually assisted instruments usually have a contact tip of about 127 mm<sup>2</sup>, and the applied force vector coincides with the axis of the instrument. Therefore, the point of force application and the direction vector of the force can be defined and controlled [142]. In the past, these instruments were criticized for delivering low peak force. However, a previous study has described that if the force magnitudes of clinical SMTs are normalized to a similar contact area of these instruments, the peak force magnitudes are very similar between clinical SMT and mechanical force manually assisted instruments [142]. Kawchuk and colleagues have demonstrated that the use of MFMA instruments generally reduces SMT force variability. However, since MFMA instruments are handled by clinicians and researchers, the variability between operators and trials remains significant [36]. Although the peak force magnitudes are similar between clinical and instrument-delivered SMT, it has been described that some responses, such as vertebral movements and spinal reflex activities, are substantially different between methods of SMT application [126,143].



Given the great force variability between operators and trials applying SMT with or without MFMA instruments, an innovative servo-controlled linear actuator motor has been developed to provide standardized SMT applications [39]. This recently developed device has also been described to deliver repeatable, controlled and safe SMT forces with optimized precision (average differences in applied peak force= $\leq 3$ N; correlation coefficient=0.98). It simulates SMT applications with specified parameters and force-time profiles and is being used in studies investigating the SMT dose-physiological response relation in humans [28,56,57].

#### ***2.5.4 Thrust duration***

Also referred as time to peak, thrust duration refers to the time from the end of the preload phase to the peak force. Thrust duration has been described to vary from 30 to 300 ms with an average of 160 ms when SMT is performed in humans [20,142]. Studies have been investigating thrust duration effects on both biomechanical and neurophysiological SMT responses. Biomechanically, Colloca and colleagues [32] have described shorter SMT thrust duration (10 ms) to produce greater adjacent segment vertebral motions in comparison to longer thrust durations (100 and 200 ms). A recent study, on the other hand, investigated thrust durations between 125 and 275 ms and observed similar vertebral displacements across them [56]. Neurophysiological responses to different thrust durations have also been investigated. Sung and colleagues [140] observed significant changes in neural discharge of low threshold muscle mechanoreceptors as the duration of the SMT thrust approached the one used in clinical settings. Similarly, thrust duration has also been described to have a significant effect on increasing muscle spindle activity during SMT application [30,31,133,139]. On the other hand, according to Reed and colleagues [34], SMT thrust duration has no effect on nociceptive specific lateral thalamic mechanical trunk responses.

Changes in electromyographic responses have also been demonstrated when SMT with different thrust durations were applied [32,56].

#### ***2.5.5 Loading rate***

Loading rate describes the changes in SMT loading as a function of the time the thrust is being applied. Loading rates during the application of a SMT thrust have been described to range from 400 N/s to 3000 N/s [104,122,144]. As an effect of varying the loading rates during SMT thrust application, lumbar spinal stiffness has been described to increase with increasing loading rate [104,145]. High loading rates have also shown to produce unique strain patterns in facet joint capsule, which could affect responses from mechanoreceptors localized at the facet joint capsule [145]. Additionally, the investigation conducted by Reed and colleagues [31] found an increase in muscle spindle discharge as loading rate also increased.

#### ***2.5.6 Application site***

The application of SMT at different levels of the spine has been investigated. Generally, it has been described that SMT thrusts displace not only the target vertebra, but also adjacent segments of the spine [46,47]. Significant changes in axial displacements of L1 or L3 vertebrae when SMT was delivered at L5/S1 facet joint using different SMT force magnitudes have been observed [47]. Displacements of remote regions are potential contributors to the biomechanical and neurophysiological responses evoked both locally and remotely from the SMT application site [32,48,49]. Specifically, the study of Herzog et al. [48] has shown EMG reflex responses of muscles away from the SMT application site. Similarly, Colloca & Keller [49] elicited different EMG responses of erector spinae muscles at L3 and L5 levels when SMT was applied at the

thoracic and lumbar spinous or transverse processes. Spinal stiffness has also been reported to decrease when SMT is applied at specific spinal locations in a feline model [45]. By also using a feline model, Reed and colleagues [44] observed that SMT application site significantly affect muscle spindles' sensory input magnitude.

## **2.6 Animal Models**

The investigation of specific spinal structures (e.g. ligaments, facet joints, intervertebral disc) in living humans can be very challenging to conduct not only due to the difficult access to these structures, but also due to ethical issues. For that reason, *in vitro* experiments using human cadaveric specimens have been conducted to investigate the biomechanical behavior of normal and pathological human spinal structures as well as the spinal responses to mechanical LBP interventions, such as SMT [143,146–148]. However, not only the availability of human cadaveric specimen is very limited but also the large variation in geometry and biomechanical properties of specimens due to differences in age, sex, bone mineral density, pathological conditions, degenerative changes, shape and size of vertebral body and intervertebral disc motivated researchers to look for alternative specimens [146,149,150]. Due to these difficulties, several animals have been used as alternative specimens for *in vitro* spinal research [24,132,151–155]. Advantageously, animal specimens are more easily available and have more uniform geometrical and biomechanical properties [146,149,150]. From a clinical point of view, their similarity with human spines from the anatomical and biomechanical aspects has been described [146,149,150].

Anatomically, differences between human and bovine vertebral body parameters (width, length, height, and area) were found at all three levels (cervical, thoracic and lumbar) with no obvious

pattern [156]. Despite of these differences, bovine spines can be an alternative to human thoracic and lumbar specimens if the differences, such as growth speed, vertebral body size and growth plates, are taken into consideration [146]. Sheep and human vertebrae are most similar at the thoracic and lumbar regions, although they show substantial differences in certain dimensions, such as vertebral body height, width and pedicle width [146,157]. Sheep spine has been described larger than the human, particularly in vertebral body height, but despite these differences, sheep spine may be useful model for experiments related to the gross structure of the thoracic or lumbar spine [146]. A comparison between deer and human spines revealed many similarities in the lower thoracic and upper lumbar spine, yet they show substantial differences in certain dimensions, such as endplate surface area and pedicular geometry [158]. Porcine specimens have been described to present several anatomical similarities, such as vertebral body height, end-plates, spinal canal shape, and pedicle sizes [159]. Nevertheless, specimen age will greatly influence on anatomical similarities as older pigs will present smaller end plate area, larger pedicles, taller vertebral bodies, narrower spinal canals and smaller spinous process lengths compared to humans [160]. Despite of those differences, porcine segments between T6 and T10 and the lumbar spine are a suitable alternative to human specimens [146].

Biomechanically, range of motion, neutral zone and neutral zone stiffness of thoracic and lumbar spines of calf and humans have been compared and was found to be substitutes for humans when range of motion is the parameter of interest [161]. Biomechanical similarities between sheep and human spines have also been found, and sheep spine might be a useful model for disc surgery, bone healing processes and evaluation of spinal implants [157]. A comparison between deer and human spine showed that the lower thoracic/upper lumbar region of the deer spine can be used as a

model for some human biomechanical experiments due to its biomechanical and material similarities to the human spine of the corresponding region [146,158,162]. The porcine and human spinal segments have been described to have quantitatively similar values for range of motion [95]. Neutral zone was found to be larger in porcine specimens when compared to humans, but not significant in all regions and effects of creep and recovery observed in porcine specimens have been shown to be representative of the human spine [93]. Therefore, the porcine spine has been considered to be a good biomechanical model for the human spine, specially the lower thoracic and lumbar regions [93,95].

### ***2.6.1 Specific differences between porcine and human lumbar spines***

#### ***2.6.1.1 Anatomical differences***

Although porcine lumbar spines have been described as suitable models for the human lumbar spine, important anatomical differences have been described and are summarized in Table 2.2 [146,150,159,160].

**Table 2.2 Anatomical characteristics of porcine and human lumbar spines**

Spinal characteristic	Porcine spine	Human spine	Notes
Vertebral body height	<ul style="list-style-type: none"> <li>• Increase from L1 to L5</li> <li>• ~ 36.3mm</li> </ul>	<ul style="list-style-type: none"> <li>• Constant from L1 to L5</li> <li>• ~ 23.8mm</li> </ul>	Overall, porcine vertebrae were taller and narrower in comparison to human vertebrae that were shorter and broader
Vertebral body width	<ul style="list-style-type: none"> <li>• Increase from L1 to L5</li> <li>• ~ 36.51mm</li> </ul>	<ul style="list-style-type: none"> <li>• Increase from L1 to L5</li> <li>• ~ 45.5mm</li> </ul>	
Upper end plate width	<ul style="list-style-type: none"> <li>• Increase from L1 to L5</li> <li>• ~ 36.35mm</li> </ul>	<ul style="list-style-type: none"> <li>• Increase from L1 to L5</li> <li>• ~ 45.35mm</li> </ul>	
Upper end plate depth	<ul style="list-style-type: none"> <li>• Constant from L1 to L5</li> <li>• ~ 24.35mm</li> </ul>	<ul style="list-style-type: none"> <li>• Constant from L1 to L5</li> <li>• ~ 35.35mm</li> </ul>	
Lower end plate width	<ul style="list-style-type: none"> <li>• Increase from L1 to L5</li> <li>• ~ 39.1mm</li> </ul>	<ul style="list-style-type: none"> <li>• Increase from L1 to L5</li> <li>• ~ 48.75mm</li> </ul>	
Lower end plate depth	<ul style="list-style-type: none"> <li>• Decrease from L1 to L5</li> <li>• ~ 22.9mm</li> </ul>	<ul style="list-style-type: none"> <li>• Decrease from L1 to L5</li> <li>• ~ 34.35mm</li> </ul>	
Pedicle width	<ul style="list-style-type: none"> <li>• Constant from L1 to L5</li> <li>• ~ 11.8mm</li> </ul>	<ul style="list-style-type: none"> <li>• Increase from L1 to L5</li> <li>• ~ 11.8mm</li> </ul>	Cross section was pear shaped on porcine pedicles whereas oval shaped in human pedicles
Pedicle height	<ul style="list-style-type: none"> <li>• Increase from L1 to L4</li> <li>• ~ 22.15mm</li> </ul>	<ul style="list-style-type: none"> <li>• Decrease from L1 to L4</li> <li>• ~ 14.95mm</li> </ul>	
Pedicle angle	<ul style="list-style-type: none"> <li>• Increase from L1 to L6</li> <li>• ~ 27deg</li> </ul>	<ul style="list-style-type: none"> <li>• Increase from L3 to L5</li> <li>• ~ 10deg</li> </ul>	
Spinal canal width	<ul style="list-style-type: none"> <li>• Increase from L1 to L6</li> <li>• ~ 17.91mm</li> </ul>	<ul style="list-style-type: none"> <li>• Increase from L1 to L5</li> <li>• ~ 24.76mm</li> </ul>	Spinal canal is wider than it is deep for both porcine and human
Spinal canal length	<ul style="list-style-type: none"> <li>• Constant from L1 to L6</li> <li>• ~ 11.6mm</li> </ul>	<ul style="list-style-type: none"> <li>• Constant from L1 to L5</li> <li>• ~ 18.1mm</li> </ul>	
Intervertebral disc height	<ul style="list-style-type: none"> <li>• Constant from L1 to L4</li> <li>• ~ 2.8mm</li> </ul>	<ul style="list-style-type: none"> <li>• Increase from L1 to L4</li> <li>• ~ 12.25mm</li> </ul>	
Transverse process length	<ul style="list-style-type: none"> <li>• Decrease from L2 to L6</li> <li>• ~ 75mm</li> </ul>	<ul style="list-style-type: none"> <li>• Increase from L1 to L5</li> <li>• ~ 90mm</li> </ul>	
Spinous process length	<ul style="list-style-type: none"> <li>• Decrease from L1 to L6</li> <li>• ~ 13mm</li> </ul>	<ul style="list-style-type: none"> <li>• Decrease from L3 to L5</li> <li>• ~ 30mm</li> </ul>	
Spinous process angle	<ul style="list-style-type: none"> <li>• Constant from L1 to L6</li> <li>• ~ 8deg</li> </ul>	<ul style="list-style-type: none"> <li>• Increase from L1 to L4</li> <li>• ~ 10deg</li> </ul>	
Interfacet distance	•	•	No data shown, but porcine and human spines presented similar dimension between facet joints.
Facet surface contour	• Radius: ~ 19.6mm	• Radius: ~ 20mm	

### 2.6.1.2 Biomechanical differences

In addition to anatomical differences, biomechanical particularities in both porcine and human lumbar spines have been previously described. Table 2.3 compiles and summarizes the specific biomechanical differences between porcine and human lumbar spines [93,95].

**Table 2.3 Biomechanical characteristics of porcine and human lumbar spines**

Biomechanical characteristic		Porcine spine	Human spine	Notes
Flexion/Extension	Range of motion	• ~10 deg • ~ 8.8 deg	• ~ 3.6 deg • ~ 14.9 deg	± 2Nm test ±7.5Nm test
	Neutral zone	• ~ 4.1 deg • ~ 1.58 deg	• ~ 2.1 deg	± 2Nm test ±7.5Nm test
	Neutral zone stiffness	• ~ 0.05Nm/deg • ~ 0.84Nm/deg	• ~ 0.64Nm/deg	± 2Nm test ±7.5Nm test
Lateral bending	Range of motion	• ~ 7.6 deg • ~ 11.2 deg	• ~ 4.5 deg • ~ 11.5 deg	± 2Nm test ±7.5Nm test
	Neutral zone	• ~ 3.2 deg • ~ 1.74 deg	• ~ 2.0 deg	± 2Nm test ±7.5Nm test
	Neutral zone stiffness	• ~ 0.05Nm/deg • ~ 0.18Nm/deg	• ~ 0.55Nm/deg	± 2Nm test ±7.5Nm test
Axial rotation	Range of motion	• ~ 2.9 deg • ~ 3 deg	• ~ 1.6 deg • ~ 5 deg	± 2Nm test ±7.5Nm test
	Neutral zone	• ~ 1.0 deg • ~ 0.3 deg	• ~ 0.9 deg	± 2Nm test ±7.5Nm test
	Neutral zone stiffness	• ~ 0.36Nm/deg • ~ 4.04Nm/deg	• ~ 2.63Nm/deg	± 2Nm test ±7.5Nm test

Nevertheless, despite of the abovedescribed anatomical and biomechanical differences between porcine and human spines, porcine spines have been demonstrated to be suitable models to investigate lumbar human spines [69,93,95,159].

## 2.7 Robotic Biomechanical Testing

The accurate determination and understanding of the *in situ* forces developed in a ligament as a response to motion or external loads of intact joints is fundamental in determining the ligament's function and contribution to the overall joint kinematics [163,164]. Previous studies developed a

new methodology using robotics technology to investigate joint biomechanics by controlling the position or the forces applied to the joint [165]. By associating the robotics technology with a universal force-moment sensor, it was possible to determine the *in situ* forces magnitude, direction, and point of application in the anterior cruciate ligament in intact knees of human cadavers [163,164,166].

The description of the load-displacement characteristics of specific spinal structures is fundamental to understanding structural biomechanical behavior and spinal function [167,168]. Biomechanical testing of cadaveric spines has been described as the greatest method to investigate the mechanical function and failure of spinal structures [168]. Consequently, several apparatus have been developed for *in vitro* biomechanical testing of spine segments by adapting servo-hydraulic dynamic testing machines or applying systems of cables and pulleys [147,169–171]. The servo-hydraulic dynamic testing machine has been widely used in the application of shear loads [147,169,172–174]. Although a system of cables and pulleys has been used to apply coupled moments in spinal segments [171,175], this approach is usually applied to investigate how joint loading is altered when one structure has been injured (or removed). Nevertheless, this system has limited results as the resulting joint movements may change with each tissue removal as the joint moves along the path of least resistance [170]. Consequently, stable six-degree-of-freedom hexapod or parallel linkage robots have also been developed and widely used to reproduce identical *in vitro* motion profiles of the spine [24,176–178]. These robots have six degrees of freedom and are considered highly stable robots capable of repeatedly applying identical 3-dimensional kinematic to the specimen, regardless of any alteration within the specimen [24,178].



In addition to testing apparatus, spinal *in vitro* biomechanical testing requires definition of control methods to conduct the application of loads and/or displacements to the spinal segment being tested. Force-controlled, displacement-controlled and hybrid controlled methods have been described and discussed in previous studies [179,180]. Specifically, the force-controlled method applies a pure controlled force or moment to the specimen and the consequent unconstrained displacements are measured [179]. This method has been described to be less appropriate in regions with low stiffness, such as the neutral zone, since small changes in the applied force can produce large changes in displacement [167,180]. On the other hand, the displacement-controlled method moves the specimen to a defined displacement and the resulting complex loads along the spine segment are measured and recorded [179]. It has been reported that the displacement-controlled method is less appropriate in regions with high stiffness, such as the elastic zone, since small changes in the applied displacement can generate large changes in load [167,180]. Alternatively, the hybrid controlled method integrates aspects of both force-controlled and displacement-controlled methods to obtain a new, hybrid method that is better suited for specific applications, such as displacement-controlled testing with the addition of achieving a specific load [167]. While hybrid control method is being studied and refined with recent findings describing its ability to actively control secondary displacements and off-axis forces while applying pure moments [181], it does not ensure a smooth and even movement throughout the testing, with further improvements being necessary [180]. Recently, a robotic Cartesian force controlled biomechanical testing system with 6 degrees-of-freedom real-time cascaded load control capability has been introduced and validated to biomechanical testing [182]. This system has been developed to apply real-time dynamic force vectors through the physiological range of movement, but tracking errors during direction reversal have been observed [183].

Constrained or unconstrained testing method should also be defined for spinal segments biomechanical testing. The constrained testing method restricts the movement of the spine segment to one specific direction. In this method, the center of rotation is also fixed and is not allowed to move [184,185]. While constrained testing can easily apply required loads or displacements with several testing apparatus, it has been described to limit coupled motion which are not representative of *in vivo* spinal movements [185]. On the other hand, the unconstrained testing method leaves the spine segment free to move in all six degrees of freedom. When a load is applied using this method, the center of rotation can change depending on the load magnitude and specimen condition, allowing the movement around its own axis of rotation [184,185]. This method is usually performed by using system of cables and pulleys, but unconstrained method for robotic biomechanical tests has also been developed and described [186]. Unconstrained testing methods enabled the description of coupled motions in the lumbar spine that are also known to occur *in vivo*. Nevertheless, *in vivo* loads are much more complex than those applied in the laboratory environment and the complete three-dimensional motion analysis of unconstrained testing involve more technical expertise [184,185].

Creep and stress relaxation are phenomena related to biological tissues' time-dependant, non-linear properties. While creep is characterized by the structural units deformation in response to a constant applied load [187], stress relaxation characterizes the temporal stress behavior of the tissue in response to an applied strain [188]. Although related, the microstructural mechanism of biological tissues experiencing creep has been described to be different from those observed during stress relaxation [188,189]. Specifically, spinal ligaments have been described to have different

morphology and function, which result in unique time-dependent, non-linear behavior [190]. However, both phenomena are biomechanically important due to their influence on the kinetics and kinematics of the spine [191]. For example, increase in overall spinal flexibility after 30 minutes of loading has been observed [192] and, similarly, Little and Khalsa (2005) [193] observed increase in intervertebral motion as a result of sustained and repetitive lumbar flexion.

## **2.8 Robotic Biomechanical Testing of the Lumbar Spine**

The identification of spinal tissues mechanical behavior is fundamental for understanding normal spinal function and identifying spinal tissues dysfunction and injury [72]. The study of specific motion segments behavior is fundamental for biomechanical characterization of the spine, including the analyses of spinal loading [194] and spinal stability [147,195]. Specifically, *in vitro* investigations have been widely conducted aiming to characterize spinal tissues mechanical behavior during physiologic movements and the application of external loads [24,169,170,174,178].

The supraspinous/interspinous ligament complex has been described to be great contributor in resisting moments created by flexion movements in the porcine lumbar spine [178]. Additionally, while the posterior elements have been identified as efficient structures in resisting anterior and posterior shear loadings [174], greater shear strains have been observed to increase the intervertebral disc stiffness contributing to resisting shear loading [174] even when the facet joints are damaged [169]. Similarly when facet joints are removed from the spine, axial loads are transferred to the annulus fibrosus and longitudinal ligaments [147].

Biomechanical fatigue failure tests of lumbar spine segments have also been conducted. Repetitive shear loads have been demonstrated to induce failure of porcine spine segments, likely caused by fracture of the posterior elements [173]. The intervertebral disc has been described to be responsible for approximately 74% of the total loads caused by a posterior shear loading and that the predominant injuries resulting from this loading are avulsions of the end plate [172]. Similarly, fatigue properties of human trabecular vertebral body have also been investigated and age, sex and vertebral position were found to have a significant effect on vertebral body fatigue strength [196,197].

Lumbar spine segments have also been biomechanically investigated both *in vivo* and *in vitro*. While *in vivo* studies are conducted in living models, *in vitro* investigations use cadaveric models and the biomechanical tests are usually conducted in a controlled environment. *In vitro* testing limitations are usually related to the *ex vivo* differences, such as soft tissue stiffness changes and the difficulty in replicating *in vivo* loading characteristics and physiologic responses [198]. Results from previous studies revealed that *in vitro* applied loading modes do not simulate spinal movements as the simplified loads cannot realistically mimic the *in vivo* situation [52,199]. Indeed, although *in vitro* biomechanical testing does not take into consideration the muscular activities and neuromuscular controls [200,201], optimized loads can show the best agreement with averaged *in vivo* measured data and lead to a reasonable simulation of the spinal compression and intervertebral movements [52,199]. Therefore, *in vivo* studies are often based on the findings from *in vitro* biomechanical studies for data validation [200].

## **2.9 Robotic Biomechanical Testing and Spinal Manipulative Therapy**

As previously stated, SMT is a clinical intervention based on the application of a mechanical force to a specific segment of the spine [20]. As a result of the external mechanical force applied during SMT, several biomechanical and neurophysiological responses have been demonstrated and previously described [21,22,104,112]. Although previous studies have provided important information regarding SMT physiological effects, the kinematics of lumbar vertebrae during SMT is still under investigation. Therefore, studies focusing on the spinal tissues mechanical behavior and loading characteristics during the application of SMT are fundamental to elucidating and understanding of the underlying mechanisms of SMT [24,145,202]

While several studies have been conducted investigating SMT biomechanical characteristics, input parameters, and basic and clinical effects [21,47,104,120,122,203], only one study have combined SMT with robotic biomechanical testing [24]. In this study, the loads experienced by each spinal structure during the application of a general SMT were quantified. The loading characteristics during SMT were found to be non-uniform among spinal tissues with the intervertebral disc experiencing the greatest forces and moments [24].

## Chapter 3.

### Quantification of loading in biomechanical testing: the influence of dissection sequence\*

#### 3.1 Introduction

Unconstrained testing of joint segments is performed by fixing one end of an articulation and leaving the other end to move freely. Traditionally performed by servo-hydraulic machines or cables/pulleys systems to move the free end of the specimen [147,169–171], this approach has been used to investigate how joint loading is altered after one structure has been injured (or removed). Importantly, this technique is limited in that the resulting joint movements may change with each tissue transection as the joint moves along the path of least resistance [170]. Alternatively, robots with sufficient rigidity and six degrees-of-freedom can reproduce identical kinematics trajectories following tissue removal [24,178]. By combining this technique with serial dissection, loads experienced by each joint structure can be quantified [24,170,178].

However, combining robotics with serial dissection does not assure that the resulting tissue loads remain equal when the dissection sequence is changed. Although this is true for linear systems, the nature and material properties (nonlinearity, viscosity, porosity etc.) of biological structures may not result in similar loads when biomechanical tests are used with different sequences of dissection [191,204].

Given the above, this experiment was conducted to investigate structural response to mechanical loading created through robotic testing when different sequence of structural removal is used.

---

\* This chapter has been published at the *Journal of Biomechanics*: Funabashi M, El-Rich M, Prasad N, Kawchuk GN. 43  
Quantification of loading in biomechanical testing: the influence of dissection sequence. J Biomech 2015; 48(12): 3522-6.

## **3.2 Materials and Methods**

### ***3.2.1 Model design and fabrication***

A simple vertebral motion segment facsimile (model) was made from two rigid objects joined together by multiple, flexible connectors of different dimensions (Figure 3.1). To minimize variability between copies of the model, 3D printing was used to fabricate 6 replicates. Based on the dimensional data from Panjabi [205], the model consisted of two rigid blocks printed in VeroWhitePlus, a rigid material that simulated vertebral bodies. Joining these two rigid blocks were three connectors made of a rubber-like material. Connectors 1 and 2 (7.5 mm diameter, 36 mm height) were composed of A40-shore TangoBlackPlus while Connector 3 (elliptical shaped: 15.75 mm height, 22.5 mm width, 17.25 mm length) was composed of A50 shore TangoBlackPlus (Figure 3.1). The resulting combination of these materials created a motion segment presumed to have a time-dependent, nonlinear behavior.

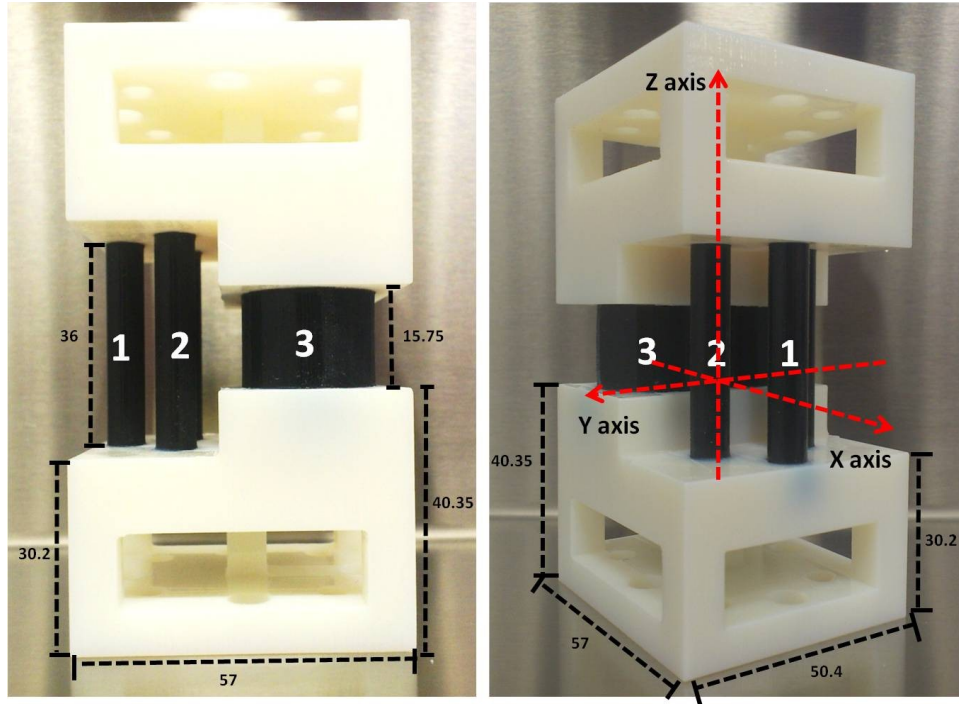


Figure 3.1 Multi-material 3D print model and Cartesian axes. Numbers indicate the connector. Measures are given in millimetres.

### 3.2.2 Model preparation and mounting

All six 3D print models were potted simultaneously with a standardized technique using dental stone (Modern Materials, South Bend, IN). A 6-axis load cell (AMTI MC3A-1000, Advanced Mechanical Technology, Inc., Watertown, MA) was used to record forces and moments generated in the models along and around each of the three Cartesian axes (x axis = anterior/posterior, y-axis = medial/lateral, z-axis = cranial/caudal) (Figure 3.1). The load cell was mounted rigidly to the platform of a parallel robot (Parallel Robotics Systems Corp., Hampton, NH) and zeroed.

The parallel robot is comprised of a rigid platform suspended by 6 rigid struts of fixed length. Each strut is attached to an electromechanical motor that travels about a circular track. Changes in the position and orientation of the robot platform are achieved by computer-controlled movement of



each motor around the track. The linear and angular resolution of the robot is approximately  $1\mu\text{m}$  and  $0.001^\circ$  respectively.

Both ends of the potted 3D model were rigidly fixed: the upper end bolted to a stationary cross-beam and the lower end bolted to the load cell mounted rigidly to the parallel robotic platform. The robot was then moved until the loads and moments on the model were minimized in all axes. This was considered the starting neutral position and from this position, spatial reference points were collected from the external surface of connector 3 with an optical tracking system (NDI, Waterloo, Canada) and customized software (LabVIEW, National Instruments, Austin, TX). From these data, a static center of rotation (COR) was calculated for subsequent testing as  $\frac{1}{3}$  the length of connector 3 from the posterior wall.

### ***3.2.3 Testing protocol***

Pilot testing was conducted to verify the maximum angular displacement of the 3D print models. Based on the properties of the materials used, the maximum angular displacement was considered the angular displacement that created relative peak moments of  $\pm 2\text{ Nm}$  and was found to be  $\pm 7^\circ$  about y-axis,  $\pm 6^\circ$  about the x-axis, and  $\pm 5^\circ$  for torsion (rotation around z-axis). Starting from the neutral position, 3 cycles of pure rotation were applied about each axis around the same COR. In each cycle, rotations were applied first in the positive direction, returning to neutral position, followed by rotation in the negative direction. After each rotation, the model was allowed to recover for a defined period of time to allow internal forces of the materials to minimize (7 minutes for rotation about y-axis, and 5 minutes for rotation about both x- and z-axes as determined from pilot testing). The return of forces and moments to baseline was assured before the following test commenced. All angular

displacements were applied at a rate of 1°/sec and all testing was performed in a room at 23°C with data sampling at 1 kHz.

### 3.2.3.1 Sequential connector removal

Following baseline testing, the three connectors were removed using predetermined sequences (Table 3.1). After the removal of each connector, the same kinematic trajectory was performed with standardized recovery time between trials.

<b>Table 3.1 Sequence of connector removal for each 3D print model</b>			
	<b>Cut 1</b>	<b>Cut 2</b>	<b>Cut 3</b>
<b>Model A</b>	Connector1	Connector2	Connector3
<b>Model B</b>	Connector1	Connector3	Connector2
<b>Model C</b>	Connector2	Connector1	Connector3
<b>Model D</b>	Connector2	Connector3	Connector1
<b>Model E</b>	Connector3	Connector1	Connector2
<b>Model F</b>	Connector3	Connector2	Connector1

### 3.2.4 Statistical Analysis

For each 3D print model, the resulting moments were plotted against time for the intact condition and following the removal of each connector. The relative mean and peak moments experienced by each connector were identified, calculated, and considered to be the primary outcome. Relative mean and peak moments were calculated as the difference between the mean and peak moments and the moments in the previous condition. The relative area between curves of the moment-rotation graph (Figure 3.2), was also calculated and analyzed. The measurements of the 3 trials were averaged and considered as dependent variables.

Descriptive statistics were reported for moments around each specific axis. As measurements were taken after the removal of each connector, the dependent variables were correlated. A linear mixed model analysis was performed using IBM SPSS Statistics version 22 with 3 fixed factors: connector, movement, and sequence of connector removal. For all statistical tests, a level of significance  $p=0.05$  was considered.

### **3.3 Results**

The variance between three repeated trials was found to be negligible (analysis of variance  $p=0.805$ ), therefore the average of the 3 trials was used. Figure 3.2 illustrates moment-rotation curves observed about the y-axis. From these average curves, the interaction between the 3 fixed factors (connector, movement, and sequence of removal) was shown to be significant and was therefore retained in the analysis. The linear mixed models analysis revealed a significant difference in the moments borne by each connector when removed in different sequences ( $p<0.001$ ) for all dependent variables. Linear mixed model tables are shown in Appendix I. The relative area between curves of the moment-displacement graph of each connector during all movements tested are displayed in Table 3.2.

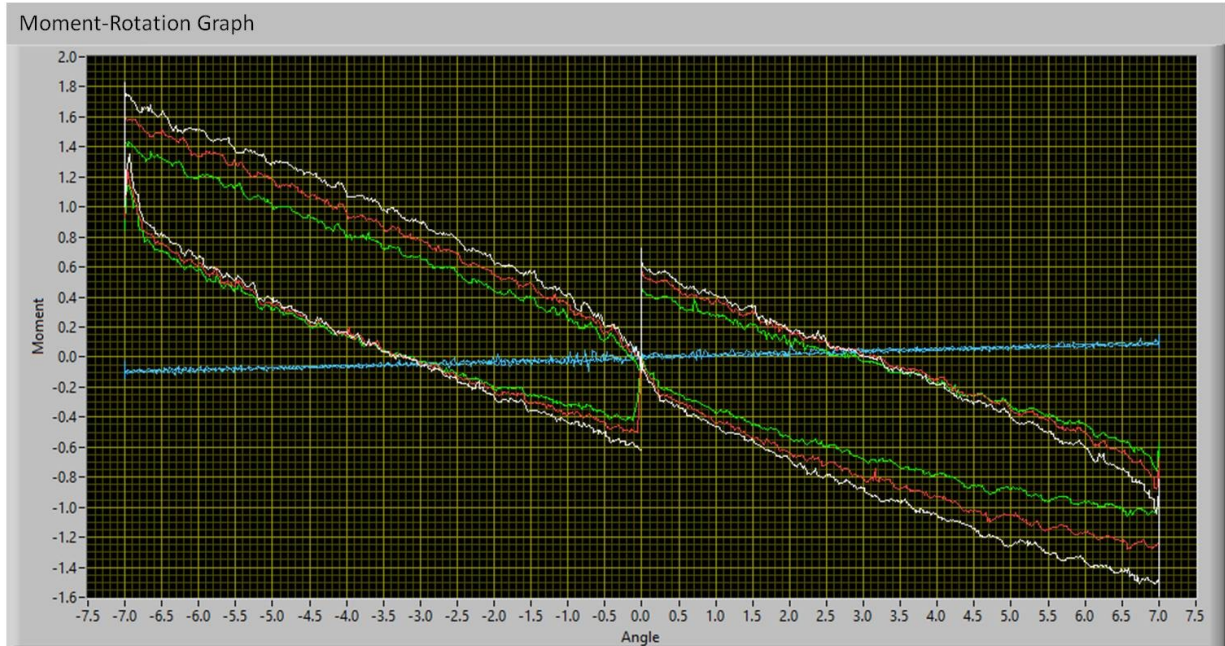


Figure 3.2 Moment-rotation graph during positive and negative rotation around y-axis. White line represents the moments observed when the model was intact. The red line corresponds to the moments after connector 1 was removed, green line after connector 2 was also removed and blue line after all connectors (1, 2 and 3) were removed. For positive rotation, bottom line corresponds to loading curve and upper line to unloading curve. For negative rotation, upper line corresponds to loading curve and bottom line to unloading curve.

**Table 3.2 Area between curves of moment-displacement graph (Nm-deg) of each connector during rotations about all three axes.**

Connector	Positive rotation			Negative rotation			Positive Rotation			Negative rotation			Positive rotation			Negative Rotation		
	y-axis			y-axis			x-axis			x-axis			z-axis			z-axis		
	1	2	3	1	2	3	1	2	3	1	2	3	1	2	3	1	2	3
<b>Specimen</b>																		
<b>A</b>	-3.46	-1.01	-0.50	-3.65	-0.82	-0.69	-5.11	-0.17	-0.27	-4.67	-0.03	-0.16	-0.88	-0.02	0.01	-0.86	-0.04	0.02
<b>B</b>	-4.94	-0.56	-0.70	-5.95	-0.36	-0.78	-4.39	-0.19	-0.01	-4.32	-0.21	-0.02	-0.98	-0.01	-0.03	-0.99	-0.00	-0.01
<b>C</b>	-4.35	-0.82	-0.68	-4.66	-0.53	-0.71	-4.22	-0.04	-0.54	-4.25	0.09	-0.64	-0.72	0.04	-0.14	-0.70	0.02	-0.13
<b>D</b>	-4.51	-0.69	-0.62	-5.26	-0.77	-0.49	-4.71	-0.47	-0.27	-4.31	-0.35	-0.17	-0.86	-0.04	-0.00	-0.83	-0.02	-0.00
<b>E</b>	-3.66	-0.52	-0.67	-3.87	-0.39	-0.57	-4.01	-0.16	-0.01	-4.00	-0.18	-0.00	-0.85	-0.00	-0.00	-0.82	-0.00	-0.00
<b>F</b>	-4.07	-0.58	-0.68	-3.75	-0.45	-0.57	-4.64	-0.19	-0.02	-3.76	-0.20	-0.00	-1.05	-0.00	-0.01	-1.05	-0.00	-0.01

Figure 3.3 shows the relative peak moments borne by each connector during positive rotation about y-axis. There was no statistically significant difference in moments when the same connector was removed first between models (i.e. moments borne by connector 1 between model A and B, connector 2 between models C and D, and connector 3 between models E and F - Mann-Whitney U;  $p>0.05$ ). Relative mean moments and area under the curve borne by each connector during positive rotation about y-axis are shown on Figures 3.4 and 3.5, respectively.

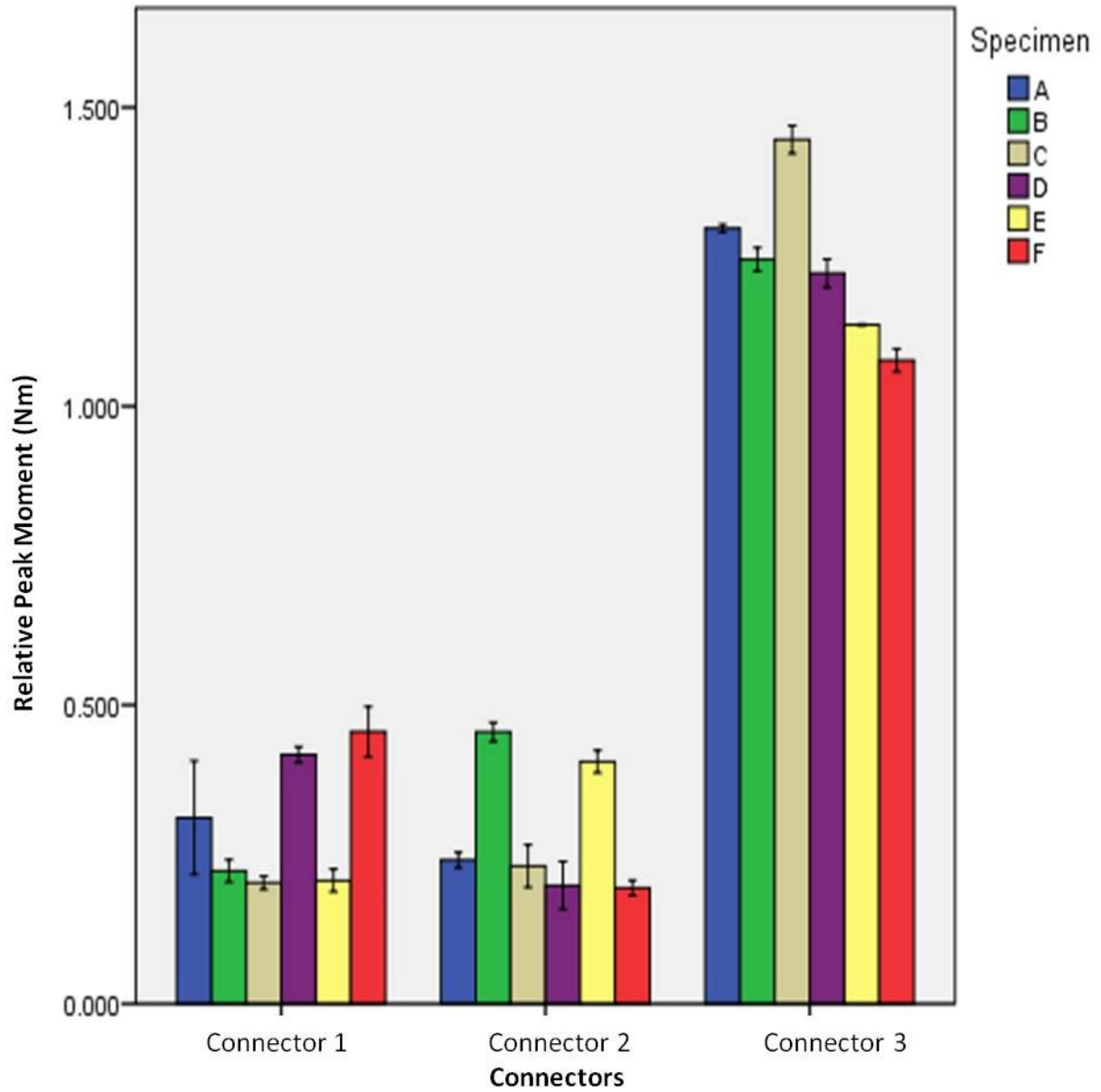


Figure 3.3 Bar chart showing the relative peak moments ( $\pm 2SE$ ) carried by each connector in different sequence of connector removal during positive rotation around y-axis.

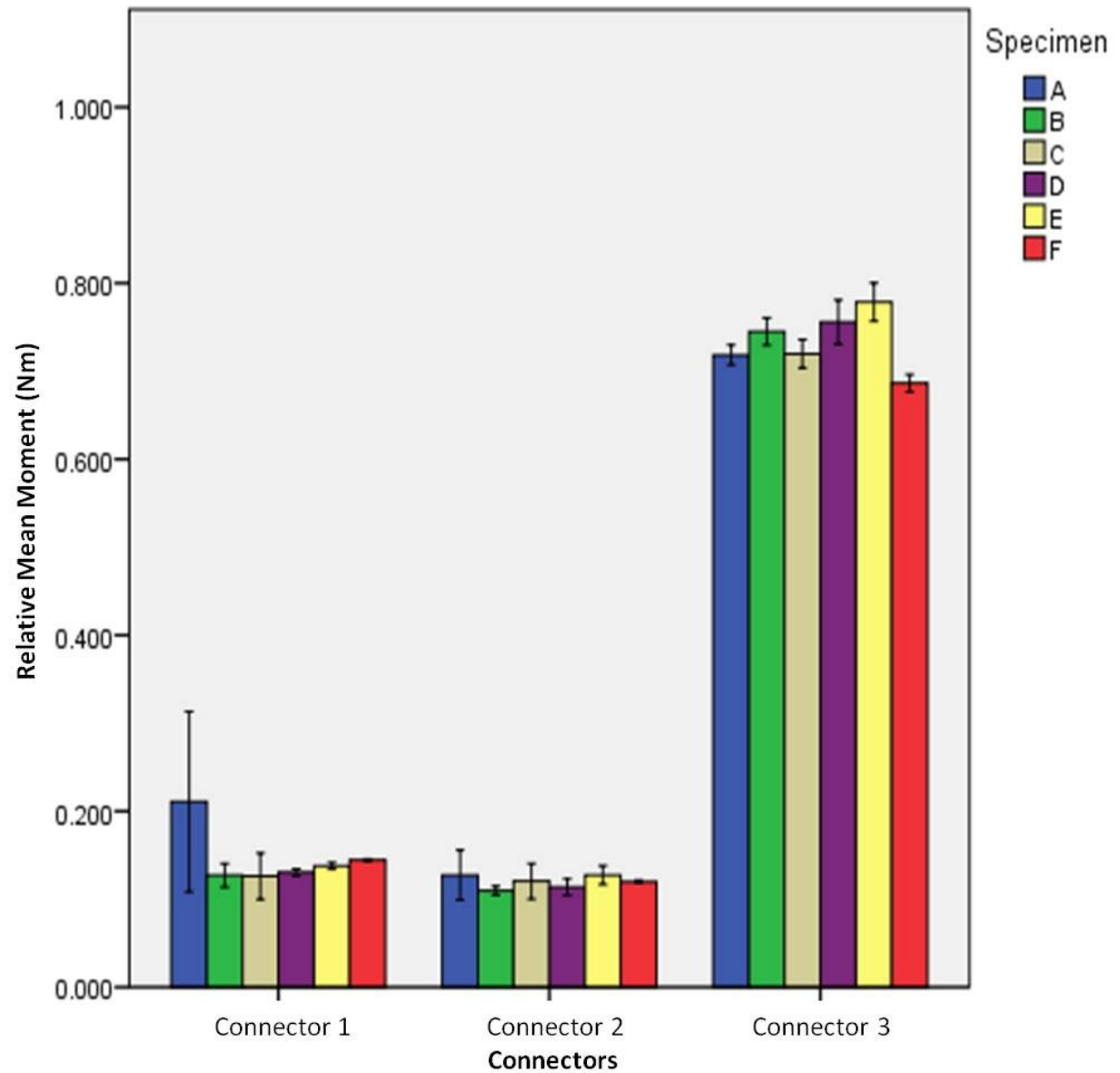


Figure 3.4 Bar chart showing the relative mean moments ( $\pm 2SE$ ) carried by each connector in different sequence of connector removal during positive rotation around y-axis.



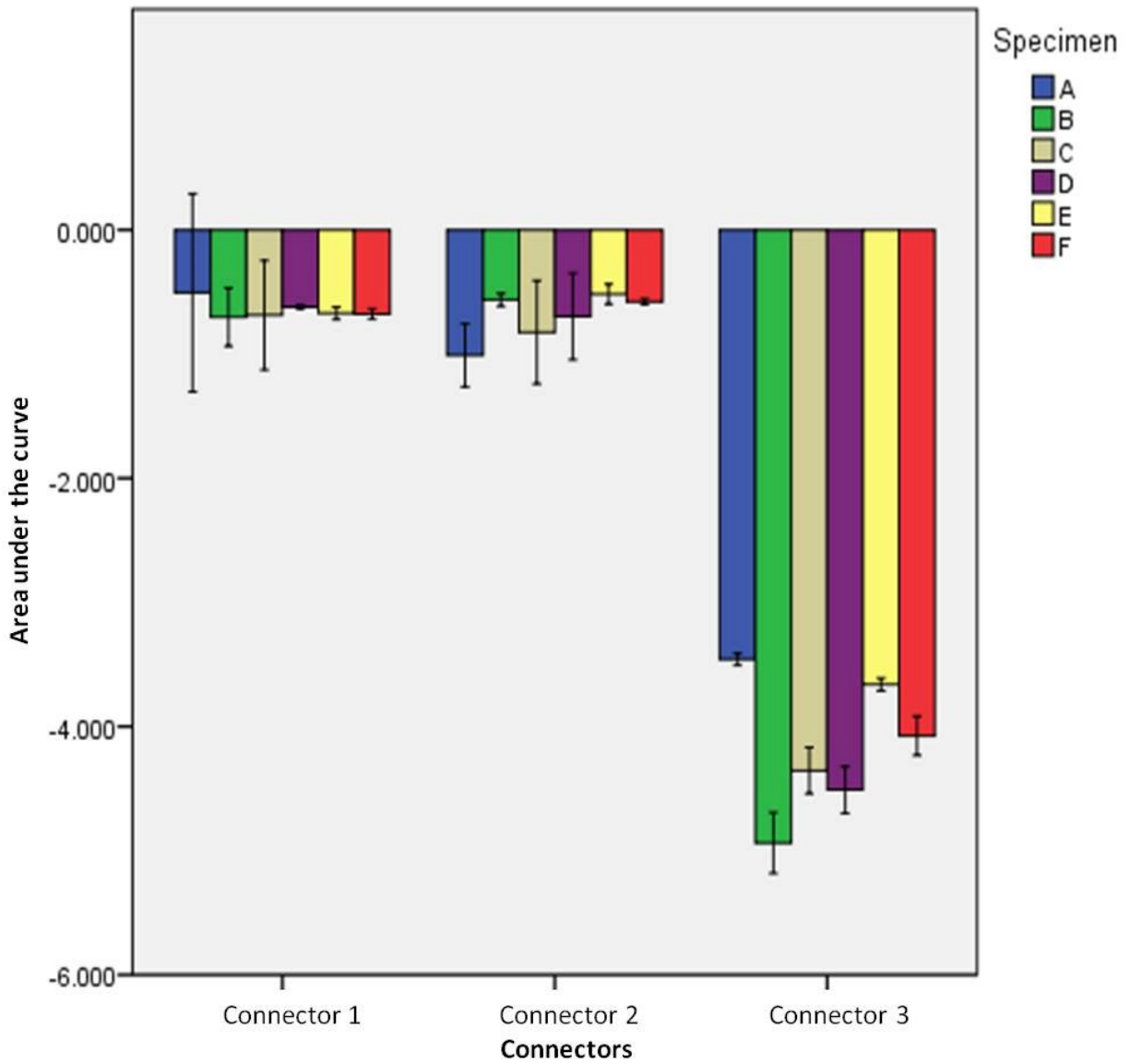


Figure 3.5 Bar chart showing the area under the curve ( $\pm 2SE$ ) of each connector in different sequence of connector removal during positive rotation around y-axis.

### **3.4 Discussion**

The results of this study demonstrate that structure loading created through robotic testing is dependent on connector removal order. Although several studies have assumed identical load sharing regardless of sequence of structure removal [24,178,206], our results illustrate that even when using fabricated replicates and standardized robotic testing protocols with kinematic replication, model loading is dependent on removal sequence. This suggests an interaction between connectors while carrying load: the removal of one structure influences the loads borne by the remaining structures.

The previous study of Lu and colleagues [174] support our findings. Their results showed that the sum of the loads experienced by the anterior and posterior columns during pure anterior and posterior shear were not equal to the load experienced by the intact specimen. They concluded that structures of the intervertebral joint act in cooperation and that the removal of one structure affects the mechanical function of the remaining structures [174].

Although our protocols were carefully developed and executed to minimize error, variability in our protocol may have occurred. These error sources however would be minimal as preliminary testing showed no statistically significant difference in the spatial orientation between the six 3D print models.

Although a standardized recovery time was defined during pilot testing and used during testing, our findings may be partly explained by insufficient recovery time even though loads were

confirmed to return to baseline before each rotation. This is unlikely for several reasons. First, rotation about the three axes were applied in the same order for all models before any connector was removed: rotation around y-axis was applied first, followed by rotation around the x- and then z-axes, so that no rotation in the same direction would be performed consecutively. Additionally, each connector was removed while the specimen was mounted in the specimen's position and loads. Finally, there was no significant difference between any of the repeat trials obtained for any given axis and any connector condition.

The current study used a parallel robotic platform to repeatedly apply identical kinematics to the 3D print models and measured the loads experienced by each connector. The study of Gillespie and Dickey [178] has also used a parallel robotic manipulator to replay identical kinematics of flexion and extension on porcine spines. By using a rotational potentiometer, they described small joint motion differences between trials, indicating deformation within the specimen [178]. In the current study however, given the known materials used to print the models, the deformation observed within the biological specimens is not likely to have occurred within our model.

This study used identical testing objects, followed standardized procedures and protocols, and performed stable robotic biomechanical testing with exact kinematics being repeated between tests. The connectors of the 3D print models used in this study were printed with rubber-like materials which were observed in our study to have nonlinear viscoelastic material behavior [207,208] (Figure 3.2). As a result, model loading was influenced by the order in which connectors were removed.

### **3.4.1 Limitations**

In our model, we used a rubber-like material which was observed to have nonlinear viscoelastic behavior as do biological tissues (Figure 3.2). However, the response of biological tissues during a biomechanical test is much more complex [209,210] and would likely result in greater differences in loading arising from changes in dissection sequence. Therefore, extrapolation of these results to biological circumstances is not appropriate. Additionally, despite the known migration of the COR during movement in biological structures, this study utilized a fixed COR based on the location reported by Xia and colleagues [211] for flexion-extension. The use of a different COR could potentially load the specimen differently.

In conclusion, this study demonstrated that the sequence in which connectors were removed from testing object affected their loading characteristics. The methodology used in the current study does not allow us to ascribe the results here observed to any one of the discussed phenomenon (e.g. viscoelasticity properties, nonlinearity behaviour, specimen preparation differences, testing error, etc). However, these results emphasize that if sequence-dependency was observed in such a simplified system, it will likely be observed in other systems composed of complex biological tissues. Based on these findings, the authors recommend that during robotic testing, tissues should be removed from all the specimens in the same sequence to facilitate appropriate comparison.

### **3.5 Acknowledgements**

This study was supported by the Canadian Research Chair Program, CIHR and NSERC through the SafetyNET grant.

## **Chapter 4.**

### **Spinal tissues loaded by spinal manipulative therapy (SMT).**

#### **Part I: the influence of SMT force magnitude and application site**

##### **4.1 Introduction**

Spinal manipulative therapy (SMT) is defined as a high velocity, low amplitude dynamic force applied to a specific location of the spine for therapeutic reasons resulting in a mechanical deformation of the spine and surrounding tissues [20–22]. It is a common intervention to treat low back pain and its usage has increased over the last decade due to the public's interest in complementary and alternative therapies [99,102]. Despite an increase in SMT usage, the underlying mechanisms of SMT (beneficial or harmful) are still not well understood.

To date, investigations of SMT mechanisms have focused on two domains: physiological outcomes, including both biomechanical and neurophysiological [22,113,132], and SMT input parameters (e.g. thrust duration, loading rate) [30,56,212].

For SMT input parameters, peak force magnitudes and application site have been described as important parameters as they influence both neurophysiological and biomechanical outcomes elicited by SMT [28,32,45,56,133,139,140]. Vertebral displacement and acceleration as well as electromyographic responses and muscle spindles neural responsiveness have been reported to change depending on the applied SMT force magnitude [28,30,31,33]. Similarly, SMT application site has been demonstrated to influence spinal stiffness and muscle spindles sensory input magnitude [44,45].

Unfortunately, few studies have succeeded in linking these domains together (i.e. SMT input parameters and physiological outcomes) by investigating how altering SMT input parameters can change the response of spinal tissues. If it can be shown that spinal tissue response is modified by SMT input parameters, then important indicators as to why SMT has specific health outcomes may be revealed.

Toward understanding SMT underlying mechanisms, a previous study conducted by Kawchuk and colleagues [24] identified the loads experienced by spinal tissues during a general clinical application of SMT. They found that within the boundaries of a specific SMT application in a cadaveric preparation, the intervertebral disc is the spinal structure that experiences the greatest loads [24]. Despite these findings, it remains unknown if changes in SMT application parameters can modify the load distribution within spinal tissues. Specifically, the investigation of loading distribution within spinal tissues when SMT is applied with different peak force magnitudes and at different application sites has not been conducted to elucidate the relation between SMT input parameters and spinal tissue response.

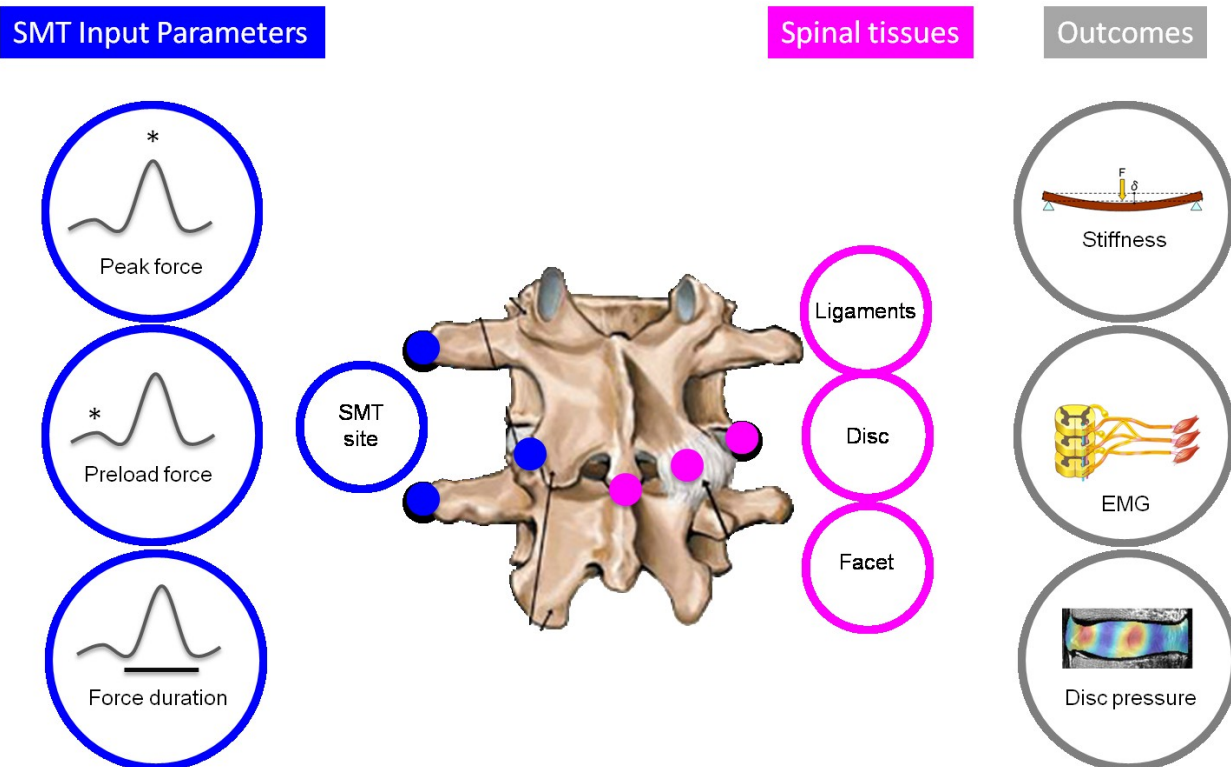


Figure 4.1 Potential relation between spinal tissue targeting and influence on physiological outcomes by adjusting SMT input parameters.

Given the lack of studies investigating SMT input parameters and their effect on spinal tissue load distribution, exploratory studies are needed to define the relation between SMT input parameters and the distribution of load within spinal tissues. Therefore, the objective of this study was to evaluate the relation between SMT input parameters and their effect on spinal tissues loading to guide the following studies of this dissertation.

## 4.2 Methods

### 4.2.1 Overview

The overall methodology used in this study is summarized in Figure 4.2.

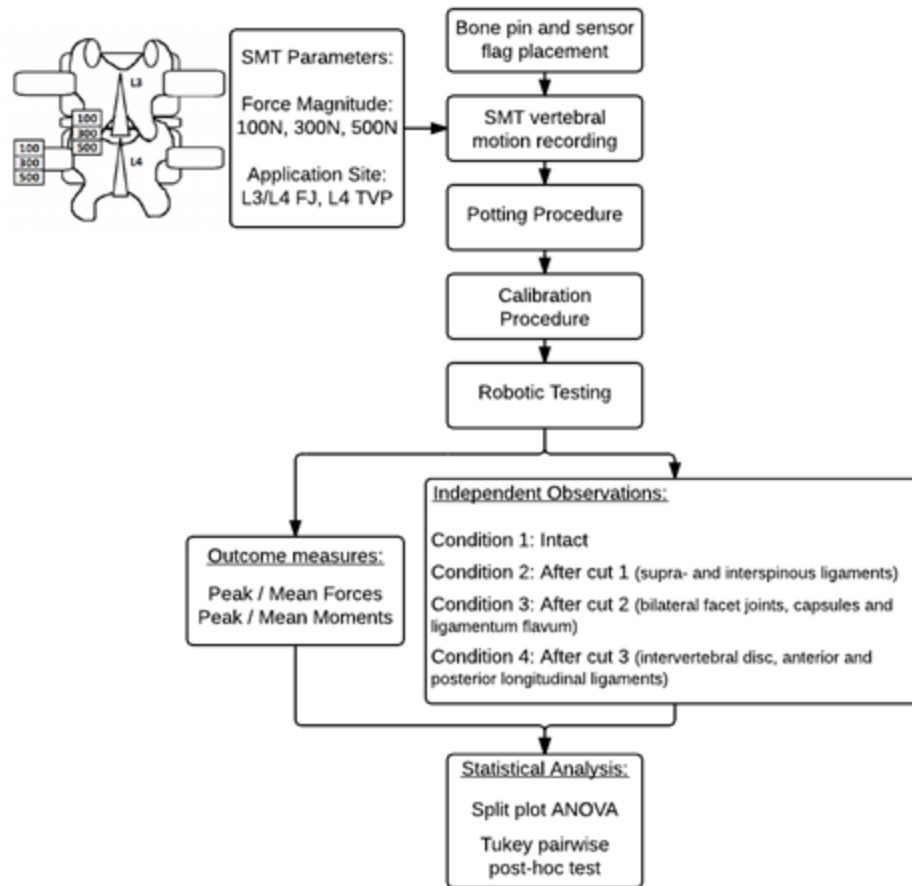


Figure 4.2 Summary of the overall methodology

#### 4.2.2 Sample Size Calculation

The sample size calculation was conducted based on the data previously reported by Kawchuk and colleagues (2010) [24] using the General Power Analysis Program (G\*Power 2) (University of Trier, Germany). With a statistical power was set at 0.80 (80%), two-tailed tests with level of significance set at  $\alpha=0.05$  (5%) and an effect size of 0.99-1.2, a sample size of 9 porcine models was required. Five additional porcine models were included to account for possible specimen loss due to data collection, potting procedure or testing complications and a total of 14 cadaveric porcine specimens were included. Given that the study from Kawchuk and colleagues also observed 12 variables, the use of the effect size reported by these authors for the current sample



size calculation is appropriate. Therefore, with a level of significance set at 0.05 and statistical power set 0.80, the chances of having types I and II errors were 5% and 20%, respectively.

#### ***4.2.3 Specimen Preparation***

Ten porcine cadavers (Duroc X [Large White X Landrace breeds]) of approximately 60-65kg were used in this study (four specimens were excluded due to technical complications during data collection). In each intact porcine cadaver, the L3 and L4 spinous processes were identified by palpation and confirmed by two techniques: 1) ultra-sound imaging and 2) needle probing. About 1.5 cm to the right of the L3 and L4 spinous processes and with approximately 20° of inclination in the clockwise direction relative to the vertical position, pilot cuts were made through the skin and paravertebral muscles until the right L3 and L4 vertebral laminae were contacted. Through each cut, a 3.2 mm diameter bone pin (Zimmer Spine, Minneapolis, MN) with the same 20° of inclination were drilled through the right lamina, into the vertebral body (Figure 4.3).

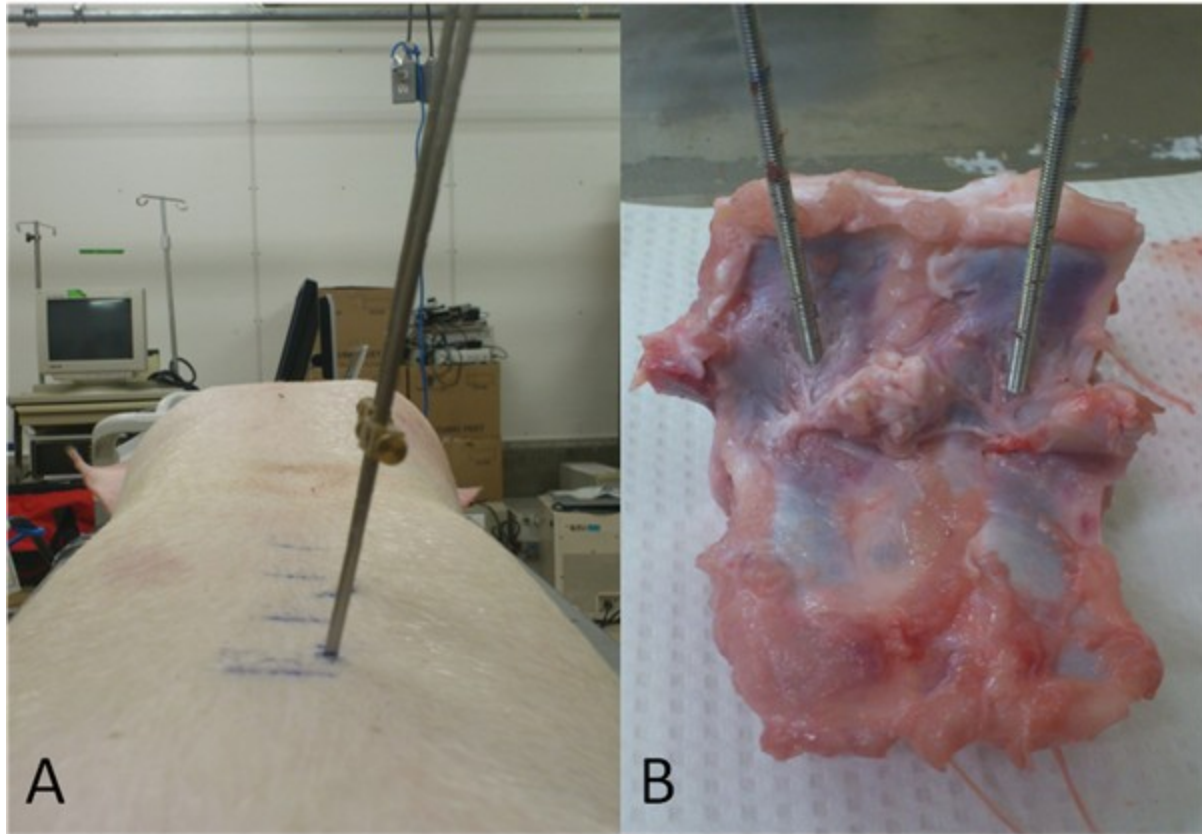


Figure 4.3 Bone pin positioning. A. Intact cadaveric specimen. B. After spine was removed.

A rectangular flag having 4 infrared light-emitting diode markers was attached to the upper end of each bone pin (Figure 4.4). Ultra-sound imaging and needle probing technique were also used on the left side of the lumbar spine to identify the L4 left transverse process (TVP) and L3/L4 facet joint (FJ). Following the application of SMT on the intact porcine cadaver (described in the following section), the lumbar spine was removed *en bloc* by reciprocating saw [24]. The vertebrae superior to L3 and inferior to L4 were extracted, the non-ligamentous tissues were removed with a scalpel and the L3/L4 segment cleaned of remaining non-ligamentous tissues with a water jet dissector (Smith and Nephew, St. Petersburg, FL). The segment was then sealed in plastic bag and kept refrigerated at 3°C for a few hours until potting and testing on the

following day [213]. The specimen was kept moist with physiologic saline throughout preparation, embedding and testing [214,215].



Figure 4.4 Rectangular flag with 4 infrared light-emitting diode markers.

#### ***4.2.4 Spinal Manipulation and Kinematic Recording***

In order to minimize significant SMT force-time profile variance known to exist between clinicians [21], SMT was delivered by a servo-controlled linear actuator motor [39] (Appendix II). A posterior to anterior spinal manipulative thrust was delivered using 3 different peak force magnitudes (100 N, 300 N, and 500 N) at 2 different application sites: L4 left TVP, and L3/L4

left FJ. For all SMTs, the preload was adjusted at 10% of the peak force and the slope of the force curve from preload to peak load (loading rate) was kept constant at 2.6 N/ms. Therefore time to peak was 37.5 ms, 112.5 ms, and 187.5 ms for SMT with 100 N, 300 N and 500 N peak force, respectively.

During the application of each SMT the resulting motion of each bone pin and sensor flag was recorded in 3 dimensions by an optical tracking system at a rate of 400 Hz (0.01 mm system resolution with 0.15 mm rigid body resolution; NDI, Waterloo, Canada) (Appendix III).

#### ***4.2.5 Potting Procedure***

Prior to robotic testing, all porcine lumbar spines had 3 pilot holes drilled in the exposed L3 and L4 endplates to accommodate 3 anchor screws per endplate (Figure 4.5).

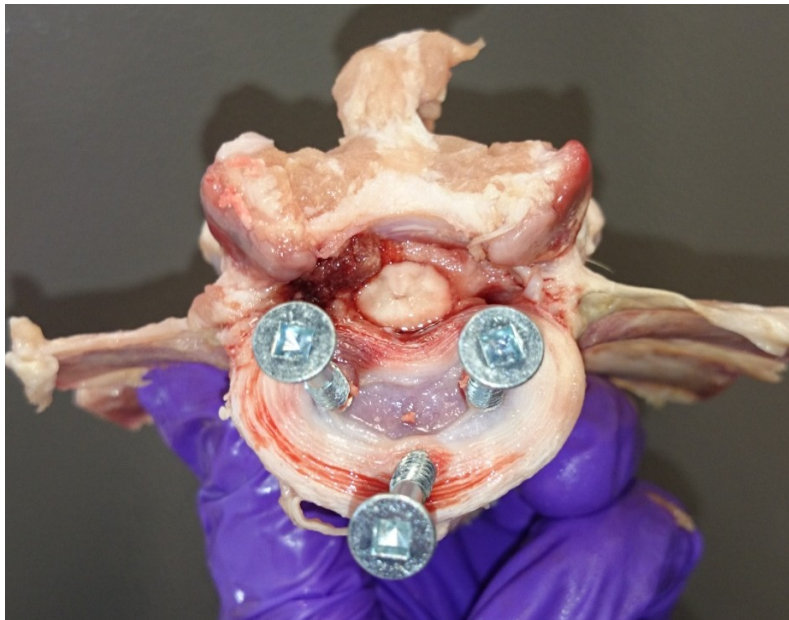


Figure 4.5 Anchor screws placement on porcine lumbar segments.



The specimens were then potted in a vertical orientation using dental stone (Modern Materials, South Bend, IN): in a horizontal surface, the spine segment was suspended in the pot by a hanger bolt drilled into L3 endplate and fixed to a ball-and-socket head attached to a cross beam (Figure 4.6A). A horizontal laser level (DeWalt Industrial Tool Co., Baltimore, MD) was used to ensure that the intervertebral disc was parallel to the horizontal. After the dental stone was dry, the pot was turned up-side down, fixed to the cross beam, and the L3 vertebra was then potted (Figure 4.6 B and C). All potting procedures were standardized to reduce variation in potting.

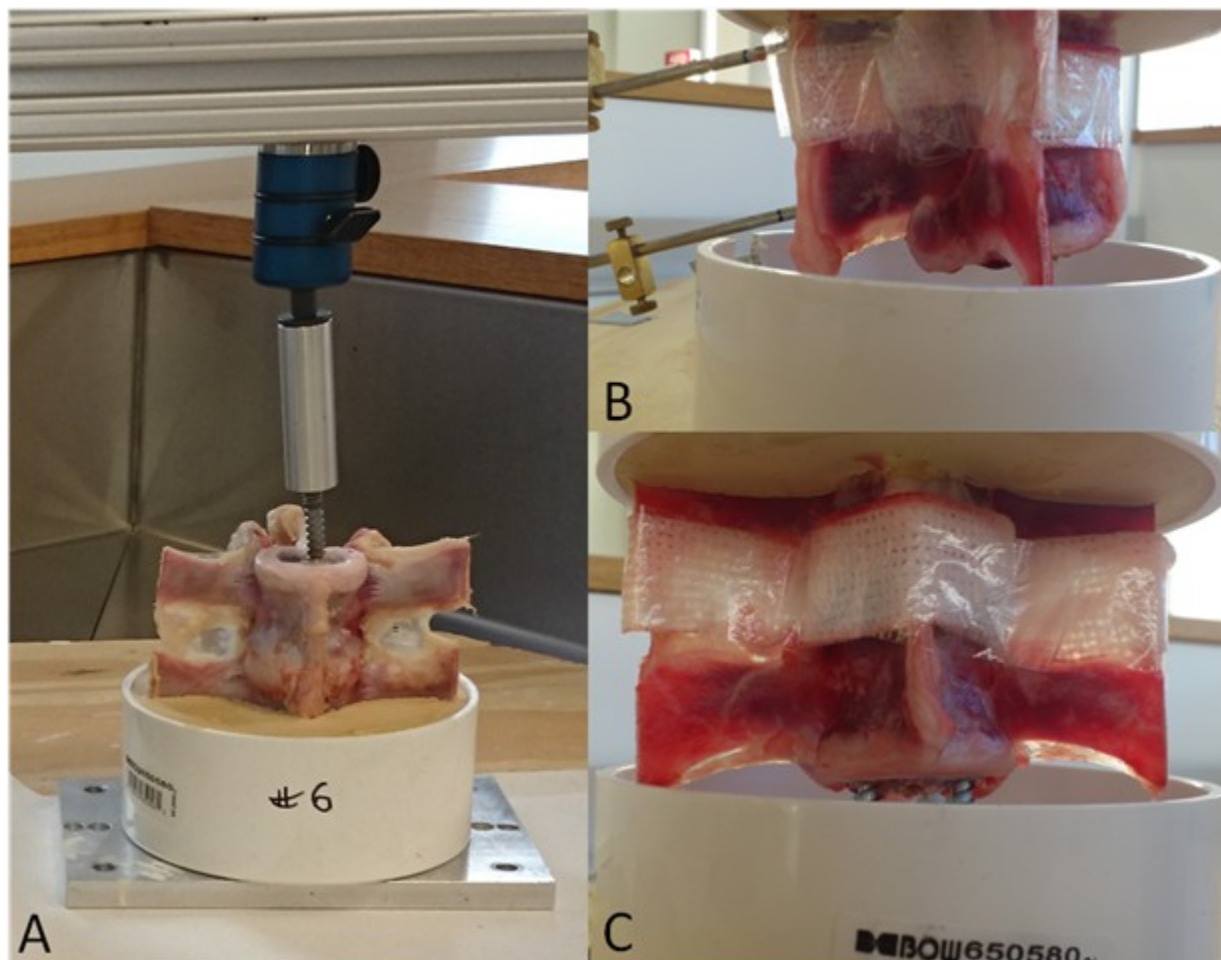


Figure 4.6 Potting procedure of porcine lumbar spine specimens. A. Potting of L4 vertebra. B and C. Potting of L3 vertebra.

#### 4.2.6 Robotic Testing

Following the potting procedure, the caudal end (L4) of the potted spinal segment was fixed to a 6-axis load cell (AMTI MC3A-1000, Advanced Mechanical Technology, Inc., Watertown, MA) and the load cell rigidly mounted to a parallel robot platform (Parallel Robotics Systems corp., Hampton, NH) (Figure 4.7A). The parallel robot is composed of a rigid circular platform with 80 cm of diameter, suspended by 6 rigid arms with 35 cm of length (Figure 4.7B). Each arm travels along a circular track moved by an electromechanical motor that is controlled by custom-designed software (LabVIEW, National Instruments, Austin, TX). By changing the commands on the software, the robot's arms move around the track and change the position and orientation of the platform. The resolution of the robot is a function of the motor performance (0.05 mm with a repeatability of 0.025 mm; Mikrolar, Hampton, NH), which translates into a linear resolution of less than 1  $\mu\text{m}$  and an angular resolution of 0.001°.

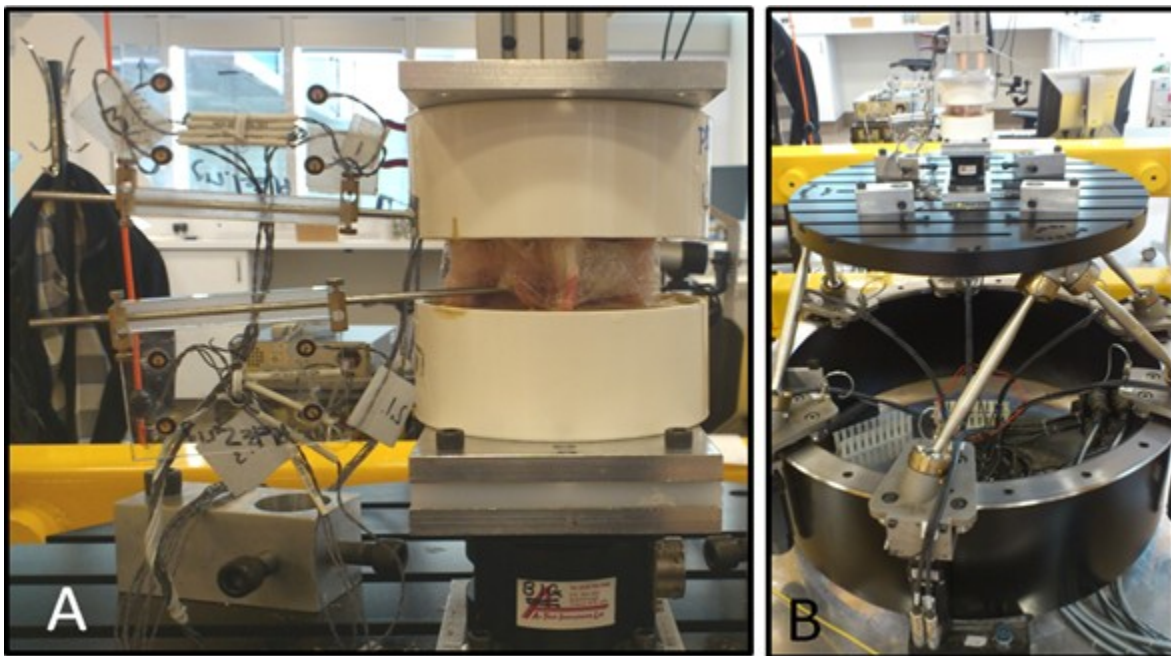


Figure 4.7 Robotic testing. A. Specimen fixed to the load cell. B. Parallel robot platform with load cell and specimen attached.

After the potted specimen was rigidly mounted to the load cell/robot, a calibration process consisted of a series of known translations and rotations of the robot platform was performed and compared to the resulting change in the sensor position (Appendix IV). This calibration was executed to position the specimen in the same position and orientation previously recorded from the *ex vivo* neutral pose. By using known mathematical processes [216], the sensor movements caused by all SMTs were transposed into the robotic frame of reference. As a result, 6 robotic trajectories with each unique parameter combination (force magnitude and SMT application site) generated a separate robotic trajectory file consisting of a series of commands. The robot accepts commands less frequently than data points are generated by the optical system. Therefore the robotic command files were re-sampled to move the robotic platform in displacement control method reproducing the path of each SMT previously recorded. Given the safety settings of the robot, the SMT path replication was approximately 10% slower than the original SMT application. Once the calibration process was complete, the cranial end of the potted specimen was fixed to a stationary cross beam, the segment positioned in the initial neutral position and the load cell zeroed.

By inputting the robotic trajectory file created in the custom-designed software, the robot moved through a series of events in the following the order: SMT application from medial to lateral and increasing SMT force magnitudes. This way, starting from the initial neutral position, SMTs were reproduced in the following sequence: 100 N at L3/L4 FJ and L4 TVP; 300 N at L3/L4 FJ and L4 TVP; and 500 N at L3/L4 FJ and L4 TVP. Each event was separated by a 2 minutes recovery time. This time was employed as it was the minimum time necessary to perform all the tasks between tests (saving data, removing spinal structures, setting up for next test) and satisfied

the minimum time for loads to return to baseline [24]. Feasibility tests performed by Kawchuk and colleagues [24] also demonstrated that peak loads in the specimen change with repeated applications of the robotic trajectory, but this phenomenon reached equilibrium within 2 or 3 trials. Therefore, 3 pre-conditioning trials were executed prior to testing.

The forces and moments generated during robotic simulation of SMT movements were recorded at 50 Hz (axes of movement: x = medial/ lateral, y = anterior/posterior, and z = superior/inferior). Following the replication of the SMT paths by the robot, spinal structures were removed and/or transected from the specimen and the exact same kinematic events repeated by the robot. Based on the previous study of this dissertation [217], spinal structures were removed using the same sequence in all 10 specimens. Therefore, spinal structures were removed/transected (via scalpel unless otherwise noted) in the following order: 1) supra- and interspinous ligament (SL), 2) bilateral facet capsules, facet joints (via rongeur) and ligamentum flavum (PJ), 3) intervertebral disc and anterior and posterior longitudinal ligaments (IVD). Since some intertransverse ligaments were not intact after removing the spine from *ex vivo* and dissection process, the intertransverse ligaments from all specimens were removed prior to testing.

#### ***4.2.7 Statistical Analysis***

##### ***4.2.7.1 Variables***

In summary, this study had 2 independent variables, 12 dependent variables with 4 conditions independently observed. The description of the conditions and variables here used are detailed in Table 4.1.



**Table 4.1 Description of conditions and variables used throughout the chapter**

Term	Definition
Condition (n=4)	State in which specimens were tested. This study investigated 4 different conditions: 1. Intact specimen, 2. after cut 1 where supra- and interspinous ligaments (SL) were removed, 3. after cut 2 removing bilateral facet joints, capsules and ligamentum flavum (PJ) and 4. after cut 3 removing intervertebral disc and anterior and posterior longitudinal ligaments (IVD).
SMT input parameter (n=6)	Characteristics of the SMT force. In this study, peak force magnitude (100N, 300N, 500N) and application site (L3/L4 facet joint and L4 transverse process) parameters were included.
Independent variable	Variable under investigation. In this study, independent variables are SMT peak force magnitude and application site.
Dependent variable	Measured variable, outcome. In this study, dependent variables are peak and mean forces and moments along and around all 3 axes of movement, respectively.

#### 4.2.7.2 Statistical Tests

For each porcine lumbar specimen, the resulting forces and moments were plotted against time for the intact condition and following the removal of each spinal structure. By using customized software (LabVIEW, National Instruments, Austin, TX), the baseline forces and moments along and around the 3 Cartesian axes were considered to be those measured when the specimen was positioned in the same initial position as *ex vivo*. The peak and mean forces and moments along and around each axis (x-, y-, and z-axes) were identified by customized software for the intact condition and following each spinal structure removal. For the spinal structures, the relative peak and mean forces and moments were normalized to the respective load experienced by the intact condition during the application of each SMT trajectory. Peak force and moment correspond to the maximum measured force and moment during the SMT thrust phase. Mean forces and moments correspond to the average value of forces and moments involving both the preload and

thrust phases of SMT. The customized software also determined the magnitude of displacements (translation and rotation) where peak loads occurred.

Given our objective of describing the relation between SMT input parameters of force magnitude and application site and spinal tissues loading characteristics, each spinal structure removal condition was analyzed independently. Therefore, a split plot analysis of variance (ANOVA) was performed using R: A language and environment for statistical computing (R Foundation for Statistical Computing, Vienna, Austria) with 2 factors: force magnitude (main-plot factor) and SMT application site (subplot factor). A Tukey multiple comparison post-hoc test was performed for pairwise analysis of significant interaction between factors. Force magnitude and application site main effects were analyzed on the conditions (intact condition or following spinal structure removal) and variables that did not reveal a significant interaction. For all statistical tests an  $\alpha$ -level of 0.05 was considered.

## **4.3 Results**

### ***4.3.1 Overview***

Table 4.2 provides an overview of the significant interactions and main effects found in this experiment. Figure 4.8 shows an overview of the peak and mean forces and moments along and around the 3 axes of movement experienced by the intact specimen and by spinal structures isolated by sequential dissection.

**Table 4.2 Summary of significant interactions and main effects**

Condition	Dependant Variable	Axes of movement		
		X	Y	Z
Intact	Peak Force	Force magnitude	Force magnitude	Force magnitude, Application site
	Mean Force	Force magnitude	Force magnitude	Application site
	Peak Moment	Interaction	Force magnitude	Force magnitude, Application site
	Mean Moment	Interaction	Application site	Force magnitude, Application site
Cut 1 (SL)	Peak Force	-	-	-
	Mean Force	Force magnitude	-	-
	Peak Moment	-	Force magnitude	-
	Mean Moment	-	-	-
Cut 2 (PJ)	Peak Force	Application site	-	-
	Mean Force	-	-	-
	Peak Moment	-	Application site	-
	Mean Moment	-	-	Force magnitude
Cut 3 (IVD)	Peak Force	-	-	-
	Mean Force	-	-	-
	Peak Moment	Interaction	-	-
	Mean Moment	-	-	-



Figure 4.8 Combined loads of all conditions

### ***4.3.2 Vertebral Displacements***

Exact vertebral displacements resulting from each SMT were replicated during robotic testing of all conditions. Relative translations and rotations of L4 vertebra in relation to L3 arising from SMT parameters of force magnitude and application site are displayed by axis of movement in Table 4.3. The greatest translation was observed along the y-axis (posterior to anterior translation) ( $5.16 \pm 2.76$  mm) and the greatest rotations around the x- ( $1.77^\circ \pm 0.87$ ) and z-axes ( $-1.85^\circ \pm 1.10$ ) (flexion-extension and axial rotation, respectively). Table 4.4 shows the average ( $\pm$ SD) relative vertebral displacement and rotation caused by SMT in comparison to values reported Kawchuk et al. (2010).

**Table 4.3 Maximal displacement (mm) and rotation (°) (SD) created in the cadaveric specimens with the application of SMT (with different force magnitudes at different application sites) trajectories for all conditions**

SMT Parameters		Displacement (mm)			Rotation (°)		
Location	Force Magnitude (N)	X (lateral)	Y (ant post)	Z (sup inf)	X (flx ext)	Y (lat bending)	Z (axial rot)
L3/L4 FJ	100	2.89 (1.72)	4.00 (2.54)	0.73 (0.27)	1.34 (0.78)	-0.72 (0.45)	-0.78 (0.66)
L3/L4 FJ	300	2.17 (1.48)	3.98 (2.47)	1.19 (0.16)	1.36 (0.84)	-0.10 (0.17)	-1.47 (1.08)
L3/L4 FJ	500	1.93 (2.08)	4.74 (3.39)	1.42 (0.22)	1.58 (1.02)	-0.70 (0.40)	-1.91 (1.12)
L4 TVP	100	2.47 (1.96)	5.76 (2.16)	0.73 (0.42)	1.90 (0.67)	-0.67 (0.57)	-1.54 (0.71)
L4 TVP	300	1.32 (1.60)	5.99 (2.66)	1.03 (0.31)	2.14 (0.85)	-0.47 (0.46)	-2.17 (1.32)
L4 TVP	500	1.50 (1.06)	6.49 (3.31)	1.12 (0.32)	2.32 (1.04)	-0.49 (0.21)	-3.22 (1.70)
Average		2.05 (1.65)	5.16 (2.76)	1.04 (0.28)	1.77 (0.87)	-0.53 (0.64)	-1.85 (1.10)

SD = standard deviation; FJ = facet joint; TVP= transverse process, N=Newtons

**Table 4.4 Average (SD) maximum displacement (mm) and rotation (°) of the current study and the previous study conducted by Kawchuk et al. (2010)**

Study	Displacement (mm)			Rotation (°)		
	X (lateral)	Y (ant post)	Z (sup inf)	X (lateral)	Y (ant post)	Z (sup inf)
Current Study	2.05 (1.65)	5.16 (2.76)	1.04 (0.28)	1.77 (0.87)	-0.53 (0.64)	-1.85 (1.10)
Kawchuk et al. (2010)	2.15 (0.47)	5.35 (0.86)	0.5 (0.07)	1.96 (0.29)	0.61 (0.17)	0.45 (0.15)

### ***4.3.3 Intact Specimen***

Figure 4.9 reports the average peak force, mean force, peak moment and mean moment experienced by the intact specimen while changing SMT parameters of applied force magnitude and application site.

#### ***4.3.3.1 Interaction effect***

With the intact specimen, a significant interaction between SMT force magnitude and application site was observed in flexion extension moments (peak and mean moments around x-axis) (Table 4.5). Specifically, the interaction between 300 N and 500 N force magnitudes with L4 TVP application site created peak moments around x-axis (average: 0.95 Nm  $\pm$ 0.97, 95% CI [0.44, 1.56]; and average: 1.24 Nm  $\pm$ 1.24, 95% CI [0.41, 1.99], respectively) significantly greater than the other possible interactions (Figure 4.10A). The interaction between 500 N force magnitude with L3/L4 FJ application site created a mean moment around x-axis (average: -0.80 Nm  $\pm$ 0.72, 95% CI [-1.22, -0.28]) significantly greater in comparison to the other possible interactions (Figure 4.10B).



Figure 4.9 Average and standard deviation of peak and mean forces and moments experienced by the intact specimen during the SMT application with each force magnitude (bottom of each graph) at each application site (bar colors). **Red boxes** indicate significant interaction between force magnitude and application site effects. **Yellow boxes** indicate significant force magnitude main effect. A **green boxes** indicates significant application site main effect.



**Table 4.5 Split plot ANOVA table for the intact condition**

Peak force along x-axis						Mean force along x-axis				
<i>Factor</i>	<i>DF</i>	<i>Sum Sq</i>	<i>Mean Sq</i>	<i>F-value</i>	<i>p-value</i>	<i>DF</i>	<i>Sum Sq</i>	<i>Mean Sq</i>	<i>F-value</i>	<i>p-value</i>
<i>Force</i>	2	1214.2	1157.09	15.09	<b>0.001</b>	2	22.45	11.225	0.2968	0.74
<i>Ea</i>	18	1380.2	76.68			18	680.87	37.826		
<i>Location</i>	1	140.6	140.58	3.2233	0.08	1	138.71	137.712	4.9646	<b>0.03</b>
<i>Force:Location</i>	2	41.2	20.59	0.4720	0.62	2	50.62	25.311	0.9059	0.41
<i>Eb</i>	27	1177.6	43.61			27	754.38	27.940		
Peak force along y-axis						Mean force along y-axis				
<i>Factor</i>	<i>DF</i>	<i>Sum Sq</i>	<i>Mean Sq</i>	<i>F-value</i>	<i>p-value</i>	<i>DF</i>	<i>Sum Sq</i>	<i>Mean Sq</i>	<i>F-value</i>	<i>p-value</i>
<i>Force</i>	2	2891.0	1445.49	32.0610	<b>&lt;0.001</b>	2	78.9	39.46	9.5985	<b>0.001</b>
<i>Ea</i>	18	811.5	45.09			18	74.0	4.11		
<i>Location</i>	1	86.3	86.28	2.9814	0.09	1	0.3	0.28	0.0552	0.81
<i>Force:Location</i>	2	106.7	53.33	1.8428	0.17	2	4.3	2.16	0.4289	0.65
<i>Eb</i>	27	781.4	28.94			27	136.2	5.04		
Peak force along z-axis						Mean force along z-axis				
<i>Factor</i>	<i>DF</i>	<i>Sum Sq</i>	<i>Mean Sq</i>	<i>F-value</i>	<i>p-value</i>	<i>DF</i>	<i>Sum Sq</i>	<i>Mean Sq</i>	<i>F-value</i>	<i>p-value</i>
<i>Force</i>	2	426.7	213.37	4.0065	<b>0.03</b>	2	86.29	43.144	2.5240	0.10
<i>Ea</i>	18	958.6	53.26			18	307.68	17.094		
<i>Location</i>	1	1431.5	1431.52	12.0459	<b>0.001</b>	1	91.71	91.712	4.6859	<b>0.03</b>
<i>Force:Location</i>	2	42.7	21.35	0.1796	0.83	2	17.95	8.974	0.4585	0.63
<i>Eb</i>	27	3208.7	118.84			27	528.44	19.572		
Peak moment around x-axis						Mean moment around x-axis				
<i>Factor</i>	<i>DF</i>	<i>Sum Sq</i>	<i>Mean Sq</i>	<i>F-value</i>	<i>p-value</i>	<i>DF</i>	<i>Sum Sq</i>	<i>Mean Sq</i>	<i>F-value</i>	<i>p-value</i>
<i>Force</i>	2	2.928	1.4639	3.6005	0.04	2	0.1027	0.05137	0.5801	0.56
<i>Ea</i>	18	7.319	0.4066			18	1.5938	0.08855		
<i>Location</i>	1	8.943	8.9434	65.4513	<b>&lt;0.001</b>	1	0.7628	0.76281	25.3743	<b>&lt;0.001</b>
<i>Force:Location</i>	2	0.930	0.4650	3.1032	<b>0.04*</b>	2	0.6135	0.30673	10.2031	<b>&lt;0.001*</b>
<i>Eb</i>	27	3.689	0.1366			27	0.8117	0.03006		
Peak moment around y-axis						Mean moment around y-axis				
<i>Factor</i>	<i>DF</i>	<i>Sum Sq</i>	<i>Mean Sq</i>	<i>F-value</i>	<i>p-value</i>	<i>DF</i>	<i>Sum Sq</i>	<i>Mean Sq</i>	<i>F-value</i>	<i>p-value</i>
<i>Force</i>	2	17.953	8.9766	25.1463	<b>&lt;0.001</b>	2	0.1169	0.05847	0.3398	0.71
<i>Ea</i>	18	6.426	0.3570			18	3.0974	0.17208		
<i>Location</i>	1	0.074	0.0744	0.0965	0.75	1	1.1354	1.13542	7.8484	<b>&lt;0.001</b>
<i>Force:Location</i>	2	0.363	0.1817	0.2357	0.79	2	0.1888	0.09440	0.6525	0.52
<i>Eb</i>	27	20.813	0.7709			27	3.9061	0.14467		
Peak moment around z-axis						Mean moment around z-axis				
<i>Factor</i>	<i>DF</i>	<i>Sum Sq</i>	<i>Mean Sq</i>	<i>F-value</i>	<i>p-value</i>	<i>DF</i>	<i>Sum Sq</i>	<i>Mean Sq</i>	<i>F-value</i>	<i>p-value</i>
<i>Force</i>	2	133.546	66.773	14.8692	<b>&lt;0.001</b>	2	4.6993	2.34964	11.9448	<b>&lt;0.001</b>
<i>Ea</i>	18	80.832	4.491			18	3.5407	0.19671		
<i>Location</i>	1	64.679	64.879	16.2209	<b>&lt;0.001</b>	1	2.6332	2.63323	31.0537	<b>&lt;0.001</b>
<i>Force:Location</i>	2	18.114	9.057	2.2644	0.12	2	0.2541	0.12706	1.4984	0.24
<i>Eb</i>	27	107.993	4.000			27	2.2895	0.08480		

\* - p-value < 0.05

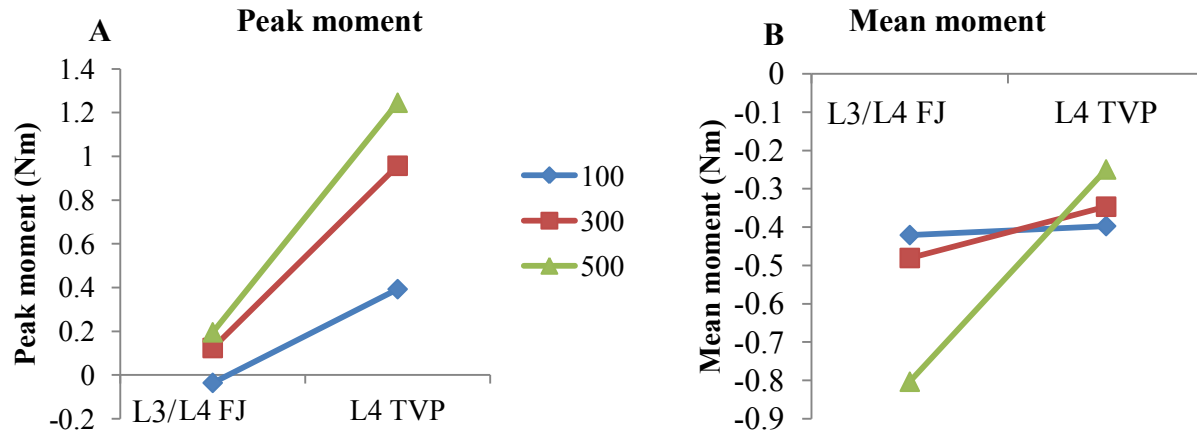


Figure 4.10 Interaction between force magnitude and application site for peak (A) and mean (B) moment around x-axis (flexion extension moment) in the intact condition. FJ=Facet joint; TVP=Transverse process.

#### 4.3.3.2 Force magnitude main effect

Significant SMT force magnitude main effect was observed in all peak forces and moments, mean anterior-posterior forces (force along y-axis), and mean axial rotation moment (moment around z-axis). Overall, the intact specimen experienced significantly greater loads and moments with the application of a SMT with greater force magnitudes (Table 4.5 and Figure 4.9).

#### 4.3.3.3 Application site main effect

Significant application site main effect was observed in peak and mean superior-inferior forces and axial rotation moments (forces along and moments around z-axis). Mean lateral moment (moment around y-axis) was also affected by SMT application site main effect. Generally, the intact specimen experienced greater superior inferior forces when SMT was applied at FJ than when applied at TVP. On the other hand, axial rotation and lateral bending moments experienced by the intact specimen were greater when SMT was applied at TVP in comparison to when applied at FJ (Table 4.5 and Figure 4.9).

#### ***4.3.4 Cut 1: Supra- and interspinous ligaments (SL)***

Figure 4.11 shows the average of normalized relative peak and mean forces and moments experienced by the SL structures during the SMT application with each force magnitude at each application site. Generally, from the total loads experienced by the intact specimen, SL structures experienced about 0.2% of the peak forces, 0.7% of the mean forces, 3% of the peak moments and 7.2% of the mean moments (Figure 4.8).

##### ***4.3.4.1 Interaction effect***

The SL structures removed in cut 1 did not present any significant interaction between force magnitude and SMT application site (Table 4.6).

##### ***4.3.4.2 Force magnitude main effect***

Statistically significant main effect of force magnitude was observed in mean lateral force and peak lateral bending moment (mean force along x-axis and peak moment around y-axis, respectively) (Table 4.6). Paradoxically, lateral loads borne by SL when SMT was applied with 100 N force magnitude (average mean force along x-axis:  $-0.18 \text{ N} \pm 0.21$ , 95% CI  $[-0.31, -0.02]$ ; average peak moment around y-axis:  $-0.10 \text{ Nm} \pm 0.06$ , 95% CI  $[-0.25, -0.04]$ ) were significantly greater than with 500 N (average mean force along x-axis:  $-0.04 \text{ N} \pm 0.12$ , 95% CI  $[-0.08, 0.00]$ ; average peak moment around y-axis:  $0.01 \text{ Nm} \pm 0.25$ , 95% CI  $[-0.07, 0.10]$ ) (Figure 4.12).

##### ***4.3.4.3 Application site main effect***

Application site main effect did not reveal a statistically significant difference.

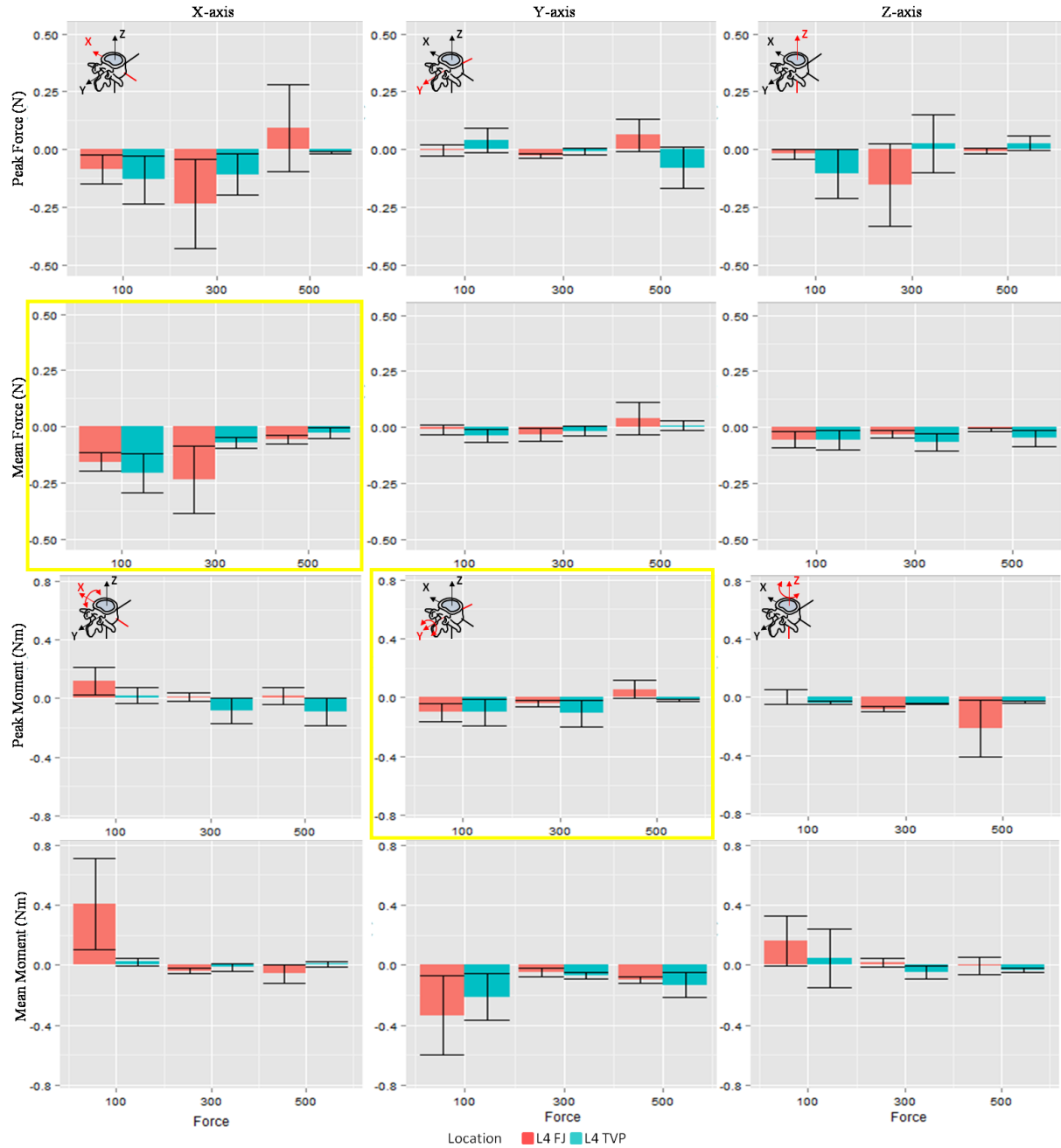


Figure 4.11 Average and standard deviation of normalized relative peak and mean forces and moments experienced by the supra- and interspinous ligaments during the SMT application with each force magnitude (bottom of each graph) at each application site (bar colors). **Yellow boxes** indicate significant force magnitude main effect.

**Table 4.6 Split plot ANOVA table for the supra- and interspinous ligaments**

Peak force along x-axis						Mean force along x-axis				
<i>Factor</i>	<i>DF</i>	<i>Sum Sq</i>	<i>Mean Sq</i>	<i>F-value</i>	<i>p-value</i>	<i>DF</i>	<i>Sum Sq</i>	<i>Mean Sq</i>	<i>F-value</i>	<i>p-value</i>
<i>Force</i>	2	0.4738	0.23689	1.3052	0.29	2	0.19636	0.09818	4.3454	<b>0.02</b>
<i>Ea</i>	18	3.2670	0.18150			18	0.40669	0.02259		
<i>Location</i>	1	0.0011	0.00112	0.0108	0.91	1	0.00159	0.00158	0.1136	0.73
<i>Force:Location</i>	2	0.1482	0.07411	0.7127	0.49	2	0.02840	0.014200	1.0160	0.37
<i>Eb</i>	27	2.8080	0.10400			27	0.37734	0.013976		
Peak force along y-axis						Mean force along y-axis				
<i>Factor</i>	<i>DF</i>	<i>Sum Sq</i>	<i>Mean Sq</i>	<i>F-value</i>	<i>p-value</i>	<i>DF</i>	<i>Sum Sq</i>	<i>Mean Sq</i>	<i>F-value</i>	<i>p-value</i>
<i>Force</i>	2	0.01444	0.00721	0.2351	0.79	2	0.02978	0.014889	1.6817	0.21
<i>Ea</i>	18	0.55272	0.03070			18	0.15936	0.00885		
<i>Location</i>	1	0.01102	0.01021	0.5754	0.45	1	0.00258	0.002582	0.3455	0.56
<i>Force:Location</i>	2	0.1021	0.05109	2.8776	0.07	2	0.00747	0.003735	0.4999	0.61
<i>Eb</i>	27	0.4793	0.01775			27	0.20174	0.007472		
Peak force along z-axis						Mean force along z-axis				
<i>Factor</i>	<i>DF</i>	<i>Sum Sq</i>	<i>Mean Sq</i>	<i>F-value</i>	<i>p-value</i>	<i>DF</i>	<i>Sum Sq</i>	<i>Mean Sq</i>	<i>F-value</i>	<i>p-value</i>
<i>Force</i>	2	0.06956	0.034778	0.4383	0.65	2	0.00739	0.003696	0.7087	0.50
<i>Ea</i>	18	1.42837	0.079354			18	0.09388	0.00521		
<i>Location</i>	1	0.02752	0.02751	0.2406	0.62	1	0.01002	0.010024	2.888	0.10
<i>Force:Location</i>	2	0.17410	0.08705	0.7612	0.47	2	0.00404	0.002022	0.5826	0.56
<i>Eb</i>	27	3.08763	0.114357			27	0.09369	0.003470		
Peak moment around x-axis						Mean moment around x-axis				
<i>Factor</i>	<i>DF</i>	<i>Sum Sq</i>	<i>Mean Sq</i>	<i>F-value</i>	<i>p-value</i>	<i>DF</i>	<i>Sum Sq</i>	<i>Mean Sq</i>	<i>F-value</i>	<i>p-value</i>
<i>Force</i>	2	0.04988	0.024942	1.3812	0.27	2	0.06025	0.03012	0.6736	0.52
<i>Ea</i>	18	0.32505	0.018058			18	0.80500	0.044722		
<i>Location</i>	1	0.07215	0.072152	1.7173	0.20	1	0.00400	0.003999	0.0672	0.79
<i>Force:Location</i>	2	0.02919	0.14594	0.3474	0.70	2	0.02799	0.013997	0.2352	0.79
<i>Eb</i>	27	1.13439	0.042014			27	1.60678	0.059510		
Peak moment around y-axis						Mean moment around y-axis				
<i>Factor</i>	<i>DF</i>	<i>Sum Sq</i>	<i>Mean Sq</i>	<i>F-value</i>	<i>p-value</i>	<i>DF</i>	<i>Sum Sq</i>	<i>Mean Sq</i>	<i>F-value</i>	<i>p-value</i>
<i>Force</i>	2	0.15788	0.078939	4.3191	<b>0.02</b>	2	0.2820	0.140991	1.0428	0.37
<i>Ea</i>	18	0.32898	0.018277			18	2.4337	0.135204		
<i>Location</i>	1	0.03591	0.035907	0.7271	0.40	1	0.0459	0.045894	0.2911	0.59
<i>Force:Location</i>	2	0.01811	0.009053	0.1833	0.83	2	0.2120	0.105989	0.6724	0.51
<i>Eb</i>	27	1.3336	0.049384			27	4.2561	0.157635		
Peak moment around z-axis						Mean moment around z-axis				
<i>Factor</i>	<i>DF</i>	<i>Sum Sq</i>	<i>Mean Sq</i>	<i>F-value</i>	<i>p-value</i>	<i>DF</i>	<i>Sum Sq</i>	<i>Mean Sq</i>	<i>F-value</i>	<i>p-value</i>
<i>Force</i>	2	0.03492	0.017459	0.7265	0.49	2	0.00012	0.000059	0.0031	0.99
<i>Ea</i>	18	0.43258	0.024032			18	0.33562	0.018646		
<i>Location</i>	1	0.00895	0.008948	0.4100	0.52	1	0.00113	0.001133	0.2070	0.87
<i>Force:Location</i>	2	0.03634	0.018171	0.8327	0.44	2	0.09972	0.049861	1.1905	0.31
<i>Eb</i>	27	0.58922	0.021822			27	1.13084	0.041883		

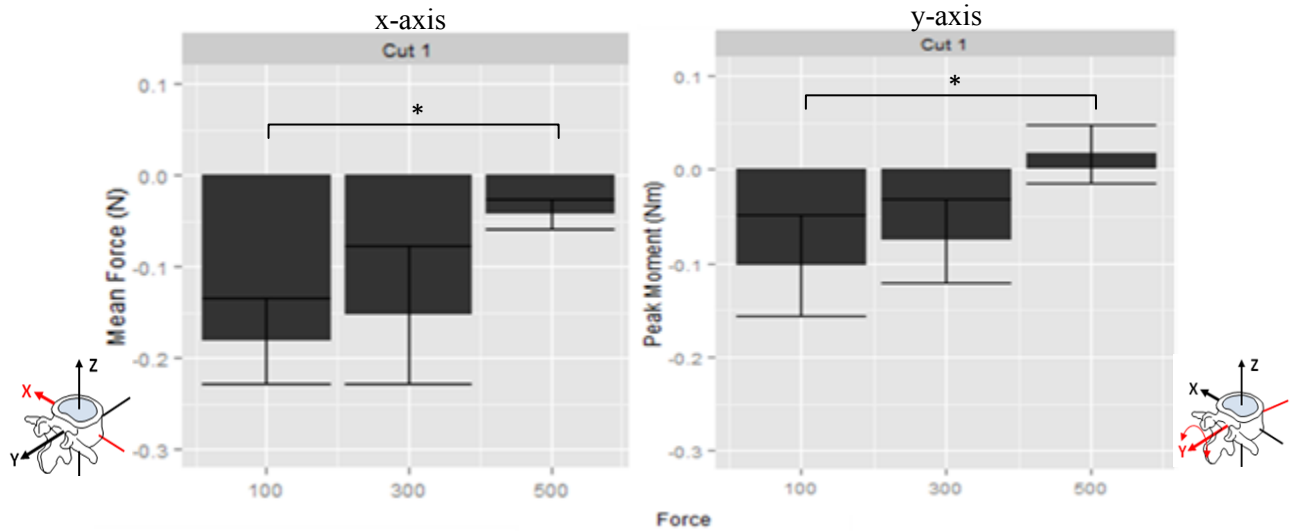


Figure 4.12 Force magnitude main effect of average (and standard deviation) mean force along x-axis (lateral force) and peak moment around y-axis (lateral bending) for supra- and interspinous ligaments.

#### 4.3.5 Cut 2: Bilateral facet joints, capsules and ligamentum flavum (PJ)

Figure 4.13 shows the average of normalized relative peak and mean forces and moments experienced by the PJ structures during the SMT application with each force magnitude at each application site. Generally, from the total loads experienced by the intact specimen, PJ structures experienced 0.1% of the peak forces, 1.4% of the mean forces, 2.1% of the peak moments and 75% of the mean moments (Figure 4.8).

##### 4.3.5.1 Interaction effects

The PJ structures removed in cut 2 did not reveal a statistically significant interaction between force magnitude and SMT application site (Table 4.7).

#### *4.3.5.2 Force magnitude main effect*

Force magnitude main effect was only observed in mean moment around z-axis (axial rotation moment) (Table 4.7): a SMT applied with a force magnitude of 100 N created moments in PJ structures (average:  $-0.17 \text{ Nm} \pm 0.51$ , 95% CI  $[-1.52, 1.17]$ ) significantly smaller than a SMT with 500 N (average:  $-0.79 \text{ Nm} \pm 0.50$ , 95% CI  $[-1.08, -0.49]$ ) (Figure 4.14 and Table 4.7).

#### *4.3.5.3 Application site main effect*

Application site main effect was also statistically significant for lateral force and lateral bending moment (peak force along x-axis and peak moment around y-axis, respectively): loads experienced by PJ structures were significantly greater when SMT was applied at L4 TVP than at L3/L4 FJ (Figure 4.15 and Table 4.7).

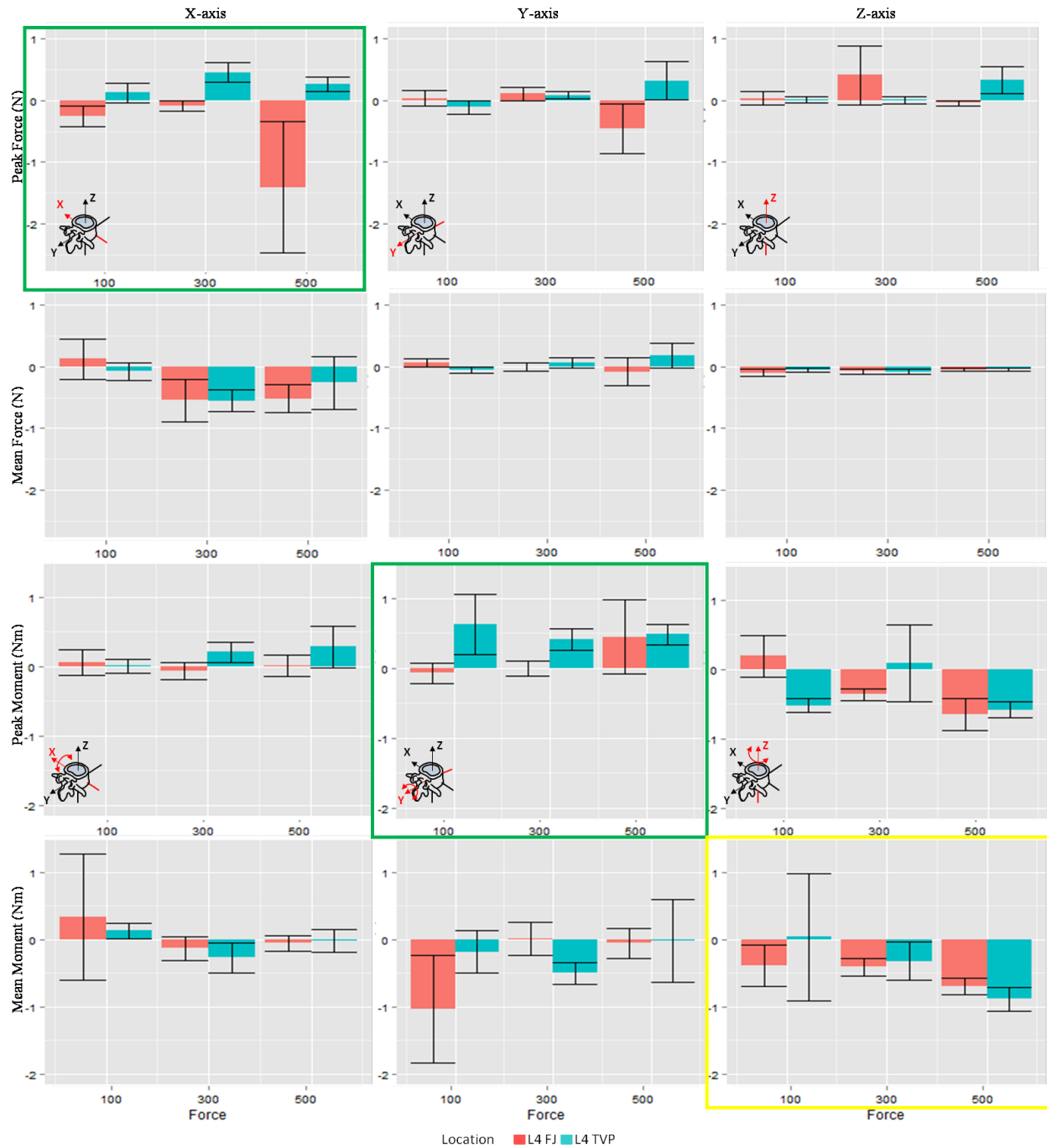


Figure 4.13 Average and standard deviation of normalized relative peak and mean forces and moments experienced by the bilateral facet joints, capsules and ligamentum flavum during the SMT application with each force magnitude (bottom of each graph) at each application site (bar colors). A **yellow box** indicates significant force magnitude main effect. **Green boxes** indicate significant application site main effect.



**Table 4.7 Split plot ANOVA table for the bilateral facet joints, capsules and ligamentum flavum**

Peak force along x-axis						Mean force along x-axis				
Factor	DF	Sum Sq	Mean Sq	F-value	p-value	DF	Sum Sq	Mean Sq	F-value	p-value
Force	2	2.939	2.9694	1.5459	0.24	2	4.1084	2.05418	2.2088	0.13
Ea	18	34.574	1.9208			18	16.7399	0.9300		
Location	1	11.199	11.1986	5.8021	0.02	1	0.0431	0.04311	0.0438	0.83
Force:Location	2	4.960	2.4798	1.2848	0.29	2	0.5451	0.27254	0.2768	0.76
Eb	27	52.112	1.9301			27	26.5833	0.98457		
Peak force along y-axis						Mean force along y-axis				
Factor	DF	Sum Sq	Mean Sq	F-value	p-value	DF	Sum Sq	Mean Sq	F-value	p-value
Force	2	0.3195	0.1597	0.5116	0.60	2	0.0205	0.01026	0.0643	0.93
Ea	18	5.6201	0.3122			18	2.8715	0.15953		
Location	1	0.6248	0.62483	1.2356	0.27	1	0.0794	0.07941	0.9995	0.32
Force:Location	2	2.5118	1.2559	2.4835	0.10	2	0.3645	0.18227	2.2944	0.12
Eb	27	13.6541	0.50571			27	2.1450	0.07944		
Peak force along z-axis						Mean force along z-axis				
Factor	DF	Sum Sq	Mean Sq	F-value	p-value	DF	Sum Sq	Mean Sq	F-value	p-value
Force	2	0.3476	0.1782	0.4433	0.64	2	0.01303	0.006516	0.7452	0.48
Ea	18	7.0583	0.39213			18	0.15738	0.008743		
Location	1	0.0045	0.00445	0.0095	0.92	1	0.00351	0.003509	0.8884	0.35
Force:Location	2	1.5229	0.76143	1.6179	0.21	2	0.00709	0.003546	0.8976	0.41
Eb	27	12.7070	0.47063			27	0.10666	0.003950		
Peak moment around x-axis						Mean moment around x-axis				
Factor	DF	Sum Sq	Mean Sq	F-value	p-value	DF	Sum Sq	Mean Sq	F-value	p-value
Force	2	0.0905	0.04525	0.2452	0.78	2	0.7544	0.37719	2.7347	0.09
Ea	18	3.3216	0.18453			18	2.4826	0.13792		
Location	1	0.2831	0.28314	0.8939	0.35	1	0.0548	0.05476	0.1550	0.69
Force:Location	2	0.5129	0.25646	0.8096	0.45	2	0.0790	0.03948	0.1118	0.89
Eb	27	8.5527	0.31677			27	9.5355	0.3517		
Peak moment around y-axis						Mean moment around y-axis				
Factor	DF	Sum Sq	Mean Sq	F-value	p-value	DF	Sum Sq	Mean Sq	F-value	p-value
Force	2	0.1420	0.07101	0.2145	0.80	2	0.4615	0.23076	0.1441	0.86
Ea	18	5.9584	0.33102			18	28.8186	1.60103		
Location	1	3.0531	3.05309	8.1190	<0.01	1	0.3616	0.36157	0.3611	0.55
Force:Location	2	0.1792	0.08959	0.2383	0.78	2	0.9484	0.47422	0.4736	0.62
Eb	27	10.1531	0.37604			27	27.0359	1.00133		
Peak moment around z-axis						Mean moment around z-axis				
Factor	DF	Sum Sq	Mean Sq	F-value	p-value	DF	Sum Sq	Mean Sq	F-value	p-value
Force	2	2.6353	1.31766	1.4245	0.26	2	5.9178	2.95889	4.9126	0.01
Ea	18	16.6498	0.9249			18	10.8414	0.60230		
Location	1	0.0144	0.01440	0.0209	0.88	1	0.0880	0.08798	0.1863	0.66
Force:Location	2	2.8818	1.44091	2.0901	0.14	2	0.6562	0.32808	0.6947	0.50
Eb	27	18.6138	0.68940			27	12.7513	0.47227		

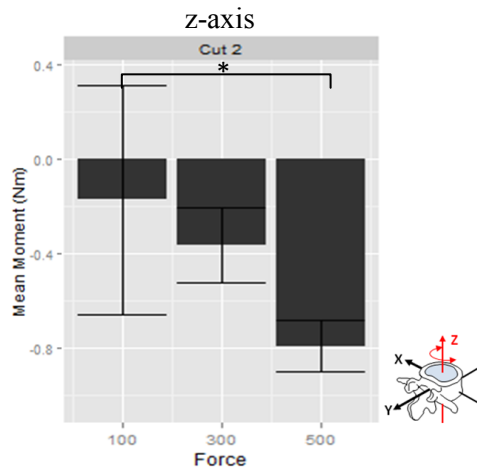


Figure 4.14 Force magnitude main effect of average (and standard deviation) mean moment around z-axis (axial rotation) for bilateral facet joints, capsules and ligamentum flavum.

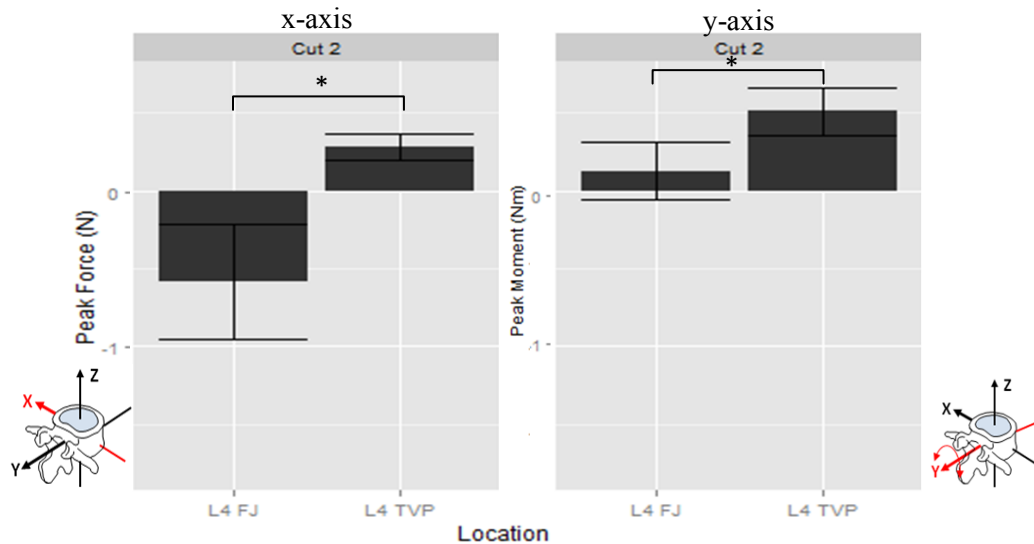


Figure 4.15 Application site main effect of average (and standard deviation) peak force along x-axis (lateral force) and peak moment around y-axis (lateral bending moment) for bilateral facet joints, capsules and ligamentum flavum.

#### 4.3.6 Cut 3: Intervertebral disc and anterior and posterior longitudinal ligaments (IVD)

Figure 4.16 shows the average of normalized peak and mean forces and moments experienced by IVD structures during the SMT application with each force magnitude at each application site. Generally, from the total loads experienced by the intact specimen, IVD structures experienced

about 2.3% of the peak forces, 2.6% of the mean forces, 58.1% of the peak moments and 77.7% of the mean moments (Figure 4.8).

#### *4.3.6.1 Interaction effects*

For the IVD structures, although a statistically significant interaction between force magnitude and SMT application site in flexion extension moment (peak moment around x-axis) was observed (Table 4.8), post-hoc analysis did not reveal any significant pairwise comparison.

#### *4.3.6.2 Force magnitude main effect*

No significant force magnitude main effect was observed.

#### *4.3.6.3 Application site main effect*

Application site main effect did not reveal a statistically significance difference.

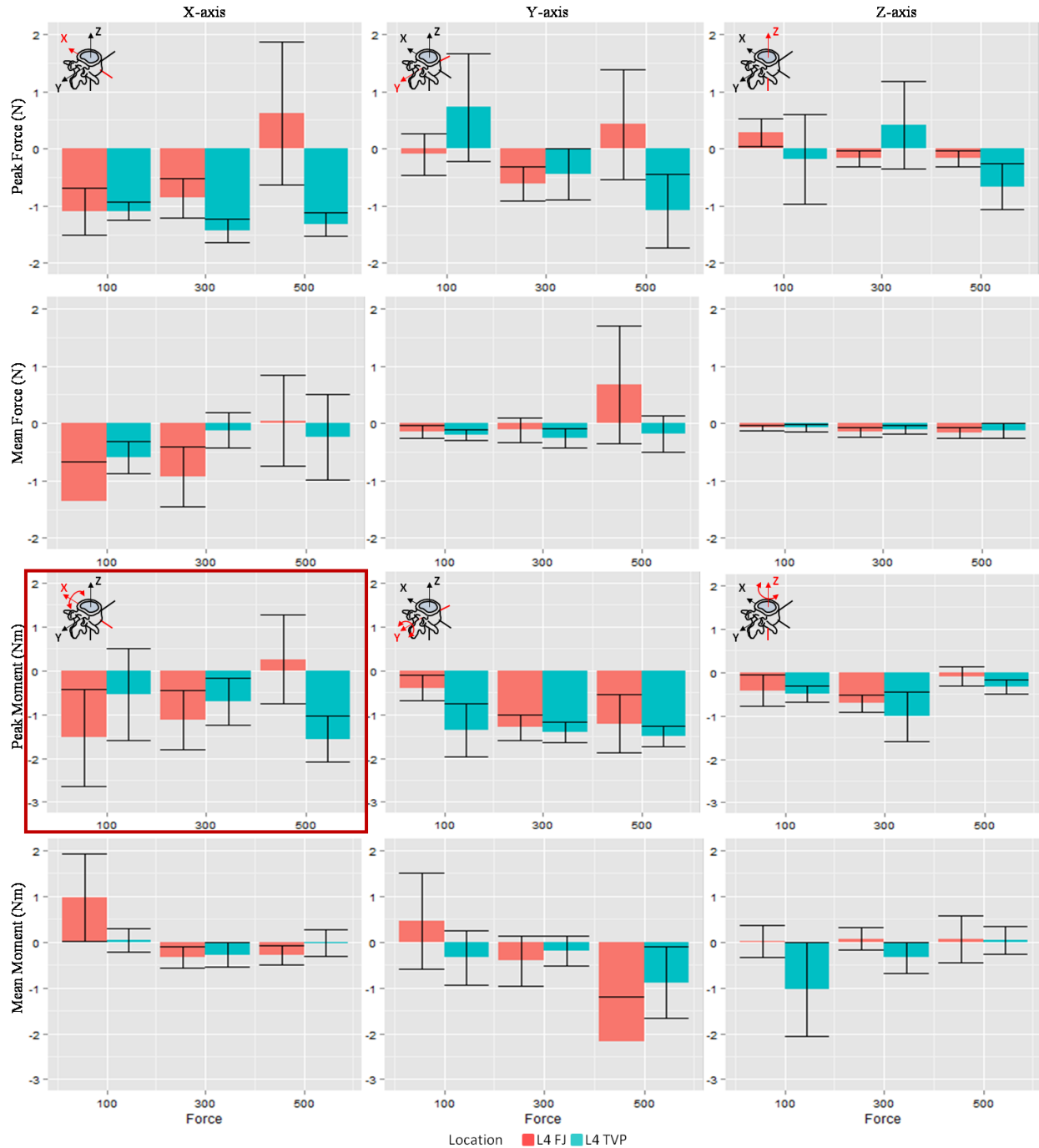


Figure 4.16 Average and standard deviation of normalized peak and mean forces and moments experienced by intervertebral disc and anterior and posterior longitudinal ligaments during the SMT application with different force magnitudes (bottom of each graph) at each application site (bar colors). A **red box** indicate significant interaction between force magnitude and application site effects.

**Table 4.8. Split plot ANOVA table for the intervertebral disc and anterior and posterior longitudinal ligaments**

Peak force along x-axis						Mean force along x-axis				
<i>Factor</i>	<i>DF</i>	<i>Sum Sq</i>	<i>Mean Sq</i>	<i>F-value</i>	<i>p-value</i>	<i>DF</i>	<i>Sum Sq</i>	<i>Mean Sq</i>	<i>F-value</i>	<i>p-value</i>
<i>Force</i>	2	7.925	3.9625	0.9616	0.40	2	7.784	3.8922	1.7808	0.19
<i>Ea</i>	18	74.148	4.1193			18	39.342	2.1857		
<i>Location</i>	1	10.453	10.4526	3.5390	0.07	1	2.835	2.8353	0.7488	0.39
<i>Force:Location</i>	2	10.039	5.0195	1.6995	0.20	2	3.838	1.9192	0.5069	0.60
<i>Eb</i>	27	79.746	2.9535			27	102.22	3.7863		
Peak force along y-axis						Mean force along y-axis				
<i>Factor</i>	<i>DF</i>	<i>Sum Sq</i>	<i>Mean Sq</i>	<i>F-value</i>	<i>p-value</i>	<i>DF</i>	<i>Sum Sq</i>	<i>Mean Sq</i>	<i>F-value</i>	<i>p-value</i>
<i>Force</i>	2	7.680	3.8402	0.7902	0.46	2	2.445	1.2223	0.6185	0.54
<i>Ea</i>	18	87.478	4.8599			18	35.751	1.9762		
<i>Location</i>	1	0.446	0.4464	0.1825	0.67	1	1.872	1.8715	1.7852	0.19
<i>Force:Location</i>	2	14.462	7.2312	2.9561	0.06	2	1.954	0.9771	0.9320	0.40
<i>Eb</i>	27	66.047	2.4462			27	28.306	1.0484		
Peak force along z-axis						Mean force along z-axis				
<i>Factor</i>	<i>DF</i>	<i>Sum Sq</i>	<i>Mean Sq</i>	<i>F-value</i>	<i>p-value</i>	<i>DF</i>	<i>Sum Sq</i>	<i>Mean Sq</i>	<i>F-value</i>	<i>p-value</i>
<i>Force</i>	2	3.317	1.6585	0.7519	0.48	2	0.0556	0.02779	1.2155	0.31
<i>Ea</i>	18	39.702	2.2057			18	0.4115	0.02286		
<i>Location</i>	1	0.233	0.2335	0.1040	0.74	1	0.0103	0.01026	0.9099	0.34
<i>Force:Location</i>	2	3.714	1.8568	0.8271	0.44	2	0.0042	0.00209	0.1852	0.83
<i>Eb</i>	27	60.612	2.2449			27	0.6044	0.0128		
Peak moment around x-axis						Mean moment around x-axis				
<i>Factor</i>	<i>DF</i>	<i>Sum Sq</i>	<i>Mean Sq</i>	<i>F-value</i>	<i>p-value</i>	<i>DF</i>	<i>Sum Sq</i>	<i>Mean Sq</i>	<i>F-value</i>	<i>p-value</i>
<i>Force</i>	2	1.461	0.7307	0.2286	0.79	2	0.7544	0.37719	2.7347	0.09
<i>Ea</i>	18	57.523	3.1957			18	2.4826	0.13792		
<i>Location</i>	1	3.301	3.3015	1.6622	0.20	1	0.0548	0.05476	0.1550	0.69
<i>Force:Location</i>	2	13.882	6.9410	3.4946	<b>0.04*</b>	2	0.0790	0.03948	0.1118	0.89
<i>Eb</i>	27	53.628	1.9862			27	9.5355	0.35317		
Peak moment around y-axis						Mean moment around y-axis				
<i>Factor</i>	<i>DF</i>	<i>Sum Sq</i>	<i>Mean Sq</i>	<i>F-value</i>	<i>p-value</i>	<i>DF</i>	<i>Sum Sq</i>	<i>Mean Sq</i>	<i>F-value</i>	<i>p-value</i>
<i>Force</i>	2	3.001	1.5003	0.9875	0.39	2	19.293	9.6466	2.6230	0.10
<i>Ea</i>	18	27.347	1.5193			18	66.199	3.6777		
<i>Location</i>	1	3.076	3.0759	2.6579	0.11	1	3.715	3.7153	0.8488	0.36
<i>Force:Location</i>	2	2.102	1.0509	0.9081	0.41	2	4.763	2.3814	0.5441	0.58
<i>Eb</i>	27	31.246	1.1573			27	118.183	4.3771		
Peak moment around z-axis						Mean moment around z-axis				
<i>Factor</i>	<i>DF</i>	<i>Sum Sq</i>	<i>Mean Sq</i>	<i>F-value</i>	<i>p-value</i>	<i>DF</i>	<i>Sum Sq</i>	<i>Mean Sq</i>	<i>F-value</i>	<i>p-value</i>
<i>Force</i>	2	4.3912	2.19562	1.9527	0.17	2	2.619	1.30969	0.4990	0.61
<i>Ea</i>	18	20.2397	1.12443			18	47.240	2.6244		
<i>Location</i>	1	0.6285	0.62854	0.6138	0.44	1	1.661	1.66109	1.0396	0.31
<i>Force:Location</i>	2	0.1380	0.06899	0.0674	0.93	2	0.739	0.36961	0.2313	0.79
<i>Eb</i>	27	27.6466	1.02395			27	43.139	1.59775		

\* - p-value &lt; 0.05

In summary, the interaction between SMT force magnitude and application site parameters with significant pairwise comparisons was only observed on the intact condition. Significant differences in loads due to force magnitude main effect were observed in the intact specimen and for SL and PJ structures. Application site main effect significantly influenced the intact specimen and PJ structures loading.

#### **4.4 Discussion**

This study aimed to describe the loading characteristics of cadaveric spinal tissues receiving SMT of different application parameters. The results demonstrate that SMT force magnitude and application site parameters influenced spinal tissues loading. The interaction effect between SMT force magnitude and SMT application site influenced the intact specimen in flexion and extension, while main significant effects were observed in all other axes. Specifically for unique spinal structures, while PJ structures were influenced by both force magnitude and application site main effects, SL structures were only influenced by SMT force magnitude. Sequential dissection revealed that lateral forces and moments experienced by SL and PJ structures were influenced by force magnitude and application site main effects respectively, and that axial moments experienced by PJ structures were also influenced by SMT force magnitude main effect. Overall, the results of this study suggest that SMT input parameters of force magnitude and application site significantly change SMT load distribution within spinal tissues and, consequently, the forces and moments experienced by the intact specimen and by spinal structures. Although several studies have been conducted investigating the effects of various SMT parameters on biomechanical and neurophysiological responses [28,30,34,45,56], this is

the first study to quantify the effect of changing SMT application parameters on spinal tissue response.

#### ***4.4.1 Methodological choices***

Significant differences in force-time profiles of manual SMT have been described in the literature [21,35,36]. It is thought that this variation in consistent application of manual SMT impedes systematic investigation of the effects of SMT parameters on various outcomes [35,36]. For this reason, a servo-controlled linear actuator motor (Linear Motor Series P01-48x360; LinMot, Inc, Zurich, Switzerland) was developed to standardize SMT force-time profiles and simulate a precise and repeatable SMT (average differences in applied peak force= $\leq 3$ N; correlation coefficient=0.98) [39]. In order to ensure that accurate and repeatable SMT force-time profiles were being applied, the current study used the Descarreaux device [39] to apply SMTs with specific parameters. In this way, it is more certain that the observed response of spinal loading is attributable to SMT parameters.

Based on these results from the first study of this dissertation, the sequence in which spinal structures are removed from the specimen influence the loads each structure experiences. Therefore, in order to avoid confounding load differences related to the sequence of structure removal, this experiment removed spinal structures from all the specimens following the same sequence: SL structures were removed first, followed by PJ structures, and IVD were the last structures to be removed [217].

#### ***4.4.2 Interpretation of Results***

##### *4.4.2.1 Vertebral displacements and rotations*

A posterior to anterior SMT thrust was applied at the overlying skin of the left L3/L4 FJ and L4 TVP and the resulting kinematics replicated for the intact specimen and following each cut. As expected, given the posterior to anterior direction of SMT application, the greatest vertebral translation was observed to occur in the postero-anterior axis (y-axis). Similarly, the greatest rotations were observed to occur around the x- (flexion-extension) and z-axes (axial rotation).

These results are in agreement with Kawchuk and colleagues (2010) [24] who applied manual SMT at the overlying skin of left L3 TVP. Kawchuk et al. [24] not only observed maximal translations in the posterior to anterior axis and greatest rotation around the medial-lateral axis (flexion-extension movement), but the magnitude of the anterior posterior displacement and flexion extension rotation were similar to the ones observed in the current study (Table 4.4). Despite these similar displacement and rotation, the rotation about z-axis observed in this study was similar in magnitude to the rotation about x-axis, and greater to the one observed by Kawchuk et al. [24]. These differing observations could be explained by the method used for SMT application. While a trained clinician applied manual SMT in the study conducted by Kawchuk and colleagues [24], our study used a servo-controlled linear actuator motor. In addition to possible force-time profile differences between manual and instrument-based SMT, the area of pressure through which the forces were applied in manual versus instrument-based SMT could additionally be the source of this observed difference in angular displacement. Although Kawchuk and colleagues [24] did not describe the position of the clinician's hand at the time of the SMT application, peak pressure migration and area of pressure distribution have been



associated with hand configuration during SMT application [218]. Given these results, it is possible that the use of a linear motor actuator created more focused and precise SMT which in turn created different angular displacements around z-axis. This suggests that in addition to SMT input parameters, other SMT characteristics, such as contact area and area of pressure distribution, may potentially play an important role in spinal tissue loading during SMT. Notwithstanding, despite the difference observed in rotation about z-axis (axial rotation), similar spinal loading magnitudes were observed on the displacements and rotations of the remaining axes (Table 4.4). This indicates that the SMT applied in the current study is representative of a clinical SMT application and, in regard to vertebral motion, the clinical implications of this study will only have a limitation on inferences regarding rotation around z-axis (axial rotation).

#### *4.4.2.2 Intact Specimen*

In the intact specimen, the interaction between 300 N and 500 N SMT magnitudes with a L4 TVP application site generated significantly greater peak flexion-extension moments (about x-axis) when compared to the other possible interactions (Figure 4.10A). In addition to the greater extension rotations caused by the application of 300 N and 500 N SMT at a TVP application site (Table 4.3), peak extension moments generally increased with greater SMT force magnitude as well as when SMT was applied at the TVP versus the FJ (Figure 4.8). Additionally, the anatomical position of L3/L4 FJ and L4 TVP gives SMT applied at the L4 TVP a mechanical advantage to producing greater moments. Therefore, by applying basic mechanical foundations and combining a longer moment arm with greater applied forces, greater moments are created in the intact specimen.

Interestingly, the interaction between L3/L4 FJ application site with 500 N force magnitude created a mean moment around the x-axis (flexion-extension moment) greater than all other interactions in this study (Figure 4.10B). While the measurement of peak moments is related to the maximum measured moment experienced during the SMT thrust phase only, the mean moments take into consideration the loads experienced during both preload and thrust phases of SMT. Therefore, when the moments experienced during the preload phase are taken into consideration, the interaction between 500 N force magnitude with L3/L4 FJ application site creates flexion-extension moments that are significantly greater. Related to the significance of preload characteristics, the study conducted by Nougrou and colleagues [57] observed that increasing forces of the preload phase significantly increased the sagittal vertebral displacement during this phase. Reed and colleagues [141] also reported preload phase parameters to influence muscle spindles responses. This indicates that SMT preload phase does not only influence neuromuscular and biomechanical responses [57,141], but also the loads experienced by the motion segment.

The significant interactions between 300 N and 500 N force magnitudes with L4 TVP application site and between 500 N force magnitude with L3/L4 FJ application site indicate that for the extension moments experienced by the intact specimen, SMT force magnitude is related to the location in which SMT is applied. Therefore, the combination of a specific force magnitude with a specific application site has a different effect than each main effect would have by itself. Consequently, future studies investigating the SMT input parameters of force magnitude and application site should consider both parameters and the interaction between them when designing the study.

Of note, only flexion-extension moments (moments around x-axis) experienced by the intact specimen were influenced by the interaction between force magnitude and application site effects. Peak and mean forces as well as moments around y- and z-axes were influenced by either force magnitude or application site main effects or both, but no interaction was observed. This observation, that main effects occur in most, but not all axes indicates that for those axes where force magnitude main effect was observed, spinal responses to SMT are not dependent on where these SMT forces are applied. Similarly, the specific spinal responses significantly influenced by SMT application site are not dependent on the SMT force magnitude. These observations indicate that for all peak and mean forces and moments around y- and z-axis, the combination of a specific force magnitude with a specific application site does not have a different effect than each main effect would have by itself.

Regarding the main effects in the intact segment, significant main effects were observed and only considered for variables in which the interaction effect was not significant. Specifically, significant force magnitude main effect was observed and SMT with greater force magnitudes increased all experienced peak forces and peak lateral and axial rotation moments. This demonstrates that generally, SMT with greater force magnitudes caused greater vertebral displacements, which is in agreement with previous observations reported by Keller et al. (2003) [46]. The current study goes further by demonstrating that in addition to the greater vertebral displacements, SMT with greater force magnitude also created greater loads in the intact specimen. Although our data support the intuitive rationale that greater vertebral displacements create greater loads in the specimen, this relation still needs to be further investigated as there

were occasions in which greater loads were not observed during great vertebral displacements. For example, although the application of a 100 N SMT at L3/L4 FJ caused the greatest lateral translation (displacement along x-axis) (Table 4.2), the forces experienced by the intact specimen along this axis (force along x-axis) was not the greatest force observed (Figure 4.9). Despite this, applying SMT with greater force magnitudes created greater peak forces in all directions as well as peak lateral bending and axial rotation moments in the intact specimen.

Regarding main effects in the intact segment, it was expected that the SMT application at TVP created greater moments than when applied at FJ. Additionally, greater vertebral axial rotation (rotation about z-axis) can be observed when SMT is applied at L4 TVP in comparison to when applied at L3/L4 FJ (Table 4.3). On the other hand, the superior-inferior forces experienced by the intact specimen were significantly greater when SMT was applied at FJ than at TVP. Table 4.3 shows that SMT application at L3/L4 FJ causes slightly greater vertebral superior translations than when applied at L4 TVP. One potential explanation for this finding is related to the existing natural pretension of the ligamentum flavum [97]. Heuer and colleagues [97] have observed a  $0.5^{\circ}$  change in lordosis angle following the transection of the ligamentum flavum indicating the presence of a natural pretension of this ligament. Therefore, it is possible that this pretension might assist the superior vertebral translation when SMT is applied at L3/L4 FJ. Therefore, while the SMT application at the TVP creates greater axial rotation moments, the SMT application at the FJ creates greater superior-inferior forces in the spinal segment.

#### *4.4.2.3 Cut 1: Supra- and interspinous ligaments (SL)*

Specifically, Table 4.3 shows the displacements of L4 vertebra in relation to L3 during the application of each SMT trajectory. Force magnitude main effect was the only significant effect observed to influence SL structures, an effect limited to lateral forces and moments. A previous study conducted by Heuer and colleagues [97] support our findings that the SL structures contribute to resisting lateral bending moments. Unexpectedly and paradoxically, SL structures experienced significantly greater lateral force (mean force along x-axis) and lateral bending moment (peak moment around y-axis) with lesser (100N), not greater SMT application (500 N). Specifically, 100 N SMT trajectories caused greater lateral translation (displacement along x-axis) and rotation (rotation around y-axis) than the 500 N SMT trajectory. Although the underlying mechanism to this paradoxical relation is not forthcoming from our data, it can be speculated that when SMT is applied with greater force magnitudes, additional spinal structures, (e.g. facet joints) are engaged thereby changing the resulting vertebral movement as well as taking over the loads previously experienced by SL structures.

In summary, although SL structures experience greater loads when SMT is applied with smaller force magnitudes, the amount of load borne by SL structures remains smaller in magnitude than the ones borne by the LF and IVD structures.

#### *4.4.2.4 Cut 2: Bilateral facet joints, capsules and ligamentum flavum (PJ)*

Both force magnitude and application site main effects significantly influenced loads experienced by PJ structures. Specifically for the force magnitude main effect, moments around z-axis (axial rotation moment) were significantly smaller when SMT was applied with 100 N

than the ones experienced during the 500 N SMT. This agrees with the previous speculation that as greater force magnitudes of SMT are applied, facet joints (and potentially ligamentum flavum) become engaged and change the resulting vertebral motion and spinal loads.

Application site main effect was also observed to significantly affect the relative load experienced by the PJ structures. For these structures, SMT applied at L4 FJ created relative peak lateral forces (along x-axis) in the opposite direction than the ones created when SMT was applied at L4 TVP. Given that the SMT application at L3/L4 FJ and at L4 TVP caused lateral translations in the same direction (Table 4.3), the reason for PJ structures to experience lateral forces (along x-axis) in opposite directions it is not completely understood. One potential explanation for this finding is related to the previously described natural pretension of the ligamentum flavum [97]. Given that 1) SMT application causes a complex movement involving 3-dimensional translations and rotations [125], 2) SMT was applied unilaterally at the left L3/L4 FJ and TVP, and 3) ligamentum flavum is included in the PJ structures, it is possible to speculate that given the combination of translations and rotations caused by SMT at each application site, ligamentum flavum pretension influences SMT loading distribution and alters loads experienced by PJ structures. Specifically, it is possible that when SMT was applied at L3/L4 FJ, the ligamentum flavum pretension imposed a greater resistance to the lateral displacement creating a lateral force in the opposite direction compared to SMT application at L4 TVP. Additionally, Table 4.3 shows that despite being in the same direction, the SMT application at L3/L4 FJ created lateral vertebral translations slightly greater than when applied at TVP. Therefore, given the oblique orientation of the facet joints in the lumbar spine [219,220], it is possible that this

slight vertebral translation increase caused a greater contact between facet joints surfaces, increasing the lateral forces borne by the PJ structures.

On the other hand, PJ structures experienced greater peak lateral bending moments (around y-axis) when SMT was applied at L4 TVP than at L3/L4 FJ. Previous studies have reported lateral displacements and rotations as a consequence of SMT application [104,125,126]. Given the anatomical position of L3/L4 FJ and L4 TVP, and the length of the moment arm when SMT is applied at each of these application sites, greater moments experienced by PJ structures when SMT is applied at L4 TVP (longer moment arm than L3/L4 FJ) were expected. Keller and colleagues (2003) [46] have described that the observed 3-dimensional vertebral motions during the SMT application is influenced by the location in which SMT is applied. Although specific lateral bending was not greatly different between L3/L4 FJ and L4 TVP SMT application sites in the current study, the total movement resulting from the combination of translations and rotations along and around all 3 Cartesian axes potentially play a significant role in loading PJ structures when SMT is applied at different application sites. This suggests that the resulting vertebral motion arising from the application of SMT at different application sites influence the SMT load distribution.

In summary, PJ structures experienced greater loads when SMT was applied with greater force magnitudes and when applied at the TVP. With the exception of mean moments around z-axis, from the total loads experienced by the intact specimen, the overall loads borne by posterior joint structures were smaller than the ones borne by IVD structures.

#### *4.4.2.5 Cut 3: Intervertebral disc, anterior and posterior longitudinal ligaments (IVD)*

While statistical analysis revealed a significant interaction in the normalized relative peak flexion-extension moments experienced by IVD structures, post-hoc testing did not reveal any significant pairwise comparison. Significant interactions with no significant pairwise comparisons may be observed when the interaction between effects are significant in the overall test, but the difference between specific levels of effects during pairwise comparisons are not large enough to reach the predetermined level of significance [221]. This indicates that there might be a trend with potential interaction between force magnitude and application site effect on peak flexion extension moments (moments around x-axis) that our study did not identify, most likely due to the small sample size. Therefore, future studies with larger sample size should be conducted to investigate this trend. Loads experienced by IVD structures were also not influenced by either force magnitude or application site main effects. Despite this, from the total loads experienced by the intact specimen, generally, the IVD were the structures that experienced the greatest loads. This finding is in accordance to the previous study conducted by Kawchuk et al. (2010) [24] and indicate that by adjusting SMT input parameters of force magnitude and application site, it might not be possible to specifically target or avoid one particular spinal structure without concurrently loading the IVD structures. Nevertheless, this exploratory study has demonstrated that by applying SMT with different force magnitudes and at different application sites, the SMT resulting load distribution within spinal tissues is altered.

#### *4.4.2.6 General Discussion*

In the intact specimen, although differences in spinal forces and moments were observed when SMT was applied with 100 N, 300 N and 500 N, the observation of significant differences in



loads experienced by SL and PJ structures when SMT with different force magnitudes were applied were only present in specific axes of movement and when a 100 N force magnitude was compared to 500 N. For these structures, the comparison between 100 N with 300 N and 300 N with 500 N force magnitudes did not reveal any significant difference in experienced loads. This indicates that a difference of applied forces greater than 200 N is required to influence the loads experienced by spinal structures.

Despite the observation that greater loads were generally observed when greater vertebral displacements were also present, some exceptions could be observed. For example, even though the application of 100 N SMT at L3/L4 FJ caused the greatest lateral translation (displacement along x-axis) and lateral bending rotation (rotation about y-axis) (Table 4.3), the forces in the intact specimen along x-axis and the moments about y-axis were not maximal (Figure 4.8). Similarly, even though lateral translations occurred in the same direction when SMT was applied at L4 TVP and at L3/L4 FJ, the PJ structures experienced lateral forces in opposite directions. Likewise, Kawchuk and colleagues (2010) [24] observed that the axis presenting greater displacements were not the same axes experiencing the greater loads. This demonstrates that greatest vertebral displacement is not always associated with greatest loading; a result most likely explained by different anatomic connections and boundaries between axes. This suggests that some displacements and rotations caused by SMT application occur within the neutral zone, where vertebral motion is produced with minimal resistance [222]. As neutral zone has been described to be a result of the nonlinear load-displacement curves presented by biological structures [222], this indicates that the nonlinear, time-dependent behavior of spinal structures also play an important role on the SMT load distribution. Even when greater vertebral

displacements are produced, if they exist within the neutral zone of the motion segment, small loads will result.

This study analysed the peak and mean forces and moments experienced by intact specimen as well as spinal structures during the SMT application with different input parameters of force magnitude and application site. While peak forces and moments correspond to the maximum load during the SMT thrust phase only, the mean forces and moments reflected on the overall loads as it is the average of loads during both preload and thrust phases. In addition to the different outcome they represent, peak and mean forces and moments showed considerable difference in magnitude with the peak loads generally having greater magnitudes and, consequently, more evident effect sizes.

Although no significant pairwise comparisons was observed, statistical analysis revealed a significant interaction between SMT force magnitude and application site only for mean flexion extension moments of the IVD structures suggesting a trend to be further investigated. No significant interaction between SMT force magnitude and application site was observed for SL and PJ structures. This indicates that for those spinal structures, the effects of force magnitude and application site are independent from each other and that the effect of one does not change the effect of the other.

Interestingly, considerably different displacements and rotations were observed when SMT was applied with different input parameters of force magnitude and application site (Table 4.3). Specifically, while most of the great translations and rotations were caused by greater force

magnitudes, greater lateral translation and rotation were caused by smaller SMT force magnitudes. Additionally, the SMT application at L4 TVP caused greater vertebral displacements and rotation only in specific axes (e.g. translation along y-axis and rotation about z-axis). This indicates that SMT input parameters of force magnitude and application site not only significantly influence on SMT load distribution within spinal structures, but also influences the coupled motion of the spinal segment. It is possible that SMT input parameters of force magnitude and application site affect spinal structures engagement as well as the length of moment arms created, influencing the resulting vertebral motion.

Given that this was the first study to investigate the differences in spinal structures loading characteristics due to the different SMT input parameters of force magnitude and application site, a comparison to existing literature is limited. Results from the current study indicate that SMT force magnitude and application site parameters influence the resulting complex 3-dimensional vertebral motion as well as the loading distribution within spinal tissues and, consequently, the loads spinal structures experience during SMT.

Of note, given the findings of the first study of this dissertation (Chapter 3), the results of the current study is limited to the order in which structures were removed from the specimen during biomechanical testing. By changing the order of structure removal, the loading characteristics experienced by spinal structures during SMT with different force magnitudes and application site would also be changed. Given the composition and biomechanical function of spinal structures investigated here, it is possible to speculate that structure removal order will not significantly

impact the loading characteristics of spinal structures. Nevertheless, future studies are needed to quantify the load difference when different orders of structure removal are used.

#### *4.4.2.5 Clinical implications*

Based on the results of this study, the application of SMT with different force magnitudes and at different application sites alter the loading distribution within spinal tissues.

Generally, for the intact spinal segment, greater SMT force magnitude created greater forces and moments, while applying greater force magnitudes at L4 TVP and at L3/L4 FJ increases the maximum and the overall (respectively) flexion-extension moment experienced by the intact specimen. In addition, the SMT application at L4 TVP created greater lateral bending and axial rotation moments and smaller superior-inferior forces while application at the FJ created greater superior inferior forces.

For SL structures, SMT with smaller force magnitudes created greater lateral loads. Alternatively, in order to avoid loading SL structures, SMT with greater force magnitudes are recommended.

For PJ structures, greater force magnitudes created greater axial rotation moments. The SMT application at L4 TVP created greater lateral bending moments. Alternatively, in order to avoid loading PJ structures, SMT with smaller force magnitudes should be applied.

Force magnitude and application site did not influence the loads experienced by IVD structures. It may not be possible to avoid loading IVD structures by changing SMT force magnitudes and application site parameters. Figure 4.17 summarizes the abovedescribed clinical implications. Noteworthy, given that the current study was conducted using porcine cadaveric models, the clinical implications described here are speculative and further clinical studies are needed to verify their application to human spines.







































Spinal Structure	SMT input parameter	Loading	Vertebral motion
 Whole Segment	 Force Magnitude	 All forces All moments	 Ant-post/sup-inf translation Flex-ext/axial rotation  Lat translation Lat bending
	 TVP	 Ant-post/lat forces Lat Bend/axial rot. moment	 Ant-post translation Flex-ext/axial rotation
	 FJ	 Sup-inf forces	 Lat translation
 Posterior Ligaments <small>From whole segment total, generally carry: 0.2% peak forces; 0.7% mean forces 3% peak moments; 7.2% mean moments</small>	 Force Magnitude  FJ or TVP	 Lat forces Lat bend. moment  No specific effect	
 Facet complex + Lig. Flavum <small>From whole segment total, generally carry: 0.1% peak forces; 1.4% mean forces 2.1% peak moments; 75% mean moments</small>	 Force Magnitude  TVP	 Axial rot. moment   Lat forces Lat Bend moments	
 Disc + Longitudinal ligs. <small>From whole segment total, generally carry: 2.3% peak forces; 2.6% mean forces 58.1% peak moments; 77.7% mean moments</small>	Are always loaded. SMT force magnitude and application site did not increase/decrease loads.		
<b>To Avoid:</b>	<b>SMT input parameter</b>	<b>Loading</b>	
 Whole Segment	 Force Magnitude	 All forces All moments	
	 TVP	 Sup-inf forces	
	 FJ	 Ant-post/lat forces Lat Bend/axial rot. moment	
 Posterior Ligaments	 Force Magnitude  FJ or TVP	 Lat forces Lat bend. moment  No specific effect	
 Facet complex + Lig. Flavum	 Force Magnitude  FJ	 Axial rot. moment   Lat forces Lat bend moments	
 Disc + Longitudinal ligs.	Are always loaded. SMT force magnitude and application site did not increase/decrease loads.		

Figure 4.17 Summary of clinical implications

#### **4.4.3 Limitations**

First, a porcine cadaveric model was used. Although porcine lumbar spine models have been described to be suitable alternative to human spines [93,95,146], anatomical and biomechanical differences can be observed. Therefore, the extrapolation of these results to human spines are limited. Second, by using cadaveric models limitations associated with differences between *in vivo* and *in vitro* conditions such as physiological and muscular effects, and potential differences in repeated loading testing are also present. Third, given the results of the first study of this dissertation, the loads here observed are specific to the order in which spinal structures were removed from the specimen. Fourth, this was an exploratory study initiating scientific investigations regarding the effect of SMT input parameters of force magnitude and application site on spinal tissues load distribution. More research is necessary to further investigate these parameters as well as other SMT input parameters, such as thrust duration and loading rate.

#### **4.5 Conclusion**

Based on the findings of this study, SMT input parameters of force magnitude and application site significantly influence the distribution of forces and moments within the motion segment. Consequently, forces and moments experienced by the intact L3/L4 spinal segment, and SL and PJ structures were significantly influenced by force magnitudes and application site parameters of SMT. Given the findings of this study that smaller force magnitudes may influence some spinal structures and greater force magnitudes may influence others, a 300 N force magnitude was chosen for the following studies of this dissertation.

## **Chapter 5.**

### **Spinal tissues loaded by spinal manipulative therapy (SMT).**

#### **Part II: the influence of application site**

##### **5.1 Introduction**

Randomized controlled trials investigating spinal manipulative therapy (SMT) have reported conflicting evidence. While some studies observed significant improvement in low back pain patients following SMT interventions [101,105–107], other studies reported that SMT was not significantly superior to other types of intervention (e.g. exercise; standard medical care) [108–110]. While this conflicting evidence can be explained partially in light of recent findings that suggest SMT affects some, but not all low back pain patients [111], another explanation is that variability in SMT application may create varied responses to SMT [21]. Similar to other treatment parameter that have been described to significantly affect the outcome of physical interventions such as dosage and application site [223–225], SMT input parameters likely modulate the physiological outcomes following a SMT application.

Specifically, SMT input parameters have been reported to significantly vary between clinicians and applications [36,43,226]. With respect to application site, previous investigations have reported not only the limited ability of manual therapists to accurately identify the site of application [40,41,226], but also that the location in which SMT is actually applied may shift about 10 mm during SMT application [142]. Based on that, basic and clinical research has been conducted to assess the influence of SMT input parameters on both biomechanical and neurophysiological responses to SMT. Specifically, Colloca & Keller [49] observed differences



in electromyographic response (EMG) of the erector spinae muscle when SMT was delivered at the spinous or transverse process of different spinal levels. Additionally, while Reed and colleagues [44] demonstrated that the site in which SMT was applied significantly affected muscle spindles sensory input, a biomechanical study conducted by Edgecombe and colleagues [45] showed significant changes in spinal stiffness related to SMT application site.

Although the abovementioned findings indicate that SMT application site significantly affects the physiological outcomes elicited by SMT, many other SMT parameters have yet to be studied including SMT loading characteristics as they relate to influencing specific spinal tissues. By elucidating the SMT load distribution within spinal tissues when SMT is applied at different application sites, the relation between SMT application site and spinal tissue response could be defined. Importantly, if it can be shown that the SMT application at specific sites preferentially load particular spinal structures, then SMT could be provided to a specific location tailored to each individual's condition, improving SMT efficacy and safety.

Given the above, the objective of this study was to describe the effect of a standardized SMT application on load distribution within spinal tissues as a function of application site. Specifically, this study aimed to describe if the application of a SMT with standardized force provided at different application sites (including adjacent spinal segments) influenced loads experienced by spinal structures.

## **5.2 Methods**

### ***5.2.1 Overview***

The methodology used in this study was previously described in detail in Chapter 4 of this dissertation. Briefly, a linear actuator motor was used to provide a standardized application of SMT at 6 distinct application sites of the lumbar spine. The resulting SMT vertebral motions were tracked by an optical system and then replicated by a parallel robotic platform. By combining kinematics replication and serial dissection, the forces and moments experienced by spinal tissues were recorded using a 6 degrees-of-freedom load cell and analysed.

### ***5.2.2 Sample Size Calculation***

The sample size calculation was conducted based on the data previously reported by Kawchuk and colleagues (2010) [24] using the General Power Analysis Program (G\*Power 2) (University of Trier, Germany). With a statistical power was set at 0.80 (80%), two-tailed tests with level of significance set at  $\alpha=0.05$  (5%) and an effect size of 0.99-1.2, a sample size of 9 porcine models was required. Five additional porcine models were included to account for possible specimen loss due to data collection, potting procedure or testing complications and a total of 14 cadaveric porcine specimens were included. Given that the study from Kawchuk and colleagues also observed 12 variables, the use of the effect size reported by these authors for the current sample size calculation is appropriate. Therefore, with a level of significance set at 0.05 and statistical power set 0.80, the chances of having types I and II errors were 5% and 20%, respectively.

### 5.2.3 Specimen Preparation

Thirteen fresh porcine cadavers (Duroc X [Large White X Landrace breeds]) of approximately 60-65 kg were used in this study (one specimen was excluded due to calibration error and consequent robotic testing complication). In each intact porcine cadaver, bone pins were drilled into the L3 and L4 vertebral bodies and a rectangular flag having 4 infrared light-emitting diode markers was attached to the exposed end of each bone pin (Figure 5.1). Following SMT application to the intact porcine cadaver (detailed in the following section), the lumbar spine was removed *en bloc* [24]. The L3/L4 spinal segment was cleaned of non-ligamentous tissues, sealed in a plastic bag and kept refrigerated at 3°C until potting and testing on the following day [213]. The specimen was kept moist with physiologic saline throughout preparation, embedding and testing [170,178].

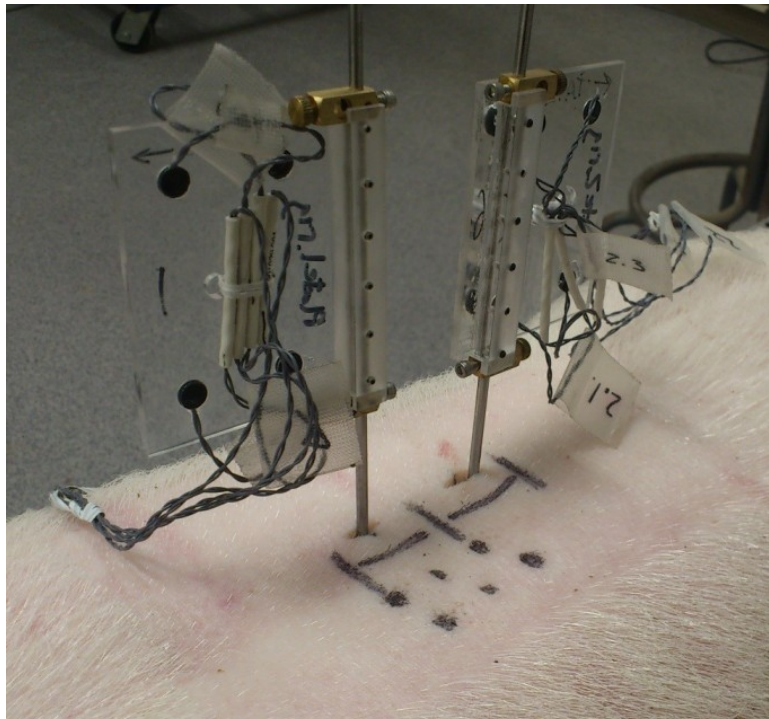


Figure 5.1 Rectangular flags with 4 infrared light-emitting diode markers attached to bone pins drilled into L3 and L4 vertebrae.

#### ***5.2.4 Spinal Manipulation***

Ultrasonic imaging and needle probing were used to identify skin locations of 6 distinct anatomic landmarks used as application sites: L2/L3 facet joints (FJ), L3/L4 FJ, L3 transverse process (TVP), L4 TVP, the space between those FJs (BTW FJ) and the space between those TVPs (BTW TVP). In order to minimize the known and significant SMT force-time profile variance that occurs within clinical SMT [21], this study used a servo-controlled linear actuator motor [39] to apply all SMTs (Appendix II). This device provided a posteroanterior spinal manipulative thrust with peak force magnitude chosen from data provided in Chapter 4. Specifically, given that low force magnitude SMT (100 N) influenced some spinal structures and greater SMT force magnitudes (500 N) influenced others, a 300 N force magnitude was selected to best affect all possible spinal tissues. Therefore, all SMT in this study was provided with a peak force magnitude of 300 N with a preload adjusted to be 10% of the peak force (30 N) and the slope of the force curve from preload to peak load being 2.6 N/ms with a time to peak of 112.5 ms.

#### ***5.2.5 Kinematic Recording***

During the application of SMT at each site, the resulting motion of L3 and L4 was captured by an optical tracking system that recorded the movement of each bone pin/sensor flag in 3 dimensions at a rate of 400 Hz (0.01 mm system resolution with 0.15 mm rigid body resolution; NDI, Waterloo, Canada) (Appendix III).

### **5.2.6 Potting Procedure**

This study followed the standardized potting procedure described in the previous chapter where specimens were potted in a vertical orientation using dental stone (Modern Materials, South Bend, IN) with the intervertebral disc positioned parallel to the horizontal plane (Figure 5.2).



Figure 5.2 Standardized potting procedure and L3/L4 spinal segment.

### **5.2.7 Robotic Testing**

Following the potting procedure, robotic testing was conducted as previously described in Chapter 4. In brief, the caudal end (L4) of the potted spinal segment was fixed to a 6-axis load cell (AMTI MC3A-1000, Advanced Mechanical Technology, Inc., Watertown, MA) and the load cell mounted rigidly to a parallel robotic platform (Parallel Robotics Systems corp., Hampton, NH). A calibration process was performed [216] (Appendix IV) resulting in 6 robotic trajectory files consisting of a series of commands corresponding to the vertebral trajectories during SMT application at each of the 6 different application sites. The robot accepts commands less frequently than data points are generated by the optical system. Therefore the robotic command

files were re-sampled to move the robotic platform in displacement control method reproducing the path of each SMT previously recorded. Given the safety settings of the robot, the SMT path replication was approximately 10% slower than the original SMT application. The cranial end of the potted specimen was then fixed to a stationary cross beam and the segment positioned in the initial neutral position.

Starting from this initial neutral position, SMTs were replayed in the robot in the following sequence from cranial to caudal and from medial to lateral: L2/L3 FJ, BTW FJs, L3/L4 FJ, L3 TVP, BTW TVP, and L4 TVP. Each SMT replication by the robot was separated by a 2 minutes recovery time as it was the minimum time necessary to perform all the tasks between tests (saving data, removing spinal structures, setting up for next test) and satisfied the minimum time for loads to return to baseline [24]. Based on feasibility tests performed by Kawchuk and colleagues (2010) [24], 3 pre-conditioning trials were executed prior to testing.

The forces and moments experienced by the specimen during robotic replication of SMT movements were recorded (axes of movement: x = medial/ lateral, y = anterior/posterior, and z = superior/inferior). Following the robotic replication of the SMT trajectories, spinal structures were removed and/or transected from the specimen and the same 6 trajectories repeated in the same order by the robot. Based on the findings reported by Funabashi et al. (2015) [217] that the order in which structures are removed from the specimen influence their loading characteristics, spinal structures were removed/transected (via scalpel unless otherwise noted) in the same order from all specimens: 1) supra- and interspinous ligament (SL), 2) bilateral facet capsules, facet

joints (via rongeur) and ligamentum flavum (PJ), 3) intervertebral disc and anterior and posterior longitudinal ligaments (IVD).

### **5.2.8 Data Analysis**

#### *5.2.8.1 Overview*

Similar to Chapter 4, this study analysed 12 dependent variables corresponding to the peak and mean forces and moments measured and recorded along and around each of the 3 Cartesian axes, in 4 conditions independently observed (intact and following the removal of spinal structures). In contrast to the previous chapter, this study investigated only 1 independent variable: SMT application site.

#### *5.2.8.2. Data Processing*

Detailed data extraction and processing was described in the previous chapter of this dissertation (Chapter 4). Briefly, baseline forces and moments were considered to be those recorded when the specimen was positioned in the same initial position as in its *ex vivo* state. The resulting forces and moments for each SMT trajectory of each specimen were plotted against time for each condition (intact and following the removal of spinal structures) and peak and mean forces and moments along and around each axis (x-, y-, z-axes) identified by customized software (LabVIEW, National Instruments, Austin, TX). Like Chapter 4, relative peak and mean forces and moments experienced by spinal structures were normalized to the respective load experienced by the intact condition during the application of each SMT trajectory. Table 5.1 presents the description of conditions and variables, and the definition of included dependent

variables. The magnitude of displacements (translation and rotation) where peak forces and moments occurred was also identified by the customized software.

**Table 5.1. Description of conditions and variables used throughout the chapter**

Term	Definition
Condition (n=4)	State in which specimens were tested. This study investigated 4 different conditions: 1. Intact specimen, 2. after cut 1 where supra- and interspinous ligaments (SL) were removed, 3. after cut 2 removing bilateral facet joints, capsules and ligamentum flavum (PJ) and 4. after cut 3 removing intervertebral disc and anterior and posterior longitudinal ligaments (IVD).
SMT input parameter (n=6)	Characteristics the SMT force. In this study, application site parameter was included (L2/L3 and L3/L4 facet joints, L3 and L4 transverse processes and the interspace between those facet joints and transverse processes).
Independent variable	Variable under investigation. In this study, independent variable is SMT application site.
Dependent variable	Measured variable, outcome. In this study, dependent variables are peak and mean forces and moments along and around all 3 axes of movement, respectively.
<ul style="list-style-type: none"> <li>• Peak forces and moments</li> </ul>	maximum measured force and moment during the SMT thrust phase
<ul style="list-style-type: none"> <li>• Mean forces and moments</li> </ul>	average value of forces and moments involving both the preload and thrust phases of SMT

### 5.2.8.3 Statistical Tests

As the objective of this study was to describe the effects of SMT application site on spinal tissues loading, each condition (intact specimen and following the removal of spinal structures) was analyzed independently. Given that all 6 locations were applied on the same specimen, each SMT application at a different application site was considered a repeated measure. Therefore, for the intact specimen, a repeated measures multivariate analysis of variance (MANOVA) was conducted followed by a Bonferroni post-hoc analysis for pairwise comparisons. For the analysis of loads experienced by each spinal structure, a MANOVA was conducted for the regression coefficients. A Tukey post-hoc test was performed for the multiple pairwise comparisons of the removed spinal



structures. Statistical tests were performed combining IBM SPSS Statistics for Windows, Version 22.0 (Armonk, NY: IBM Corp.) and R: A language and environment for statistical computing (R Foundation for Statistical Computing, Vienna, Austria).

## **5.3 Results**

### ***5.3.1 Overview***

Overall, SMT application site significantly affected the loads experienced by spinal structures. Generally, forces and moments experienced by the intact specimen and spinal structures changed significantly in terms of direction when SMT was applied at adjacent spinal levels and significantly decreased when SMT was applied between vertebrae.

### ***5.3.2 General descriptive statistics***

Given a non-parametric distribution of the resulting data, descriptive statistics include median and interquartile range (IQR). Median peak and mean forces experienced by the intact specimen are shown in Figures 5.3 and 5.4, respectively. The median of normalized relative peak and mean forces experienced by spinal structures following each cut are also shown. Similarly, median peak and mean moments experienced by the intact specimen as well as the median of normalized relative peak and mean moments experienced by isolated spinal structures are shown in Figures 5.5 and 5.6, respectively. Only significant comparisons are shown and are identified according to the legend provided in each figure.

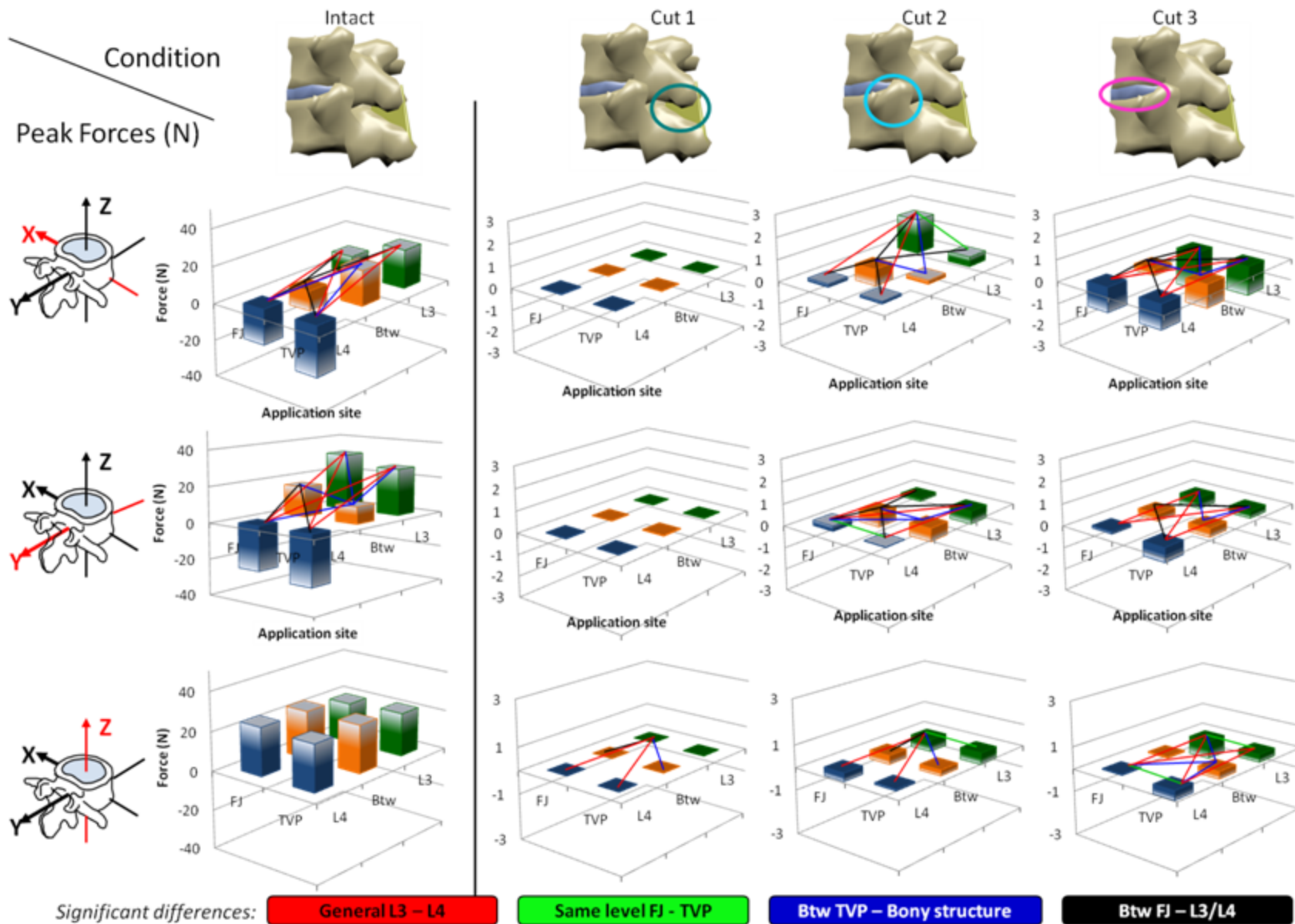


Figure 5.3 Median value of peak forces experienced by the intact specimen and median value of normalized peak forces experienced by spinal structures.

Only significant comparisons ( $p < 0.05$ ) are shown according to the legend: significant differences when SMT was applied at L3 or at L4 vertebrae are shown in **red**; differences when SMT was applied at the facet joint or the transverse process of the same vertebra are shown in **green**; differences when SMT was applied between L3 and L4 transverse processes in comparison to the remaining application sites are shown in **blue**; differences when SMT was applied between L2/L3 and L3/L4 facet joints in comparison to either facet joints or transverse processes of L3 or L4 vertebrae are shown in **black**. FJ=facet joint; TVP=transverse process; Btw=between; Cut 1=supra- and interspinous ligaments; Cut 2=bilateral facet joints, capsules and ligamentum flavum; Cut 3=intervertebral disc, anterior and posterior longitudinal ligament.

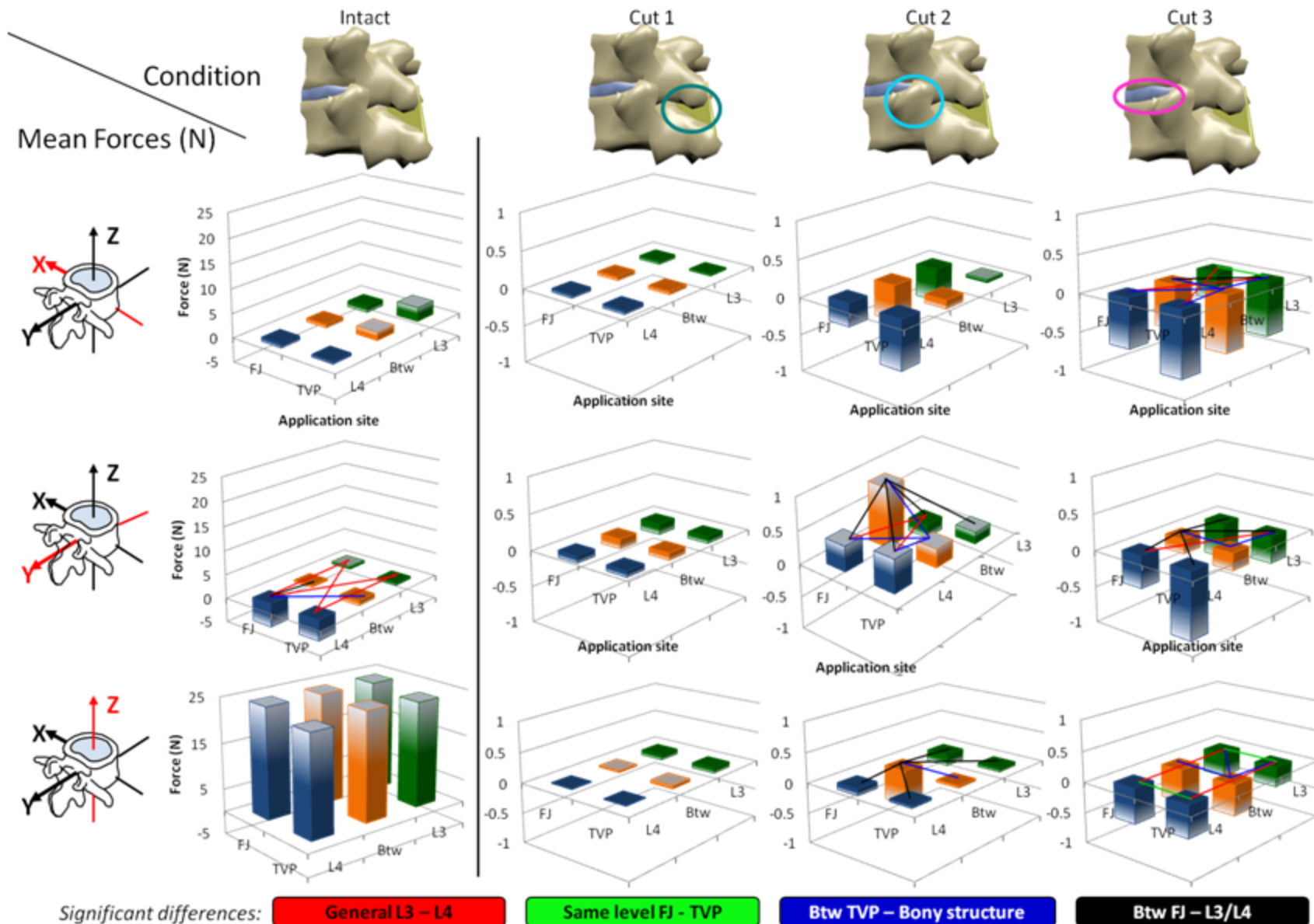


Figure 5.4 Median values of mean forces experienced by the intact specimen and median values of normalized mean forces experienced by spinal structures.

Only significant comparisons ( $p < 0.05$ ) are shown according to the legend: significant differences when SMT was applied at L3 or at L4 vertebrae are shown in **red**; differences when SMT was applied at the facet joint or the transverse process of the same vertebra are shown in **green**; differences when SMT was applied between L3 and L4 transverse processes in comparison to the remaining application sites are shown in **blue**; differences when SMT was applied between L2/L3 and L3/L4 facet joints in comparison to either facet joints or transverse processes of L3 or L4 vertebrae are shown in **black**. FJ=facet joint; TVP=transverse process; Btw=between; Cut 1=supra- and interspinous ligaments; Cut 2=bilateral facet joints, capsules and ligamentum flavum; Cut 3=intervertebral disc, anterior and posterior longitudinal ligament.

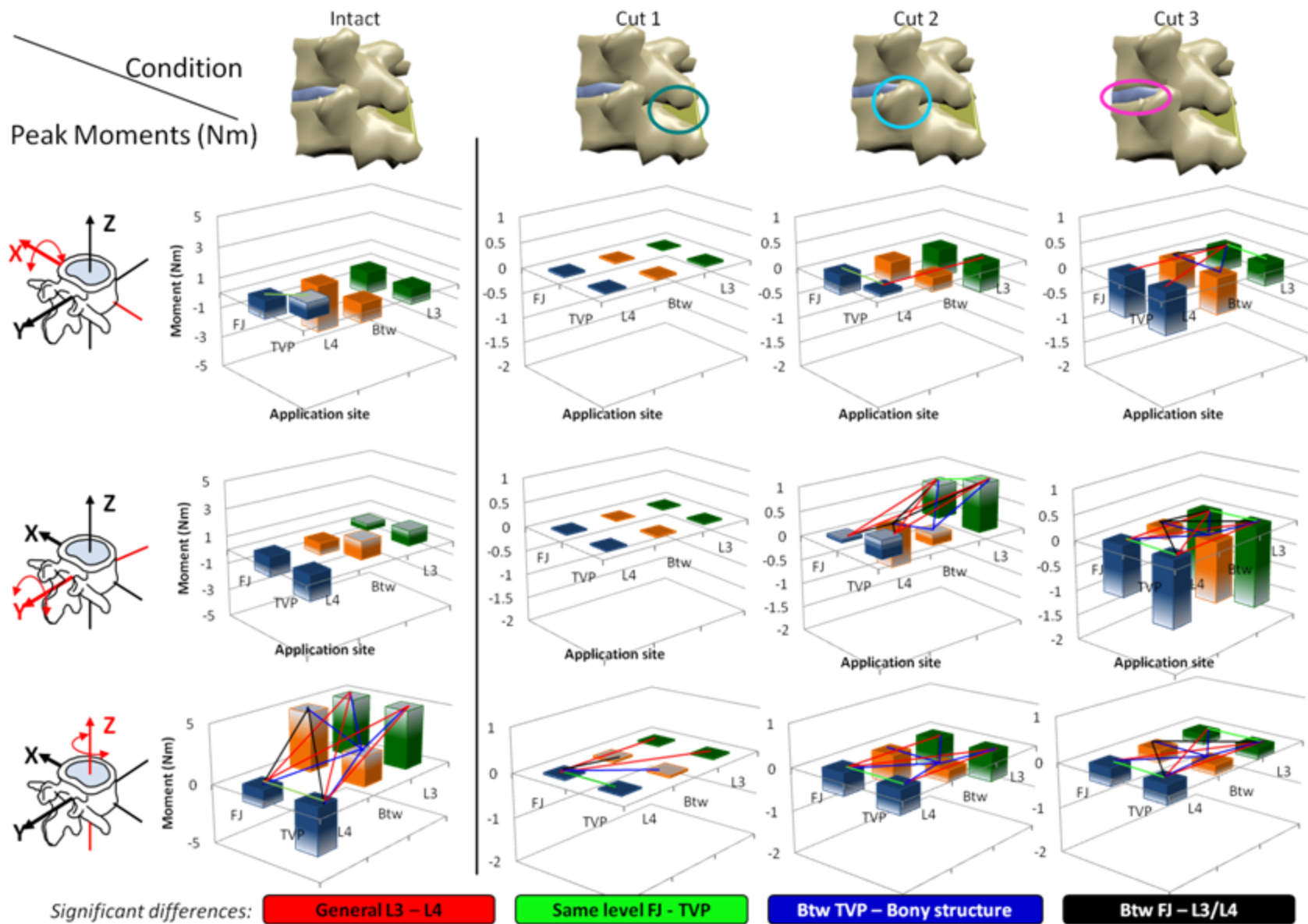


Figure 5.5 Median values of peak moments experienced by the intact specimen and median values of normalized peak moments experienced by spinal structures.

Only significant comparisons ( $p < 0.05$ ) are shown according to the legend: significant differences when SMT was applied at L3 or at L4 vertebrae are shown in **red**; differences when SMT was applied at the facet joint or the transverse process of the same vertebra are shown in **green**; differences when SMT was applied between L3 and L4 transverse processes in comparison to the remaining application sites are shown in **blue**; differences when SMT was applied between L2/L3 and L3/L4 facet joints in comparison to either facet joints or transverse processes of L3 or L4 vertebrae are shown in **black**. FJ=facet joint; TVP=transverse process; Btw=between; Cut 1=supra- and interspinous ligaments; Cut 2=bilateral facet joints, capsules and ligamentum flavum; Cut 3=intervertebral disc, anterior and posterior longitudinal ligament.



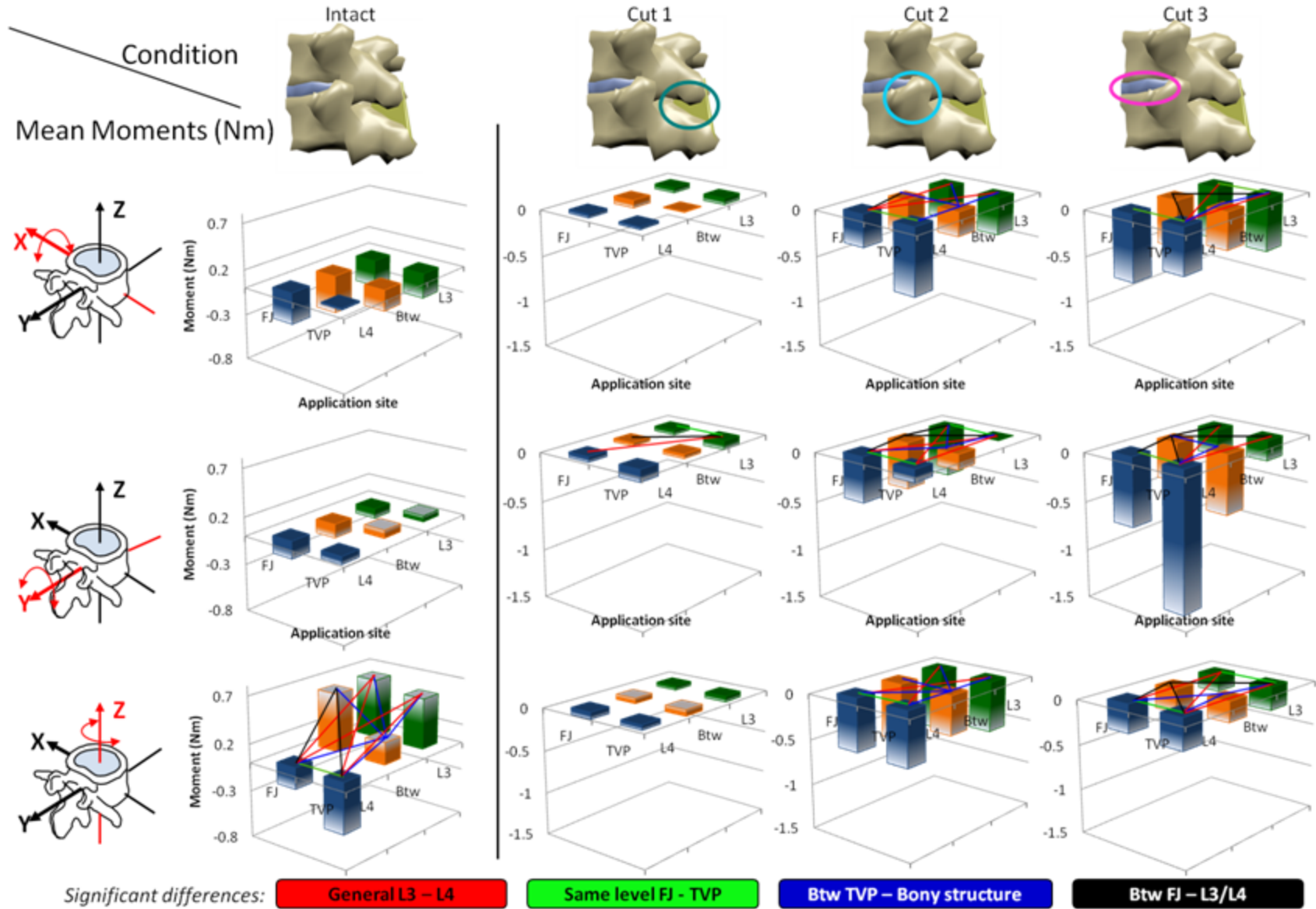




Figure 5.6 Median values of mean moments experienced by the intact specimen and median values of normalized mean moments experienced by spinal structures.

Only significant comparisons ( $p < 0.05$ ) are shown according to the legend: significant differences when SMT was applied at L3 or at L4 vertebrae are shown in **red**; differences when SMT was applied at the facet joint or the transverse process of the same vertebra are shown in **green**; differences when SMT was applied between L3 and L4 transverse processes in comparison to the remaining application sites are shown in **blue**; differences when SMT was applied between L2/L3 and L3/L4 facet joints in comparison to either facet joints or transverse processes of L3 or L4 vertebrae are shown in **black**. FJ=facet joint; TVP=transverse process; Btw=between; Cut 1=supra- and interspinous ligaments; Cut 2=bilateral facet joints, capsules and ligamentum flavum; Cut 3=intervertebral disc, anterior and posterior longitudinal ligament.

### 5.3.2.1 Vertebral displacements and rotations

The same vertebral displacements arising from each SMT application were replicated during robotic testing of all conditions. Relative L4 displacements (translations and rotations) in relation to L3 vertebra are shown in Table 5.2 by SMT application site and axis of movement. The greatest translation was observed in the y-axis (postero-anterior axis) (average: 5.33 mm  $\pm$ SD: 3.55) and the greatest rotation around the z-axis (axial rotation) (absolute average: 2.31°  $\pm$ SD: 0.93). Absolute values of vertebral displacements and rotations were used to calculate the overall average displacement and rotations including all application sites as negative values only indicate the direction of displacement and rotation on the axis of movement (bottom of Table 5.2). Table 5.3 shows the average ( $\pm$ SD) relative displacement and rotation of the present study, the study described in Chapter 4 and the study previously conducted by Kawchuk and colleagues (2010) [24].

**Table 5.2. Maximal displacement (mm) and rotation (°) (SD) created in the cadaveric specimens with the application of SMT (at different application sites) trajectories**

SMT Application site	Displacement (mm)			Rotation (°)		
	X (lateral)	Y (ant post)	Z (sup inf)	X (flx ext)	Y (lat bending)	Z (axial rot)
L2/L3 FJ	2.01 (1.33)	9.95 (3.46)	0.77 (0.41)	2.95 (1.18)	-0.72 (0.40)	3.48 (1.06)
L3 TVP	2.69 (1.69)	7.52 (2.89)	0.82 (0.34)	2.22 (1.08)	-0.87 (0.40)	3.21 (1.11)
Btw FJ	2.44 (1.61)	6.06 (3.39)	0.87 (0.42)	1.69 (1.21)	-0.78 (0.46)	3.10 (1.11)
Btw TVP	2.29 (1.05)	4.01 (3.49)	0.88 (0.31)	1.22 (1.11)	-0.74 (0.29)	1.75 (0.85)
L3/L4 FJ	1.48 (1.30)	1.56 (3.96)	0.99 (0.39)	0.90 (1.05)	-0.59 (0.33)	-0.41 (0.83)
L4 TVP	-0.95 (1.09)	2.91 (4.12)	0.73 (0.51)	1.35 (0.81)	-0.07 (0.47)	-1.93 (0.62)
Average of absolute values	1.98 (1.34)	5.33 (3.55)	0.84 (0.40)	1.72 (1.78)	0.63 (0.39)	2.31 (0.93)

SD=standard deviation; SMT=spinal manipulative therapy; FJ=facet joint; TVP=transverse process, Btw=between; ant post=anterior posterior; sup inf=superior inferior; flx ext=flexion extension; lat bending=lateral bending; axial rot=axial rotation; for lateral displacement: +=left direction, -=right direction; for lateral bending: -=right lateral bending; for axial rotation: +=right axial rotation, -= left axial rotation

**Table 5.3 Average (SD) maximum displacement (mm) and rotation (°) of the current study, study described in Chapter 4 and the previous study conducted by Kawchuk et al. (2010)**

Study	Displacement (mm)			Rotation (°)		
	X (lateral)	Y (ant post)	Z (sup inf)	X (flx ext)	Y (lat bending)	Z (axial rot)
Current Study*	1.98 (1.34)	5.33 (3.55)	0.84 (0.40)	1.72 (1.78)	0.63 (0.39)	2.31 (0.93)
Chapter 4	2.05 (1.65)	5.16 (2.76)	1.04 (0.28)	1.77 (0.87)	-0.53 (0.64)	-1.85 (1.10)
Kawchuk et al. (2010)*	2.15 (0.47)	5.35 (0.86)	0.5 (0.07)	1.96 (0.29)	0.61 (0.17)	0.45 (0.15)

\* - Average of absolute values

ant post = anterior posterior; sup inf = superior inferior; flx ext = flexion extension; lat bending = lateral bending; axial rot = axial rotation

### 5.3.3 Intact Specimen

Table 5.4 shows the values of median (IQR) of peak and mean forces and moments experienced by the intact specimen when SMT was applied at each application site. The analysis of the intact specimen revealed significant differences in experienced forces and moments when SMT was applied at different application sites. Generally, significant differences in forces and moments were observed when SMT was applied at L3 vertebra (FJ and TVP), BTW FJ and BTW TVP in comparison to when applied at L4 vertebra (FJ and TVP). Specifically, SMT application at L3, BTW FJ and BTW TVP generally created peak lateral and anterior posterior forces (forces along x- and y-axis, respectively), and torsion moments (moment around z-axis) in the opposite direction to the ones created during SMT application at L4 vertebra (FJ and TVP) (Figures 5.3, 5.5, 5.6). Additionally, peak anterior posterior forces (forces along y-axis) and torsion moments (moments around z-axis) were significantly smaller when SMT was applied BTW TVP in comparison to when applied at the remaining application sites (Table 5.4). While peak extension moment (moment around x-axis) was significantly greater and in opposite direction when SMT was applied at L3/L4 FJ in comparison to L4 TVP, torsion moments (moments around z-axis) were significantly greater when SMT was applied at L4 TVP (Table 5.4).

**Table 5.4. Median (IQR) forces and moments experienced by the intact specimen during the SMT application at each application site**

Condition	Variable	Axis	Application Site					
			L2/L3 FJ	L3 TVP	BTW FJ	BTW TVP	L3/L4 FJ	L4 TVP
Intact	Peak Force	X	10.06 (10.77) <sup>c,e,f</sup> 95% CI [-0.27, 18.62]	21.10 (12.61) <sup>c,e,f</sup> 95% CI [4.39, 25.38]	-11.12 (6.88) <sup>a,b,e,f</sup> 95% CI [-15.37, 2.6]	19.12 (13.05) <sup>e,f</sup> 95% CI [-29.80, -21.80]	-19.58 (8.82) <sup>a,b,c,d</sup> 95% CI [-24.79, -14.39]	-27.69 (9.58) <sup>a,b,c,d</sup> 95% CI [-29.8, -21.8]
		Y	31.61 (6.70) <sup>d,e,f</sup> 95% CI [14.95, 35.65]	26.23 (13.92) <sup>d,e,f</sup> 95% CI [10.40, 30.50]	16.84 (22.02) <sup>d,e,f</sup> 95% CI [7.14, 27.90]	9.46 (23.01) <sup>a,b,c,e</sup> 95% CI [-6.74, 11.85]	-25.12 (21.72) <sup>a,b,c,d</sup> 95% CI [-29.29, -16.00]	-28.47 (8.56) <sup>a,b,c</sup> 95% CI [-32.62, -13.9]
		Z	20.21 (32.17) 95% CI [-1.51, 21.15]	21.88 (14.17) 95% CI [4.56, 23.85]	24.32 (36.15) 95% CI [1.16, 24.9]	24.36 (10.31) 95% CI [21.93, 29.38]	24.64 (8.09) 95% CI [21.10, 29.60]	23.82 (13.60) 95% CI [16.65, 27.19]
		X	-1.33 (11.21) 95% CI [-2.29, 6.79]	2.87 (7.30) 95% CI [1.53, 7.28]	-0.80 (7.33) 95% CI [-3.64, 7.17]	1.64 (10.02) 95% CI [-2.23, 3.96]	-0.87 (14.68) 95% CI [-7.53, 4.49]	-0.53 (6.62) 95% CI [-2.89, 1.80]
		Y	0.58 (4.56) <sup>e,f</sup> 95% CI [-2.05, 2.37]	-0.51 (3.24) <sup>e,f</sup> 95% CI [-2.74, 1.95]	-0.35 (2.79) <sup>e</sup> 95% CI [-1.58, 1.43]	-1.08 (3.41) <sup>e</sup> 95% CI [-5.27, 0.13]	-5.15 (6.52) <sup>a,b,c,d</sup> 95% CI [-10.99, -3.84]	-4.37 (3.46) <sup>a,b</sup> 95% CI [-7.27, -2.47]
		Z	24.27 (4.79) 95% CI [-6.91, 26.47]	23.12 (3.10) 95% CI [-5.82, 25.28]	24.32 (8.60) 95% CI [-8.64, 28.09]	24.01 (10.22) 95% CI [-5.67, 26.26]	24.28 (8.02) 95% CI [-2.80, 28.39]	22.47 (10.65) 95% CI [-4.56, 25.00]
	Peak Moment	X	-1.50 (1.65) 95% CI [-2.84, 0.37]	-1.05 (1.55) 95% CI [-2.44, 0.11]	-3.15 (2.18) 95% CI [-3.96, 1.00]	-1.27 (2.19) 95% CI [-2.08, 0.39]	-1.22 (2.63) <sup>f</sup> 95% CI [-3.08, -1.00]	1.04 (1.26) <sup>e</sup> 95% CI [-0.46, 2.30]
		Y	0.48 (1.70) 95% CI [-1.68, 1.07]	1.09 (0.94) 95% CI [-0.96, 1.54]	-0.89 (0.55) 95% CI [-1.83, 0.01]	1.32 (3.09) 95% CI [-0.58, 1.86]	-1.44 (0.79) 95% CI [-1.98, 1.09]	-1.88 (0.82) 95% CI [-2.25, 1.23]
		Z	5.70 (3.65) <sup>d,e,f</sup> 95% CI [4.98, 7.70]	5.22 (2.52) <sup>d,e,f</sup> 95% CI [4.35, 6.47]	5.29 (2.19) <sup>d,e,f</sup> 95% CI [4.27, 6.56]	2.49 (1.56) <sup>a,b,c,e,f</sup> 95% CI [2.01, 3.45]	-1.48 (1.74) <sup>a,b,c,d,f</sup> 95% CI [-2.52, -0.47]	-4.02 (1.36) <sup>a,b,c,d,e</sup> 95% CI [-4.66, -3.23]
		X	-0.30 (0.63) 95% CI [-0.50, 0.01]	-0.28 (0.48) 95% CI [-0.48, 0.07]	-0.42 (0.72) 95% CI [-0.56, 0.09]	-0.23 (0.56) 95% CI [-0.39, 0.02]	-0.35 (0.56) 95% CI [-0.42, 0.01]	-0.02 (0.56) 95% CI [-0.20, 0.16]
		Y	-0.10 (0.90) 95% CI [-0.26, 0.37]	0.06 (0.54) 95% CI [-0.01, 0.40]	-0.15 (0.65) 95% CI [-0.32, 0.42]	0.08 (0.80) 95% CI [-0.19, 0.26]	-0.19 (0.87) 95% CI [-0.53, 0.21]	-0.08 (0.39) 95% CI [-0.22, 0.08]
		Z	0.62 (0.46) <sup>d,e,f</sup> 95% CI [0.46, 0.82]	0.54 (0.29) <sup>d,e,f</sup> 95% CI [0.38, 0.71]	0.62 (0.27) <sup>d,e,f</sup> 95% CI [0.49, 0.81]	0.23 (0.18) <sup>a,b,c,e,f</sup> 95% CI [0.14, 0.41]	-0.23 (0.51) <sup>a,b,c,d,f</sup> 95% CI [-0.48, -0.01]	-0.55 (0.43) <sup>a,b,c,d,e</sup> 95% CI [-0.67, -0.33]

IQR=interquartile range; 95% CI= 95% confidence interval; FJ=facet joint; TVP=transverse process; BTW=between

<sup>a</sup> - significant difference in comparison (p<0.05) with L2/L3 FJ

<sup>b</sup> - significant difference in comparison (p<0.05) with L3 TVP

<sup>c</sup> - significant difference in comparison (p<0.05) with BTW FJ

<sup>d</sup> - significant difference in comparison (p<0.05) with BTW TVP

<sup>e</sup> - significant difference in comparison (p<0.05) with L3/L4 FJ

<sup>f</sup> - significant difference in comparison (p<0.05) with L4 TVP

#### ***5.3.4 Cut 1: Supra- and interspinous ligaments (SL)***

Table 5.5 shows the values of median (IQR) of normalized forces and moments experienced by the SL structures when SMT was applied at each application site relative to the intact condition. Generally, considering 100% the total forces and moments experienced by the intact specimen, SL structures experienced about 0.5% of the peak forces, 1.8% of the mean forces, 4% of the peak moments and 74% of the mean moments.

The analysis revealed significant change in loads experienced by SL structures when SMT was applied at different locations of the spine. Specifically, change in peak superior inferior force (force along z-axis) experienced by SL structures was significantly greater when SMT was applied at L2/L3 FJ in comparison to L4 vertebra (FJ and TVP), BTW FJ and BTW TVP (Table 5.5). Change in mean lateral bending moment (moment around y-axis) was significantly greater when SMT was applied at L3 TVP (median: -0.09Nm (IQR: 0.11)) in comparison to when applied at the FJ of L2/L3 (median: -0.05Nm (IQR: 0.10)), L3/L4 (median: -0.05Nm (IQR: 0.12)) and BTW FJ (median: -0.03Nm (IQR: 0.06)). Additionally, change in peak torsion moment (moment around z-axis) was significantly greater when SMT was applied at L3/L4 FJ when compared to all other application sites (Figure 5.5).

**Table 5.5. Median (IQR) value of normalized forces and moments (relative to the intact condition) experienced by the supra- and interspinous ligaments during the SMT application at each application site**

Condition	Variable	Axis	Application Site					
			L2/L3 FJ	L3 TVP	BTW FJ	BTW TVP	L3/L4 FJ	L4 TVP
Cut 1 (SL)	Peak Force	X	-0.06 (0.13)	-0.01 (0.02)	-0.00 (0.06)	-0.02 (0.01)	-0.04 (0.03)	-0.02 (0.03)
			95% CI [-0.85, 1.21]	95% CI [-0.13, 0.34]	95% CI [-0.04, 0.01]	95% CI [-0.03, 0.01]	95% CI [-0.09, 0.00]	95% CI [-0.04, 0.00]
		Y	-0.01 (0.01)	-0.02 (0.02)	-0.01 (0.02)	-0.03 (0.06)	-0.03 (0.07)	-0.02 (0.01)
			95% CI [-0.30, 0.08]	95% CI [-0.14, 0.02]	95% CI [-0.02, 0.00]	95% CI [-0.07, 0.01]	95% CI [-0.08, 0.00]	95% CI [-0.04, 0.05]
		Z	-0.01 (0.16) <sup>c,d,e,f</sup>	-0.00 (0.11)	0.00 (0.08) <sup>a</sup>	-0.00 (0.02) <sup>a</sup>	0.00 (0.01) <sup>a</sup>	-0.00 (0.01) <sup>a</sup>
			95% CI [-1.06, 0.19]	95% CI [-0.27, 0.04]	95% CI [-0.04, 0.10]	95% CI [-0.08, 0.01]	95% CI [-0.05, 0.02]	95% CI [-0.08, 0.12]
	Mean Force	X	-0.05 (0.10)	-0.03 (0.11)	-0.05 (0.07)	-0.04 (0.05)	-0.05 (0.10)	-0.05 (0.22)
			95% CI [-0.21, 0.07]	95% CI [-0.16, 0.09]	95% CI [-0.22, 0.00]	95% CI [-0.24, 0.07]	95% CI [-0.01, 0.00]	95% CI [-0.15, 0.07]
		Y	-0.16 (0.42)	-0.10 (0.32)	-0.14 (0.56)	-0.10 (0.27)	-0.10 (0.09)	-0.08 (0.04)
			95% CI [-0.57, 0.01]	95% CI [-0.43, 0.00]	95% CI [-0.80, 0.06]	95% CI [-0.17, 0.11]	95% CI [-0.30, 0.03]	95% CI [-0.13, 0.02]
		Z	-0.09 (0.11)	-0.09 (0.21)	-0.03 (0.16)	-0.05 (0.09)	-0.01 (0.04)	-0.01 (0.06)
			95% CI [-0.18, 0.10]	95% CI [-0.23, 0.13]	95% CI [-0.61, 0.09]	95% CI [-0.21, 0.04]	95% CI [-0.18, 0.09]	95% CI [-0.15, 0.02]
	Peak Moment	X	-0.01 (0.07)	-0.04 (0.05)	-0.03 (0.01)	-0.04 (0.06)	-0.04 (0.03)	-0.03 (0.02)
			95% CI [-0.05, 0.18]	95% CI [-0.10, 0.11]	95% CI [-0.07, 0.04]	95% CI [-0.16, 0.01]	95% CI [-0.31, 0.01]	95% CI [-0.05, 0.00]
		Y	-0.02 (0.11)	-0.03 (0.03)	-0.01 (0.05)	-0.03 (0.02)	-0.03 (0.03)	-0.03 (0.02)
			95% CI [-0.41, 0.00]	95% CI [-0.50, 0.60]	95% CI [-0.05, 0.02]	95% CI [-0.04, 0.01]	95% CI [-0.15, 0.03]	95% CI [-0.04, 0.01]
		Z	-0.03 (0.01) <sup>e</sup>	-0.03 (0.002) <sup>e</sup>	-0.05 (0.01) <sup>e</sup>	-0.05 (0.02) <sup>e</sup>	-0.04 (0.12) <sup>a,b,c,d,f</sup>	-0.03 (0.01) <sup>e</sup>
			95% CI [-0.19, 0.01]	95% CI [-0.04, -0.03]	95% CI [-0.05, -0.04]	95% CI [-0.06, 0.04]	95% CI [-0.59, -0.04]	95% CI [-0.04, -0.02]
	Mean Moment	X	-0.06 (0.13)	-0.07 (0.17)	-0.08 (0.09)	-0.01 (0.11)	-0.04 (0.09)	-0.03 (0.13)
			95% CI [-0.27, 0.01]	95% CI [-0.37, 0.02]	95% CI [-0.32, 0.02]	95% CI [-0.06, 0.03]	95% CI [-0.08, 0.02]	95% CI [-0.18, 0.12]
		Y	-0.05 (0.10) <sup>b</sup>	-0.09 (0.11) <sup>a,c,e</sup>	-0.03 (0.06) <sup>b</sup>	-0.04 (0.08)	-0.05 (0.12) <sup>b</sup>	-0.12 (0.18)
			95% CI [-0.05, 0.03]	95% CI [-1.07, -0.08]	95% CI [-0.10, -0.00]	95% CI [-0.03, 0.01]	95% CI [-0.07, 0.00]	95% CI [-1.08, 0.24]
		Z	-0.05 (0.05)	-0.07 (0.03)	-0.06 (0.02)	-0.07 (0.11)	-0.08 (0.09)	-0.06 (0.03)
			95% CI [-0.07, 0.03]	95% CI [-0.08, 0.03]	95% CI [-0.07, 0.03]	95% CI [-0.12, 0.00]	95% CI [-0.16, 0.08]	95% CI [-0.34, 0.12]

IQR=interquartile range; 95%CI=95% confidence interval; SL=supra- and interspinous ligaments; FJ=facet joint; TVP=transverse process; BTW=between

<sup>a</sup> - significant difference in comparison (p<0.05) with L2/L3 FJ

<sup>b</sup> - significant difference in comparison (p<0.05) with L3 TVP

<sup>c</sup> - significant difference in comparison (p<0.05) with BTW FJ

<sup>d</sup> - significant difference in comparison (p<0.05) with BTW TVP

<sup>e</sup> - significant difference in comparison (p<0.05) with L3/L4 FJ

<sup>f</sup> - significant difference in comparison (p<0.05) with L4 TVP

### **5.3.5 Cut 2: Facet capsules, facet joints and ligamentum flavum (PJ)**

Table 5.6 shows the values of median (IQR) of forces and moments experienced by the PJ structures when SMT was applied at each application site. Generally, considering 100% the total forces and moments experienced by the intact specimen, PJ structures experienced loads equivalent to about 2.5% of the peak forces, 25.3% of the mean forces, 7.3% of the peak moments and 257.6% of the mean moments.

The analysis of change in loads experienced by PJ structures also showed significant differences when SMT was provided at different application sites. Generally, changes in specific forces and moments experienced by PJ structures were significantly smaller when SMT was applied BTW TVP in comparison to when applied at other application sites (Table 5.6). Forces and moments experienced by PJ structures differed in direction and magnitude when SMT was applied at L3 and L4 vertebrae. Specifically during the SMT application at L3 vertebra (FJ and TVP), BTW FJ and BTW TVP, PJ structures experienced peak anterior posterior forces (force along y-axis) in the opposite direction to when applied at L4 vertebra (FJ and TVP) (Figure 5.3). Particularly in each axis, change in peak lateral force (force along x-axis) was significantly greater when SMT was applied at L2/L3 FJ and BTW FJ (even though in opposite direction) when compared to the other application sites (Table 5.6). While change in peak and mean anterior posterior forces (force along y-axis) and mean superior inferior forces (force along z-axis) were significantly greater when SMT was applied BTW FJ than when applied at the other application sites (Table 5.6 and Figure 5.4), change in peak superior inferior forces (forces along z-axis) were significantly greater when SMT was applied at L2/L3 FJ than in other application sites (Figure 5.3).

Specifically for moments and similarly to the intact specimen, change in peak flexion extension moment (moment around x-axis) was significantly greater when SMT was applied at L3/L4 FJ (median: -0.38Nm (IQR: 0.38)) in comparison to when applied at L4 TVP (median: -0.08Nm (IQR: 0.24)). Additionally, change in peak torsion moments were significantly smaller during SMT application at L3/L4 FJ (median: -0.52Nm (IQR: 0.29)) and BTW TVP (median: -0.27Nm (IQR: 0.34)) than the application at L4 TVP (median: -0.56Nm (IQR: 0.08)) and L3 vertebra (FJ and TVP) (Table 5.6). While changes in peak lateral bending were significantly greater during SMT application at L3 vertebra (FJ and TVP) than at L4 vertebra (FJ and TVP), it was in the opposite direction during a SMT application at BTW FJ in comparison to the other application sites (Figure 5.5). While changes in mean extension moments experienced by PJ structures during a SMT application at L3/L4 FJ and BTW TVP were significantly smaller than the other application sites, changes in mean lateral bending moments (moment around y-axis) were significantly greater when SMT was applied at FJs in comparison to TVPs (Table 5.6). Additionally, mean torsion moments were significantly smaller during a SMT application at BTW TVP than other application sites, whereas SMT application at TVPs generally created mean torsion moments significantly greater than when SMT was applied at FJs (Table 5.6).



**Table 5.6. Median (IQR) value of normalized forces and moments (relative to the intact condition) experienced by the bilateral facet joints, capsules and ligamentum flavum during the SMT application at each application site**

Condition	Variable	Axis	Application Site					
			L2/L3 FJ	L3 TVP	BTW FJ	BTW TVP	L3/L4 FJ	L4 TVP
Cut 2 (PJ)	Peak Force	X	1.62 (1.84) <sup>b,c,d,e,f</sup>	0.45 (0.54) <sup>a,c</sup>	-0.79 (1.48) <sup>a,b,d,e,f</sup>	0.17 (0.47) <sup>a,c</sup>	0.14 (0.35) <sup>a,c</sup>	0.10 (0.23) <sup>a,c</sup>
			95% CI [0.97, 3.52]	95% CI [0.06, 0.66]	95% CI [-1.40, -0.15]	95% CI [0.01, 0.61]	95% CI [-0.05, 0.27]	95% CI [0.08, 0.32]
		Y	-0.17 (0.39) <sup>c,e</sup>	-0.62 (0.44) <sup>c,d,e,f</sup>	-0.63 (0.57) <sup>a,b,d,e,f</sup>	-0.61 (0.87) <sup>b,c,e</sup>	0.23 (0.31) <sup>a,b,c,d,f</sup>	0.02 (0.08) <sup>b,c,e</sup>
			95% CI [-0.49, -0.06]	95% CI [-0.69, -0.39]	95% CI [-1.33, -0.41]	95% CI [-0.99, 0.68]	95% CI [0.16, 0.42]	95% CI [-0.69, -0.39]
		Z	0.00 (0.75) <sup>b,c,d,e,f</sup>	-0.01 (0.56) <sup>a</sup>	0.00 (0.13) <sup>a</sup>	-0.01 (0.07) <sup>a</sup>	0.00 (0.06) <sup>a</sup>	-0.01 (0.02) <sup>a</sup>
			95% CI [0.06, 1.32]	95% CI [-0.07, 0.25]	95% CI [-0.10, 0.18]	95% CI [-0.19, 0.09]	95% CI [-0.12, 0.00]	95% CI [-0.30, 0.35]
	Mean Force	X	-0.45 (1.07)	0.04 (0.30)	-0.49 (1.62)	-0.12 (0.52)	-0.32 (0.49)	-0.68 (1.30)
			95% CI [-1.15, 0.25]	95% CI [-1.39, 0.97]	95% CI [-1.01, 0.04]	95% CI [-0.60, 0.56]	95% CI [-0.84, 0.17]	95% CI [-2.14, 1.96]
		Y	-0.20 (2.12) <sup>c,e,f</sup>	0.18 (2.38) <sup>c</sup>	0.89 (5.62) <sup>a,b,d,e,f</sup>	0.28 (2.90) <sup>c,e,f</sup>	0.38 (0.69) <sup>a,c,d</sup>	0.50 (0.40) <sup>a,c,d</sup>
			95% CI [-0.98, 0.94]	95% CI [-0.80, 1.21]	95% CI [0.47, 3.18]	95% CI [-1.18, 1.07]	95% CI [0.00, 0.99]	95% CI [0.27, 0.93]
		Z	-0.42 (0.45) <sup>c</sup>	-0.18 (0.50) <sup>c</sup>	-0.23 (0.48) <sup>a,b,d,e,f</sup>	-0.17 (0.29) <sup>c</sup>	-0.02 (0.13) <sup>c</sup>	-0.08 (0.34) <sup>c</sup>
			95% CI [-0.47, 0.09]	95% CI [-0.56, 0.43]	95% CI [-1.27, -0.09]	95% CI [-0.69, 0.61]	95% CI [-0.24, 0.01]	95% CI [-0.58, 0.49]
	Peak Moment	X	-0.56 (0.35)	-0.55 (0.33) <sup>f</sup>	-0.41 (0.33)	-0.26 (0.52)	-0.38 (0.38) <sup>f</sup>	-0.08 (0.24) <sup>b,e</sup>
			95% CI [-0.68, 0.27]	95% CI [-1.12, -0.24]	95% CI [-0.65, 0.22]	95% CI [-0.88, 0.01]	95% CI [-0.95, -0.12]	95% CI [-0.76, -0.29]
		Y	0.69 (3.18) <sup>b,c,d,e,f</sup>	0.99 (1.02) <sup>a,c,d,e,f</sup>	-0.79 (1.05) <sup>a,b,d,e,f</sup>	0.21 (0.67) <sup>a,b,c,f</sup>	0.07 (0.54) <sup>a,b,c</sup>	0.37 (0.36) <sup>a,b,c,d</sup>
			95% CI [0.25, 2.34]	95% CI [0.51, 1.36]	95% CI [-1.30, 0.59]	95% CI [-0.10, 0.43]	95% CI [-0.47, 1.08]	95% CI [-0.09, 0.50]
		Z	-0.71 (0.09) <sup>d,e</sup>	-0.69 (0.05) <sup>d,e,f</sup>	-0.66 (0.06) <sup>d</sup>	-0.27 (0.34) <sup>a,b,c,e,f</sup>	-0.52 (0.29) <sup>a,b,d,f</sup>	-0.56 (0.08) <sup>b,d,e</sup>
			95% CI [-0.74, -0.53]	95% CI [-0.71, -0.59]	95% CI [-0.69, -0.59]	95% CI [-0.33, -0.14]	95% CI [-0.75, -0.17]	95% CI [-0.62, -0.50]
	Mean Moment	X	-0.35 (0.41) <sup>d,e</sup>	-0.40 (0.42) <sup>d,e</sup>	-0.37 (0.23) <sup>d,e</sup>	-0.26 (1.07) <sup>a,b,c,f</sup>	-0.35 (1.19) <sup>a,b,c,f</sup>	-0.72 (2.04) <sup>d,e</sup>
			95% CI [-1.68, 0.07]	95% CI [-1.17, 0.02]	95% CI [-2.02, 0.39]	95% CI [-0.31, -0.21]	95% CI [-0.63, -0.01]	95% CI [-1.68, -0.09]
		Y	-0.48 (1.23) <sup>b,c,d,f</sup>	0.01 (1.99) <sup>a,c,d,e,f</sup>	-0.48 (1.47) <sup>a,b,e</sup>	-0.15 (0.50) <sup>a,b,e</sup>	-0.46 (0.83) <sup>b,c,d,f</sup>	-0.13 (1.35) <sup>a,b,e</sup>
			95% CI [-1.49, -0.02]	95% CI [-2.62, -0.14]	95% CI [-0.71, 0.53]	95% CI [-0.44, 0.10]	95% CI [-1.27, -0.14]	95% CI [-1.18, 0.72]
		Z	-0.60 (0.38) <sup>d,f</sup>	-0.56 (0.23) <sup>e</sup>	-0.64 (0.28) <sup>d</sup>	-0.43 (0.55) <sup>a,b,c,e,f</sup>	-0.59 (0.47) <sup>b,d,f</sup>	-0.60 (0.11) <sup>a,e</sup>
			95% CI [-0.87, -0.52]	95% CI [-0.73, -0.43]	95% CI [-0.75, -0.53]	95% CI [-0.86, -0.01]	95% CI [-1.27, -0.21]	95% CI [-0.78, -0.20]

IQR=interquartile range; 95%CI=95% confidence interval; PJ=bilateral facet joints, capsules and ligamentum flavum; FJ=facet joint; TVP=transverse process; BTW=between

<sup>a</sup> - significant difference in comparison (p<0.05) with L2/L3 FJ

<sup>b</sup> - significant difference in comparison (p<0.05) with L3 TVP

<sup>c</sup> - significant difference in comparison (p<0.05) with BTW FJ

<sup>d</sup> - significant difference in comparison (p<0.05) with BTW TVP

<sup>e</sup> - significant difference in comparison (p<0.05) with L3/L4 FJ

<sup>f</sup> - significant difference in comparison (p<0.05) with L4 TVP

### ***5.3.6 Cut 3: Intervertebral disc and anterior and posterior longitudinal ligaments (IVD)***

Table 5.7 shows the values of median (IQR) of forces and moments experienced by the IVD structures when SMT was applied at each application site. Generally, considering 100% the total forces and moments experienced by the intact specimen, IVD structures experienced loads equivalent to about 4.4% of the peak forces, 34% of the mean forces, 7.7% of the peak moments and 238.4% of the mean moments.

Statistical analysis revealed significant changes in loads experienced by IVD structures as a function of the application site. Particularly for forces, change in lateral forces (forces along x-axis) were generally greater when SMT was applied at TVP in comparison to when applied at FJ. Specifically, change in mean lateral force (force along x-axis) was significantly greater when SMT was applied at L3 TVP (median: -0.73N (IQR: 0.94)) than when applied at L2/L3 FJ (median: -0.37N (IQR: 0.79)). Additionally, while change in peak lateral forces (force along x-axis) and mean anterior posterior forces (force along y-axis) were significantly smaller during SMT application at BTW FJ than in other application sites, peak lateral forces were also significantly greater when SMT was applied at L3 vertebra (FJ and TVP) in comparison to L4 vertebra (FJ and TVP) and BTW TVP (Table 5.7). Change in peak anterior posterior forces significantly differed in magnitude during a SMT at L3 vertebra (FJ and TVP) and at L4 vertebra (FJ and TVP). On the other hand, although change in peak superior inferior force (force along z-axis) was significantly greater when SMT was applied at L2/L3 FJ (median: -0.84N (IQR: 0.97)) than when applied at L3 TVP (median: -0.37N (IQR: 0.94)), it was also greater when SMT was applied at L4 TVP (median: -0.43N (IQR: 0.97)) than at L3/L4 FJ (median: -0.05N (IQR: 0.11)). Additionally, while changes in peak superior inferior forces also significantly differed as a

function of the spinal level in which SMT was applied, change in mean superior inferior forces were significantly greater during a SMT application at the FJ in comparison to its respective spinal level TVP, with the SMT application at L4 (FJ and TVP) also creating greater change in mean superior inferior forces than its respective landmark at L3 (FJ and TVP, respectively).

Specifically for moments, while change in lateral bending and torsion moments (moments around y- and z-axis, respectively) were generally greater when SMT was applied at TVP in comparison to when applied at FJ, extension moments (moments around x-axis) were generally greater when SMT was applied at FJ than at TVP (Figures 5.3 to 5.6). While change in peak flexion extension moments (moments around x-axis) was significantly smaller when SMT was applied at L2/L3 FJ than at L4 vertebra (FJ and TVP), mean flexion extension moments were significantly greater during a SMT application at L4 TVP in comparison to L3 vertebra (FJ and TVP) (Table 5.7). Change in peak and mean lateral bending moments (moments around y-axis) were significantly smaller during a SMT application at BTW FJ in comparison to other application sites. While change in mean lateral bending moment was significantly greater when SMT was applied at L4 TVP than at L3 vertebra (FJ and TVP), change in peak lateral bending moment was significantly greater during SMT application at L3 vertebra (FJ and TVP) in comparison to the other application sites (Table 5.7). Although change in peak torsion moments (moment around z-axis) experienced by IVD structures was significantly greater when SMT was applied at L3 and L4 TVPs in comparison to BTW FJ, it was also significantly smaller when SMT was applied at BTW TVP in comparison to when applied at the other application sites and significantly greater during SMT application at L4 TVP than at L3 vertebra (FJ and TVP) (Table 5.7).

**Table 5.7. Median (IQR) value of normalized forces and moments (relative to the intact condition) experienced by the intervertebral disc, anterior and posterior longitudinal ligaments during the SMT application at each application site**

Condition	Variable	Axis	Application Site					
			L2/L3 FJ	L3 TVP	BTW FJ	BTW TVP	L3/L4 FJ	L4 TVP
Cut 3 (IVD)	Peak Force	X	-1.81 (1.67) <sup>c,d,e,f</sup>	-1.38 (0.42) <sup>c,d,e,f</sup>	-0.31 (1.02) <sup>a,b,d,e,f</sup>	-1.10 (0.35) <sup>a,b,c</sup>	-1.16 (0.33) <sup>a,b,c</sup>	-1.14 (0.54) <sup>a,b,c</sup>
			95% CI [-5.05, -1.01]	95% CI [-1.79, -1.03]	95% CI [-0.58, 0.38]	95% CI [-1.47, -1.00]	95% CI [-1.34, -1.04]	95% CI [-1.44, -1.00]
		Y	-0.53 (0.50) <sup>d,e,f</sup>	-0.34 (0.28) <sup>c,d,e,f</sup>	-0.35 (0.69) <sup>b,f</sup>	-0.41 (0.84) <sup>a,b</sup>	-0.13 (0.47) <sup>a,b</sup>	-0.66 (0.24) <sup>a,b,c</sup>
			95% CI [-0.07, -0.40]	95% CI [-0.53, -0.22]	95% CI [-0.57, -0.00]	95% CI [-0.75, 0.49]	95% CI [-0.70, 0.19]	95% CI [-1.46, 1.50]
		Z	-0.84 (0.97) <sup>b,d,e,f</sup>	-0.37 (0.94) <sup>a,e,f</sup>	-0.06 (0.92)	-0.34 (1.06) <sup>a,e,f</sup>	-0.05 (0.11) <sup>a,b,d,f</sup>	-0.43 (0.97) <sup>a,b,d,e</sup>
			95% CI [-2.26, -0.28]	95% CI [-0.85, 0.36]	95% CI [-0.78, 0.05]	95% CI [-0.89, -0.00]	95% CI [-0.31, 0.7]	95% CI [-1.88, -0.17]
	Mean Force	X	-0.37 (0.79) <sup>b,f</sup>	-0.73 (0.94) <sup>a,c,d,e</sup>	-0.61 (0.95) <sup>b,d</sup>	-0.76 (0.45) <sup>b,c,e,f</sup>	-0.67 (0.58) <sup>b,d</sup>	-0.87 (2.89) <sup>a,d</sup>
			95% CI [-0.71, 0.10]	95% CI [-1.88, 0.12]	95% CI [-1.43, -0.07]	95% CI [-1.18, 1.15]	95% CI [-1.65, 0.02]	95% CI [-3.46, -0.87]
		Y	-0.50 (0.80) <sup>c</sup>	-0.38 (0.45) <sup>c,d,e</sup>	-0.21 (2.07) <sup>a,b,d,e,f</sup>	-0.25 (0.38) <sup>b,c</sup>	-0.45 (0.40) <sup>b,c</sup>	-0.95 (0.52) <sup>c</sup>
			95% CI [-1.06, 0.03]	95% CI [-0.82, 0.10]	95% CI [-1.80, -0.78]	95% CI [-0.86, 0.45]	95% CI [-1.29, 1.07]	95% CI [-1.38, 0.52]
		Z	-0.39 (0.63) <sup>b,d,e</sup>	-0.33 (0.54) <sup>a,d,f</sup>	-0.55 (0.73) <sup>d</sup>	-0.51 (0.77) <sup>a,b,c</sup>	-0.59 (0.61) <sup>a,f</sup>	-0.53 (0.81) <sup>b,e</sup>
			95% CI [-0.97, 0.93]	95% CI [-0.70, -0.02]	95% CI [-1.51, -0.08]	95% CI [-0.72, -0.07]	95% CI [-0.77, -0.33]	95% CI [-0.78, 0.26]
	Peak Moment	X	-0.43 (0.30) <sup>b,c,d,e,f</sup>	-0.43 (0.37) <sup>a</sup>	-0.61 (0.41) <sup>a,d</sup>	-0.72 (0.65) <sup>a,c</sup>	-0.84 (0.66) <sup>a</sup>	-0.82 (0.35) <sup>a</sup>
			95% CI [-1.13, -0.09]	95% CI [-1.49, 0.82]	95% CI [-0.81, -0.16]	95% CI [-1.14, -0.57]	95% CI [-0.98, -0.25]	95% CI [-1.00, -0.42]
		Y	-1.59 (3.10) <sup>b,c,d,e,f</sup>	-1.68 (1.71) <sup>a,c,d,e,f</sup>	-0.20 (0.94) <sup>a,b,d,f</sup>	-1.20 (0.31) <sup>a,b,c,e</sup>	-1.03 (0.69) <sup>a,b,d,f</sup>	-1.34 (0.39) <sup>a,b,c,e</sup>
			95% CI [-4.66, -0.96]	95% CI [-2.64, -1.18]	95% CI [-0.68, 0.14]	95% CI [-1.37, -0.98]	95% CI [-1.36, -0.02]	95% CI [-1.59, -0.94]
		Z	-0.23 (0.06) <sup>b,d,f</sup>	-0.26 (0.09) <sup>a,c,d,e,f</sup>	-0.28 (0.09) <sup>b,d,f</sup>	-0.21 (0.20) <sup>a,b,c,e,f</sup>	-0.39 (0.56) <sup>b,d,f</sup>	-0.42 (0.08) <sup>a,b,c,d,e</sup>
			95% CI [-0.31, -0.19]	95% CI [-0.35, -0.22]	95% CI [-0.34, -0.23]	95% CI [-0.22, -0.10]	95% CI [-0.63, 0.03]	95% CI [-0.50, -0.35]
	Mean Moment	X	-0.59 (0.53) <sup>b,f</sup>	-0.59 (0.33) <sup>a,c,d,f</sup>	-0.52 (0.49) <sup>b,f</sup>	-0.41 (0.51) <sup>b,f</sup>	-0.73 (0.71) <sup>f</sup>	-0.51 (2.24) <sup>a,b,c,d,e</sup>
			95% CI [-0.83, 0.03]	95% CI [-0.77, -0.25]	95% CI [-1.33, 0.25]	95% CI [-0.99, -0.14]	95% CI [-1.15, -0.18]	95% CI [-1.81, -0.67]
		Y	-0.26 (0.69) <sup>c,f</sup>	-0.21 (1.53) <sup>c,f</sup>	-0.40 (1.54) <sup>a,b,d,e,f</sup>	-0.62 (0.94) <sup>c,f</sup>	-0.71 (1.08) <sup>c,f</sup>	-1.46 (4.37) <sup>a,b,c,d,e</sup>
			95% CI [-0.67, 0.56]	95% CI [-1.05, 0.66]	95% CI [-1.74, -0.29]	95% CI [-0.96, 0.01]	95% CI [-1.04, 0.30]	95% CI [-3.29, -0.47]
		Z	-0.18 (0.22) <sup>b,e,f</sup>	-0.26 (0.14) <sup>a,c,d,f</sup>	-0.26 (0.17) <sup>b,e,f</sup>	-0.23 (0.40) <sup>b,e,f</sup>	-0.32 (0.63) <sup>a,c,d,f</sup>	-0.35 (0.37) <sup>a,b,c,d,e</sup>
			95% CI [-0.29, -0.06]	95% CI [-0.37, -0.17]	95% CI [-0.38, 0.00]	95% CI [-0.55, 0.04]	95% CI [-0.91, -0.12]	95% CI [-1.32, -0.26]

IQR=interquartile range; 95%CI=95% confidence interval; IVD=intervertebral disc, anterior and posterior longitudinal ligaments; FJ=facet joint; TVP=transverse process; BTW=between

<sup>a</sup> - significant difference in comparison (p<0.05) with L2/L3 FJ

<sup>b</sup> - significant difference in comparison (p<0.05) with L3 TVP

<sup>c</sup> - significant difference in comparison (p<0.05) with BTW FJ

<sup>d</sup> - significant difference in comparison (p<0.05) with BTW TVP

<sup>e</sup> - significant difference in comparison (p<0.05) with L3/L4 FJ

<sup>f</sup> - significant difference in comparison (p<0.05) with L4 TVP

## 5.4 Discussion

This study aimed to describe the loading characteristics of spinal tissues when SMT with a fixed peak force magnitude was applied at different application sites. The results indicate that the location in which SMT was applied significantly influenced spinal tissue loading characteristics. In general, a posterior to anterior SMT thrust application at the L3 vertebra caused vertebral movement, forces and moments between L3 and L4 spinal segment which were in reversed direction when SMT was applied at L4 vertebra. In contrast, when SMT was applied on the soft tissue between adjacent vertebrae (BTW TVP), vertebral movement did not significantly change while forces and moments were similar in direction to L3 TVP but smaller in magnitude. When changing SMT application sites within the same vertebra, greater torsion moments were generally experienced when SMT was applied at TVP compared to FJ. Overall, the results of this study suggest that SMT application site significantly influences SMT load distribution within spinal tissues and consequently, the forces and moments experienced by spinal structures. Although previous studies have described biomechanical and neurophysiological responses as a result of SMT application at a specific site [44,45,48,49], this is the first study to quantify the forces and moments experienced by spinal structures and describe how SMT loading distribution changes as a function of the application site. Figure 5.7 presents a summary of the general findings of this study.

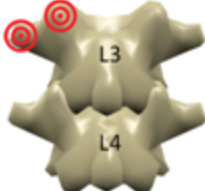
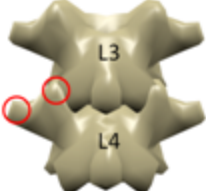

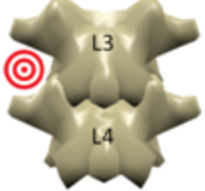
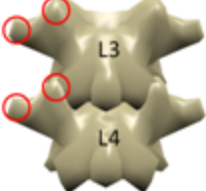


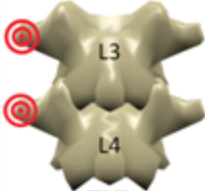
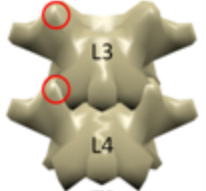


SMT application site:	In comparison to:	General effect on vertebral movement	General effect on loading
 L3 FJ and TVP	Vs.  L4 FJ and TVP	 Vertebral motion generally in opposite directions relatively to each other <small>(mainly lateral translation and axial rotation)</small>	L3-L4 spinal segment experiences overall forces and moments in opposite direction
 Between TVPs	Vs.  Bony structures	 No substantial change on vertebral motion	 Forces and moments
 TVP	Vs.  FJ	 Axial rotation <small>(mainly when applied at L4 TVP)</small>	 Torsion moments <small>(mainly when applied at L4 TVP)</small>

Figure 5.7 Summary of general findings of this study.

#### 5.4.1 Vertebral displacements and rotations

In this study, a posterior to anterior SMT thrust was applied at the skin overlying L3 and L4 vertebrae landmarks (FJs and TVPs) and at the interspace between them. The resulting L4 vertebral displacements and rotations in relation to L3 vertebra were replicated during robotic testing of all conditions. Interestingly, vertebral motions were considerably different when SMT was applied at each application site, with SMT application at L3 vertebra (FJ and TVP) generally creating the greatest displacements and rotations magnitudes, and SMT application at L4 vertebra (FJ and TVP) generally creating the smallest magnitudes of displacements and rotations. Given the posterior to anterior SMT thrust application, the observed opposite relative lateral translation and axial rotation when SMT was applied at L3 vertebra in comparison to when applied at L4 vertebra

was expected. Similar magnitudes of displacements in opposite directions, however, were not observed. For example, while the SMT application at L3 TVP created an axial rotation of  $3.21^{\circ}$  (L4 right axial rotation in relation to L3), SMT application at L4 TVP caused  $1.93^{\circ}$  of L4 left axial rotation. This indicates that for a SMT application with a constant force magnitude, the spinal level in which SMT is applied generally creates motions in opposite directions but not of opposing magnitudes. This difference in magnitudes is likely the result of variation in the specimens themselves, such as vertebral position (angulation and distance from skin) [227,228] and facet joint orientation [73] that may influence vertebral motion arising from SMT.

The greatest linear displacements were observed along the anterior posterior axis (y-axis) and greatest rotations in axial rotation movement (around z-axis). Given the posterior to anterior direction of SMT thrust application, the great displacement along the posterior-anterior axis was expected and supported by previous studies [24]. In contrast to the observation of greater axial rotation in the current study, the study conducted by Kawchuk and colleagues (2010) [24], observed rotations in flexion extension to be greater than around the other axes. On the other hand, the previous study described in Chapter 4 observed large rotations in both flexion extension and axial rotation. While Kawchuk et al. (2010) [24] applied a manual SMT provided by a trained clinician, both the study described on Chapter 4 and the current study applied SMT by using a linear actuator motor with a contact area of approximately  $0.8 \text{ cm}^2$ . Based on a previous finding that hand configuration during SMT application influence SMT's resultant magnitude, location and pressure distribution [218], differences in angular displacements observed between the current study and the one conducted by Kawchuk and colleagues (2010) [24] are likely related to differences in SMT force-time profile and area of pressure distribution.

This observation supports Chapter 4's speculation suggesting that in addition to SMT force-time characteristics (e.g. force magnitude, loading rate, application site), contact area and area of pressure distribution are also important aspects of SMT application. Additionally, differences in SMT input parameters between this study, Chapter 4 of this dissertation and the study conducted by Kawchuk and colleagues may also contribute to the observed difference in vertebral motion. While the current study applied 300N peak force SMT at 6 different application sites (L2/L3 and L3/L4 FJs, L3 and L4 TVP and the interspace between those FJs and TVPs), Chapter 4 of this dissertation applied SMT with 3 different peak force magnitudes at L3/L4 FJ and L4 TVP, and Kawchuk and colleagues (2010) applied a manual SMT (peak force magnitude not measured) at L3 TVP. Despite the difference observed in rotation about the axial axis (z-axis), the magnitudes of the remaining displacements and rotations along and around all other axes were similar to the ones observed in previous studies (Table 5.3). Therefore, similar to Chapter 4, SMT used in the current study is representative of a clinical SMT and clinical implications arising from this study are only limited in regards to vertebral axial rotation movement.

Noteworthy, no statistical analysis was conducted on vertebral motion displacements and rotations during SMT applications and differences between displacements and rotations were only described here with the purpose of putting SMT input parameter and consequent vertebral motion into perspective. Despite of this, the description of spinal segment vertebral motion during the SMT application with different parameters is of great importance to demonstrate that SMT input parameters does affect the vertebral motion path and may contribute to the different physiological responses observed following SMT application [22,29,44,45].



### ***5.4.2 Interpretation of Results***

#### ***5.4.2.1 Forces and moments in the intact specimen***

The direction of particular forces and moments experienced by the intact specimen when SMT was applied at L3 vertebra (FJ and TVP), BTW FJ and BTW TVP reversed when SMT was applied at L4 vertebra (FJ and TVP) (Table 5.4). More specifically, peak anterior posterior and lateral forces (forces along y- and x-axis, respectively), and torsion moments (moments around z-axis) created when SMT was applied at L3 vertebra (FJ and TVP), BTW FJ and BTW TVP, were in opposite direction compared to the ones created when SMT was applied at L4. Although a SMT application at L4 vertebra did not cause vertebral motions in anterior posterior and lateral translations completely in the opposite direction as to when applied at L3 vertebra, translations during the SMT application at L3/L4 FJ were considerably smaller than the ones during SMT application at L3 vertebra (L2/L3 FJ and L3 TVP), BTW FJ and BTW TVP. Therefore, even though relative vertebral displacements during SMT application at adjacent levels (L3 and L4 vertebrae FJ and TVP) was not always opposite relatively to each other, anterior posterior and lateral forces and axial moments were opposite. This indicates that spinal loading is not always a reflection of the vertebral displacement (i.e. the axis with the greatest displacement does not always experience the greatest forces or moments) given the unequal dimensions of the vertebral neutral zone combined with directionality in various anatomic conditions and constraints.

The intact specimen also experienced peak anterior posterior forces (forces along y-axis) and torsion moments (moments around z-axis) significantly smaller when SMT was applied at BTW TVP than when applied at any other application site involved in this study. This was expected given that only soft tissues are present underneath the skin overlying BTW TVP. In contrast,

bony structures are present below all other application sites: L2/L3 and L3/L4 FJs, L3 and L4 TVPs and L3 lamina (underneath BTW FJ overlying skin). This suggests that when SMT is provided at the skin overlying soft tissues with no bony structures, SMT forces are dissipated through those soft tissues and significantly smaller loads are transmitted and experienced by the vertebral segment.

Based on the data observed in this study, in order to compensate for applying SMT at BTW TVP, the SMT would require about 2x the force magnitude to create approximately similar torsion moments in the spinal segment as created during a SMT application at L3 vertebra (FJ and TVP). Similarly, for a SMT application at BTW TVP to create anterior posterior forces approximately similar to the ones created by a SMT application at L3 (FJ and TVP), the SMT force magnitude would need to be approximately 8x the one applied in this study, which corresponds to a force magnitude of approximately 2400 N. In order for a SMT application at BTW TVP create anterior posterior forces and torsion moments similar to the ones created during a SMT application at L4 vertebra, the SMT thrust would have to be applied in the opposite direction to the one used in this study, i.e. a thrust applied from anterior to posterior (which may not be clinically possible). Although a SMT with approximately 2400 N was estimated to create similar anterior posterior forces to the ones created when SMT was applied at L3 vertebra (about 30 N), previous research reported failure shear forces ranging from 800 N to 8700 N in porcine spines [173,229,230] and from 700 N to 1000 N in human spines [231,232]. Since a 300N-SMT application at L3 (FJ and TVP) created an average anterior posterior force of 30 N (equivalent to 10% of the applied force), the application of a 2400N-SMT on a vertebral landmark during a mistargeted SMT application is estimated to create an anterior posterior force

of approximately 240N, which would still be below the values reported to cause spinal failure [173,231]. Nevertheless, it is important to emphasize that these are estimates based on the values observed in this study. The application of SMT with greater force magnitudes however will alter the resulting 3-dimensional vertebral motion of the spinal segment, potentially altering the forces and moments created at the specimen.

Peak extension moment (moment around x-axis) was significantly greater when SMT was applied at L3/L4 FJ in comparison to when applied at L4 TVP. Even with a smaller extension rotation during SMT application at L3/L4 FJ than when applied at L4 TVP, the anatomical position of both structures might suggest an explanation for this finding. Given that the spinal segment included in this study is composed of the L3 and L4 vertebrae and the interconnecting structures between them (except muscular tissues), SMT motions applied to this unit falls in between those vertebrae within the mobile portion of the functional spinal unit [126] which is more closely located to the L3/L4 FJ (Figure 5.8) than to L4 TVP. With these anatomical positions, the observation that the application of a posterior-to-anterior SMT thrust on the overlying skin of L3/L4 FJ creates greater extension moments is comprehensible.

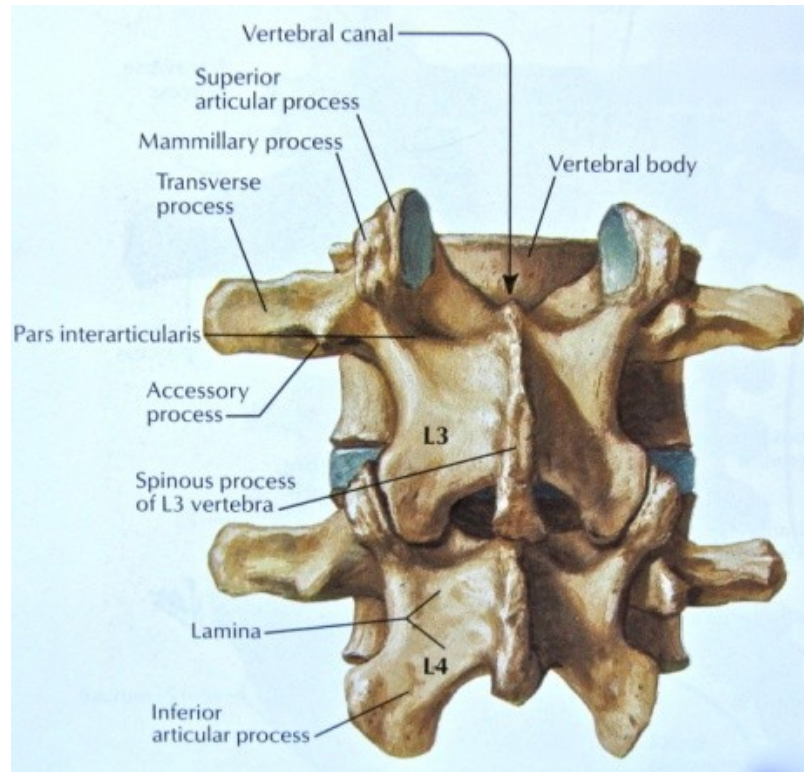


Figure 5.8 Posterior view of the L3-L4 motion segment. [Source: Netter FH. Atlas of human anatomy. 4th ed., 2006. Saunders Elsevier]

Significant differences in experienced torsion moments (moments around z-axis) were also observed when SMT was applied at L4 TVP in comparison to when applied at L3/L4 FJ. The significantly greater torsion moment experienced when SMT was applied at L4 TVP was expected not only due to the greater vertebral axial rotation (Table 5.2), but also due to the anatomical location of both structures in relation to the axial axis of the spinal segment. The longer moment arm presented by the TVP combined with applied forces (such as SMT) gives this structure a mechanical advantage of producing greater moments in comparison to the FJ. Therefore, applying SMT at the TVP creates significantly greater torsion moments on the intact specimen. The effect of SMT application at anatomic landmarks (e.g. FJ and TVP) of adjacent spinal levels on the resulting SMT 3-dimensional vertebral movement remains not completely clear. Despite the limited evidence regarding the specific reasons to why the same significant changes in torsion moments

were not observed when SMT was applied at L3 TVP in comparison to when applied at L2/L3 FJ, it can be speculated that this was likely due to the anatomical position of both structures and their distance to the overlying skin of SMT application sites. In support of this, previous studies have described the distance from the skin to spinal anatomical landmarks and reported TVP structures to be approximately 10 mm further from the skin than FJ and 26 mm further from the skin than spinous process [227,228]. This demonstrates that although a TVP application site presents a longer moment arm, it is also further from the skin, topped with more soft tissue through which SMT forces can rapidly dissipate with a resulting smaller transmission of force to the TVP in comparison to FJ. Therefore, the thickness of soft tissues between the skin and vertebral structures might influence the transmitted SMT forces as well as the SMT resulting vertebral motions.

In summary, the intact spinal segment experienced torsion moments, anterior posterior and lateral forces in opposite direction when SMT is applied at adjacent spinal level (L3 and L4 FJ and TVPs). The anterior posterior and lateral forces and torsion moments were significantly smaller with the SMT application at BTW TVP, with an estimate of significantly greater SMT force magnitude to create loads similar to the ones created during a SMT application at the L3 vertebra. Applying SMT at FJ significantly increases the extension moments while SMT application at the TVP significantly increases the torsion moments experienced by the intact spinal segment.

#### *5.4.2.2 Cut 1: Supra- and interspinous ligaments (SL)*

Overall, SL structures experienced significant change in loads when SMT was applied at different application sites. Importantly, sequential dissection technique revealed that the loads

experienced by SL structures were substantially smaller than the ones experienced by the other spinal structures (PJ and IVD). This indicates that even when SMT is applied at a location that SL structures experienced significantly greater change in loads, PJ and IVD structures will still be experiencing greater loads than SL structures. More specifically, while SL structures experienced, on average, the greatest change in forces and moments during a SMT application at L3 TVP, PJ and IVD structures experienced forces and moments 3x and 6x greater during the SMT application on the same application site, respectively.

Nevertheless, significant change in peak superior inferior forces (forces along z-axis) experienced by SL structures was still observed and a SMT application at L2/L3 FJ created significantly greater change in superior inferior forces in comparison to when applied at L4 vertebra (FJ and TVP), BTW FJ and BTW TVP. Of note, the superior inferior forces (forces along z-axis) experienced by SL structures were in the negative direction of z-axis, which translates into a force in the caudal direction. Even though the SMT application at L2/L3 FJ did not create superior inferior translations considerably different than the ones of the other SMT trajectories, SMT application at L2/L3 FJ created greater rotation in extension movement (rotation around x-axis) which brings the L3 and L4 spinous processes closer together compressing the SL structures. Therefore, the caudal force experienced by SL structures is created to resist the compression occurring during extension movement [91,97].

Change in mean lateral bending moment (moment around y-axis) experienced by SL structures was significantly greater when SMT was applied at L3 TVP than when applied at L2/L3 FJ,

L3/L4 FJ and BTW FJ. This was expected given the anatomical position of TVP and FJ, and the longer moment arm presented by TVP in comparison to FJ.

Significant change in peak torsion moment (moment around z-axis) was also experienced by SL structures. Unexpectedly, and in contrast to the intact specimens, SL structures experienced greater torsion moments with the SMT application at L3/L4 FJ. Table 5.2 shows a smaller vertebral axial rotation when SMT was applied at L3/L4 FJ. Combining a smaller moment arm (in comparison to TVP) and a smaller angular displacement (rotation around z-axis), it is likely that SL structures are resistors of small degrees of axial rotations [97]. When greater rotations are produced, other structures, such as facet joints, are likely engaged and take over the loads in resisting the axial rotation.

In summary, while SMT application at L2/L3 FJ generally increases the forces experienced by SL structures, increased moments are observed when SMT is applied at L3 TVP. Importantly, although SMT application at specific application sites significantly changed loads experienced by SL structures, the amount of loads SL structures carry are substantially smaller than the ones carried by PJ and IVD structures.

#### *5.4.2.3 Cut 2: Bilateral facet joints, capsules and ligamentum flavum (PJ)*

Overall, significant changes in loads experienced by PJ structures were observed when SMT was applied at different application sites. Although the overall forces experienced by PJ structures were generally smaller than the ones experienced by IVD structures, PJ structures experienced greater torsion moments than SL and IVD structures. This indicates that by applying SMT at

TVP (instead of FJ), it is possible to preferentially increase torsion moments in PJ structures without concurrently increasing these same moments experienced by other spinal structures.

Similar to the intact specimen, the change in peak anterior posterior forces (forces along y-axis) experienced by PJ structures when SMT was applied at L3 vertebra (FJ and TVP), BTW FJ and BTW TVP were in the opposite direction to when applied at L4 vertebra indicating that the SMT application at adjacent spinal levels create opposite loads experienced by PJ structures. Also, as observed in the intact specimen, change in forces and moments experienced by PJ structures when SMT was applied at BTW TVP were generally smaller than when SMT was applied at other application sites, likely due to the dissipation of the majority of forces through soft tissues and significantly smaller forces being transmitted to the spinal segment. Additionally, change in torsion moments (moments around z-axis) were also significantly greater when SMT was applied at L4 TVP in comparison to when applied at L3/L4 FJ, which is likely related to the mechanical advantage of TVP's longer moment arm in comparison to FJs, producing greater torsion moments.

Specifically for PJ structures, a significantly greater change in peak lateral force (force along x-axis) was observed when SMT was applied at L2/L3 FJ and BTW FJ (even though in opposite direction) than other application sites. Although SMT application at L2/L3 FJ and BTW FJ did not cause the greatest lateral translations (Table 5.2), facet joint contact and natural ligamentum flavum pretension may have contributed to lateral translation resistance. Supporting this idea, previous studies have described the mechanical function of the facet joint in resisting anterior



and lateral shear movements [74,75]. This indicates that even under small displacements, PJ structures are the main resistors to intervertebral lateral translation movements.

The change in anterior posterior forces (forces along y-axis) and mean superior inferior force (force along z-axis) experienced by PJ structures were significantly greater when SMT was applied at BTW FJ in comparison to when applied at other application sites. Additionally, similarly to SL structures, change in peak superior inferior forces (forces along z-axis) were significantly greater when SMT was applied at L2/L3 FJ than in other application sites. While the significant change in superior inferior forces experienced by PJ structures might be related to the resistance of facet joints to intervertebral compression when extension movement is associated [71,233], significant changes in the anterior posterior forces might be related to the facet joint surface orientation and ligamentum flavum pretension imposing great resistance to anterior posterior shear movements [71,72,234]. While the anterior translation of the superior vertebra in relation to the inferior is resisted by facet joint surface contact, the posterior translation has been described to be resisted by posterior elements of the spine, specifically, spinal ligaments [75,174]. Given that SL structures did not present a significant change in anterior posterior forces, this indicates that ligamentum flavum and facet joint capsules might be important resistors to posterior shear translation.

Similarly to the intact specimen, peak flexion extension moment (moment around x-axis) experienced by PJ structures was significantly greater when SMT was applied at L3/L4 FJ in comparison to when applied at L4 TVP. Despite the smaller extension angular displacement, Schendel and colleagues [76] have described the contact of the anterior inferior portion of facet joint surfaces during extension movement. Therefore, it is possible that when SMT forces were

applied directly on the skin overlying the FJs, less force were dissipated and were more effectively transmitted through these contact points, significantly increasing the moments in extension experienced by PJ structures.

Changes in mean extension moments experienced by PJ structures during a SMT application at L3/L4 FJ and BTW TVP were significantly smaller than the other application sites. This was expected given the smaller vertebral extension rotation caused by the SMT application at these locations.

Interestingly, changes in mean lateral bending moments (moment around y-axis) were significantly greater when SMT was applied at FJs in comparison to TVPs. As similar observation was not revealed for peak lateral bending, it is possible that the preload phase of SMT created greater lateral bending moments on PJ structures when it was being applied at FJs in comparison to at TVPs. Additionally, changes in peak lateral bending were significantly greater during SMT application at L3 vertebra (FJ and TVP) in comparison to at L4 vertebra (FJ and TVP) and may be explained by the greater lateral bending rotations caused by a SMT application at L3 vertebra.

In summary, despite the significant changes in forces experienced by PJ structures when SMT was applied at different application sites, with the greatest changes in force being generally observed when SMT was applied at L2/L3 FJ, overall forces experienced by IVD structures were, on average, approximately 3x greater than PJ structures during a SMT application at the same application site. Notwithstanding, PJ structures were the structures that experienced greater

torsion moments, suggesting that when SMT is applied at TVP (rather than at FJ), PJ structures are loaded preferentially in comparison to other spinal structures.

#### *5.4.2.4 Cut 3: Intervertebral disc, anterior and posterior longitudinal ligaments (IVD)*

Application of SMT at different application sites significantly influenced change in loads experienced by IVD structures. Overall, IVD structures experienced greater forces and moments than the other spinal structures (SL and PJ), with the exception of torsion moments (mainly experienced by PJ structures). This suggests that applying SMT at different application sites may not increase the forces experienced by other spinal structures without concurrently increasing the forces experienced by the IVD structures.

Similar to the intact specimen and PJ structures, change in torsion moments (moments around z-axis) experienced by IVD structures were significantly greater when SMT was applied at TVP in comparison to when applied at FJ, and significantly smaller when SMT was applied on soft tissues (BTW TVP) than at application sites involving bony structures. This again is related to the longer moment arm of TVP structures in comparison to FJ structures, and the force dissipation through soft tissues, respectively.

Generally, a greater change in mean lateral force (force along x-axis) was generally observed when SMT was applied at TVP than when applied at FJ and significant change in mean lateral force was observed when SMT was applied at L3 TVP in comparison to when applied at L2/L3 FJ. This observation may be related to the magnitude of lateral displacement that occurred when SMT was applied at L3 TVP in comparison to when applied at other application sites. Although

PJ structures have been described to be the main resistors to lateral translation, studies have also described the intervertebral disc to contribute to resisting anterior posterior and lateral shear movements [74,174]. This indicates that when significant lateral vertebral translations are produced, not only the PJ structures impose resistance, but also the IVD structures are involved in assisting the resistance to lateral translation movement.

Changes in peak lateral forces and mean anterior posterior forces (forces along x- and y-axis) experienced by IVD structures were significantly smaller during SMT application at BTW FJ in comparison to other application sites. Although the reason for this observation is not clear from the current data, this can potentially be related to the anatomic structures underneath the location in which SMT was applied (L3 left lamina) and the resultant 3-dimensional vertebral movement. Given that vertebral lamina is not a landmark usually targeted during a clinical SMT application, this suggests that applying SMT off-target significantly reduces anterior posterior and lateral forces experienced by IVD structures.

Change in peak anterior posterior forces significantly differed in magnitude during a SMT at adjacent spinal levels and significantly greater anterior posterior forces were observed during SMT application at L2/L3 FJ and L4 TVP. While the greater anterior posterior force experienced by IVD structures during SMT application at L2/L3 FJ can be explained by the greater anterior posterior displacement caused by the SMT application at this location (Table 5.2), the reason for the greater force during SMT application at L4 TVP is less clear. Nevertheless, Table 5.2 shows that the SMT application at L4 TVP caused smallest lateral and superior inferior displacements as well as lateral bending. Therefore, it is possible that the resulting 3-dimensional vertebral

motion caused by the SMT application L4 TVP moved the spinal segment through a specific path in which IVD structures were the main resistors to anterior posterior displacements.

Significant changes in superior inferior forces (forces along z-axis) experienced by IVD structures were observed when SMT was applied at L3 and L4 vertebrae with SMT application at L2/L3 FJ and L4 TVP creating the greatest changes. Interestingly, SMT application at L2/L3 FJ and L4 TVP trajectories presented similar superior inferior translations but smaller than other application sites. The intervertebral disc resistance to compression has been widely described [72,235]. Greater superior inferior translations, however, have been observed to significantly load the PJ structures. Therefore, it can be speculated that with greater superior inferior displacements, the facet joint surfaces become engaged and take over the forces previously experienced by the intervertebral disc during smaller superior inferior translations. In support of this, neural arch and facet joint engagement have been reported to stress shield the anterior elements of the vertebral column during specific postures and movements of the spine [83,85]. Additionally, intervertebral disc height of porcine animals are smaller than humans [159] potentially increasing the stress shield effect of facet joints on the intervertebral disc.

Similarly, changes in mean flexion extension moments (moments around x-axis) were significantly greater when SMT was applied at L3/L4 FJ in comparison to when applied at L4 TVP. Despite the smaller extension rotation occurred during SMT application at L3/L4 FJ (Table 5.2), the IVD structures resistance to extension movements has been previously described [97,236]. Nevertheless, Ryan and colleagues [85] reported that facet joint engagement stress shields the posterior annulus fibrosus of the intervertebral disc during extension movement. This

indicates that IVD structures are greater contributors to resisting small extension movements. Greater extension rotations engage facet joints, which again take over the loads previously experienced by the IVD structures.

Changes in lateral bending moments (moments around y-axis) were significantly greater when SMT was applied at TVP in comparison to when applied at FJ. This might also be related to the longer moment arm presented by TVP structures in comparison to FJ structures. By applying a constant force magnitude, greater moment arms produce greater moments.

Change in peak lateral bending moment was significantly greater during SMT application at L3 vertebra (FJ and TVP) in comparison to the other application sites. The intervertebral disc resistance to lateral bending has been previously described [78,97]. Therefore, given the greater distance from L3 FJ and TVP to the mobile portion of the L3/L4 spinal segment in comparison to the other application sites (Figure 5.8), this observation is comprehensible.

In summary, despite the significant change in torsion moments when SMT was applied at TVP in comparison to FJ, IVD structures experienced smaller torsion moments than PJ structures. Nevertheless, IVD structures generally experienced greater overall forces compared to all other spinal structures suggesting that how ever SMT may be modified in its application, it is difficult to reduce forces imparted to the IVDs.

#### *5.4.2.5 General discussion*

Based on the results of this study, providing SMT at different application sites significantly influenced SMT loading distribution within spinal tissues. Specifically, SMT application site changed the SMT resulting vertebral motion and consequently, significantly influenced the loads experienced by the intact specimen and spinal structures. Although speculations can be made to explain specific significant differences here observed, these results should be carefully interpreted. The observed difference in loads experienced by the intact specimen and by spinal structures should be interpreted as how the distribution of SMT loads change when SMT is applied at different application sites. For example, change in mean lateral bending moment (moment around y-axis) was significantly greater when SMT was applied at L3/L4 FJ for PJ structures, but significantly greater when SMT was applied at L4 TVP for IVD structures. As the discussion of this study provided potential biomechanical explanations for each of these observations, one could interpret these findings as conflicting. However, given the methodology used allowing for the comparison of experienced loads during each SMT trajectory within each set of spinal structures, this should rather be interpreted as difference in SMT loading distribution. Therefore, these results indicate that although the SMT application at L3/L4 FJ and L4 TVP, for example, did not cause a significant lateral bending moment difference in the intact specimen, the distribution of SMT loads change as a function of the application site: PJ structures experience greater lateral bending moment with SMT application at L3/L4 FJ and IVD structures experience the greatest lateral bending moments when SMT is applied at L4 TVP.

Of note, this study observed that the mean moments experienced by PJ and IVD structures are greater than the ones experienced by the intact specimen, with these structures experiencing

mean moments equivalent to 257% and 238% of the mean moments experienced by the intact specimen, respectively. Given that the majority of this percentage correspond to the mean extension moments (around x-axis), this can be explained by the natural pretension of the ligamentum flavum [97]: when the specimen is intact, the ligamentum flavum "assists" the extension movement. Once the ligamentum flavum is removed, this "assistance" is also removed, increasing the resistance to extension movement than previously observed when the specimen was intact and ligamentum flavum was still present.

Importantly, unlike the study conducted by Kawchuk et al. (2010) [24] and the previous study of this dissertation (Chapter 4) where it was observed that the IVD structures were the structures that experienced the greatest forces and moments regardless of the SMT force magnitude and application site, the current study observed that for specific variables, PJ structures were the structures that experienced the greatest moments. Specifically, despite the differences observed within each set of spinal structures (each cut), PJ structures experienced the greatest peak and mean torsion moments (moments around z-axis) and mean flexion extension moments (moments around x-axis). This suggests that by altering SMT application site and applying SMT at TVP (instead of FJ), it is possible to preferentially increase the torsion moments of PJ structures without concurrently increasing torsion moments of IVD structures. Although the SMT application at the TVP created greater torsion moments experienced by the intact specimen as well as PJ and IVD structures in comparison to when applied at other application sites, the torsion moments experienced by PJ structures are approximately 1.6x greater than the ones experienced by IVD structures (Figures 5.5 and 5.6).



Although the previous study of this dissertation (Chapter 4) did not show the greater loads experienced by PJ structures when SMT was applied at TVP in comparison to when applied at FJ, the experiment described in Chapter 4 was an exploratory study involving both force magnitude and application site. Therefore, it is possible that confounding loads related to SMT input parameter of force magnitude did not permit this observation. This highlights the importance of choosing adequate study design and analysis in order to answering specific questions. Given this observation, further studies investigating only SMT force magnitude input parameter should be conducted.

Of note, given the findings of the first study of this dissertation (Chapter 3), the results of the current study is limited to the order in which structures were removed from the specimen during biomechanical testing. By changing the order of structure removal, the loading characteristics experienced by spinal structures during SMT application at different application sites would also be changed. Given the composition and biomechanical function of spinal structures investigated here, it is possible to speculate that structure removal order will not significantly impact the loading characteristics of spinal structures. Nevertheless, future studies are needed to quantify the load difference when different orders of structure removal are used.

#### *5.4.2.6 Clinical implications*

Based on the results of this study, the SMT application at different application sites significantly influenced the SMT loading distribution within spinal tissues.

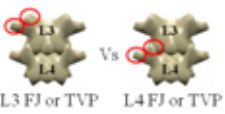

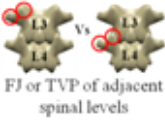












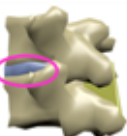

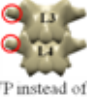

For the intact specimen, to increase the torsion moments, SMT could be applied at TVP (rather than FJ). Alternatively, to decrease the general forces and moments SMT could be applied at BTW TVP.

To generally increase forces experienced by SL structures, SMT could be applied at L2/L3 FJ. To generally increase moments experienced by SL structures, SMT application at L3 TVP could be used. Nevertheless, forces and moments experienced by SL structures are considerably smaller than the ones concurrently experienced by PJ and IVD structures.

For PJ structures, while SMT could be applied at FJ to generally increase forces, SMT could be applied at TVP to generally increase moments with torsion moments being mainly experienced by PJ structures (rather than SL and IVD structures). Of note, overall forces are still greatly experienced by IVD structures. To specifically increase extension moments, SMT application at FJ could be used. Alternatively, to reduce overall forces and moments on PJ structures, SMT could be applied at BTW TVP.

In all application sites, IVD structures experienced greater overall forces. To generally increase forces experienced by IVD structures, SMT application at L2/L3 FJ could be used. Although torsion moments experienced by IVD structures are considerably smaller than the ones concurrently experienced by PJ structures, to generally increase moments experienced by IVD structures, SMT could be applied at TVP. To specifically increase extension moments, SMT application at FJ could be used. To decrease the general forces and moments experienced by IVD structures, SMT could be applied at BTW TVP.

Figure 5.12 summarizes the resulting vertebral motion and spinal structure loading during SMT application at each application site. Noteworthy, given that the current study was conducted using porcine cadaveric models, the clinical implications described here are speculative and further clinical studies are needed to verify their application to human spines.

SMT application at:	Effect on vertebral motion:	To affect:	Apply SMT at:	To create:
 <p>L3 FJ or TVP Vs L4 FJ or TVP</p>	<p>Opposite direction of: Lateral translation Axial rotation</p>	 <p>Whole segment</p>	 <p>FJ or TVP of adjacent spinal levels</p>	<p>Ant-post / Lat forces Torsion moments in opposite directions</p>
 <p>L3 TVP</p>	<p>↑ Lateral translation Lateral bending</p>		 <p>TVP instead of FJ</p>	<p>↑ Torsion moments</p>
 <p>L2/L3 FJ</p>	<p>↑ Ant-post. translation Flexion-extension Axial rotation</p>	 <p>Posterior ligaments</p> <p>From whole segment total, generally carry: 2.3% of forces; 78% of moments</p>	 <p>L2/L3 FJ</p>	<p>↑ Overall forces</p>
 <p>L3/L4 FJ</p>	<p>↑ Sup-inf translation</p>		 <p>L3 TVP</p>	<p>↑ Overall moments</p>
 <p>L4 TVP</p>	<p>↓ Sup-inf / Lateral translation Lateral bending</p>	 <p>Facet complex + Lig. flavum</p> <p>From whole segment total, generally carry equivalent to: 27.8% forces; 264.3% moments</p>	 <p>FJ instead of TVP</p>	<p>Ant-post forces in opposite directions</p>
 <p>L3/L4 FJ</p>	<p>↓ Ant-post. translation Flexion-extension Axial rotation</p>		 <p>TVP instead of FJ</p>	<p>↑ Overall forces</p>
		 <p>Intervertebral disc + longitudinal lig</p> <p>From whole segment total, generally carry equivalent to: 38.4% of forces; 245.7% of moments</p>	 <p>L2/L3 FJ</p>	<p>↑ Overall forces</p>
			 <p>TVP instead of FJ</p>	<p>↑ Overall moments</p>
			 <p>FJ instead of TVP</p>	<p>↑ Extension moments</p>


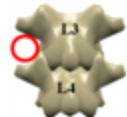


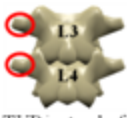


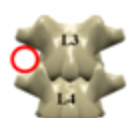


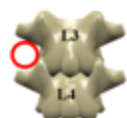

To Avoid:	Apply SMT at:	To create:
 Whole segment	 BTW L3/L4 TVP	 Ant-post / Lat. Forces Torsion moments
 Posterior ligaments	 TVP instead of FJ	 Torsion moments
 Facet complex + Lig. flavum	 BTW L3/L4 TVP	 Torsion moments
 Intervertebral disc + longitudinal ligs	 BTW L3/L4 TVP	 Torsion moments

Figure 5.12 Summary of clinical implications

### 5.4.3 Limitations

The current study investigated spinal structures loads by using a porcine cadaveric model. Although porcine lumbar spine models have been described to be suitable alternative models to human spines [93,95,146], anatomical and biomechanical differences have been described. Therefore, these results are limited in making inferences regarding living human spines. Additionally, differences between *in vivo* and *in vitro* conditions such as physiological and muscular effects, and potential differences in repeated loading testing also limit the application of these results to living condition. Specifically for this study, some specimens presented forces along z-axis reaching a ceiling effect during initial positioning of the intact specimen, reducing

the sensibility of the load cell in measuring forces along z-axis in the intact specimen. Finally, given the findings reported by Funabashi et al. (2015) [217], the loads reported in the current study are specific to the order in which spinal structures were removed from the specimen.

## **5.5 Conclusion**

Based on the findings of this study, SMT application site significantly influences the resulting complex 3-dimensional vertebral motion and spinal tissue loading distribution. The SMT application at adjacent spinal levels caused opposite relative vertebral movements relatively to each other and, consequently, opposite anterior posterior forces and torsion moments. When SMT was applied between vertebra (BTW TVP), significantly smaller forces and moments were experienced by the intact specimen, PJ and IVD structures. Additionally, when SMT was applied further from the midline within the same vertebra (at TVP versus FJ), greater torsion moments were observed. Most importantly, the results of this study demonstrated by altering SMT application site and targeting TVPs (rather than FJs), it is possible to preferentially target PJ structures.

## **Chapter 6.**

### **Spinal tissue loading as a function of the method of spinal manipulative therapy application**

#### **6.1 Introduction**

Spinal manipulative therapy (SMT) is a common intervention for low back pain and is mainly used by chiropractors and osteopaths since the late 19<sup>th</sup> century [237]. It involves the application of a dynamic, high-velocity, low-amplitude thrust, causing a mechanical deformation of the spine and surrounding soft tissues [20–22]. While SMT is used commonly by the public [102], its application is difficult to standardize for a number of reasons including variation of input parameters (e.g. thrust duration, loading rate, preload phase forces) within and between clinicians. Specifically, peak force magnitudes, application site, contact surface area and hand configuration during SMT application have been previously described to significantly vary and influence the location, magnitude and pressure distribution of SMT loads [20,21,35,142,218].

Without controlling SMT input parameters, systematic investigations on the effect of SMT is problematic [39]. Based on this limitation, mechanical devices have been developed aiming at standardizing SMT application toward minimizing variability of SMT input parameters. While the use of mechanical devices does reduce SMT variability [36], it remains unknown if these mechanical devices elicit the same outcomes as manual SMT [106]. Therefore, the clarification of SMT load distribution within spinal tissues when SMT is provided with different methods of application is fundamental not only to clarify if the SMT application by a mechanical device is representative of a clinical SMT application, but also to verify if different devices could be used to preferentially target specific spinal structures.

Specifically, mechanical force manually assisted (MFMA) instruments have been developed and used widely in both research and clinical settings [37,212]. Although the use of MFMA instruments have been described to reduce variability between clinicians, MFMA instruments are still subjected to inter-operator and inter-trials variability [36] in force magnitude and force duration as instruments are still hand-held. To address the limitation of hand-held instrumentation to provide SMTs, a servo-controlled linear actuator motor was recently developed to simulate SMT with optimized precision and repeatability [39]. Compared to hand-held MFMA instruments, the device developed by Descarreaux and colleagues is suspended from a rigid framework and can replicate specific force-time profiles which makes it ideal to investigate the relationship between SMT input parameters and physiological outcomes [28,56,57].

Given that both hand-held MFMA instruments and rigidly-supported linear actuators are thought to reduce clinical SMT force variability, studies investigating SMT underlying mechanisms and physiological outcomes have been conducted using these mechanical devices [28,56,125,212]. Unfortunately, differences in SMT input parameters between methods of application might impose significant limitations when interpreting and translating those results into clinical settings. Specifically, while SMT input parameters, such as peak force magnitude, loading rate and thrust duration have been described to change the outcomes elicited by SMT [29–31,141,145], they have not been controlled for in a single experiment.



Importantly, by identifying how load distribution within spinal tissues change when different methods of SMT application is used, it may be possible to identify if one method of SMT application preferentially loads one specific spinal structure. If it can be shown that spinal tissue response can be modified by SMT application method, then important indicators regarding SMT specific health outcomes might be revealed in addition to the potential of developing new clinical techniques tailored to a patient's specific needs. Therefore, the objective of this study was to compare the loading characteristics of spinal structures when SMT was provided with different methods of application in cadaveric porcine lumbar spines. Given that each method of SMT application present distinct force-time characteristics (e.g. peak force magnitude, contact surface area, loading rate) and those have been described to significantly influence SMT effects [142,212,218], it is hypothesized that SMT load distribution within spinal tissues will significantly differ as a function of the method of SMT application.

## **6.2 Methods**

### ***6.2.1 Overview***

Similar methodology to that used in this study was described in detail within Chapter 4 of this dissertation. Generally, an optical tracking system was used to record the vertebral motions arising from SMT application with three different methods (MFMA instrument, manual SMT and linear actuator motor). These vertebral motions were then replicated by a parallel robotic platform and through the use of kinematic replication with serial dissection, forces and moments experienced by specific spinal structures were quantified.

### ***6.2.2 Sample Size Calculation***

The sample size calculation was conducted based on the data previously reported by Kawchuk and colleagues (2010) [24] using the General Power Analysis Program (G\*Power 2) (University of Trier, Germany). With a statistical power was set at 0.80 (80%), two-tailed tests with level of significance set at  $\alpha=0.05$  (5%) and an effect size of 0.99-1.2, a sample size of 9 porcine models was required. Five additional porcine models were included to account for possible specimen loss due to data collection, potting procedure or testing complications and a total of 14 cadaveric porcine specimens were included. Given that the study from Kawchuk and colleagues also observed 12 variables, the use of the effect size reported by these authors for the current sample size calculation is appropriate. Therefore, with a level of significance set at 0.05 and statistical power set 0.80, the chances of having types I and II errors were 5% and 20%, respectively.

### ***6.2.3 Specimen Preparation***

This study used 12 fresh porcine cadavers (Duroc X [Large White X Landrace breeds]) of approximately 60-65kg (two porcine specimens were excluded due to technical complications). In each intact porcine cadaver, ultra-sound imaging and needle probing technique were used to identify L3 and L4 vertebrae and L3/L4 left facet joint (FJ). One bone pin was drilled into the each of the L3 and L4 vertebral bodies and a rectangular flag having 4 infrared light-emitting diode markers was attached to the upper end of each bone pin (Figure 6.1).

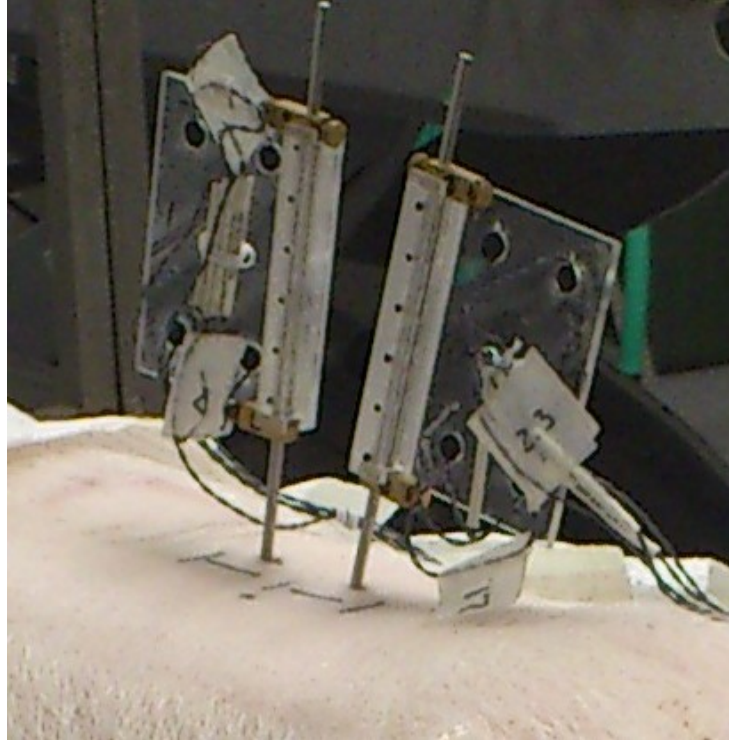


Figure 6.1 Rectangular flags with 4 infrared light-emitting diode markers attached to bone pins drilled into L3 and L4 vertebrae.

Following the application of SMT with the 3 different methods of application on the intact porcine cadaver (detailed in the following sections), the lumbar spine was removed *en bloc* [24]. The L3/L4 spinal segment was cleaned of non-ligamentous tissues, sealed in a plastic bag and kept refrigerated at 3°C for less than 5 hours until potting and testing on the following day [213]. The specimen was kept moist with physiologic saline throughout preparation, embedding and testing [170,178].

#### **6.2.4 Spinal manipulation**

Three methods of SMT were used to apply a posteroanterior thrust to the skin overlying the L3/L4 left FJ: a MFMA instrument (Activator V-E, Activator Methods International, Phoenix, AZ) (SMTact), a trained clinician with 3 years of clinical experience (SMTman), and the servo-

controlled linear actuator motor (SMTmot) [39] (Appendix II) (Figure 6.2). The SMTact was set to at maximum force and the clinician instructed to apply a general SMT using the hypothenar push manipulation in which the clinician's pisiform bone was positioned on the skin overlying L3/L4 FJ. For SMT application with SMTmot, a peak force magnitude of 300N was used, preload phase force was adjusted to be 10% of the peak force (30 N) and the slope of the force curve from preload to peak load being 2.6 N/ms with a time to peak of 112.5 ms.

A pressure array (Pressure Profile System, Inc. Los Angeles, CA) was used in 5 additional cadaveric porcine models with identical characteristics (breed, weight) to measure the SMT force-time characteristics applied by the SMTact and SMTman. The pressure array was placed between clinicians hands/SMTact contact tip and the skin overlying L3/L4 FJ. The pressure array was 1 mm thick, composed of 10x10 pressure sensors with a pressure sensitivity of 0.15% and recorded the force-time characteristics of SMT application at a rate of 120 Hz.

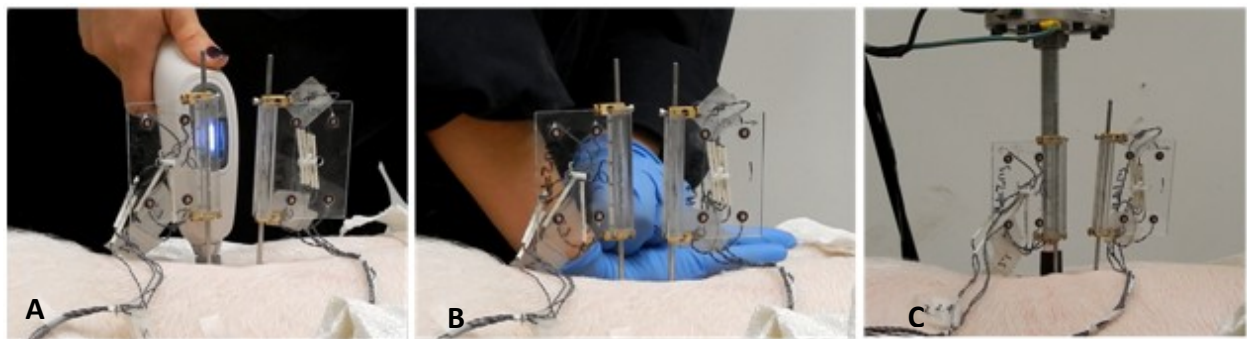


Figure 6.2 Three methods used to apply SMT: A. mechanical force manually assisted instrument (Activator V-E); B. Manual SMT; C. linear actuator motor.

### **6.2.5 Kinematic Recording**

During the application of each SMT, the resulting L3 and L4 vertebral motion was captured by each bone pin and sensor flag and recorded in 3 dimensions by an optical tracking system at a

rate of 400 Hz (0.01 mm system resolution with 0.15 mm rigid body resolution; NDI, Waterloo, Canada) (Appendix III).

#### **6.2.6 Potting Procedure**

This study followed the standardized potting procedure described in the previous chapter (Chapter 4) where specimens were potted in a vertical orientation using dental stone (Modern Materials, South Bend, IN) with the intervertebral disc positioned parallel to the horizontal plane (Figure 6.3).

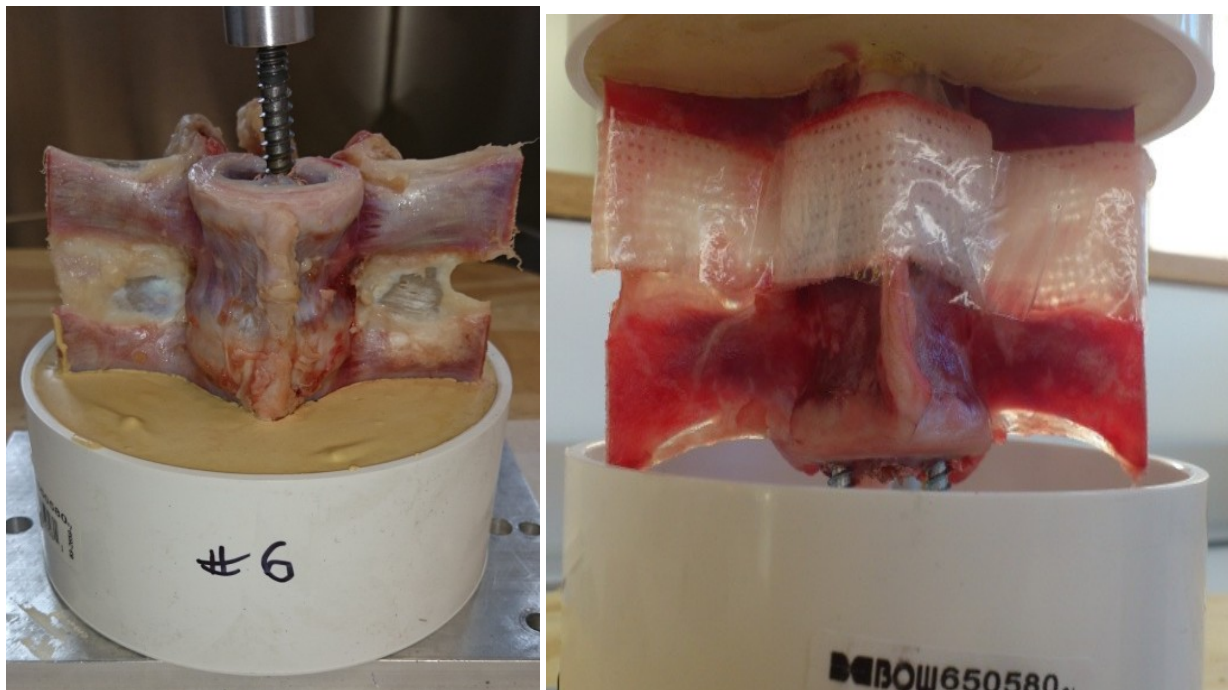


Figure 6.3 Standardized potting procedure and L3/L4 spinal segment.

#### **6.2.7 Robotic Testing**

Following the potting procedure, the robotic testing was conducted as previously described in Chapter 4. In brief, the caudal end (L4) of the potted spinal segment was fixed to a 6-axis load cell (AMTI MC3A-1000, Advanced Mechanical Technology, Inc., Watertown, MA) and the load

cell mounted rigidly to a parallel robot platform (Parallel Robotics Systems corp., Hampton, NH). A calibration process was performed [216] (Appendix IV) resulting in 3 robotic trajectories files consisting of a series of commands corresponding to each of the 3 methods of SMT application (SMTact, SMTman and SMTmot). The robot accepts commands less frequently than data points are generated by the optical system. Therefore the robotic command files were re-sampled to move the robotic platform in displacement control method reproducing the path of each SMT previously recorded. Given the safety settings of the robot, the SMT path replication was approximately 10% slower than the original SMT application. The cranial end of the potted specimen was then fixed to a stationary cross beam and the segment positioned in the initial neutral position.

The robot was then moved and, starting from the initial neutral position, SMTs replications were reproduced in the following sequence: SMTact, SMTman and SMTmot. Each movement replication was separated by a 2 minutes recovery time as it was the minimum time necessary to perform all the tasks between tests (saving data, removing spinal structures, setting up for next test) and satisfied the minimum time for loads to return to baseline [24]. Based on feasibility tests performed by Kawchuk and colleagues (2010) [24] where peak loads in the specimen reached equilibrium within 2 or 3 trials, 3 pre-conditioning trials were executed prior to testing.

The forces and moments experienced by the specimen during robotic replication of SMTs applied by different methods were recorded (axes of movement:  $x$  = medial/lateral,  $y$  = anterior/posterior, and  $z$  = superior/inferior). Following the replication of SMTs kinematics by the robot, spinal structures were removed and/or transected from the specimen and the same

robotic trajectories repeated by the robot. Based on the findings reported by Funabashi et al. (2015) [217] that the order in which structures are removed from the specimen influence their loading characteristics, spinal structures were removed/transected (via scalpel unless otherwise noted) in same order from all specimens: 1) supra- and interspinous ligament (SL), 2) bilateral facet capsules, facet joints (via rongeur) and ligamentum flavum (PJ), 3) intervertebral disc and anterior and posterior longitudinal ligaments (IVD). Given the intertransverse ligaments fragile nature and frequent damage during *en bloc* spinal removal, all specimens had their intertransverse ligaments removed prior to testing.

### **6.2.8 Data Analysis**

#### **6.2.8.1 Overview**

Similar to Chapter 4, this study also analysed 12 dependent variables corresponding to the peak and mean forces and moments measured and recorded along and around each of the 3 Cartesian axes, in 4 conditions independently observed (intact and following the removal of spinal structures). In contrast to Chapter 4, however, this study investigated only 1 independent variable: method of SMT application (SMTact, SMTman and SMTmot). Table 6.1 presents the description of conditions and variables, and the definition of included dependent variables.

**Table 6.1. Description of conditions and variables used throughout the chapter**

Term	Definition
Condition (n=4)	State in which specimens were tested. This study investigated 4 different conditions: 1.Intact specimen, 2.after cut 1 where supra- and interspinous ligaments (SL) were removed, 3.after cut 2 removing bilateral facet joints, capsules and ligamentum flavum (PJ) and 4.after cut 3 removing intervertebral disc and anterior and posterior longitudinal ligaments (IVD).
Independent variable (n=3)	Variable under investigation. In this study, independent variable is method of SMT application: SMTact, SMTman and SMTmot.
Dependent variable	Measured variable, outcome. In this study, dependent variables are peak and mean forces and moments along and around all 3 axes of movement, respectively.
• Peak forces and moments	Maximum measured force and moment during the SMT thrust phase. For passive physiological moments, the maximum force and moment during the applied motion
• Mean forces and moments	Average value of forces and moments involving both the preload and thrust phases of SMT. For passive physiological movement, the average value of forces and moments involving the entire movement.

#### 6.2.8.2 Data Processing

Data extraction and processing has been detailed in the previous chapter of this dissertation (Chapter 4). Briefly, baseline forces and moments were considered to be those recorded when the specimen was positioned in the same initial position as *ex vivo*. The resulting forces and moments of each specimen were plotted against time for each condition (intact and following the removal of spinal structures) and peak and mean forces and moments along and around each axis (x-, y-, z-axes) were identified by customized software (LabVIEW, National Instruments, Austin, TX). Similarly to Chapter 4, relative peak and mean forces and moments experienced by spinal structures were normalized to the respective load experienced by the intact condition during the SMT application with each method. The magnitude of displacements (translation and rotation) where peak loads occurred was also identified by the customized software.

Pressure data during SMT application with SMTact and SMTman was plotted against time by using the software provided by the manufacturer (Chameleon Visualization and Data Acquisition



Software 2012, Version 1.7.0.6, Pressure Profile Systems. Inc., Los Angeles, CA). Peak force magnitude during SMT thrust phase and time to peak were extracted by the software and used for SMTact and SMTman force-time characterization. Contact surface area at peak force magnitude during SMTman application was extracted by the pressure recording software and was considered to be the area around the sensor recording the peak force magnitude in which forces above 10% of the recorded peak force magnitude were observed.

#### *6.2.8.3 Statistical Tests*

Given the objective of this study to compare the loading characteristics of spinal tissues during the application of SMT with different methods, each condition (intact condition and following the removal of spinal structures) was analyzed independently. Given that all methods of SMT application were performed on the same specimen, each observation of forces and moments when SMTs with different methods of application were replicated was considered a repeated measure. Therefore, for the intact specimen, a repeated measures multivariate analysis of variance (MANOVA) followed by a Bonferroni post-hoc analysis for pairwise comparisons was conducted. For the analysis of change in loads following the removal of each spinal structures, a MANOVA for the regression coefficients was conducted followed by a Tukey post-hoc test for the multiple pairwise comparisons of the removed spinal structures. Statistical tests were performed combining IBM SPSS Statistics for Windows, Version 22.0 (Armonk, NY: IBM Corp.) and R: A language and environment for statistical computing (R Foundation for Statistical Computing, Vienna, Austria).

## 6.3 Results

### 6.3.1 Overview

Overall, the method in which SMT was applied significantly affected the loads experienced by spinal structures. Generally, SMTact created smaller forces and moments at the L3/L4 spinal segment while overall SMT forces and moments applied by SMTman and SMTmot were distributed mainly within PJ and IVD structures.

### 6.3.2 General descriptive statistics

#### 6.3.2.1 Spinal manipulative therapy characteristics

From the pressure system recordings, peak force magnitudes, contact surface area and time to peak measured during SMTact and SMTman are shown in Table 6.2 together with SMTmot characteristics. While Figure 6.4 shows an example of raw forces and moments along and around all three axes of movement during the SMT application with each method experienced by the intact L3/L4 spinal segment and following each cut, Figure 6.5 shows an example of contact surface area at peak force magnitude during SMTact and SMTman application from pressure array system recordings. As the force-time profile applied by SMTmot were defined before the SMT application and replicated by the device, pressure data were not recorded during the SMTmot application.

**Table 6.2 Average (SD) of spinal manipulative therapy characteristics of each method of application**

Method of SMT application	Applied force (N)	Contact surface area (cm <sup>2</sup> )	Time to peak (ms)	Loading rate (N/ms)	Applied stress (N/cm <sup>2</sup> )
SMTact	120 (±12.7)	0.95	99 (±31)	1.21	126.31
SMTman	524 (±41)	16.63	220 (±15)	2.38	31.51
SMTmot	300	0.8	112.5	2.6	375

SD = standard deviation; SMT = Spinal manipulative therapy; SMTact = mechanical force manually assisted instrument (Activator V-E); SMTman = Manual SMT; SMTmot = linear actuator motor.

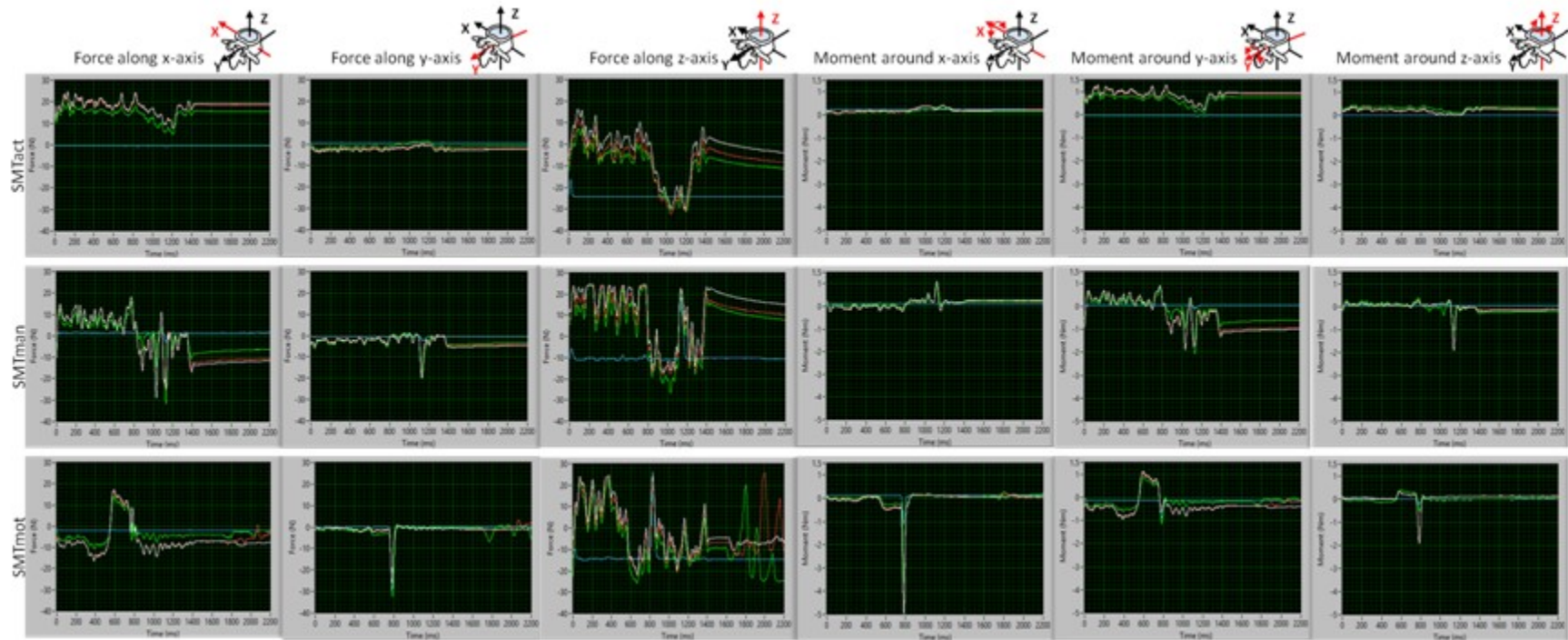


Figure 6.4 Characteristic example of force- and moment-time plots of raw forces and moments experienced by the spinal segment in all three axes of movement during SMT application with all three methods (SMTact, SMTman and SMTmot). White line represents the loads experienced by the intact specimen; red line represents the loads experienced by the whole segment after supra- and interspinous were removed; green line after bilateral facet joints, capsules and ligamentum flavum were removed and blue line after intervertebral disc, anterior and posterior ligaments were removed. SMT=spinal manipulative therapy; SMTact=mechanical force manually assisted instrument (Activator V-E); SMTman=manual SMT; SMTmot=linear actuator motor.

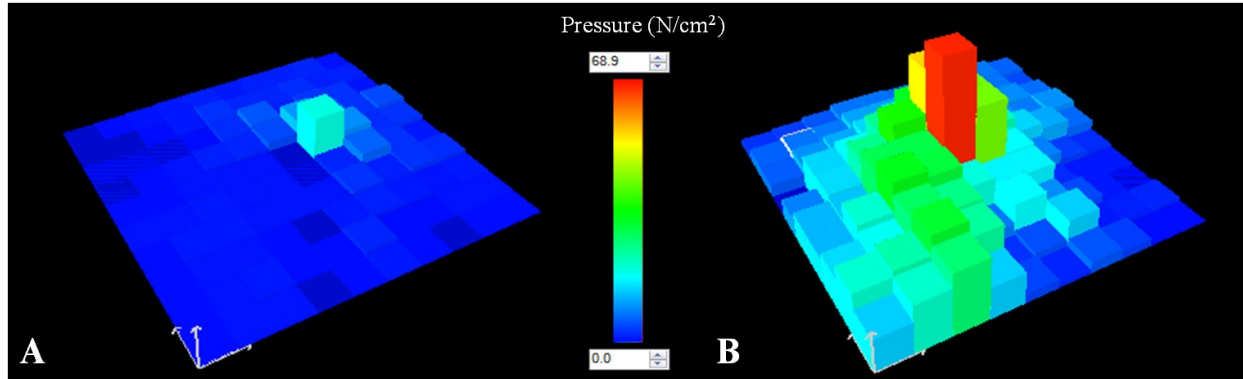


Figure 6.5 Example of contact surface area at peak force magnitude during A. mechanical force manually assisted instrument (Activator V-E) and B. manual spinal manipulative therapy application.

#### 6.3.2.2 Vertebral Displacements

In this study, vertebral displacements arising from application of SMT with different methods were replicated during robotic testing of all conditions. Relative displacements (translation and rotations) of L4 vertebra in relation to L3 vertebra are shown in Table 6.3 by method of SMT application and axis of movement. The greatest translation was observed along the y-axis (posterior to anterior translation) (average: 5.89 mm  $\pm$ SD: 3.92) and the greatest rotation around the x-axis (flexion-extension) (average: 1.97°  $\pm$ SD: 1.32). Among all three methods of SMT application, SMTmot caused the greatest lateral displacement and lateral bending, SMTman caused the greatest anterior and superior displacements as well as extension and left axial rotation.

**Table 6.3 Spinal manipulative therapy maximum displacement (mm) and rotation (°) (SD) created in the cadaveric specimen with the application of SMT (with different methods of application) trajectories**

Method of SMT application	Displacement (mm)			Rotation (°)		
	X (lateral)	Y (ant post)	Z (sup inf)	X (flx ext)	Y (lat bend)	Z (axial rot)
SMTact	0.43 (1.60)	2.16 (1.20)	0.26 (0.20)	0.65 (0.36)	-0.28 (0.28)	0.10 (0.30)
SMTman	1.26 (1.90)	9.10 (2.94)	1.39 (0.36)	3.06 (1.00)	-0.65 (0.52)	-1.71 (1.20)
SMTmot	3.34 (3.59)	6.40 (3.47)	1.33 (0.41)	2.20 (1.09)	-0.86 (0.44)	-1.09 (0.74)
Average of absolute values	1.67 (2.74)	5.89 (3.92)	0.99 (1.32)	1.97 (1.32)	0.63 (0.48)	0.96 (1.03)

SD = standard deviation; SMT = Spinal manipulative therapy; SMTact = mechanical force manually assisted instrument (Activator V-E); SMTman = Manual SMT; SMTmot = linear actuator motor.

### 6.3.2.3 General forces and moments

Figures 6.6 to 6.8 show boxplots with the median, interquartile range, distribution and outliers of peak force, mean force, peak moment and mean moment experienced by the intact specimen and spinal structures during the replication of SMT provided with different methods of application in each axis of movement.

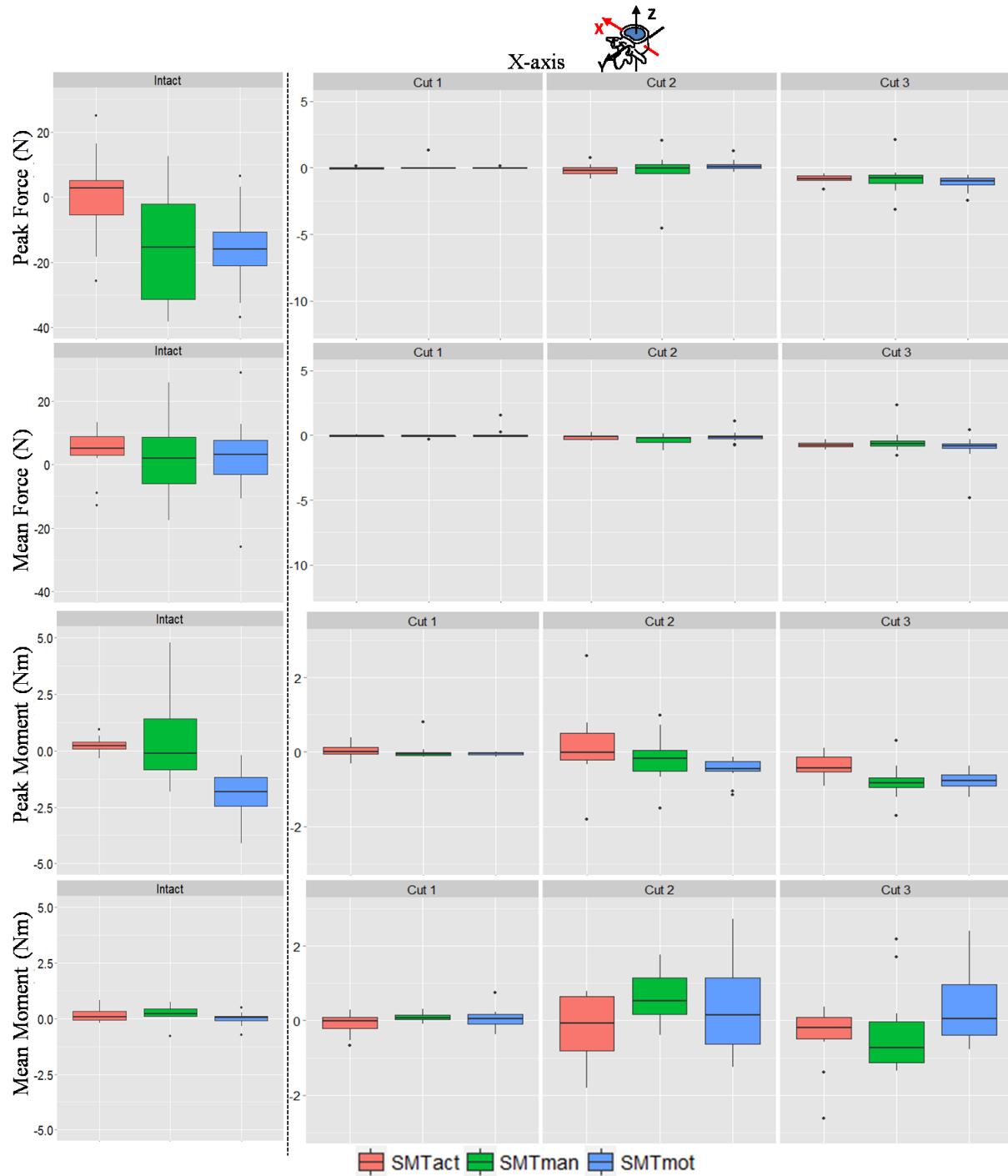


Figure 6.6 Boxplots with median, interquartile range, distribution and outliers of peak and mean forces and moments experienced by the intact specimen and following each cut in the x-axis. SMT=spinal manipulative therapy; SMTact=mechanical force manually assisted instrument (Activator V-E); SMTman=manual SMT; SMTmot=linear actuator motor; Cut 1=supra- and interspinous ligaments; Cut 2=bilateral facet joints, capsules and ligamentum flavum; Cut 3=intervertebral disc, anterior and posterior longitudinal ligaments.

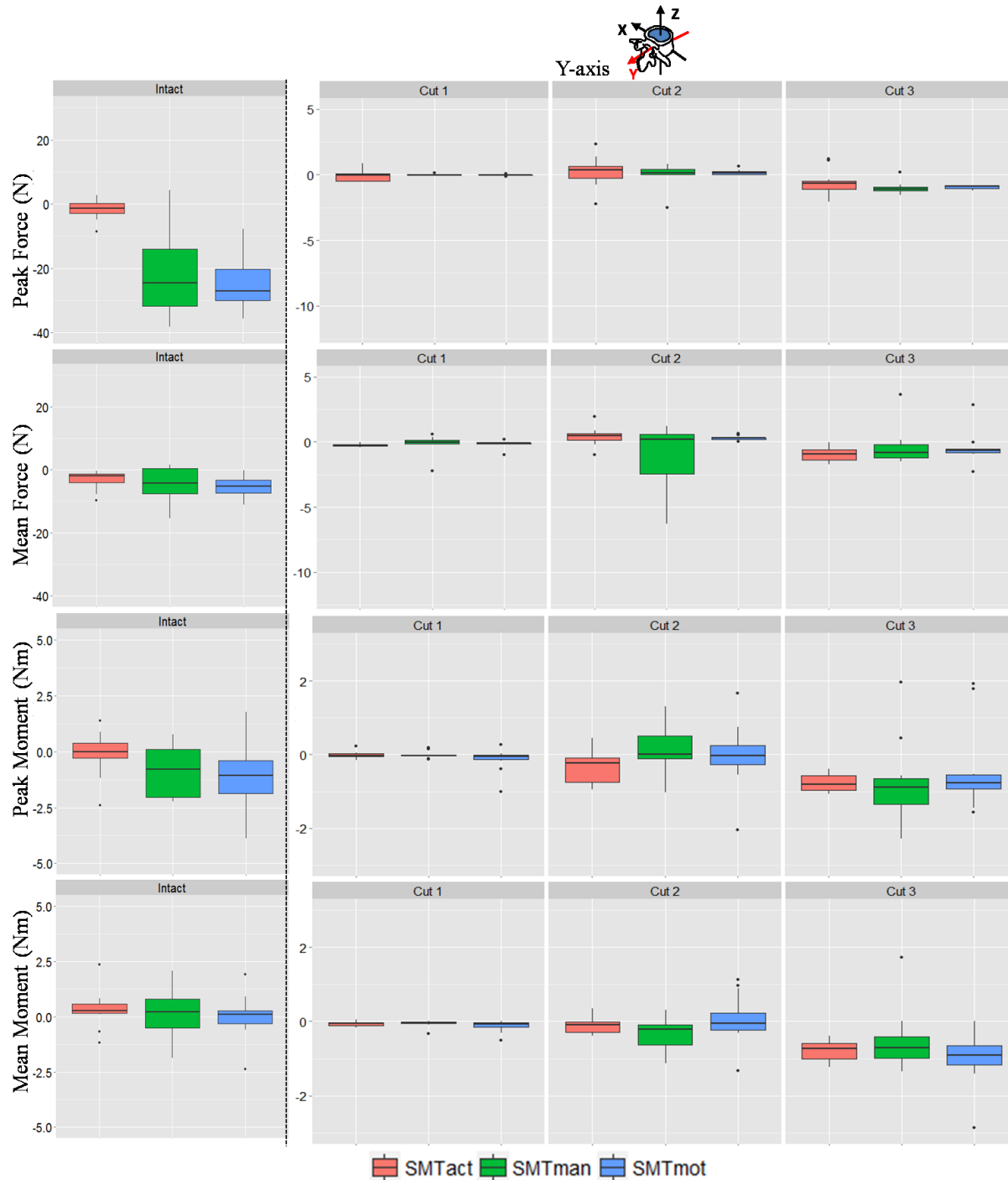


Figure 6.7 Boxplots with median, interquartile range, distribution and outliers of peak and mean forces and moments experienced by the intact specimen and following each cut in the y-axis. SMT=spinal manipulative therapy; SMTact=mechanical force manually assisted instrument (Activator V-E); SMTman=manual SMT; SMTmot=linear actuator motor; Cut 1=supra- and interspinous ligaments; Cut 2=bilateral facet joints, capsules and ligamentum flavum; Cut 3=intervertebral disc, anterior and posterior longitudinal ligaments.

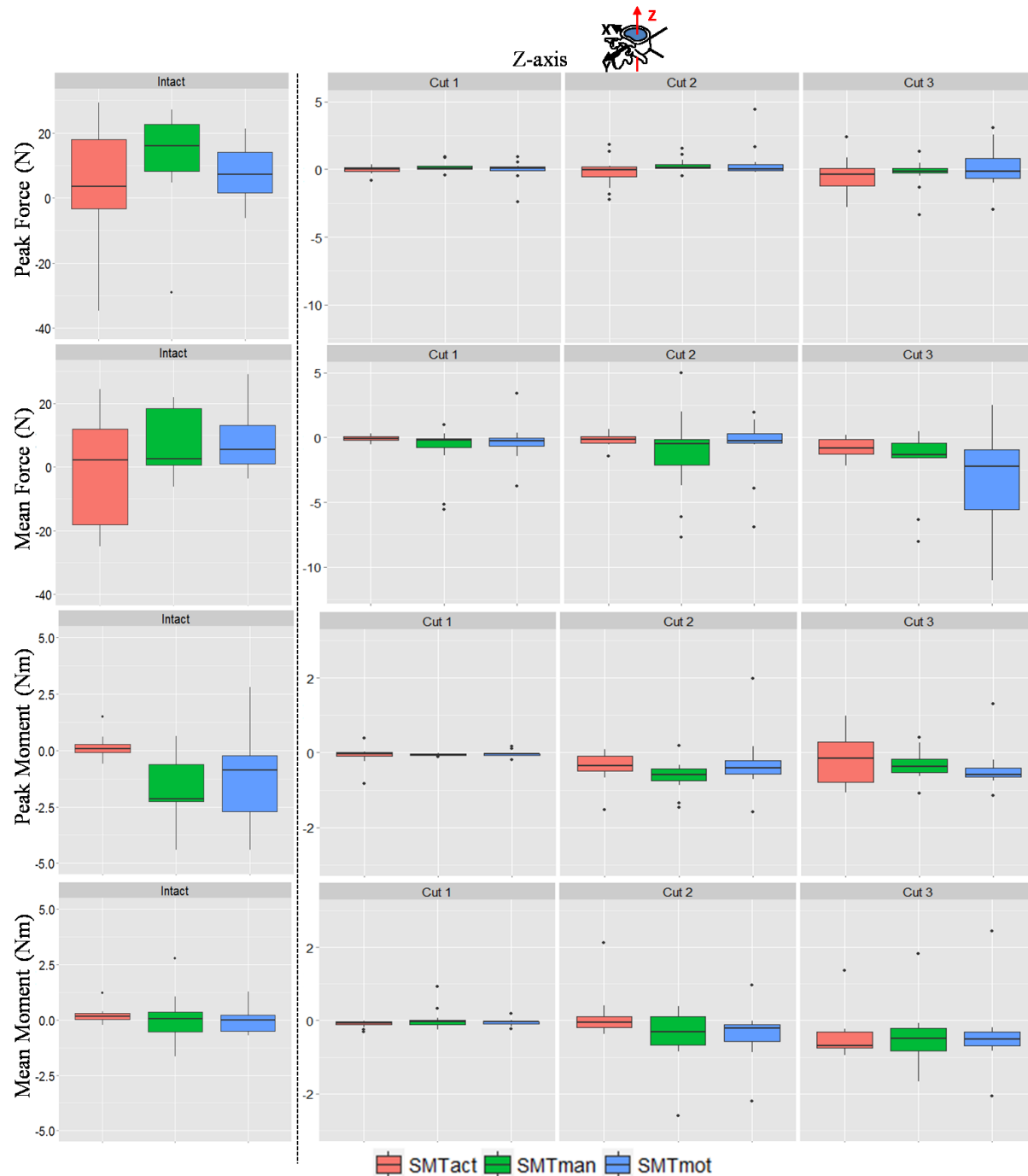


Figure 6.8 Boxplots with median, interquartile range, distribution and outliers of peak and mean forces and moments experienced by the intact specimen and following each cut in the z-axis. SMT=spinal manipulative therapy; SMTact=mechanical force manually assisted instrument (Activator V-E); SMTman=manual SMT; SMTmot=linear actuator motor; Cut 1=supra- and interspinous ligaments; Cut 2=bilateral facet joints, capsules and ligamentum flavum; Cut 3=intervertebral disc, anterior and posterior longitudinal ligaments.



### ***6.3.3 Intact Specimen***

Figure 6.9 shows the average peak force, mean force, peak moment and mean moment experienced by the intact specimen with respect to the method in which SMT was provided. The analysis revealed significant differences in forces and moments experienced by the intact specimen as a function of the method of SMT application. Generally, peak forces and moments created during a SMT application with SMTact were significantly smaller than the ones created during SMTman and SMTmot.

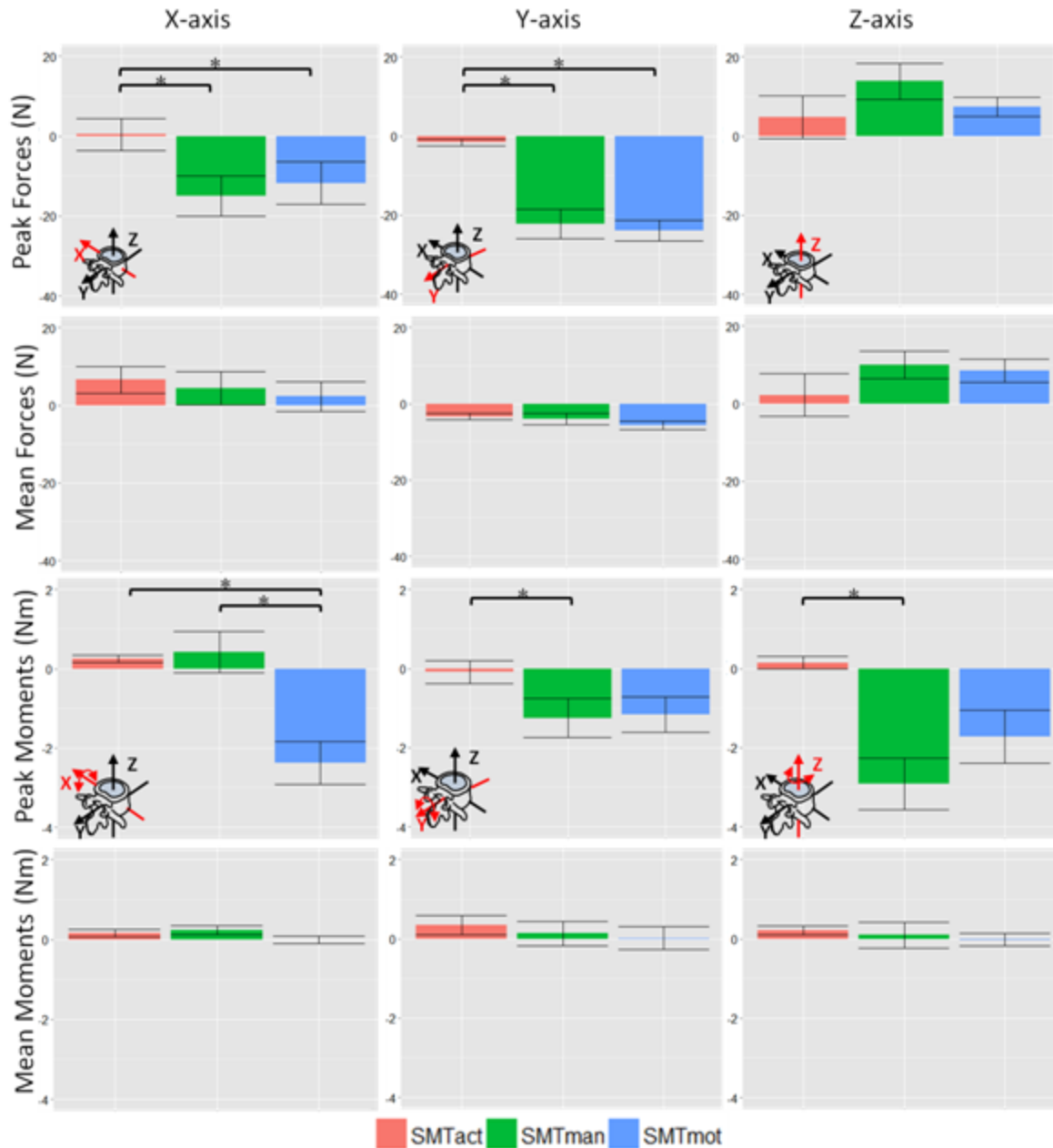


Figure 6.9 Average value of peak force, mean force, peak moment and mean moment experienced by the intact specimen during the application of SMT with different methods.

Specifically, peak lateral and anterior posterior forces (forces along x- and y-axes) experienced by the intact specimen was significantly smaller when SMT was applied with SMTact (lateral force: average: 0.41N, 95% CI [-7.37,8.20]; median: 2.73N (IQR: 10.43); anterior posterior

force: average: -1.64N, 95% CI [-3.40, 0.11]; median: -1.24N (IQR: 3.11)) than when applied with SMTmot (lateral force: average: -11.78N, 95% CI [-22.17, -1.40]; median: -14.38N (IQR: 13.95); anterior posterior force: average: -24N, 95% CI [-29.09, -18.90]; median: -26.98 (IQR: 9.80)) and SMTman (lateral force: average: -14.92N, 95% CI [-24.78, -5.06]; median: -15.46N (IQR: 29.28); anterior posterior force: average: -22.23N, 95% CI [-29.44, -15.02]; median: -24.56N (IQR: 17.62)).

Peak flexion extension moment (moment around x-axis) was significantly greater when SMT was applied with SMTmot (average: -2.37Nm, 95% CI [-3.42, -1.32]; median: -1.86Nm (IQR: 1.80)) and in opposite direction to when applied with SMTact (average: 0.25Nm, 95% CI [0.05, 0.44]; median: 0.21Nm (0.31)) and SMTman (average: 0.41Nm, 95% CI [-0.61, 1.44]; median: -0.10Nm (IQR: 2.25)). Peak lateral bending and torsion moments (moments around y- and z-axes) were significantly greater during SMTman (lateral bending moment: average: -2.91Nm, 95% CI [-2.21, -0.28]; median: -1.11Nm (IQR: 2.07); torsion moment: average: -2.91Nm, 95% CI [-4.19, -1.63]; median: -2.25Nm (IQR: 3.16)) than during SMT application with SMTact (lateral bending moment: average: -0.08Nm, 95% CI [-0.64, 0.47]; median: -0.02Nm (IQR: 0.66); torsion moment: average: 0.15Nm, 95% CI [-0.15, 0.44]; median: 0.08Nm (IQR: 0.35)).

### ***6.3.4 Cut 1: Supra- and interspinous ligaments (SL)***

Figure 6.10 presents the average of normalized peak force, mean force, peak moment and mean moment experienced by SL structures during the SMT application with different methods relative to the intact condition. Considering the total forces and moments experienced by the intact specimen 100%, the total forces and moments experienced by spinal structures during

SMT with each method of application are presented in Table 6.4. Although SL structures experienced significant changes in forces and moments as a function of the method in which SMT was applied, they were substantially smaller than the forces and moments experienced by PJ and IVD structures.

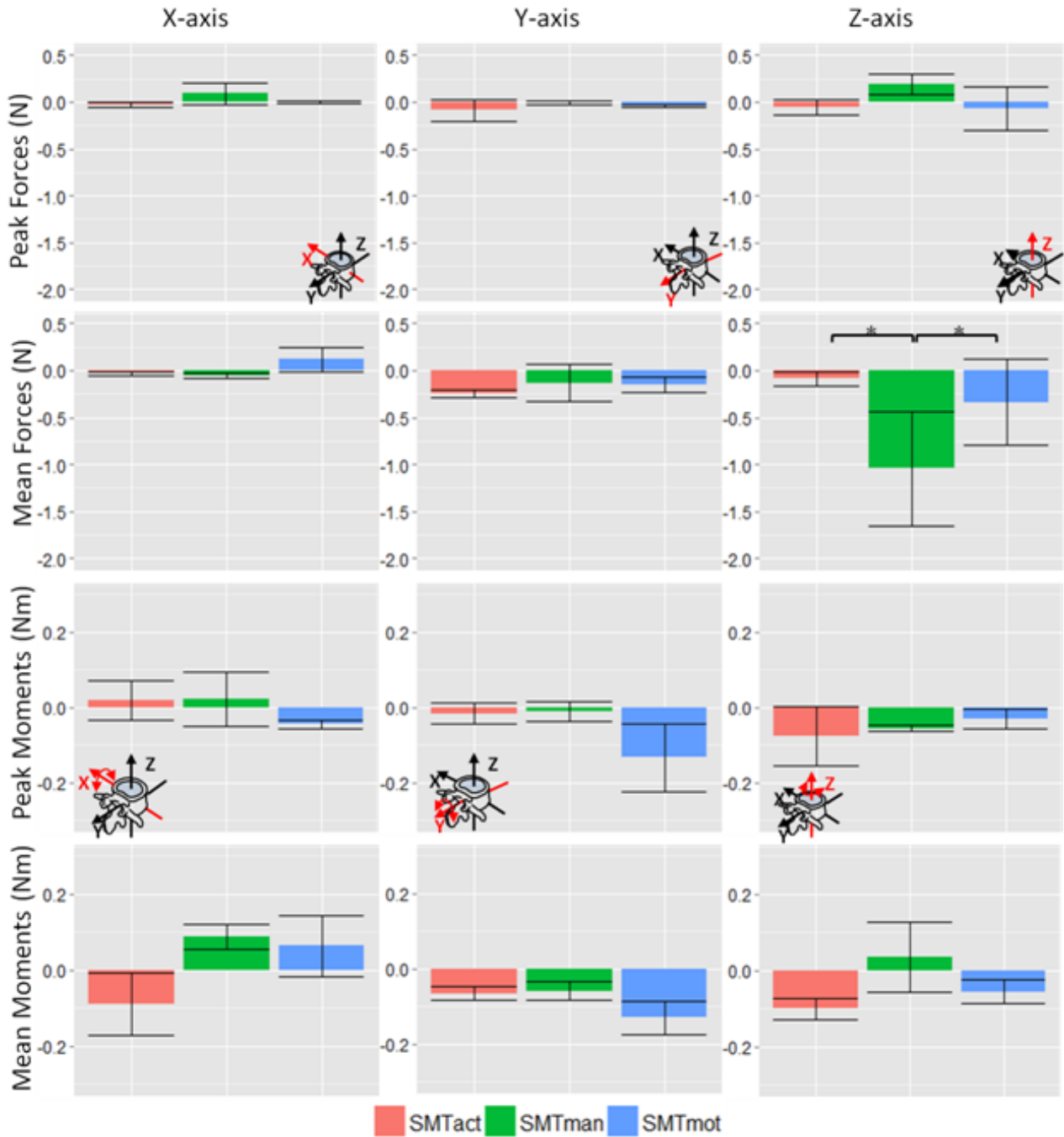


Figure 6.10 Average value of normalized peak force, mean force, peak moment and mean moment experienced by supra- and interspinous ligaments during the application of SMT with different methods.

**Table 6.4 Percentage of general forces and moments experienced by spinal structures during the SMT application with different methods in relation to the loads experienced by the intact specimen (100%)**

Spinal Structure	Method of SMT application	Peak Forces	Mean Forces	Peak Moments	Mean Moments
Cut 1 (SL)	SMTact	2.12%	1.64%	5.96%	30.77%
	SMTman	0.74%	5.94%	3.92%	17.27%
	SMTmot	0.98%	5.46%	4.76%	24.43%
Cut 2 (PJ)	SMTact	7.40%	3.82%	13.33%	17.35%
	SMTman	2.71%	18.10%	32.76%	103.14%
	SMTmot	2.10%	10.31%	26.92%	113.93%
Cut 3 (IVD)	SMTact	10.36%	8.27%	47.41%	126.32%
	SMTman	4.77%	21.12%	41.81%	147.64%
	SMTmot	7.26%	26.36%	49.92%	337.70%

SMT=spinal manipulative therapy; SL=supra- and interspinous ligaments; PJ=bilateral facet joints, capsules and ligamentum flavum; IVD=intervertebral disc, anterior and posterior longitudinal ligaments; SMTact=mechanical force manually assisted instrument (Activator V-E); SMTman=manual SMT; SMTmot=linear actuator motor

Although SL structures were less sensitive to the differences between methods of SMT application, change in mean forces along z-axis was still significantly different when SMT was applied using different methods of application. Specifically, change in mean superior inferior force (force along z-axis) experienced during SMTman (average: -1.04N, 95% CI [-2.23, 0.15]; median: -0.22N (IQR: 0.67)) was significantly greater than when applied with SMTact (average: -0.08N, 95% CI [-0.22, 0.05]; median: -0.10N (IQR: 0.28)) and SMTmot (average: -0.33N, 95% CI [-1.24, 0.56]; median: -0.25N (IQR: 0.61)).

### **6.3.5 Cut 2: Bilateral facet joints, capsules and ligamentum flavum (PJ)**

Figure 6.11 shows the average of normalized peak force, mean force, peak moment and mean moment experienced by PJ structures when SMT was applied with different methods. Despite of the significant changes in forces and moments experienced by PJ structures when using different

methods of SMT application, the changes in overall forces and moments experienced by PJ structures were smaller than the ones experienced by IVD structures (Table 6.4).

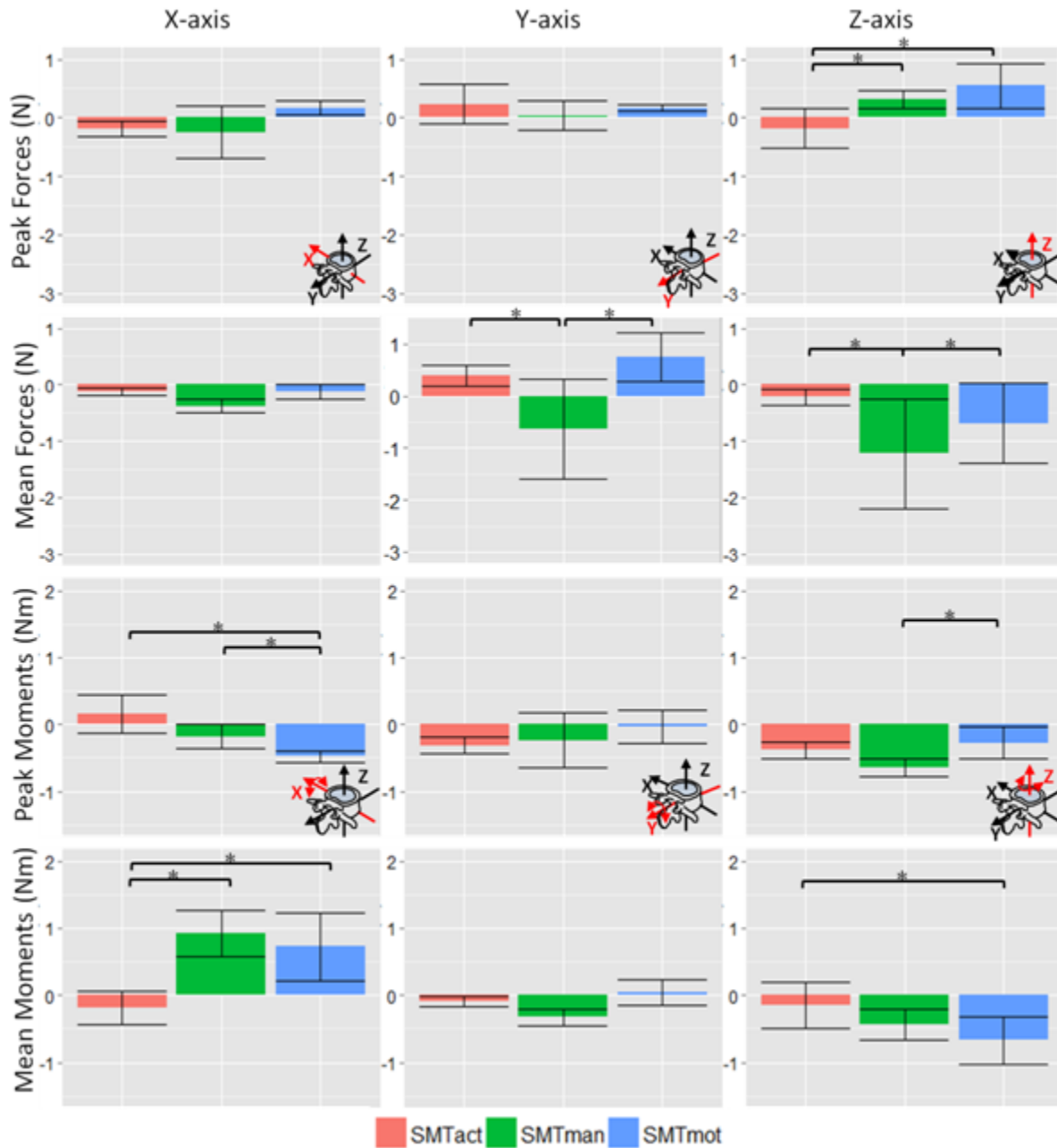


Figure 6.11 Average value of normalized peak force, mean force, peak moment and mean moment experienced by bilateral facet joints, capsules and ligamentum flavum during the application of SMT with different methods.

Specifically for forces, change in peak superior inferior force (force along z-axis) when SMT was applied with SMTact (average: -0.18N, 95% CI [-0.84, 0.47]; median: -0.00N (IQR: 0.75)) was significantly smaller and in opposite direction than both SMTmot (average: 0.54N, 95% CI [-0.20, 1.28]; median: 0.02N (IQR: 0.46)) and SMTman (average: 0.31N, 95% CI [0.00, 0.62]; median: 0.11N (IQR: 0.27)). Additionally, change in mean anterior posterior and superior inferior forces during SMTman application (anterior posterior force: average: -0.63N, 95% CI [-2.51, 1.24]; median: 0.21N (IQR: 2.79), superior inferior force: average: -1.22N, 95% CI [-3.13, 0.68]; median: -0.46N (IQR: 1.98)) were significantly greater than when SMT was applied with SMTact (anterior posterior force: average: 0.39N, 95% CI [0.00, 0.78]; median: 0.44N (IQR: 0.51), superior inferior force: average: -0.21N, 95% CI [-0.50, 0.06]; median: -0.17N (IQR: 0.53)) and SMTmot (anterior posterior force: average: 0.74N, 95% CI [-0.16, 1.66]; median: 0.28N (IQR: 0.16), superior inferior force: average: -0.68N, 95% CI [-2.06, -0.69]; median: -0.24N (IQR: 0.74)) with anterior posterior forces during SMTman being in opposite direction to the ones during SMTact and SMTmot.

Specifically for moments, while change in peak flexion extension moments (moments around x-axis) experienced by PJ structures were significantly greater when SMT was applied with SMTmot (average: -0.48Nm, 95% CI [-0.66, -0.30]; median: -0.45Nm (IQR: 0.27)) than with both SMTact (average: 0.15Nm, 95% CI [-0.41, 0.72]; median: -0.01Nm (IQR: 0.72)) and SMTman (average: -0.17Nm, 95% CI [-0.54, 0.19]; median: -0.16Nm (IQR: 0.55)), change in mean flexion extension moments when SMT was applied with SMTact (average: -0.18Nm, 95% CI [-0.66, 0.30]; median: -0.07Nm (IQR: 1.44)) was significantly smaller and in opposite direction than when applied with both SMTmot (average: 0.72Nm, 95% CI [-1.72, -0.26];



median: 0.29Nm (IQR: 1.94)) and SMTman (average: 0.91Nm, 95% CI [-1.59, -0.23]; median: 0.54Nm (IQR: 1.00)). Additionally, while changes in torsion moments (moments around z-axis) were observed and SMT applied with SMTmot (average: -0.27Nm, 95% CI [-0.74, 0.19]; median: -0.40Nm (IQR: 0.37)) created peak torsion moments significantly smaller than SMTman (average: -0.64Nm, 95% CI [-0.89, -0.39]; median: -0.58Nm (IQR: 0.31)), change in mean torsion moments were significantly smaller during a SMT applied with SMTact (average: -0.15Nm, 95% CI [-0.83, 0.52]; median: -0.08Nm (IQR: 0.32)) than with SMTmot (average: -0.67Nm, 95% CI [-1.37, -0.03]; median: -0.24Nm (IQR: 0.60)).

### ***6.3.6 Cut 3: Intervertebral disc, anterior and posterior longitudinal ligaments (IVD)***

Figure 6.12 shows the average of normalized peak force, mean force, peak moment and mean moment experienced by IVD structures when SMT was applied with different methods. In addition to the significant changes in forces and moments experienced by IVD structures when using different methods of SMT application, these were the structures that experienced the greatest changes in overall forces and moments (Table 6.4).

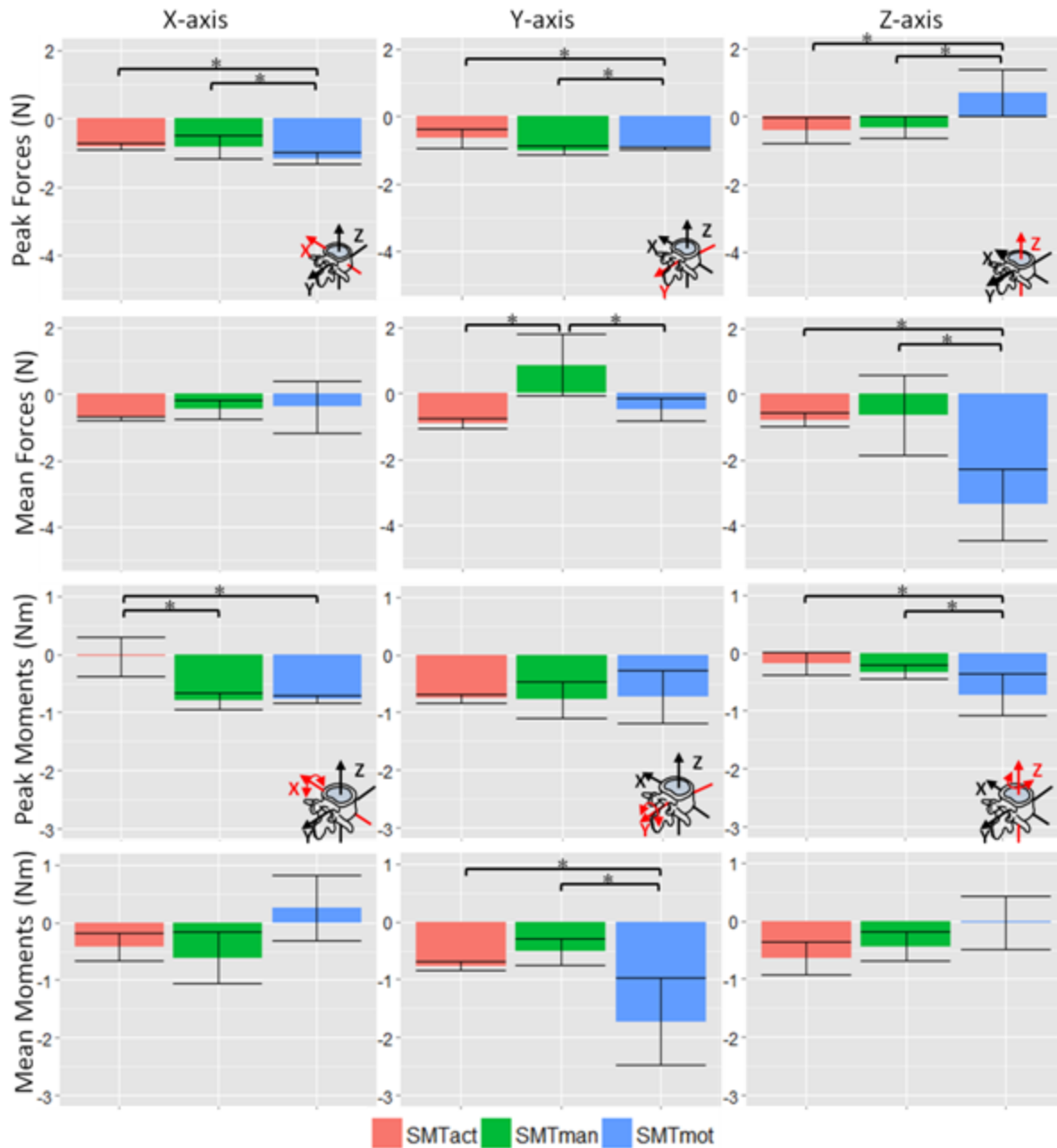


Figure 6.12 Average value of normalized peak force, mean force, peak moment and mean moment experienced by intervertebral disc, anterior and posterior longitudinal ligaments during the application of SMT with different methods.

Specifically, SMT applied with SMTmot (average: -1.16N, 95% CI [-1.49, -0.84]; median: -1.01N (IQR: 0.46)) created peak lateral force (force along x-axis) significantly greater than when applied with both SMTact (average: -0.82N, 95% CI [-1.00, -0.64]; median: -0.81N (IQR: 0.35))

and SMTman (average: -0.82N, 95% CI [-1.50, -0.14]; median: -0.77N (IQR: 0.64)). While change in peak anterior posterior force experienced by IVD structures were significantly greater when SMT was applied with SMTmot (average: -0.95N, 95% CI [-1.03, -0.87]; median: -0.89N (IQR: 0.21)) in comparison to when applied with SMTact (average: -0.65N, 95% CI [-1.23, -0.07]; median: -0.66N (IQR: 0.65)), it was significantly smaller than SMTman application (average: -1.01N, 95% CI [-1.26, -0.76]; median: -1.07N (IQR: 0.32)). Change in peak superior inferior forces during a SMT application with SMTmot (average: 0.68N, 95% CI [-2.03, -0.66]; median: 0.11N (IQR: 1.97)) was significantly greater and in opposite direction than with SMTact (average: -0.42N, 95% CI [-1.17, 0.32]; median: -0.35N (IQR: 1.30)) and SMTman (average: -0.33N, 95% CI [-0.97, 0.31]; median: -0.15N (IQR: 0.38)). While change in mean anterior posterior forces experienced by IVD structures were significantly greater and in opposite direction during SMTman (average: 0.90N, 95% CI [0.98, 2.69]; median: -0.71N (IQR: 2.22)) than with SMTact (average: -0.85N, 95% CI [-1.21, -0.60]; median: -0.90N (IQR: 0.81)) and SMTmot (average: -0.48N, 95% CI [-1.15, 0.17]; median: -0.67N (IQR: 0.30)), change in mean superior inferior forces were significantly greater during a SMT application with SMTmot (average: -3.37N, 95% CI [-5.51, -1.23]; median: -2.20N (IQR: 4.66)) than with SMTact (average: -0.78N, 95% CI [-1.19, -0.37]; median: -0.84N (IQR: 1.11)) and SMTman (average: -0.64N, 95% CI [-3.05, -0.17]; median: -0.91N (IQR: 1.42)).

Specifically for moments, change in peak flexion extension moments (moment around x-axis) was significantly smaller when SMT was applied with SMTact (average: -0.03Nm, 95% CI [-0.69, 0.62]; median: -0.35Nm (IQR: 0.41)) than with SMTmot (average: -0.77Nm, 95% CI [-0.90, -0.65]; median: -0.77Nm (IQR:0.30)) and SMTman (average: -0.80Nm, 95% CI [-1.07, -

0.52]; median: -0.83Nm (IQR: 0.25)). Change in mean lateral bending moments during a SMT application with SMTmot (average: -1.72Nm, 95% CI [-3.19, -0.25]; median: -0.96Nm (IQR: 0.63)) was significantly greater in comparison to when applied with SMTact (average: -0.76Nm, 95% CI [-0.89, 0.04]; median: -0.72Nm (IQR: 0.57)) and SMTman (average: -0.52Nm, 95% CI [-1.48, 0.26]; median: -0.70Nm (IQR: 0.57)). Additionally, significant change in peak torsion moments (moment around z-axis) was also observed and the SMT application with SMTmot (average: -0.72Nm, 95% CI [-1.41, -0.02]; median: -0.59Nm (IQR: 0.27)) created significantly greater changes in comparison to SMTact (average: -0.18Nm, 95% CI [-0.58, 0.20]; median: -0.16Nm (IQR: 1.07)) and SMTman (average: -0.32Nm, 95% CI [-0.55, -0.10]; median: -0.37Nm (IQR: 0.35)).

## **6.4 Discussion**

This study aimed to quantify and compare the loading characteristics of cadaveric porcine lumbar spine structures when SMT was provided with different methods of application (SMTact, SMTman, SMTmot). The results of this study indicate that the method in which SMT was provided significantly influenced spinal structure loading characteristics. In general, while SMT application with SMTact created forces and moments significantly smaller than SMTman and SMTmot, SMTman and SMTmot created greater forces and moments in different directions. Specifically, while SMTman created greater torsion moments in the intact specimen, SMTmot created greater extension moments. Sequential dissection of spinal structures revealed that while PJ structures experienced greater moments during SMTman application, IVD structures experienced greater moments during SMT application with SMTmot. Although studies have been investigating the biological outcomes elicited by SMT by using different devices to reduce SMT force-time characteristics variability [24,28,47,49,141], this is the first study to quantify the

forces and moments experienced by spinal structures and describe how SMT loading distribution within spinal structures changes when different method SMT application is used. Figure 6.13 presents a summary of the general findings of this study.









Spinal structure:	Method of SMT application:	Effect on loading:
 Whole segment	 Mechanical force manually assisted instrument	Create smaller forces and moments
	 Manual SMT	↑ Torsion moments
	 Linear actuator motor	↑ Extension moments
 Facet complex + Lig. flavum	 Manual SMT	↑ Overall moments
 Intervertebral disc + longitudinal ligs	 Linear actuator motor	↑ Overall moments

Figure 6.13 Summary of general findings of this study.

#### ***6.4.1 Spinal manipulative therapy characteristics - Comparison with previous studies***

In the current study, SMT application with SMTact provided an average peak force magnitude of 120N ( $\pm 12.7$ N) reached in 99ms ( $\pm 31$ ms), with a loading rate of 1.21N/ms. Previous studies have investigated the force-time characteristics of MFMA instruments [212,238] and specifically the SMT characteristics of Activator V-E have been recently reported [239]. Although Liebschner and colleagues (2014) [239] observed Activator V-E to provide peak force magnitude of 189N, a peak force magnitude of approximately 130N was measured when SMT was applied on a soft tissue analog, which is comparable to the peak force magnitude measured in the current study. Unfortunately, time to peak and loading rate of SMT applied with Activator V-E have not been reported in the literature, which impedes the comparison with the ones observed in this study.

Manual SMT was applied with an average peak force magnitude of 524N ( $\pm 41$ N) with an average time to peak of 220ms and, therefore, a loading rate of 2.38N/ms. Despite of the well-known variability in SMT force-time characteristics not only between clinicians and trials, but also depending on individual presentation, spinal region and articular stiffness [21,35,114], similar force-time characteristics have been described in previous investigations [122,240–242]. Therefore, the SMTman provided in this study is representative of a clinical SMT application on humans, even though cadaveric porcine models were used.

#### ***6.4.2 Vertebral displacements and rotations - Comparison with previous studies***

In this study, three different methods of SMT application were used to provide a posterior to anterior SMT thrust on the skin overlying L3/L4 FJ. The resulting L4 vertebral translations and rotations relative to L3 vertebra were replicated during robotic testing in all testing conditions

(intact specimen and following spinal structures removal). Table 6.3 shows that the resulting 3-dimensional vertebral displacements and rotations differed as a function of the method used. Similar to our observations, Keller and colleagues (2006) [33] investigated vertebral displacements and acceleration during SMT application with 3 different MFMA instruments on the spinous process of T12. They observed that different magnitudes of vertebral displacements and acceleration were caused by different instruments in all 3 axes of movement which is probably due to differences in force-time characteristics between instruments [33].

In this study, while SMTmot was observed to cause greater lateral displacement and lateral bending, SMTman caused greater anterior and superior displacement as well as extension and axial rotations. Considering the results observed on Chapter 4 of this dissertation where greater SMT peak force magnitude applied at L3/L4 FJ caused greater posterior and superior displacement and extension and axial rotations, and smaller SMT peak force magnitude caused greater lateral displacement and lateral bending, it is possible that the difference in vertebral motions here observed are due to the difference in applied SMT peak force magnitude between SMTman and SMTmot. Nevertheless, the greater lateral displacement and lateral bending observed in Chapter 4 of this dissertation were observed during the SMT application with 100N, which is closer to the SMT peak force during SMT application with SMTact (120N) than with SMTmot (300N). Therefore, this difference in vertebral motion could also be influenced by the contact surface area of each method of SMT application. Specifically, given that SMTman was provided through a substantially larger contact surface area than SMTmot, it is possible that not only L3/L4 FJ, but also surrounding structures were subjected to the force applied by the

SMTman, such as L3 and L4 lamina, producing increased vertebral displacement and rotation in the observed directions.

Despite the differences in magnitude of vertebral displacements and rotations between methods of SMT application observed in the current study, all three methods caused vertebral trajectories in which the greatest displacements occurred along anterior posterior axis and greatest rotations around flexion extension axis. Similar to these observations, previous studies have also reported great anterior displacements and extension rotations during SMTman [24,243] and SMT applied with SMTact [125]. Specifically, Kawchuk and colleagues (2010) [24] also applied Manual SMT in a similar model to the one used in the current study and observed anterior displacements of 5.35mm and extension rotations of 1.96°. Additionally, Gal et al. (1997) [243] observed anterior displacements of 6-12mm and extension rotations of 0.2-1.8° during Manual SMT application at the low thoracic region of human cadavers. Despite the similar axes of greatest displacements and rotations between previous and the current study, the magnitudes of displacements and rotations were considerably different and are likely related to well-known force-time profile significant variability between clinicians [20,35] and SMT application site, as Chapter 5 of this dissertation described differences in the resulting vertebral motion during the SMT application at different application sites. While the current study applied SMT at L3/L4 FJ, Kawchuk et al. (2010) [24] and Gal et al. (1997) [243] applied SMT at the L3 and T10-T12 transverse processes, respectively. Therefore, not only the force-time characteristics, but also the resulting vertebral motions indicate that SMTman applied here was representative of a clinical SMT application.



Similarly, Keller and colleagues (2003) [46] investigated vertebral motions during SMT application at lumbar FJs using a MFMA instrument and although rotations were not measured, anterior displacements of 0.58mm were observed. Given that Keller et al. (2003) [46] applied SMT at similar location to the current study, the noticeable difference in anterior displacement magnitude between studies may be related to differences in SMT force-time characteristics. Although both studies applied SMT using MFMA instruments, distinct models of MFMA instruments were used and might explain these differences in vertebral motion. While Keller and colleagues (2003) [46] used the Activator-II, the current study used Activator V-E. In addition to differences in SMT force-time characteristics between models of MFMA instruments [212], Kawchuk et al. (2006) have demonstrated that although the use of MFMA instruments generally reduces SMT force variability, they are handled by clinicians and researchers and the variability between operators and trials remains significant [36].

In summary, the vertebral displacements and rotations observed during the SMT application with different methods occurred in similar axes to those previously reported, indicating that although SMTs were applied to porcine cadaveric models, the SMT resulting vertebral motions were representative of a clinical SMT application.

### ***6.4.3 Interpretation of Results***

#### ***6.4.3.1 Intact Specimen***

The analysis of the intact specimen revealed peak lateral and anterior posterior forces (forces along x- and y-axes, respectively) significantly smaller when SMT was applied with SMTact in comparison to SMTman and SMTmot. This difference was expected not only due to the

difference in peak force magnitude between methods of SMT application, but also given the resulting vertebral motion caused by SMT application with SMTact in comparison to SMTmot and SMTman. This observation is in accordance to Chapter 4 of this dissertation where SMT application with smaller force magnitudes caused peak lateral and anterior posterior forces significantly smaller in comparison to SMT with greater force magnitudes.

Peak flexion extension moment (moment around x-axis) experienced by the intact specimen was significantly greater when SMT was applied with SMTmot compared to SMTact and SMTman. Given that Chapter 4 of this dissertation found that a minimum of 200N difference in applied SMT peak force magnitude is required to create significant differences in experienced forces and moments, the significant difference in extension moment is then likely related to the resultant direction of the SMT applied thrust. Although SMT thrust application during SMTact and SMTman were intended to be delivered purely in the posterior to anterior direction, the positioning of the instruments were not controlled and resultant direction of the force applied during SMT with both methods were potentially subjected to slight differences. Given that this study did not measure the resulting force direction in which SMT thrust was applied, it is possible that SMTact, SMTman and SMTmot applied a SMT thrust with small differences in direction, with SMTmot potentially creating significantly greater extension moments than SMTact and SMTman.

Peak lateral bending and torsion moments (moments around y- and z-axes, respectively) experienced by the intact specimen were significantly greater during SMTman in comparison to SMTact. The greater torsion moments created by SMTman can be explained by the greater axial

rotation motion it caused in comparison to SMTact (Table 6.3). The greater lateral bending moment, in turn, might be related to the difference in SMT peak force magnitude and the SMT peak force location migration during SMTman [142]. Given the previous investigation demonstrating that peak force application location may shift during the SMTman application, it is possible that the location in which the peak SMTman force was applied shifted in a direction (e.g. laterally) that a greater lateral bending moment was created. Another potential explanation for this observation is the contact surface area in which both SMTs were applied. Given that SMTman provided SMT through a contact surface that is substantially larger in comparison to SMTact, it potentially involved greater lateral area of contact, creating greater lateral bending moments.

In summary, peak forces and moments experienced by the intact specimen were generally more sensitive to differences in methods of SMT application than mean forces and moments. Additionally, SMTact created peak forces and moments significantly smaller than SMTmot and SMTman.

#### *6.4.3.2 Cut 1: Supra- and interspinous ligaments (SL)*

Overall, among the 3 methods of SMT application, SL structures generally experienced greater change in moments during the SMT application with SMTact. Despite of this, the magnitude of forces and moments experienced by SL structures were substantially smaller than those experienced by the other spinal structures, with PJ and IVD structures experiencing moments about 3x and 6x greater, respectively. This indicates that no matter how SMT is applied, the

loads arising from SMT application are distributed mainly within PJ and IVD structures and SL structures experience minor forces and moments (Table 6.4).

Changes in superior inferior forces experienced by SL structures during SMTman was significantly greater in comparison to the ones during SMT application with SMTact and SMTmot. The caudal force experienced by SL structures associated with extension movement has been previously described [91,97]. Therefore, given the greater superior displacement associated with the greater extension rotation observed during SMTman in comparison to SMTact and SMTmot, SL structures experienced greater caudal forces to resist these motions. This is in accordance to the previous Chapter 5 of this dissertation.

In summary, although the forces and moments experienced by SL structures were considerably smaller than the ones experienced by PJ and IVD structures, SL structures experienced significantly greater inferior forces during SMTman than during SMTact and SMTmot.

#### *6.4.3.3 Cut 2: Bilateral facet joints, capsules and ligamentum flavum (PJ)*

Overall, significant changes in forces and moments experienced by PJ structures were observed during the SMT application with different methods. Generally, among the 3 methods of SMT application, PJ structures experienced greater changes in peak moments during the application of SMTman (Table 6.4). Despite of this, the magnitude of the overall forces and moments experienced by PJ structures were smaller than those experienced by IVD structures, with the latter experiencing moments about 2x greater. Nevertheless, peak torsion moments and mean anterior posterior forces experienced by PJ structures during SMTman application were greater

than the ones experienced by SL and IVD structures. This indicates that PJ structures are the main resistors to the axial rotation component and contribute to resisting anterior posterior displacements during SMTman application.

Significant change in superior inferior forces (forces along z-axis) experienced by PJ structures was observed and SMTact created significantly smaller peak superior inferior forces compared to SMTman and SMTmot. The increase in forces experienced by facet joint during compression has been previously described especially when extension rotations and shear displacements are combined [233]. Therefore the significant difference between changes in peak superior inferior forces created by SMTman and SMTmot in comparison to SMTact might be explained by the greater superior and anterior displacements as well as extension rotation caused by those two methods of SMT application in comparison to SMTact (Table 6.3). Similarly, changes in mean anterior posterior and superior inferior forces were significantly greater during SMTman than during SMT application with SMTact and SMTmot, which is likely also explained by the greater vertebral displacements and rotations caused by SMTman than by SMTact and SMTmot (Table 6.3).

Significant changes in flexion extension moments experienced by PJ structures were observed and while peak flexion extension moments were significantly greater when SMT was applied with SMTmot in comparison to SMTact and SMTman, mean flexion extension moments were significantly greater during SMT applied with SMTmot and SMTman in comparison to SMTact. Therefore, extension moments experienced by PJ structures were always smaller when SMT was applied with SMTact, which is likely due to the smaller SMT force applied, causing smaller

extension rotations. Given that changes in peak extension moment created by SMT application with SMTmot in comparison to SMTman were significant, but the mean extension moments were not, it is possible to speculate that the SMT preload phase of both methods present significant differences and compensate for the differences observed in peak moments. Although preload phase was not analyzed in the current study, in Figure 6.4 it is possible to observe that the force magnitude and the duration of preload phase between methods of SMT application were different, with SMTman potentially presenting greater preload force and duration, compensating for the difference in peak extension moment.

Change in peak torsion moments experienced by PJ structures were significantly smaller during a SMT application with SMTmot than with SMTman, which was expected given the applied SMT force magnitude and the vertebral motion caused during SMT application with each method. Interestingly, despite of the smaller axial rotation caused by SMT application with SMTact, the change in peak torsion moments it created was not significantly smaller than the ones created by SMTman and SMTmot. Although we currently cannot demonstrate the exact mechanisms for this observation, it is possible that the combination the of 3-dimensional vertebral motions resulting from each SMT application might have created specific peak torsion moments on the PJ structures, suggesting that moments do not always reflect the vertebral motion. On the other hand, change in mean torsion moment created by SMT application with SMTmot was significantly greater in comparison to SMT applied with SMTact. This again suggests that the preload phase characteristics influence the moments experienced by spinal structures.

In summary, despite the significant changes in forces and moments experienced by PJ structures when SMT was applied with different methods of application, with the greatest changes being generally experienced during SMTman, overall moments experienced by IVD were, on average, approximately 2x greater than PJ structures. Importantly, SMTman not only created the greatest changes in overall moments experienced by PJ structures, but also created greater torsion moments on PJ structures than on SL or IVD structures. This indicates that a SMTman application at the lumbar FJs preferentially loads PJ structures.

#### *6.4.3.4 Cut 3: Intervertebral disc, anterior and posterior longitudinal ligaments (IVD)*

Overall, significant changes in forces and moments experienced by IVD structures were observed during the SMT application with different methods. Generally, among the 3 methods of SMT application, IVD structures experienced greater peak moments during SMTmot SMT (Table 6.4). Although specific forces and moments (mean anterior posterior forces and peak torsion moments) experienced by PJ structures during SMTman were greater than the ones experienced by SL and IVD structures, the magnitude of the overall forces and moments experienced by IVD structures were generally greater than those experienced by SL and PJ structures. This indicates that no matter what method of SMT application is used, IVD structures experience the majority of forces and moments.

Change in peak lateral force (force along x-axis) was significantly greater during SMT applied with SMTmot than with SMTact and SMTman. This was expected given the greater lateral displacement caused by SMT application with SMTmot (Table 6.3). Similarly, change in peak and mean anterior posterior forces (force along y-axis) was significantly greater during SMTman

in comparison to SMT application with SMTact and SMTmot, which is likely also related to the greater anterior translation caused by SMTman (Table 6.3).

Significant change in peak and mean superior inferior forces (force along z-axis) experienced by IVD structures was observed and SMT applied with SMTmot created significantly greater peak superior inferior forces in comparison to SMT applied with SMTact and SMTman. Given that the intervertebral disc has been previously described to resist compression [72,235] and that the greatest superior displacement during SMTman loaded PJ structures in a greater extent, it is possible that IVD structures are responsible for resisting compression during small superior displacements. Since the neural arch has been previously demonstrated to stress shield the intervertebral disc from compressive forces [83], the great superior displacements during SMTman likely engaged and increased facet joint contact, stress shielding the compression forces previously experienced by the intervertebral disc during smaller superior displacements.

Change in peak flexion extension moments (moment around x-axis) was significantly smaller during SMT application with SMTact in comparison to with SMTmot and SMTman. This was expected given the smaller extension rotation observed during the SMT application with SMTact in comparison to the other methods of SMT application (Table 6.3). Although the facet joints contact has been described to stress shield the intervertebral disc posterior annulus fibrosus during extension movement [85], anterior longitudinal ligament and intervertebral disc have been observed to significantly contribute to resisting extension movement [97]. Therefore, PJ and IVD structures experience significantly greater flexion extension moments created during greater extension rotations observed during SMT application with SMTman and SMTmot.



A significantly greater change in mean lateral bending moment (moment around y-axis) experienced by IVD structures was observed during SMT application with SMTmot when compared to SMT application with SMTact and SMTman. In addition to the previous observation from Heuer and colleagues (2007) [97] that the nucleus pulposus is great contributor to resisting lateral bending moments, this can also be explained by the greatest lateral rotation observed during SMT application with SMTmot.

Change in peak torsion moments (moment around z-axis) was also significantly greater during SMT application with SMTmot in comparison to SMTact and SMTman. Although SMT application with SMTmot did not cause the greatest axial rotation, this is likely related to the resultant direction of the SMT applied thrust. As previously mentioned, since the direction of the resultant applied thrust with SMTact and SMTman were not measured, it is possible that the resultant direction of the thrust during the SMT application with both methods were not purely in the posterior to anterior direction. As such, the thrust resultant direction during SMT application with both methods were potentially subjected to slight deviations possibly creating smaller torsion moments in the IVD structures.

In summary, the overall forces and moments created by all methods of SMT application were generally experienced by IVD structures, with the only exception of peak torsion moments during SMTman which was mainly experienced by PJ structures. Significant changes in forces and moments experienced by IVD structures was observed when SMT was applied with different methods of application, with the greatest changes being generally experienced when SMT was

applied with SMTmot. This suggests that SMT application with SMTmot at L3/L4 FJ preferentially loads IVD structures.

#### *6.4.3.5 General discussion*

Based on the results of this study, providing SMT at the L3/L4 FJ with different methods of application significantly influenced the SMT load distribution within spinal structures. For example, while SMTman created greater peak torsion moments on PJ structures, SMTmot was the method that created greater torsion moments on IVD structures (Figures 6.11 and 6.12). Additionally, while SMT application with SMTmot and SMTman created comparable posterior forces on the intact specimen, IVD structures experienced greater posterior forces during SMTman in comparison to SMTmot (Figures 6.7 and 6.12). Moreover, while SMT application with both SMTmot and SMTman generally created greater forces and moments than SMTact in all conditions, PJ structures generally experienced greater changes in moments during SMTman and IVD structures during SMT application with SMTmot (Figures 6.11 and 6.12). These observations show the difference in spinal structure loading when different methods of SMT are used and indicate that different SMT techniques may influence the SMT load distribution within spinal structures.

Given that all SMTs were applied at the same location of the spine, differences in loading distribution are likely related to differences in SMT characteristics [33,212]. Since SMTs were provided with distinct methods of SMT application, not only SMT peak force magnitudes, but also the contact surface areas between methods of SMT application were noticeably different (Table 6.2). Specifically, although the contact surface area from SMTact and SMTmot were

similar, the one from SMTman was substantially greater. Consequently, it is possible that additional structures were displaced during the SMT force application when SMTman was provided in comparison to SMTact and SMTmot.

Additionally, as each method of SMT application provided SMT with different peak force magnitudes and presented unique contact surface areas, the estimated total stress applied by each method was also substantially different: SMTmot applied considerably larger stress ( $375\text{N}/\text{cm}^2$ ) followed by SMTact ( $126.3\text{N}/\text{cm}^2$ ) and SMTman ( $31.51\text{N}/\text{cm}^2$ ) (Table 6.2). Accordingly, it is possible speculate that not only the SMT peak force magnitude and contact surface area, but also the resulting stress arising from SMT application may be an important SMT characteristic that potentially influences specific characteristics of particular spinal structures. Unfortunately, the current study did not measure the stresses experienced by the intact specimen and by spinal structures and could not verify this speculation. Therefore, further studies investigating the stresses experienced by the spinal segment and its structures during the application of SMT should be conducted.

In addition to the abovementioned SMT characteristics and given the spinal structures viscoelastic behavior, SMT loading rate has also been described to elicit specific spinal tissue responses, such as facet joint capsule strain [145]. Given that SMT was provided with different loading rates by each method (SMTact:  $1.21\text{N}/\text{ms}$ ; SMTman:  $2.38\text{N}/\text{ms}$ ; SMTmot:  $2.6\text{N}/\text{ms}$ ) (Figure 6.14), it is possible that particular loading characteristics of specific spinal structures would be more sensitive to high loading rates. Indeed, Figures 6.11 and 6.12 show that not only peak flexion extension moments experienced by PJ structures, but also peak torsion moments

experienced by IVD structures may potentially be associated with the SMT loading rate of each method. This suggests that high loading rates may elicit different responses of PJ and IVD structures.

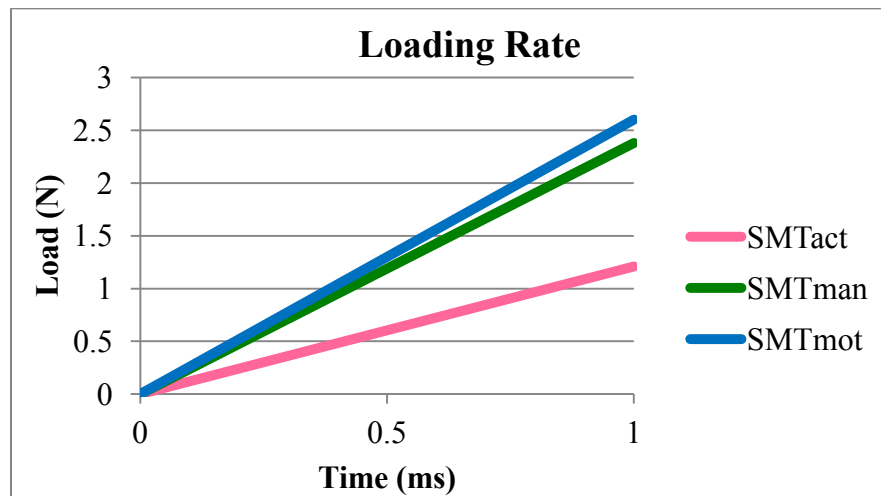


Figure 6.14 Loading rate of different methods of SMT application. SMTact=mechanical force manually assisted (Activator V-E); SMTman=manual SMT; SMTmot=linear actuator motor

Interestingly, the result of this study showed significant differences in specific mean, but not in peak forces and moments as well as differences in peak, but not in mean forces and moments. This suggests that the preload phase characteristics, such as preload force magnitude and duration, also affect the SMT load distribution within spinal tissues. In support of this, recent investigations have reported the influence of preload phase characteristics on electromyographic (EMG) and muscle spindles responses potentially due to changes in SMT loading rate as a consequence of altered preload phase characteristics [57,141]. Therefore, preload phase characteristics not only significantly affect neuromuscular responses, but also the SMT load distribution within spinal structures.

Of note, given the findings of the first study of this dissertation (Chapter 3), the results of the current study is limited to the order in which structures were removed from the specimen during biomechanical testing. By changing the order of structure removal, the loading characteristics experienced by spinal structures during SMT with methods of application would also be changed. Given the composition and biomechanical function of spinal structures investigated here, it is possible to speculate that structure removal order will not significantly impact the loading characteristics of spinal structures. Nevertheless, future studies are needed to quantify the load difference when different orders of structure removal are used.

#### *6.4.3.6 Clinical implications*

Based on the results of this study, the posterior to anterior SMT thrust application at L3/L4 FJ with different methods caused distinct vertebral motions and loaded the spinal structures in different extents. In general, while SMT applied with SMTact created smaller peak forces and moments on the intact specimen, SMTman created greater changes in moments on PJ structures and SMT application with SMTmot created greater changes in moments on IVD structures. Therefore, to preferentially load PJ structures, a SMTman application at the L3/L4 FJ could potentially be used. Similarly, to preferentially load IVD structures, a SMT application with SMTmot on the same location could be used. Figure 6.15 shows a summary of the clinical implications. Noteworthy, given that the current study was conducted using porcine cadaveric models, the clinical implications described here are speculative and further clinical studies are needed to verify their application to human spines.












To affect:	Apply SMT with:	To create:
 Whole segment	 Manual SMT  Linear actuator motor	 Overall peak forces and moments
 Posterior ligaments	Experienced smaller overall forces and moments	
 Facet complex + Lig. flavum	 Manual SMT	 Overall moments
 Intervertebral disc + longitudinal ligs	 Linear actuator motor	 Overall moments

Figure 6.15 Summary of clinical implications

#### 6.4.4 Limitations

This study used porcine lumbar spine models and although porcine models have been described to be suitable for the investigation of the human spine [93,95,146], the reported anatomical and biomechanical differences limit the application of these results to human subjects. Additionally,

the results from cadaveric models are also limited due to differences between *in vivo* and *in vitro* conditions such as muscular effects, and potential differences in repeated loading testing are also present. Given the results of the first study of this dissertation [217], the loads here observed are specific to the order in which spinal structures were removed from the specimen and by using a different order of spinal structure removal, results might also change, potentially altering the forces and moments experienced by each spinal structure. Additionally, as this study did not control for the resultant direction of the applied thrust during SMT application with SMTact and SMTman, different results could be observed between SMT applications with these methods. Finally, since only one SMT technique was provided by a single clinician in this study, different SMT techniques and force-time profiles may result in different loading experienced by spinal structures.

## **6.5 Conclusion**

Based on the findings of this study, the loads created during SMT application and its distribution within spinal structures differed significantly as a function of the method in which SMT was applied. While SMTman influenced mean forces and peak moments in PJ structures, SMT application with SMTmot influenced peak and mean moments and mean forces in IVD structures. Unique loading characteristics created by specific method of SMT application may elicit different spinal tissue responses. Consequently, care should be taken when extrapolating SMT mechanisms into clinical settings when specific method of SMT application was used. Additionally, although the linear actuator motor (SMTmot) was originally developed to standardize and conduct systematic SMT research, this study revealed that it might have a distinct clinical utilization.

## **Chapter 7.**

### **Quantification of spinal tissues loading: a comparison between spinal manipulative therapy (SMT) and passive lumbar movements.**

#### **7.1 Introduction**

Spinal manipulative therapy (SMT) is a popular, cost-effective intervention used widely for low back pain treatment by various health care providers such as chiropractors, osteopaths and physiotherapists [19,99,244]. With the increase usage of SMT [102], studies investigating its beneficial effects have described both the biomechanical and neurophysiological responses elicited by SMT [21,22]. While biomechanical studies have described vertebral motion and acceleration during SMT application as well as changes in spinal stiffness, intradiscal pressure and spinal loading following a SMT application [24,125,128,129,131], neurophysiological investigations observed that paraspinal muscle reflexes, motoneuron excitability, lateral thalamic mechanical response threshold and muscle spindle sensory input are also influenced by SMT application [44,48,134,141]. Both biomechanical and neurophysiological responses are believed to contribute to the SMT beneficial effects and initiate the clinical improvements elicited following a SMT application [112,245].

Conversely, both serious (e.g. disc herniation and cauda equina syndrome) and minor adverse events (e.g. local discomfort, increased stiffness and muscle pain) have been associated with SMT [246–250]. While the risk of serious adverse events following a SMT application is very low with no robust evidence associating them to SMT intervention [26,249–252], minor adverse events are considerably common, with about 30-50% of patients who receive SMT experiencing



some kind of adverse event following the SMT application [27,253]. Typically, most minor adverse events are benign and transient, often disappearing within 24 to 48 hours [27,250,252].

Unfortunately, the underlying mechanisms of SMT are still not completely understood and it remains unknown if unique SMT characteristics are responsible for either its therapeutic and adverse effects. Specifically, the reasons why some SMT applications cause adverse events while others elicits beneficial outcomes requires scientific clarification. Therefore, elucidation of SMT underlying mechanisms is fundamental not only to determine the relation between SMT application and its beneficial biological outcomes [21,22], but also to establish how SMT can cause harm. By identifying spinal tissue response to SMT mechanical deformation and determining the spinal structures that are most affected during a SMT application, both beneficial and potential harmful effects of SMT may be better understood.

Towards this, a basic investigation comparing how responses elicited by SMT differ from the ones elicited by daily physiological movements would be an initial step to elucidate both the beneficial and harmful mechanisms of SMT. Specifically, comparing loads borne by spinal tissues during SMT application with loads arising from physiological movements and daily activities would help put SMT loading into context.

While previous biomechanical investigations have reported vertebral motion, intradiscal pressure and spinal loading as a result of both physiological movements [51,55,254,255] and SMT [24,125,129], significant methodological differences between these investigations (e.g. specimen characteristics and testing protocol) preclude the direct comparison of biomechanical

characteristics (e.g. spinal loading) during physiological movements and SMT application. Therefore, an unified investigation of spinal tissue loading during both the application of SMT and physiological movements in one study within a single model using a standardized testing protocol would potentially identify unique kinematics related to SMT. Consequently, SMT input parameters could be adjusted to target or avoid the specific kinematics of interest.

Given the above, the objective of this study was to compare the loading characteristics of spinal tissues during the application of a manual SMT as well as the passive lumbar movements of flexion, extension and axial rotation within the lumbar spines of the same cadaveric porcine specimens. Given that SMT is based on the application of force vectors to the spine aiming to move it beyond its physiological range of motion [21,104], it is hypothesized that greater forces and moments would be experienced by spinal tissues during manual SMT than during passive lumbar movements.

## **7.2 Methods**

### ***7.2.1 Overview***

Similar methodology to that used in this study was described in detail within Chapter 4 of this dissertation. In general, an optical tracking system was used to record the vertebral motions resultant of manual SMT and passive flexion, extension and left axial rotation movements. Then, these vertebral motions were replicated by a parallel robotic platform and, by combining kinematic replication with serial dissection, forces and moments experienced by spinal tissues were measured and recorded by a load cell and further analysed.

### ***7.2.2 Sample Size Calculation***

The sample size calculation was conducted based on the data previously reported by Kawchuk and colleagues (2010) [24] using the General Power Analysis Program (G\*Power 2) (University of Trier, Germany). With a statistical power was set at 0.80 (80%), two-tailed tests with level of significance set at  $\alpha=0.05$  (5%) and an effect size of 0.99-1.2, a sample size of 9 porcine models was required. Five additional porcine models were included to account for possible specimen loss due to data collection, potting procedure or testing complications and a total of 14 cadaveric porcine specimens were included. Given that the study from Kawchuk and colleagues also observed 12 variables, the use of the effect size reported by these authors for the current sample size calculation is appropriate. Therefore, with a level of significance set at 0.05 and statistical power set 0.80, the chances of having types I and II errors were 5% and 20%, respectively.

### ***7.2.3 Specimen Preparation***

Twelve fresh porcine cadavers (Duroc X [Large White X Landrace breeds]) of approximately 60-65kg were used in this study (two specimens were excluded due to technical complications). In each intact porcine cadaver, ultra-sound imaging and needle probing technique were used to identify L3 and L4 vertebrae and L3/L4 left facet joint (FJ). One bone pin was drilled into the each of the L3 and L4 vertebral bodies and a rectangular flag having 4 infrared light-emitting diode markers was attached to the upper end of each bone pin (Figure 7.1).

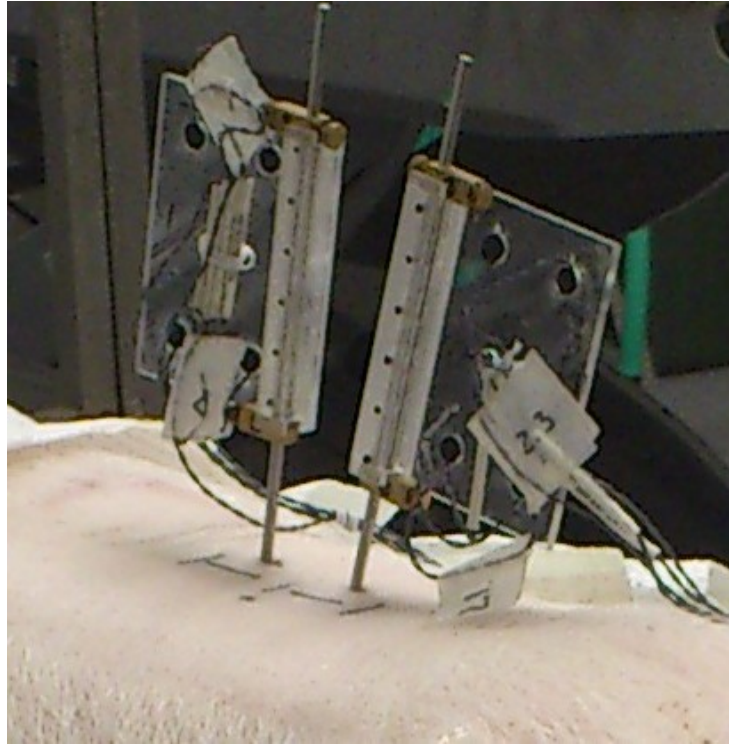


Figure 7.1 Rectangular flags with 4 infrared light-emitting diode markers attached to bone pins drilled into L3 and L4 vertebrae.

The cadaveric pig was then positioned in the neutral prone position on a hinged hardwood board that was fixed to a flexion-extension table (Leander Health Technologies, Lawrence, KS). The L3 and L4 vertebrae were positioned above and below the hinge line, respectively, and the cadaveric porcine was fixed to the table by strapping around the lower thoracic region (Figure 7.2) [256]. This way the porcine cadaver was stable with the upper body fixed to the table and movements applied on the lower body, would move the L3-L4 segment. Following the application of SMT and physiological movements on the intact porcine cadaver (detailed in the following sections), the lumbar spine was removed *en bloc* [24]. The L3/L4 spinal segment was cleaned of non-ligamentous tissues, sealed in a plastic bag and kept refrigerated at 3°C for less than 5 hours until potting and testing on the following day [213]. The specimen was kept moist with physiologic saline throughout preparation, embedding and testing [170,178].

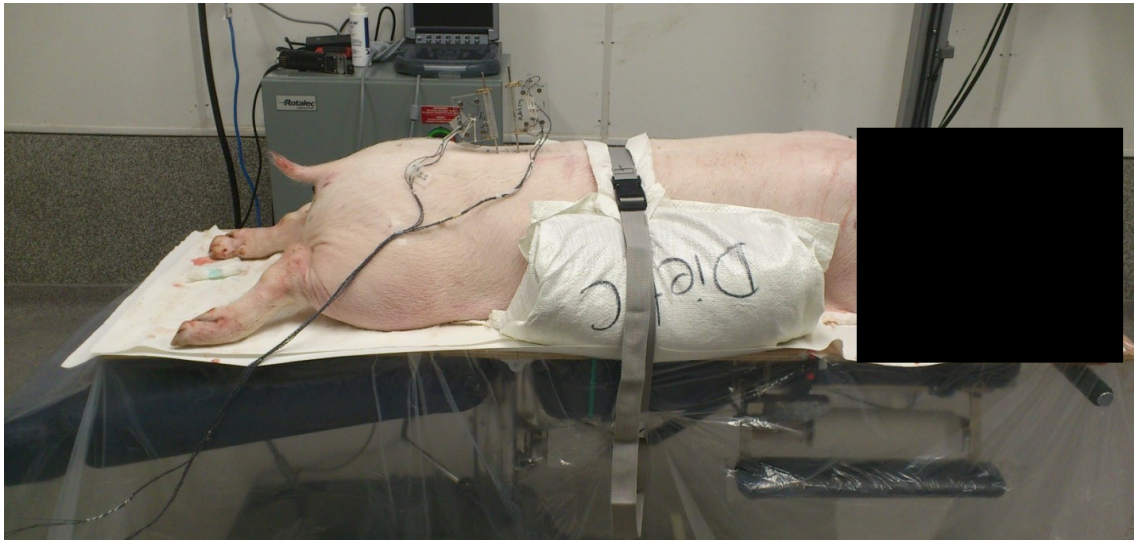


Figure 7.2 Cadaveric porcine positioning on hinged hardwood board with L3 positioned above the hinge line and L4 below.

#### ***7.2.4 Passive Lumbar Movements***

Three lumbar movements were passively performed: flexion, extension and left axial rotation. Passive flexion movement was performed by the automatic flexion movement of the flexion-extension table at a rate of approximately  $0.0008^{\circ}/\text{ms}$ . Passive extension and axial rotation were manually performed with no assistance from the table. Specifically, passive extension was performed by holding and moving both lower limbs in the upward direction at an average rate of  $0.005^{\circ}/\text{ms}$  until the maximum extension between L3/L4 segment was reached and L2/L3 segment started to visually move (Figure 7.3). Passive left axial rotation was performed by stabilizing L3 and rotating the pelvis to the left side at an averaged  $0.003^{\circ}/\text{ms}$  to the maximum range in rotation (Figure 7.4). Each passive lumbar movement was performed twice and the data from the second movement was used for analysis.



Figure 7.3 Passive extension movement



Figure 7.4 Passive left axial rotation movement

### ***7.2.5 Spinal Manipulation***

A trained clinician with 3 years of clinical experience was instructed to apply a general SMT using the hypothenar push manipulation in which the clinician's pisiform bone were positioned on the skin overlying L3/L4 FJ, previously located by using ultra-sound imaging and needle probing. A pressure array (Pressure Profile System, Inc. Los Angeles, CA) was used to measure the SMT force-time characteristics and was placed between the clinician's hands and the skin overlying L3/L4 FJ. The pressure array was 1 mm thick, composed of 10x10 pressure sensors with a pressure sensitivity of 0.15% and recorded the force-time characteristics of SMT application at a rate of 120 Hz.



### ***7.2.6 Kinematic Recording***

During the application of each passive lumbar movement and manual SMT, the resulting L3 and L4 vertebral motion was captured by each bone pin and sensor flag and recorded in 3 dimensions by an optical tracking system at a rate of 400 Hz (0.01 mm system resolution with 0.15 mm rigid body resolution; NDI, Waterloo, Canada) (Appendix III).

### ***7.2.7 Potting Procedure***

This study followed the standardized potting procedure described in the previous chapter (Chapter 4) where specimens were potted in a vertical orientation using dental stone (Modern Materials, South Bend, IN) with the intervertebral disc positioned parallel to the horizontal plane (Figure 7.5).

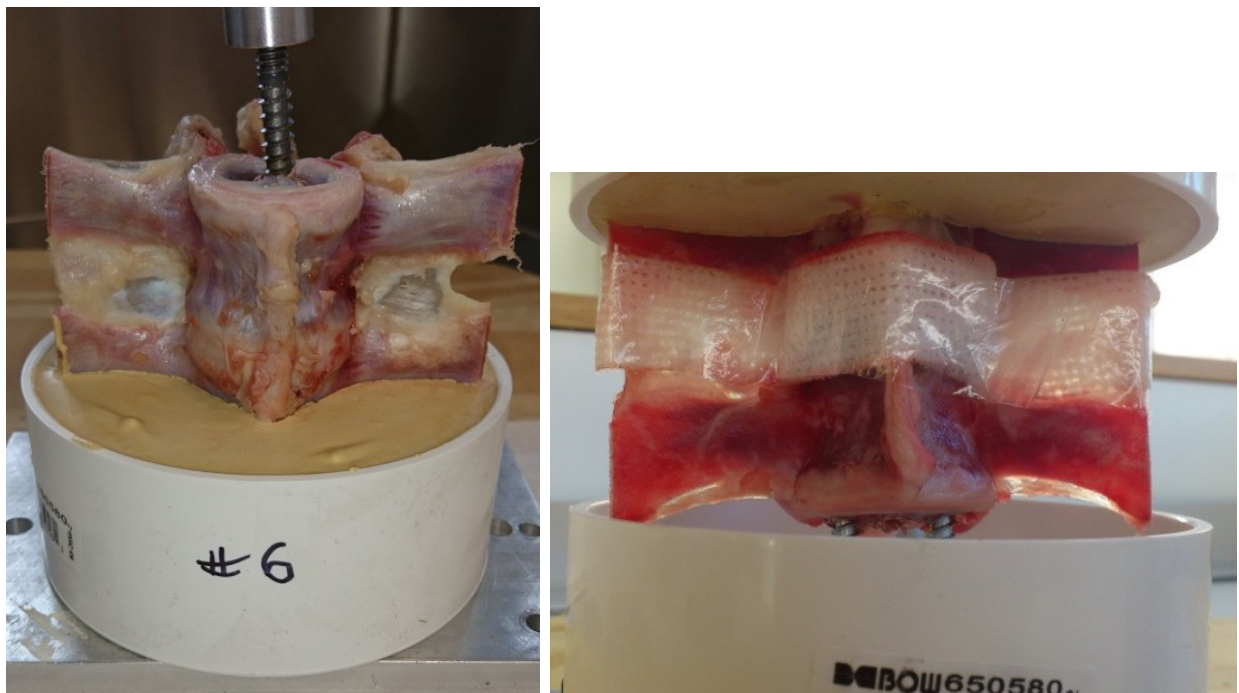


Figure 7.5 Standardized potting procedure and L3/L4 spinal segment.

### ***7.2.8 Robotic Testing***

Following the potting procedure, the robotic testing was conducted as previously described in Chapter 4. In brief, the caudal end (L4) of the potted spinal segment was fixed to a 6-axis load cell (AMTI MC3A-1000, Advanced Mechanical Technology, Inc., Watertown, MA) and the load cell mounted rigidly to a parallel robot platform (Parallel Robotics Systems corp., Hampton, NH). A calibration process was performed [216] (Appendix IV) resulting in 4 robotic trajectories files consisting of a series of commands corresponding to the passive lumbar movements (flexion, extension and left axial rotation) and the manual SMT application. The robot accepts commands less frequently than data points are generated by the optical system. Therefore the robotic command files were re-sampled to move the robotic platform in displacement control method reproducing the path of each SMT previously recorded. Given the safety settings of the robot, the SMT path replication was approximately 10% slower than the original SMT application. The cranial end of the potted specimen was then fixed to a stationary cross beam and the segment positioned in the initial neutral position.

The robot was then moved and, starting from the initial neutral position, the following passive lumbar movements were reproduced first, followed by the SMT application movement: flexion, extension, left axial rotation, then manual SMT. Each movement replication was separated by a 2 minutes recovery time as it was the minimum time necessary to perform all the tasks between tests (saving data, removing spinal structures, setting up for next test) and satisfied the minimum time for loads to return to baseline [24]. Based on feasibility tests performed by Kawchuk and colleagues (2010) [24], 3 pre-conditioning trials were executed prior to testing.



The forces and moments experienced by the specimen during robotic replication of manual SMT and passive physiological movements kinematics were recorded (axes of movement: x = medial/lateral, y = anterior/posterior, and z = superior/inferior). Following the robotic replication of the trajectories corresponding to applied motions (passive lumbar movements and manual SMT), spinal structures were removed and/or transected from the specimen and the same robotic trajectories repeated by the robot. Based on the findings reported by Funabashi et al. (2015) [217], spinal structures were removed/transected (via scalpel unless otherwise noted) in same order from all specimens: 1) supra- and interspinous ligament (SL), 2) bilateral facet capsules, facet joints (via rongeur) and ligamentum flavum (PJ), 3) intervertebral disc and anterior and posterior longitudinal ligaments (IVD). Given the intertransverse ligaments fragile nature and frequent damage during *en bloc* spinal removal, all specimens had their intertransverse ligaments removed prior to testing.

## **7.2.9 Data Analysis**

### **7.2.9.1 Overview**

Similar to Chapter 4, this study also analysed 12 dependent variables corresponding to the peak and mean forces and moments measured and recorded along and around each of the 3 Cartesian axes, in 4 conditions independently observed (intact and following the removal of spinal structures). In contrast to Chapter 4, however, this study investigated only 1 independent variable: applied motion (i.e. passive lumbar movement and SMT application). Table 7.1 presents the description of conditions and variables, and the definition of included dependent variables.

**Table 7.1. Description of conditions and variables used throughout the chapter**

Term	Definition
Condition (n=4)	State in which specimens were tested. This study investigated 4 different conditions: 1. Intact specimen, 2. after cut 1 where supra- and interspinous ligaments (SL) were removed, 3. after cut 2 removing bilateral facet joints, capsules and ligamentum flavum (PJ) and 4. after cut 3 removing intervertebral disc and anterior and posterior longitudinal ligaments (IVD).
Independent variable (n=4)	Variable under investigation. In this study, independent variable is applied motion (manual SMT application and passive lumbar movements of flexion, extension and left axial rotation).
Dependent variable	Measured variable, outcome. In this study, dependent variables are peak and mean forces and moments along and around all 3 axes of movement, respectively.
• Peak forces and moments	Maximum measured force and moment during the SMT thrust phase. For passive physiological moments, the maximum force and moment during the applied motion
• Mean forces and moments	Average value of forces and moments involving both the preload and thrust phases of SMT. For passive physiological movement, the average value of forces and moments involving the entire movement.

#### 7.2.9.2 Data Processing

Data extraction and processing has been detailed in the previous chapter of this dissertation (Chapter 4). Briefly, baseline forces and moments were considered to be those recorded when the specimen was positioned in the same initial position as *ex vivo*. The resulting forces and moments of each specimen were plotted against time for each condition (intact and following the removal of spinal structures) and peak and mean forces and moments along and around each axis (x-, y-, z-axes) were identified by customized software (LabVIEW, National Instruments, Austin, TX). Similarly to Chapter 4, relative peak and mean forces and moments experienced by spinal structures were normalized to the respective load experienced by the intact condition during the application of each movement (passive lumbar movement and manual SMT). The magnitude of displacements (translation and rotation) where peak loads occurred was also identified by the customized software.

Pressure data was plotted against time for the SMT application on each porcine cadaver by using the software provided by the manufacturer (Chameleon Visualization and Data Acquisition Software 2012, Version 1.7.0.6, Pressure Profile Systems. Inc., Los Angeles, CA). Maximum applied force and time to peak were extracted by the software and used for SMT force-time characterization.

#### *7.2.9.3 Statistical Tests*

Given the objective of this study to compare the loading characteristics of spinal tissues during the application of manual SMT and passive lumbar movements, each condition (intact condition and following the removal of spinal structures) was analyzed independently. Given that all passive lumbar movements and SMT application were performed on the same specimen, each observation of forces and moments when SMT and passive lumbar movements were replicated was considered a repeated measure. Therefore, for the intact specimen, a repeated measures multivariate analysis of variance (MANOVA) followed by a Bonferroni post-hoc analysis for pairwise comparisons was conducted. For the analysis of loads experienced by each spinal structures, a MANOVA for the regression coefficients was conducted. A Tukey post-hoc test was performed for the multiple pairwise comparisons of the removed spinal structures. Statistical tests were performed combining IBM SPSS Statistics for Windows, Version 22.0 (Armonk, NY: IBM Corp.) and R: A language and environment for statistical computing (R Foundation for Statistical Computing, Vienna, Austria).

## **7.3 Results**

### ***7.3.1 Overview***

Overall, the forces and moments experienced by the intact specimen and spinal structures significantly changed as a function of the applied motion. Despite of a few exceptions (described in detail in the following sections), forces and moments created by manual SMT were not significantly greater than the ones created during passive lumbar movements of flexion, extension and left axial rotation.

### ***7.3.2 Spinal manipulative therapy characteristics***

From pressure system recordings, manual SMT provided an average peak force magnitude of 524 N (SD:  $\pm 41$ N; range: 430 - 565N) over 220 ms ( $\pm 15$ ms) (loading rate: 2.38 N/ms).

### ***7.3.3 Vertebral displacements and rotations***

The exact vertebral displacements arising from SMT application and passive lumbar movements were replicated during robotic testing of all conditions. Relative displacements (translations and rotations) of L4 vertebra in relation to L3 are shown in Table 7.2 by applied motion (SMT and physiological movements) and axis of movement. The greatest lateral translation (along x-axis) ( $-1.28\text{mm} \pm 0.86$ ), anterior posterior translation (along y-axis) ( $9.53\text{mm} \pm 2.66$ ) and extension rotation (rotation around x-axis) ( $3.17^\circ \pm 0.78$ ) occurred during passive lumbar extension movement. The greatest superior translation (along z-axis) ( $1.40\text{mm} \pm 0.36$ ), lateral bending (rotation around y-axis) ( $-0.65^\circ \pm 0.52$ ) and axial rotation (rotation around z-axis) ( $-1.71^\circ \pm 1.20$ ) occurred during the application of manual SMT.

**Table 7.2 Maximal displacement (mm) and rotation (°) (SD) created in the cadaveric specimens with the application of manual SMT and passive lumbar movements trajectories**

Motion	Displacement (mm)			Rotation (°)		
	X (lateral)	Y (ant post)	Z (sup inf)	X (flx ext)	Y (lat bending)	Z (axial rot)
Manual SMT	1.26 (1.90)	9.10 (2.94)	1.40 (0.36)	3.06 (1.00)	-0.65 (0.52)	-1.71 (1.20)
Axial Rotation	0.66 (2.69)	4.57 (2.28)	0.49 (0.26)	1.40 (0.74)	-0.44 (0.74)	-1.24 (0.58)
Extension	-1.28 (0.86)	9.53 (2.66)	1.05 (0.34)	3.17 (0.78)	-0.07 (0.45)	-0.20 (0.27)
Flexion	-1.18 (0.64)	-1.82 (1.24)	-0.24 (0.13)	-0.58 (0.39)	0.32 (0.16)	-0.19 (0.12)

SD = standard deviation; SMT = spinal manipulative therapy

### **7.3.4 Forces and Moments**

#### *7.3.4.1 General descriptive statistics*

Figure 7.6 shows an example of raw forces and moments along and around all three axes of movement during each applied motion (manual SMT and passive lumbar movements) experienced by the intact L3/L4 spinal segment and following each cut.

Figure 7.7 shows boxplots with the median, interquartile range, distribution and outliers of peak force, mean force, peak moment and mean moment experienced by the intact specimen and following each spinal structure removal during SMT application and passive lumbar movements of flexion, extension and left axial rotation.

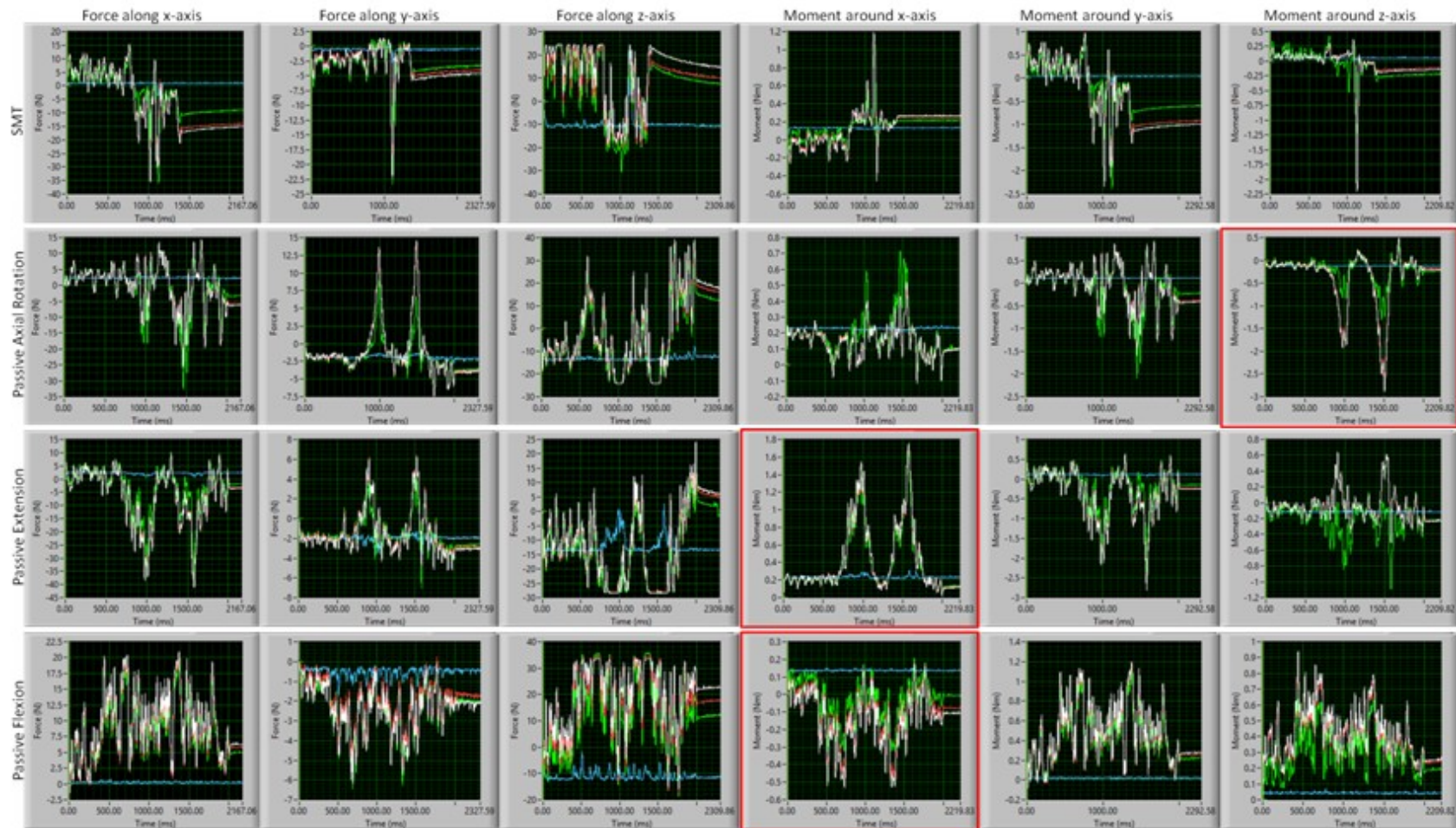


Figure 7.6 Characteristic example of force- and moment-time plots of raw forces and moments experienced by the spinal segment in all three axes of movement during manual SMT and passive lumbar movements (left axial rotation, extension and flexion). White line represents the loads experienced by the intact specimen; red line represents the loads experienced by the whole segment after supra- and interspinous were removed; green line after bilateral facet joints, capsules and ligamentum flavum were removed and blue line after intervertebral disc, anterior and posterior ligaments were removed. Red boxes indicate the moments around the main axis of motion of passive lumbar movements.

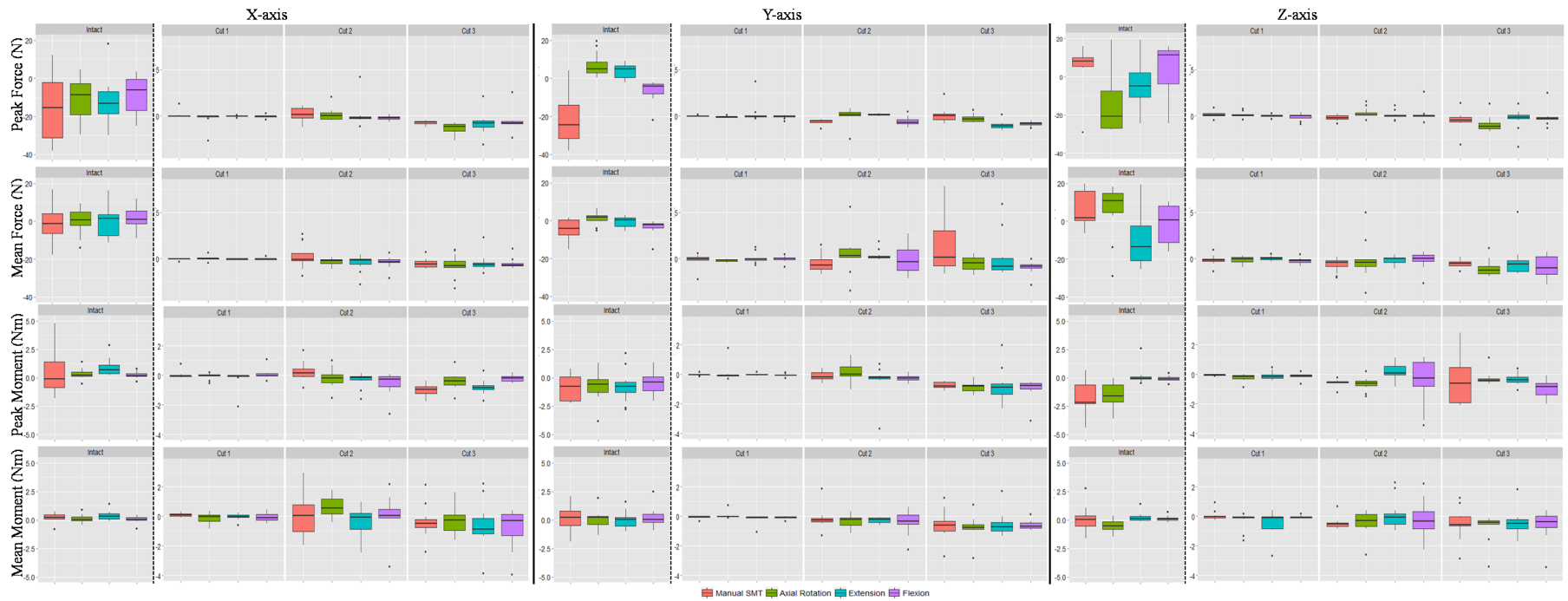


Figure 7.7 Boxplots with median, interquartile range, distribution and outliers of peak and mean forces and moments experienced by the intact specimen and following each cut. SMT=spinal manipulative therapy; Cut 1=supra- and interspinous ligaments; Cut 2=bilateral facet joints, capsules and ligamentum flavum; Cut 3=intervertebral disc, anterior and posterior longitudinal ligaments.

#### *7.3.4.2 Intact Specimen*

Figure 7.8 shows the average peak force, mean force, peak moment and mean moment experienced by the intact specimen while changing the applied motion. The analysis of the intact specimen revealed significant differences in forces and moments as a function of the applied motion. Generally, extension mean moments were significantly greater during passive extension than during flexion movement, and torsion moments were significantly greater during manual SMT and passive axial rotation in comparison to passive flexion and extension movements. From 36 comparisons between manual SMT with each passive lumbar movement (flexion, extension and left axial rotation), only 6 comparisons revealed greater specific forces and moments during manual SMT (Figure 7.8). Among those, peak anterior posterior force was the only variable in which manual SMT was significantly greater than all passive lumbar movements (Figure 7.9).



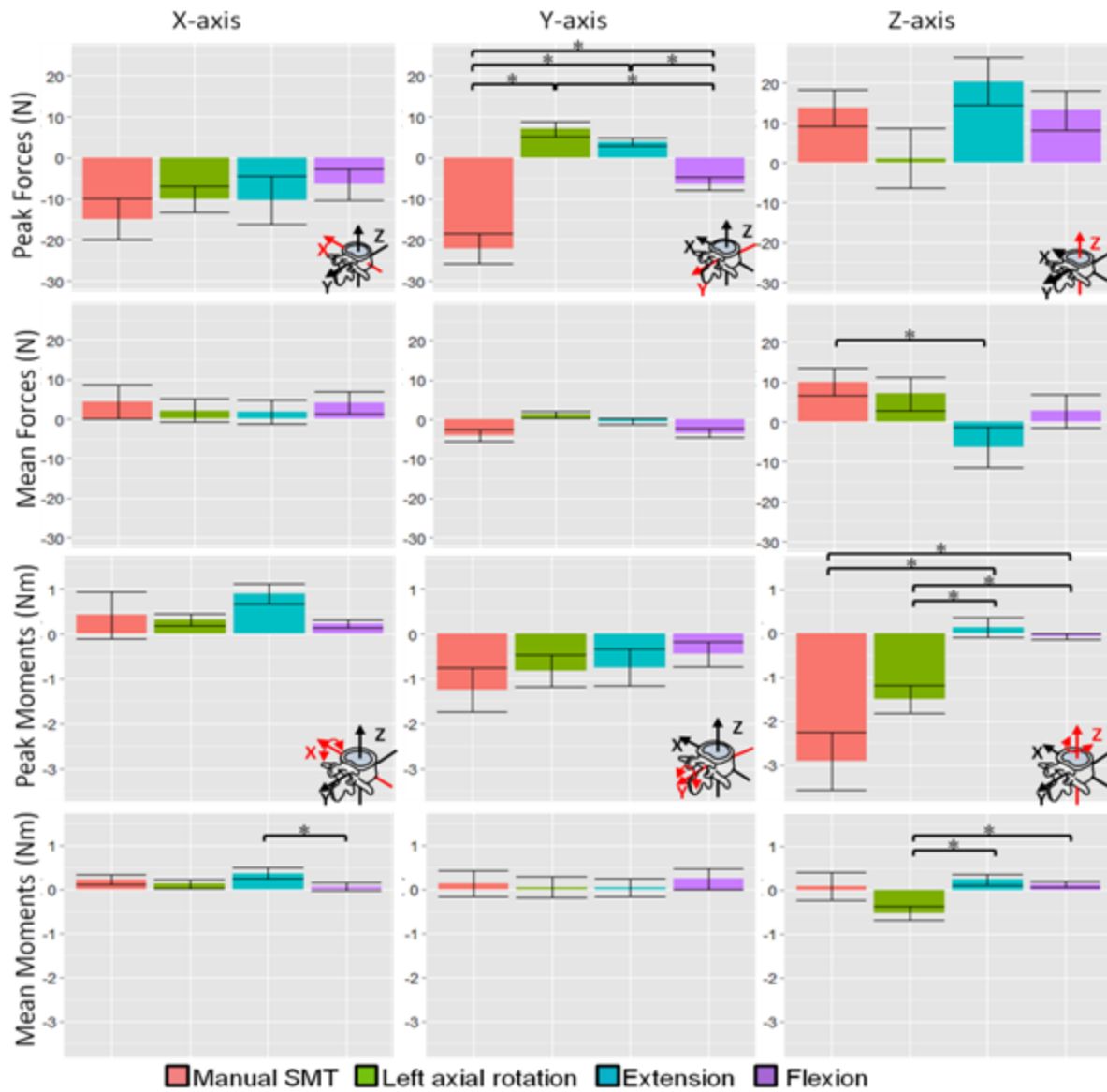


Figure 7.8 Average value of peak force, mean force, peak moment and mean moment experienced by the intact specimen during the application of manual SMT and passive lumbar movements of flexion, extension and left axial rotation.

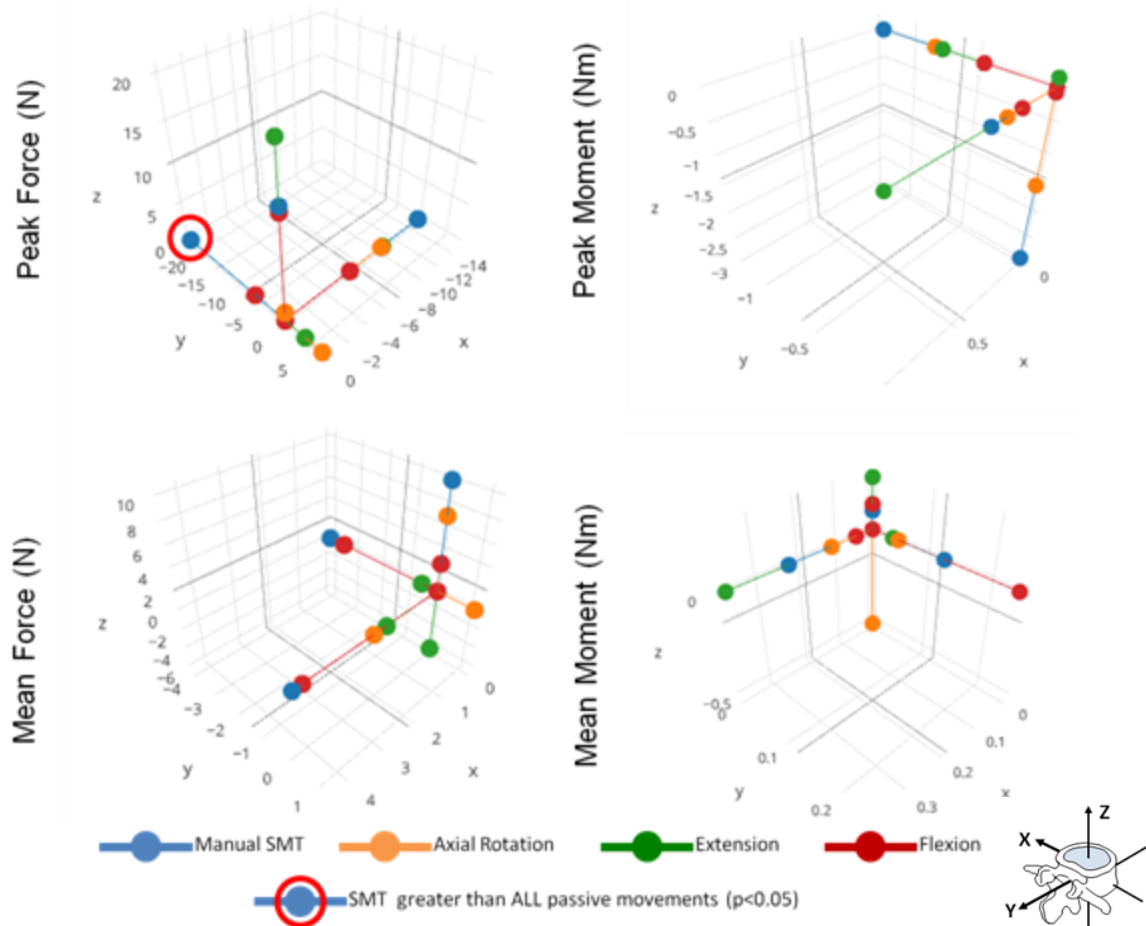


Figure 7.9 Three-dimensional plots of average values of peak force, mean force, peak moment and mean moment experienced by the intact specimen during the application of manual SMT and passive lumbar movements of flexion, extension and left axial rotation in each axis of movement.

Specifically, while peak anterior posterior force (force along y-axis) created by manual SMT (average: -22.23 N, 95% CI [-29.45, -15.02]; median: -24.56 N (IQR: 17.42)) was significantly greater than all passive lumbar movements (flexion (average: -6.33 N, 95% CI [-9.52, -3.14]; median: -4.19 N (IQR:4.99)), extension (average: 3.90 N, 95% CI [1.82, 5.99]; median: 4.83 N (IQR: 6.19)) and left axial rotation (average: 7.03 N, 95% CI [3.40, 10.67]; median: 4.97 N (IQR: 5.64))), differences between peak anterior posterior force during left axial rotation and extension were also significant in comparison to flexion. Additionally, mean superior inferior force (force along z-axis) was significantly greater during manual SMT (average: 10.01 N, 95%

CI [3.17, 16.85]; median: 7.58 N (IQR: 19.26)) in comparison to passive extension movement (average: -6.28 N, 95% CI [-2.12, 1.07]; median: -12.76 N (IQR: 27.83)).

Specifically for moments, although peak torsion moment (moment around z-axis) was significantly greater during manual SMT (average: -2.91 Nm, 95% CI [-4.19, -1.63]; median: -2.25 Nm (IQR: 3.16)) and passive left axial rotation (average: -1.50 Nm, 95% CI [-2.14, -0.87]; median: -1.62 Nm (IQR: 1.49)) than during passive extension (average: 0.13 Nm, 95% CI [-0.31, 0.58]; median: -0.07 Nm (IQR: 0.18)) and flexion (average: -0.07 Nm, 95% CI [-0.21, 0.06; median: -0.09 Nm (IQR: 0.21)), only passive left axial rotation (average: -0.52 Nm, 95% CI [-0.84, -0.20]; median: -0.53 Nm (IQR: 0.67)) was observed to create mean torsion moment significantly greater than passive extension (average: 0.23 Nm, 95% CI [0.00, 0.47]; median: 0.11Nm (IQR: 0.30)) and flexion (average: 0.12 Nm, 95% CI [-0.00, 0.26]; median: 0.08Nm (IQR: 0.18)). Additionally, the only significant difference in extension moments (moments around x-axis) was between passive extension and flexion movements, with a significantly greater mean moment during passive extension movement (average: 0.36 Nm, 95% CI [0.13, 0.60]; median: 0.30 Nm (IQR: 0.45)) in comparison to passive flexion (average: 0.05 Nm, 95% CI [-0.12, 0.23]; median: 0.05 Nm (IQR: 0.27)).

#### *7.3.4.3 Cut 1: Supra- and interspinous ligaments (SL)*

Figure 7.10 presents average peak force, mean force, peak moment and mean moment experienced by SL structures during the application of manual SMT and passive lumbar movements. Considering 100% the total forces and moments experienced by the intact specimen, the percentage of forces and moments experienced by spinal structures during manual SMT and

passive lumbar movements are presented on Table 7.4. Although significant changes in forces and moments experienced by SL structures were revealed depending on the applied motion, they were substantially smaller than the forces and moments experienced by other spinal structures (PJ and IVD). Generally, considerably fewer changes were observed to be significant within SL structures with slightly greater forces and moments being experienced during passive flexion extension movements. From 36 comparisons between manual SMT with each passive lumbar movement (flexion, extension and left axial rotation), only 3 comparisons revealed greater specific forces during manual SMT. Only mean superior inferior forces experienced by SL structures during manual SMT were significantly greater than all passive lumbar movements (Figure 7.11).

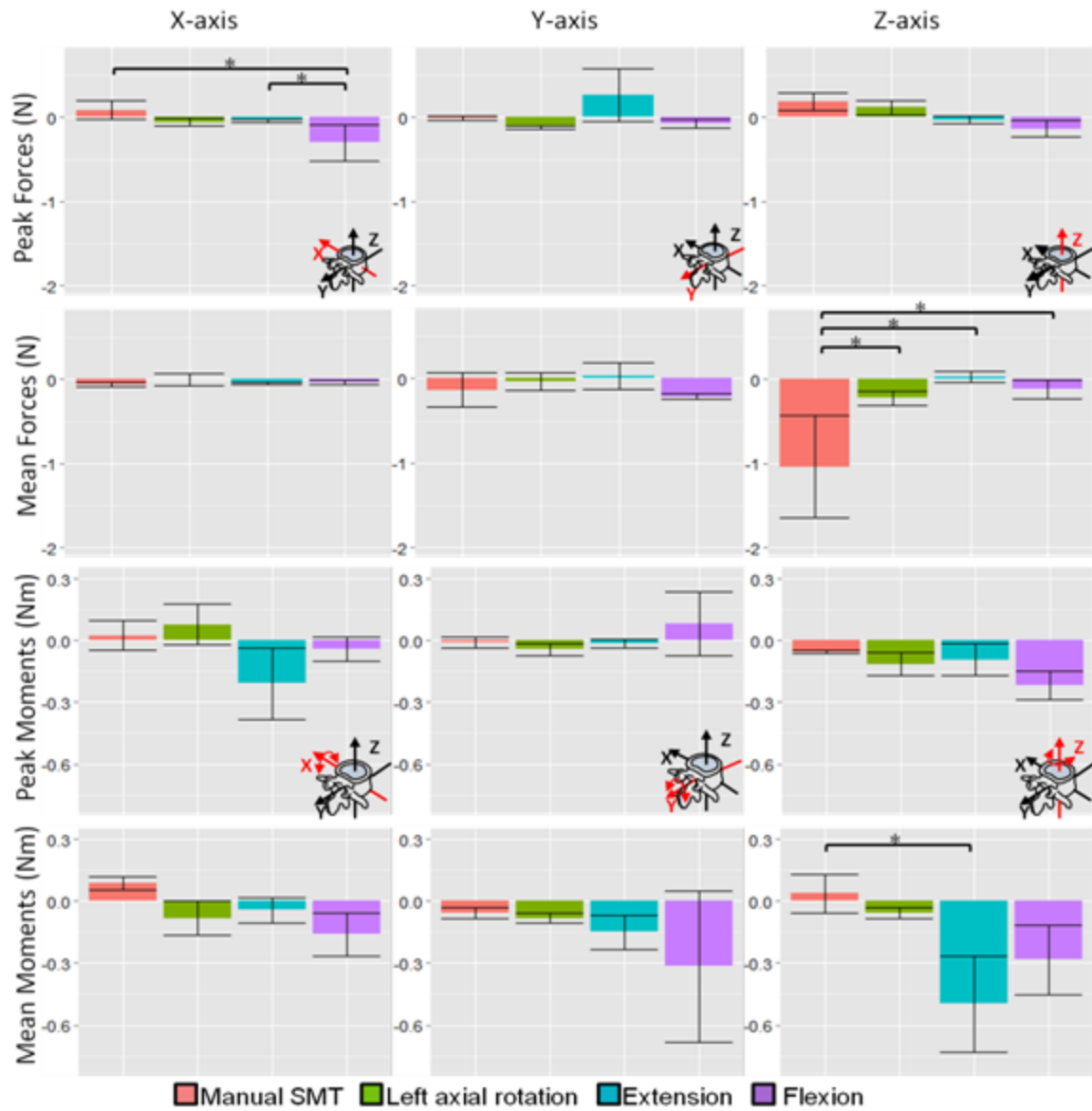


Figure 7.10 Average value of normalized peak force, mean force, peak moment and mean moment experienced by the supra- and interspinous ligaments during the application of manual SMT and passive lumbar movements of flexion, extension and left axial rotation.

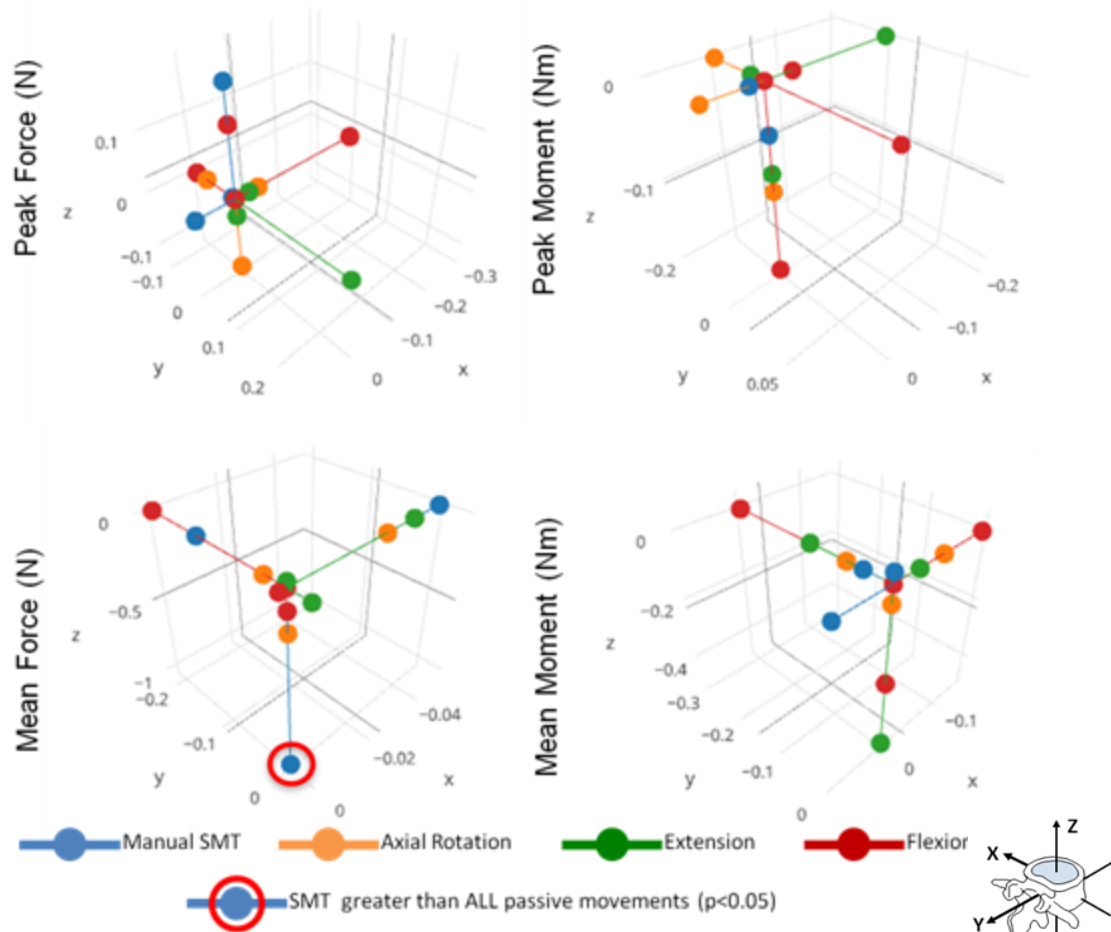


Figure 7.11 Three-dimensional plots of average values of normalized peak force, mean force, peak moment and mean moment experienced by the supra- and interspinous ligaments during the application of manual SMT and passive lumbar movements of flexion, extension and left axial rotation in each axis of movement.

**Table 7.4 Percentage of general forces and moments experienced by spinal structures during each applied motion (manual SMT and passive lumbar movements) in relation to the loads experienced by the intact specimen (100%)**

Spinal Structure	Applied Motion	Peak Forces	Mean Forces	Peak Moments	Mean Moments
Cut 1 (SL)	Manual SMT	0.74%	5.94%	3.92%	17.18%
	Axial Rotation	1.02%	2.48%	13.26%	28.37%
	Extension	1.10%	1.96%	18.75%	72.17%
	Flexion	1.67%	2.81%	42.52%	70.00%
Cut 2 (PJ)	Manual SMT	2.71%	18.10%	32.76%	103.13%
	Axial Rotation	4.38%	11.13%	44.90%	240.43%
	Extension	6.14%	12.23%	86.33%	256.52%
	Flexion	2.77%	5.31%	108.66%	261.11%
Cut 3 (IVD)	Manual SMT	4.77%	21.12%	41.81%	146.88%
	Axial Rotation	6.92%	12.85%	61.90%	200.00%
	Extension	5.01%	14.05%	130.08%	263.48%
	Flexion	6.70%	14.10%	222.83%	446.67%

SMT=spinal manipulative therapy; SL=supra- and interspinous ligaments; PJ=bilateral facet joints, capsules and ligamentum flavum; IVD=intervertebral disc, anterior and posterior longitudinal ligaments

Specifically, change in peak lateral force (force along x-axis) experienced by SL structures was significantly greater during passive flexion (average: -0.29 N, 95% CI [-0.72, -0.12]; median: -0.07 N (IQR: 0.06)) in comparison to manual SMT (average: 0.08 N, 95% CI [-0.13, 0.30]; median: -0.02 N (IQR: 0.03)) and passive extension movement (average: -0.03 N, 95% CI [-0.07, 0.00]; median: -0.03 N (IQR: 0.03)). The change in mean superior inferior force (force along z-axis) was significantly greater during manual SMT (average: -1.04 N, 95% CI [-2.23, -0.15]; median: -0.22 N (IQR: 0.67)) than during all passive lumbar movements (flexion (average: -0.11 N, 95% CI [-0.33, 0.10]; median: -0.03 N (IQR: 0.49)), extension (average: 0.02 N, 95% CI [-0.09, 0.15]; median: 0.04 N (IQR: 0.19)), left axial rotation (average: -0.22 N, 95% CI [-0.40, -0.04]; median: -0.23 N (IQR: 0.31))). Specifically for moments, change in mean torsion moment (moment around z-axis) was significantly greater during passive extension (average: -0.49 Nm, 95% CI [-0.95, -0.04]; median: -0.09 Nm (IQR: 0.79))) than during manual SMT (average: 0.03 Nm, 95% CI [-0.14, 0.21]; median: -0.03 Nm (IQR: 0.12))).

#### *7.3.4.4 Cut 2: Bilateral facet joints, capsules and ligamentum flavum (PJ)*

Figure 7.12 shows the average peak force, mean force, peak moment and mean moment experienced by PJ structures during applied motions of manual SMT and passive lumbar movements. Although significant changes in forces and moments experienced by PJ structures were observed as a function of the applied motion, overall forces and moments experienced by PJ structures were smaller than the ones experienced by IVD structure (Table 7.4), with the exception of torsion moments during manual SMT and passive axial rotation, where PJ structures experienced the greatest torsion moments. Generally, greater forces and moments were experienced during movements including large axial rotations, e.g. manual SMT and passive left axial rotation movement. From 36 comparisons between manual SMT with each passive lumbar movement (flexion, extension and left axial rotation), only 12 comparisons revealed greater specific forces and moments during manual SMT. Among those, superior inferior forces and mean extension moment were the only variables in which manual SMT was significantly greater than all passive lumbar movements (Figure 7.13).



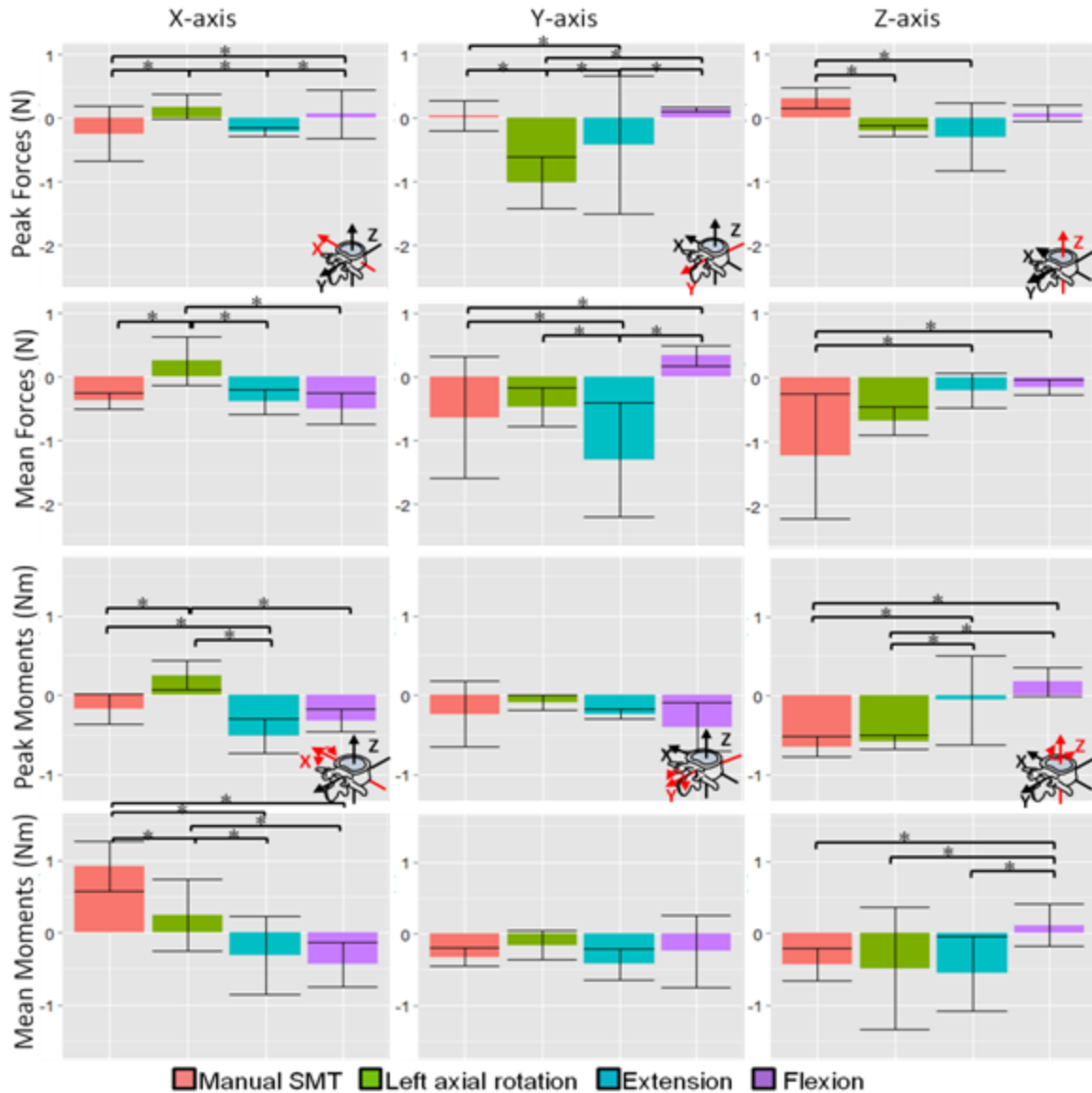


Figure 7.12 Average value of normalized peak force, mean force, peak moment and mean moment experienced by the bilateral facet joint, capsules and ligamentum flavum during the application of manual SMT and passive lumbar movements of flexion, extension and left axial rotation.

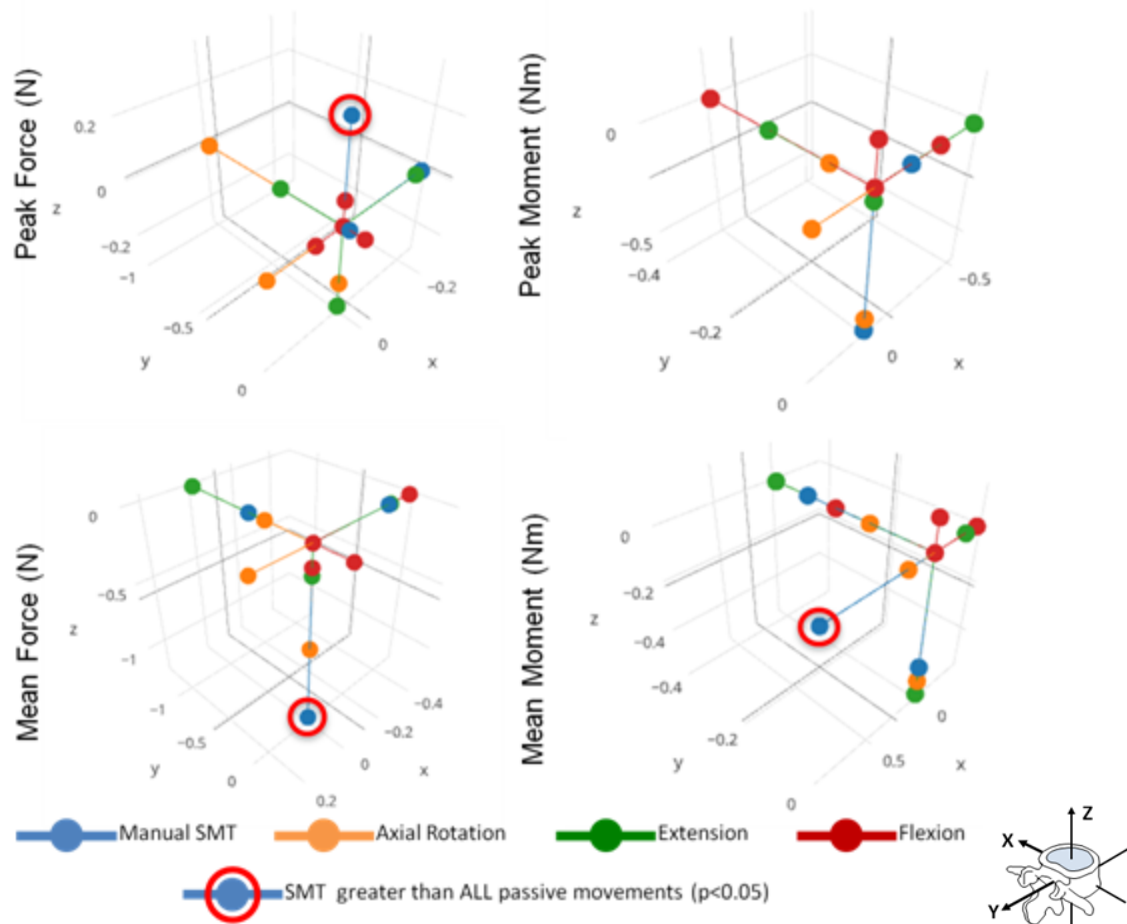


Figure 7.13 Three-dimensional plots of average values of normalized peak force, mean force, peak moment and mean moment experienced by the facet joints, capsules and ligamentum flavum during the application of manual SMT and passive lumbar movements of flexion, extension and left axial rotation in each axis of movement.

Specifically, change in peak lateral force (force along x-axis) experienced by PJ structures was significantly greater during manual SMT (average: -0.24 N, 95% CI [-1.10, -0.16]; median: -0.05 N (IQR: 0.67)) and passive extension (average: -0.21 N, 95% CI [-0.35, -0.08]; median: -0.24 N (IQR: 0.26)) in comparison to passive left axial rotation (average: 0.18 N, 95% CI [-0.21, 0.57]; median: 0.15 N (IQR: 1.05)) and passive flexion (average: 0.07 N, 95% CI [-0.67, 0.82]; median: -0.21 N (IQR: 0.18)). For peak anterior posterior forces (forces along y-axis), passive left axial rotation (average: -1.01 N, 95% CI [0.06, 0.02]; median: -0.52 N (IQR: 0.30)) and extension (average: -0.42 N, 95% CI [-2.54, -0.17]; median: -0.70 N (IQR: 0.62)) created significantly

greater changes in comparison to manual SMT (average: 0.04 N, 95% CI [-0.43, 0.51]; median: 0.15 N (IQR: 0.67)) and passive flexion movement (average: 0.13 N, 95% CI [-1.81, -0.21]; median: 0.09 N (IQR: 0.18)). Additionally, while change in mean anterior posterior forces was significantly greater during passive extension movement (average: -1.30 N, 95% CI [-3.06, 0.45]; median: -0.97 N (IQR: 2.30)) in comparison to all other applied motions (manual SMT (average: -0.63 N, 95% CI [-2.51, 1.24]; median: 0.21 N (IQR: 2.79)), passive left axial rotation (average: -0.46 N, 95% CI [-1.07, 0.13]; median: -0.69 N (IQR: 1.02)) and flexion (average: 0.34 N, 95% CI [0.03, 0.35]; median: 0.14 N (IQR: 0.15))), manual SMT also created change in mean anterior posterior force significantly greater than passive flexion movement. Change in superior inferior forces experienced by PJ structures were significantly greater during manual SMT than during all passive lumbar movements (Figure 7.13).

Specifically for moments, while change in peak flexion extension moment (moment around x-axis) during passive extension moment (average: -0.51 Nm, 95% CI [-0.93, -0.08]; median: -0.25 Nm (IQR: 0.69)) was significantly greater than during manual SMT (average: -0.17 Nm, 95% CI [-0.54, 0.19]; median: -0.16 Nm (IQR: 0.55)) and passive left axial rotation (average: 0.25 Nm, 95% CI [-0.10, 0.61]; median: 0.17 Nm (IQR: 0.26)), change in mean extension moments was significantly greater during manual SMT (average: 0.91 Nm, 95% CI [0.23, 1.59]; median: 0.54 Nm (IQR: 1.00)) than all passive lumbar movements (flexion (average: -0.43 Nm, 95% CI [-1.04, 0.17]; median: -0.07 Nm (IQR: 1.07)), extension (average: -0.31 Nm, 95% CI [-1.38, 0.74]; median: -0.02 Nm (IQR: 0.60)), left axial rotation (average: 0.24 Nm, 95% CI [-0.71, 1.20]; median: -0.09 Nm (IQR: 1.86))), with the passive left axial rotation being significantly smaller than passive extension and flexion movements. For torsion moments (moments around z-axis),

while changes in peak torsion moment during manual SMT (average: -0.64 Nm, 95% CI [-0.89, -0.39]; median: -0.58 Nm (IQR: 0.31)) and passive left axial rotation (average: -0.58 Nm, 95% CI [-0.76, -0.40]; median: -0.53 Nm (IQR: 0.07)) were significantly greater than passive extension (average: -0.05 Nm, 95% CI [-1.15, 1.04]; median: 0.09 Nm (IQR: 1.73)) and flexion (average: 0.17 Nm, 95% CI [-0.17, 0.53]; median: 0.09 Nm (IQR: 0.57)), change in mean torsion moment was significantly smaller during passive flexion (average: 0.11 Nm, 95% CI [-0.46, 0.68]; median: -0.06 Nm (IQR: 0.72)) than during manual SMT (average: -0.43 Nm, 95% CI [-0.88, -0.01]; median: -0.29 Nm (IQR: 0.77)), passive extension (average: -0.55 Nm, 95% CI [-1.57, -0.15]; median: -0.37 Nm (IQR: 1.09)) and left axial rotation (average: -0.49 Nm, 95% CI [-2.15, -0.16]; median: -0.54 Nm (IQR: 0.27)).

#### *7.3.4.5 Cut 3: Intervertebral disc, anterior and posterior longitudinal ligaments (IVD)*

Figure 7.14 presents the average peak force, mean force, peak moment and mean moment experienced by IVD structures while changing the applied motion. Significant changes in forces and moments experienced by IVD structures were revealed depending on the applied motion. Overall forces and moments experienced by IVD structures were greater than the ones experienced by SL and PJ structures, with the exception of torsion moments during manual SMT and passive axial rotation, where PJ structures were loaded to a greater extent than SL and IVD structures. Generally, there was no specific applied motions during which IVD structures experienced greater forces and moments. From 36 comparisons between manual SMT with each passive lumbar movement (flexion, extension and left axial rotation), only 5 comparisons revealed specific forces and moments that were greater during manual SMT. Despite of those,

none of the forces and moments were significantly greater during manual SMT in comparison to all passive lumbar movements (Figure 7.15).

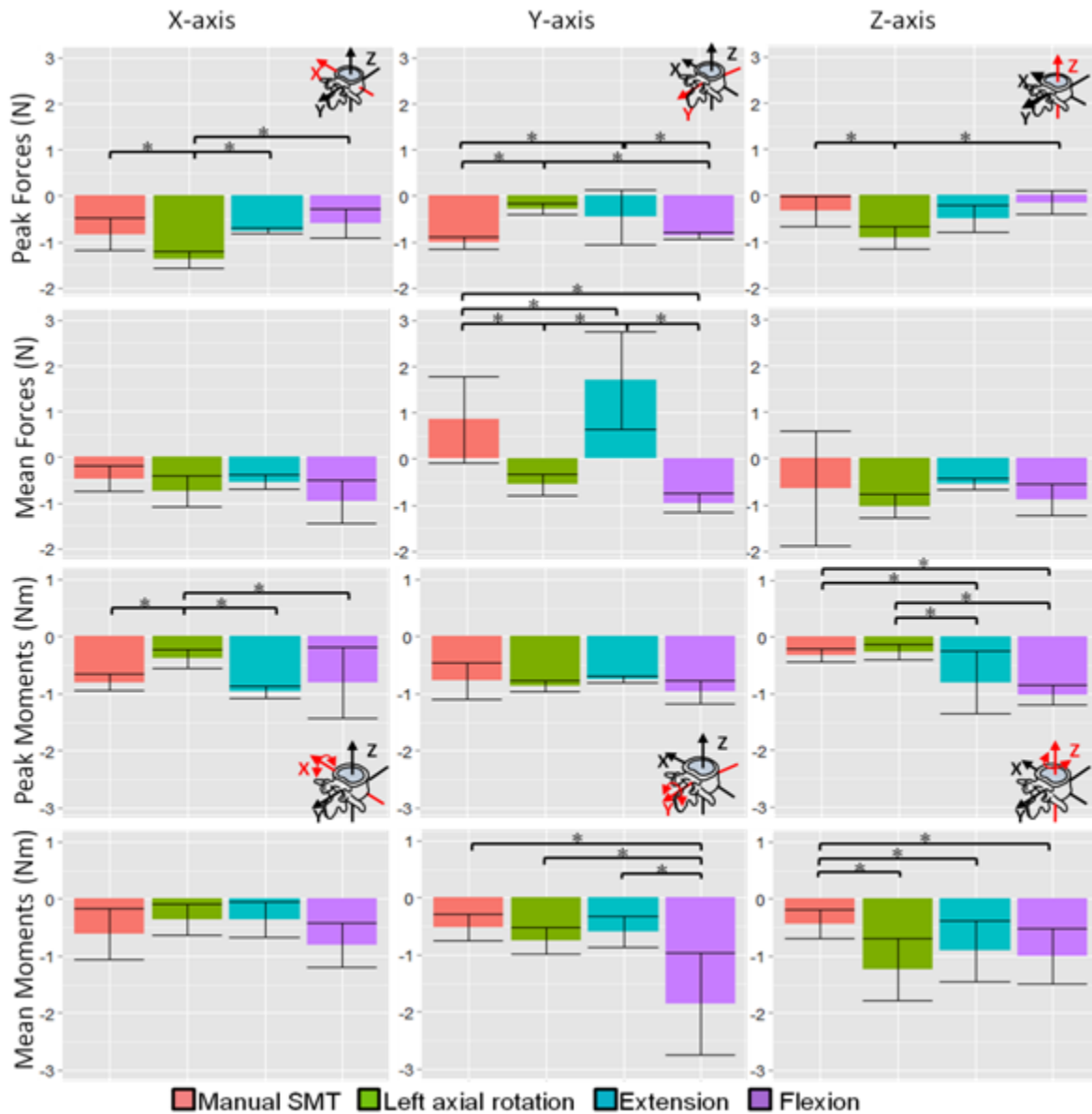


Figure 7.14 Average value of normalized peak force, mean force, peak moment and mean moment experienced by the intervertebral disc, anterior and posterior longitudinal ligaments during the application of manual SMT and passive lumbar movements of flexion, extension and left axial rotation.

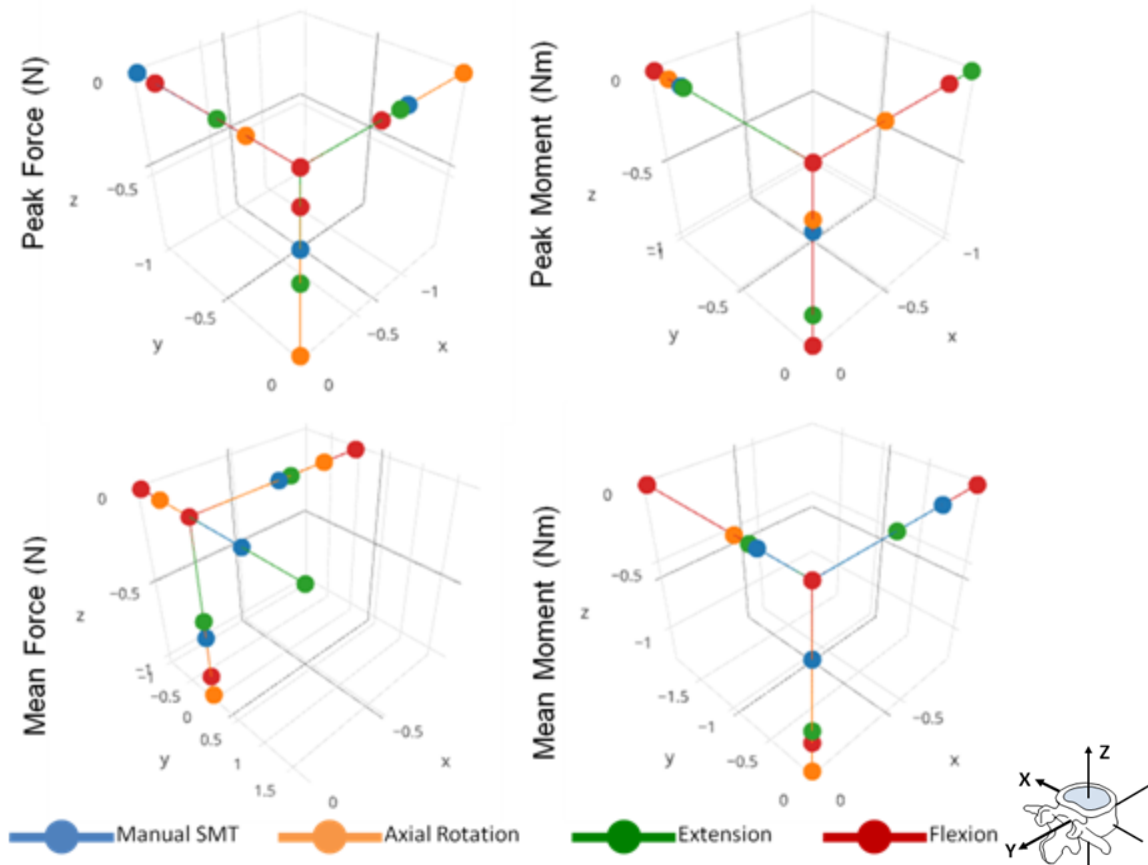


Figure 7.15 Three-dimensional plots of average values of normalized peak force, mean force, peak moment and mean moment experienced by the intervertebral disc, anterior and posterior longitudinal ligaments during the application of manual SMT and passive lumbar movements of flexion, extension and left axial rotation in each axis of movement.

Specifically, peak lateral force (force along x-axis) experienced by IVD structures was significantly greater during passive left axial rotation (average: -1.37 N, 95% CI [-1.73, -1.01]; median: -1.13 N (IQR: 0.78)) in comparison to manual SMT (average: -0.82 N, 95% CI [-1.50, -0.14]; median: -0.77 N (IQR: 0.64)), passive extension (average: -0.75 N, 95% CI [-0.88, -0.61]; median: -0.68 N (IQR: 0.24)) and flexion (average: -0.59 N, 95% CI [-1.21, 0.02]; median: -0.75 N (IQR: 0.27)). Additionally, while change in peak anterior posterior force (force along y-axis) was significantly greater during manual SMT (average: -1.01 N, 95% CI [-1.26, -0.76]; median: -1.07 N (IQR: 0.32)) and passive flexion (average: -0.87 N, 95% CI [-1.01, -0.72]; median: -0.83

N (IQR: 0.22)) than during passive extension (average: -0.45 N, 95% CI [-1.62, -0.07]; median: -0.03 N (IQR: 0.69)) and left axial rotation (average: -0.27 N, 95% CI [-0.51, -0.04]; median: -0.34 N (IQR: 0.46)), change in mean anterior posterior forces was significantly greater during passive extension movement (average: 1.70 N, 95% CI [-3.78, -0.38]; median: 0.15 N (IQR: 3.82)), followed by manual SMT (average: 0.85 N, 95% CI [-2.68, -0.98]; median: -0.71 N (IQR: 2.22)) in comparison to passive left axial rotation (average: -0.55 N, 95% CI [-1.00, -0.10]; median: -0.44 N (IQR: 1.24)) and flexion (average: -0.94 N, 95% CI [-1.33, -0.55]; median: -0.83 N (IQR: 0.39)). Change in peak superior inferior force (force along z-axis) was significantly greater during passive left axial rotation (average: -0.89 N, 95% CI [-1.37, -0.42]; median: -1.16 N (IQR: 0.59)) in comparison to manual SMT (average: -0.33 N, 95% CI [-0.97, -0.30]; median: -0.15 N (IQR: 0.38)) and passive flexion (average: -0.15 N, 95% CI [-0.65, 0.35]; median: -0.26N (IQR: 0.16)).

Specifically for moments, change in peak extension moment (moment around x-axis) was significantly smaller during passive left axial rotation (average: -0.38 Nm, 95% CI [-0.71, -0.06]; median: -0.37 Nm (IQR: 0.52)) in comparison to manual SMT (average: -0.80 Nm, 95% CI [-1.07, -0.52]; median: -0.83 Nm (IQR: 0.25)), passive extension (average: -0.97 Nm, 95% CI [-1.18, -0.75]; median: -0.93 Nm (IQR: 0.45)) and flexion (average: -0.80 Nm, 95% CI [-2.02, 0.41]; median: -0.19 Nm (IQR: 0.36)). Additionally, while change in peak torsion moments (moments around z-axis) during passive extension (average: -0.80 Nm, 95% CI [-1.87, 0.27]; median: -0.81 Nm (IQR: 2.35)) and flexion (average: -1.01 Nm, 95% CI [-1.37, -0.68]; median: -0.83 Nm (IQR: 0.75)) was significantly greater in comparison to manual SMT (average: -0.32 Nm, 95% CI [-0.55, -0.10]; median: -0.36 Nm (IQR: 0.35)) and passive left axial rotation (average: -

0.26 Nm, 95% CI [-0.52, -0.00]; median: -0.40 Nm (IQR: 0.16)), change in mean torsion moment experienced by IVD structures during manual SMT (average: -0.43 Nm, 95% CI [-0.92, -0.04]; median: -0.48 Nm (IQR: 0.62)) was significantly smaller than during passive left axial rotation (average: -1.23 Nm, 95% CI [-2.30, -0.15] ; median: -0.44 Nm (IQR: 0.50)), extension (average: -0.91 Nm, 95% CI [-1.94, 0.11]; median: -0.57 Nm (IQR: 0.82)) and flexion (average: -1.00 Nm, 95% CI [-1.95, -0.05]; median: -0.53 Nm (IQR: 0.85)).

## **7.4 Discussion**

This study aimed to quantify and compare the displacement, forces and moments experienced by spinal structures of a porcine cadaveric model during the application of manual SMT and passive lumbar movements of flexion, extension and left axial rotation. The results of this study indicate that in contrast to previous beliefs, manual SMT did not always load spinal structures to a significantly greater extent than passive lumbar movements of flexion, extension and left axial rotation. Specifically for the intact specimen, manual SMT did not create significantly greater forces and moments than the ones created during passive lumbar movements, with only one exception being observed on anterior posterior forces. Similarly for unique spinal structures, serial dissection revealed that manual SMT did not always load spinal structures to a greater extent than passive lumbar movements and the only exceptions were on superior inferior forces experienced by SL and PJ structures and extension moments experienced by PJ structures. Figure 7.16 summarizes the main findings of the current study.



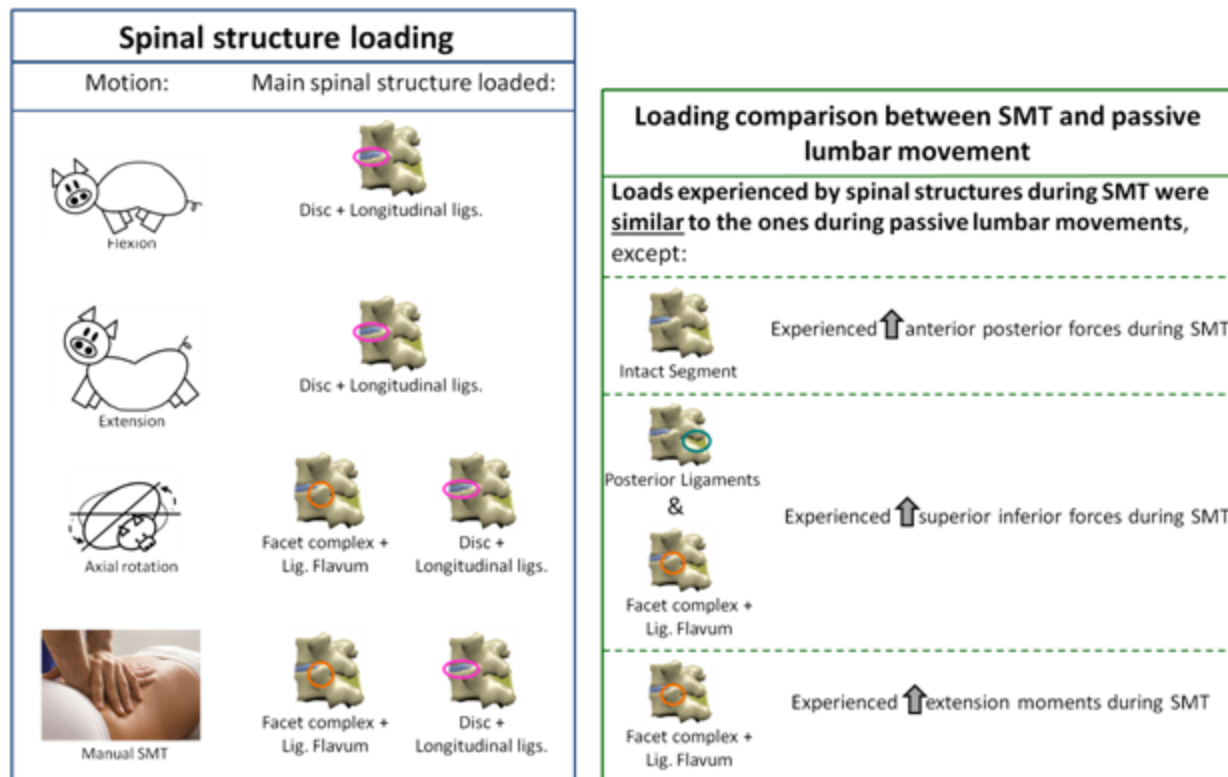


Figure 7.16 Summary of the main findings of the current study.

Spinal manipulative therapy also did not cause vertebral motions greater than passive lumbar movements in all directions: passive extension movement caused the greatest lateral and anterior translations as well as extension rotations. Therefore, even though SMT is believed to move the spinal segment beyond its physiological range of motion [21], the results of the current study demonstrate that not only the vertebral motions, but also the loads experienced by the intact specimen and spinal structures during an application of manual SMT were not always significantly greater than the ones during passive lumbar movements. Although studies have been conducted investigating spinal loading during both physiological movements [51,55] and SMT application [24], this is the first study to quantify and compare the loads arising from both passive movement and manual SMT in a unified study with comparable specimens and testing protocol.

#### ***7.4.1 Spinal manipulative therapy characteristics - Comparison with previous studies***

In the current study, manual SMT force-time characteristics were measured by a pressure array system and an average peak force magnitude of 524N ( $\pm 41$ N) was observed. Although SMT force magnitude has been described to be adjusted based on specific aspects (e.g. patient morphology and articular stiffness) [114], similar peak force magnitudes have been reported by previous investigations [114,240,241]. Likewise, time to peak of 220ms ( $\pm 15$ ms) and loading rate of 2.38N/ms here observed are also in accordance to previous reports [35,122,242]. This indicates that even though manual SMT was applied on cadaveric porcine models, force-time profile of the applied SMT was representative of a clinical manual SMT application on human subjects.

The same manual SMT resulting vertebral motions were replicated during biomechanical testing of the intact specimen and following each cut. In this study, manual SMT caused greatest translation in the anterior posterior axis (along y-axis) (9.10 mm) and the greatest rotation in flexion extension (around x-axis) ( $3.06^\circ$ ). Despite of the difference in magnitudes, Kawchuk and colleagues (2010) [24] also observed greatest displacement (5.35 mm) and rotation ( $1.96^\circ$ ) in the same axes as the current study using a similar animal model. In addition, Gal and colleagues (1997) [243] investigated the relative vertebral motions during SMT application on the thoracic region of unembalmed human cadavers and also observed significant posterior to anterior translations (6-12 mm) and flexion extension rotations ( $0.2-1.8^\circ$ ). The greater flexion extension rotation observed in the current study is likely related to differences in force-time characteristics of the applied SMT and spinal levels. Despite this difference, the SMT resulting vertebral

motions observed here also indicate that the SMT provided in the current study is representative of a clinical SMT application.

#### ***7.4.2 Vertebral motion during lumbar movements - Comparison with previous studies***

Previous investigations have reported L3/L4 intersegmental displacements and rotations of lumbar segments during functional activities and active lumbar movements of flexion, extension, lateral bending and axial rotation [88,89,96] and maximum rotations of approximately 5° during flexion extension and lateral bending and 4° during axial rotation have been reported *in vivo* [88,89,96]. Intersegmental *in vitro* range of motion of the lumbar spine has also been previously described and maximum rotations of approximately 7° during flexion extension, 8° during lateral bending and 3.5° during axial rotation have been reported [97,257,258]. In this study, Table 7.2 shows that the applied passive lumbar movements presented ranges that are within the maximum ranges reported in the literature, indicating that the passive lumbar movements here applied were representative of normal L3/L4 intersegmental lumbar movements observed in both living humans and biomechanical testing. Importantly, Table 7.2 also shows that in the current study, the maximum rotations caused by manual SMT were also within the *in vivo* and *in vitro* reported range of motion. This indicates that in contrast to previous beliefs, manual SMT application does not move the spinal segment beyond its normal range of motion, but stays within the range of movement reported in the literature [88,89,96].

Due to the coupled motions observed in the spine, *in vivo* vertebral translations during active lumbar movements of flexion, extension lateral bending and axial rotation have also been measured and anterior posterior displacements of approximately 1.8mm, lateral displacements of

2.4mm and cranio-caudal displacements of 4mm have been reported in the L3/L4 spinal segment [88,89,96]. Based on Table 7.2, only the anterior posterior displacements observed in the current study exceed the previously reported translation values and specifically the anterior posterior displacements observed during manual SMT presented significantly greater magnitudes (9.10mm). These differences were expected given that most of the studies that investigated lumbar range of motion and reported the magnitudes of the coupled motions (i.e. translations) included living participants performing active movements and fundamental factors, such as muscular activation and subject positioning, may contribute to these differences. Despite of the large anterior posterior translation observed during manual SMT, the anterior posterior translation caused by passive extension movement was even greater (9.53mm), suggesting that manual SMT does not cause larger displacements than passive lumbar movements.

Previous intersegmental *in vitro* studies reported anterior posterior displacements of approximately 3mm, lateral displacement of 2.6mm and cranio-caudal displacements of 1mm [74,91,92]. Although our study observed larger anterior posterior displacements during manual SMT and passive extension movement, vertebral failure was only observed at an anterior displacement of approximately 11.7mm with associated shear force of more than 1000N [259]. Therefore, even though anterior posterior vertebral displacements here observed were greater than the displacements reported *in vivo* and *in vitro* [74,88,89,92,96,97], both the anterior displacement and shear force was substantially smaller than the vertebral failure values, most likely due to the 3-dimensional associated vertebral motions during manual SMT and passive lumbar movements.

In summary, the vertebral motions observed during both passive lumbar movements and manual SMT generally stayed within the normal range of motion reported in the literature, with only one exception on anterior posterior displacements. This indicates that not only were the passive movements applied in this study generally representative of lumbar movements, but also that in general, manual SMT does not move the vertebrae past the limits found with active motion with the exception of in anterior posterior translation. The remaining translations and rotations along and around all other axes of movement caused by manual SMT stayed within the physiological range of motion.

### ***7.4.3 Interpretation of Results***

#### ***7.4.3.1 Intact specimen***

Given that manual SMT was applied at the left L3/L4 FJ (creating a left axial rotation component), passive axial rotation was intentionally performed to the left side so that the moments arising from both motions were observed in the same direction and more easily compared as shown on Figure 7.8. Additionally, given that flexion and extension motions occur around the same axis of movement (x-axis in this study), but with rotations in opposite directions, it was expected that the moments created by these motions were observed in opposite directions, which was not the case (Figure 7.8). This suggests that peak and mean moments do not always reflect the vertebral motions.

The analysis of the intact specimen revealed peak anterior force (force along y-axis) significantly greater during manual SMT in comparison to all passive lumbar movements included in this study. Given the posterior to anterior direction of manual SMT thrust application, a greater force

along y-axis experienced by the intact specimen resisting the thrust application was expected. Significant differences in peak anterior posterior forces during passive extension was also observed in comparison to passive flexion. As shear forces in opposite directions have been previously described during flexion and extension movements (anterior shear force during flexion and posterior shear force during extension) [260], the significant difference between anterior posterior forces during these movements was also expected.

The mean superior inferior force (force along z-axis) experienced by the intact specimen was significantly greater during manual SMT than during passive extension movement. Interestingly, although superior inferior vertebral displacements during manual SMT and passive extension were not considerably different (Table 7.2), they created mean superior forces in opposite directions, with manual SMT creating a mean cranial force and extension movement a mean caudal force (Figure 7.8). While the caudal force created to resist the superior displacement during passive extension is comprehensive, the cranial force observed during manual SMT despite of the superior displacement is an interesting finding. This is in accordance with observations from previous studies of this dissertation (chapters 4, 5 and 6) and can likely be explained by the 3-dimensional vertebral motion associated with manual SMT. It is possible that the displacements and rotations associated with manual SMT (e.g. anterior translation, extension and axial rotation) deformed the intact specimen to a particular position where a resisting force in the cranial direction was created.

Specifically for moments, apart from the expected significant differences between mean extension moment (moment around x-axis) experienced by the intact specimen during passive

flexion and extension movements, the significant differences in torsion moments (moments around z-axis) between passive left axial rotation and passive flexion and extension movements were also expected. Importantly, peak torsion moment during manual SMT was significantly greater than passive flexion and extension movements, but not than passive left axial rotation, indicating that the torsion moments created by manual SMT on the intact spinal segment does not impose a greater risk of spinal injury than a passive axial rotation movement does.

In summary, the forces and moments experienced by the intact specimen during manual SMT were generally not significantly greater than the ones during passive lumbar movements. The only exception was on forces along y-axis where greater peak anterior posterior force during manual SMT was observed in comparison to passive lumbar movements of flexion, extension and left axial rotation. This exception might be responsible for eliciting the physiological responses observed following a SMT application, but not during passive lumbar movements.

#### *7.4.3.2 Cut 1: Supra- and interspinous ligaments (SL)*

Overall, SL structures experienced significant changes in forces and moments during the application of manual SMT and passive lumbar movements. Similarly to the previous studies of this dissertation, however, the forces and moments experienced by SL structures were remarkably smaller than the ones experienced by PJ and IVD structures. This indicates that the loads arising from manual SMT and passive lumbar movements are distributed mainly within PJ and IVD structures, with SL structures generally experiencing minor loads (Table 7.4).

Significant change in peak lateral force (force along x-axis) was observed and passive flexion movement created significantly greater change in lateral force in comparison to during manual SMT and passive extension. Similarly to the current study, lateral translation coupled motion has been previously observed during flexion-extension movements [88,89]. Differences in lateral forces between manual SMT and passive flexion is likely related to the lateral translation caused by both applied motions: while manual SMT caused left lateral translation, right lateral translations was observed during passive flexion movement (Table 7.2). On the other hand, despite the similar coupled lateral translation observed during passive flexion and extension movements, the significant difference in lateral force change experienced by SL structures might be related to the biomechanical function of SL structures during these movements. While SL structures are compressed during extension [97], they have been described as important resistors to flexion movement in the porcine model [178], suggesting that when fibers of SL structures are tensioned (during flexion movement), SL structures potentially become more sensitive to lateral forces.

Change in mean superior inferior force (force along z-axis) was significantly greater during manual SMT than during all passive lumbar movements included in this study. This is likely due to the greater superior displacements caused by manual SMT in comparison to the passive lumbar movements (Table 7.2). Additionally, the combination of superior displacement with extension rotation during manual SMT potentially compresses SL structures in a significantly greater extent than passive lumbar movements of flexion, extension and left axial rotation, causing greater superior inferior forces resisting this superior displacement.



Specifically for moments, change in mean torsion moment (moment around z-axis) was significantly greater during passive extension movement in comparison to manual SMT. Table 7.2 shows a noticeable difference in axial rotation between these two applied motions, with manual SMT causing greater axial rotation than passive extension movement. Therefore, it is possible that SL structures contribute to resisting small degrees of axial rotation [97] and when greater axial rotations are performed (like during manual SMT), other spinal structures (e.g. facet joints) get engaged and take over the loads previously experienced by SL structures.

In summary, despite of the smaller magnitude of overall forces and moments experienced by SL structures in comparison to the ones experienced by PJ and IVD structures, change in forces and moments experienced by SL structures during manual SMT were generally not significantly greater than during passive lumbar movements. Importantly, the exception along z-axis where mean superior inferior force experienced by SL structures during manual SMT was significantly greater than during passive lumbar movements might contribute to the SMT therapeutic effect, in comparison to passive lumbar movements.

#### *7.4.3.3 Cut 2: Bilateral facet joints, capsules and ligamentum flavum (PJ)*

Overall, significant changes in forces and moments experienced by PJ structures were observed during the application of manual SMT and passive lumbar movements of flexion, extension and left axial rotation. While the overall forces and moments experienced by PJ structures were generally smaller than the ones experienced by IVD structures (Table 7.4), specific greater forces and moments were experienced by PJ structures during particular applied motions. More specifically, torsion moments and mean anterior posterior forces during passive left axial rotation

and manual SMT, and mean extension moments during passive extension movement and passive axial rotation experienced by PJ structures were greater than the ones experienced by SL and IVD structures. This indicates that PJ structures are the main resistors to axial rotations (both passive axial rotation movement and the axial rotation component of manual SMT), and important contributors to resisting passive extension movements, which is in accordance to the Chapter 5 of this dissertation as well as previous investigations [51,97,236,261].

Significant change in lateral forces (forces along x-axis) experienced by PJ structures was observed and manual SMT and passive extension created significantly greater peak lateral force than passive left axial rotation and flexion movements. Given the greater lateral translation observed during manual SMT and passive extension movement (Table 7.2), greater lateral forces created by these applied motions were expected as PJ structures have been described as the primary resistors to lateral displacements [74,75].

Changes in peak anterior posterior force (force along y-axis) was significantly greater during passive left axial rotation and extension in comparison to manual SMT and passive flexion movement. While this was expected during passive extension due to the greatest anterior posterior displacement (Table 7.2) and the known resistance of facet joints to extension movement [97,236], passive left axial rotation did not cause significant anterior posterior displacements. Despite this, facet joints' biomechanical function of resisting axial rotations has been widely described given the orientation of its surfaces in the lumbar spine [71,72]. Therefore, it is possible that when facet joints are already in contact due to the primary motion (in this case, left axial rotation), other movements that increase facet joint surface contact, such

as anterior translation of the superior vertebra, will increase the loads on PJ structures. Additionally, while change in mean anterior posterior force was significantly greater during passive extension movement in comparison to the remaining applied motions included in this study, it was also significantly greater during manual SMT in comparison to passive flexion. This is likely related to the greater anterior vertebral displacement observed during manual SMT (Table 7.2), creating a posterior force in comparison to the posterior vertebral displacement during passive flexion, creating an anterior force experienced by PJ structures.

Change in superior inferior forces (forces along z-axis) were significantly greater during manual SMT than all passive lumbar movements of flexion, extension and left axial rotation. In addition to the greatest superior displacement during manual SMT in comparison to the passive lumbar movements, this can also be explained by the facet joint resistance to compression, especially when combined with rotations and shear displacements [71,233]. Therefore, PJ structures experience greater superior inferior forces during manual SMT than during passive lumbar movements.

Given the applied motion, significantly greater changes in peak flexion extension moment (moment around x-axis) during passive extension movement in comparison to manual SMT and passive left axial rotation were expected. Change in peak flexion extension moment experienced by PJ structures was also significantly greater during passive left axial rotation than manual SMT and passive flexion movement. As previously mentioned, the biomechanical function of facet joints in resisting axial rotation has been widely described [71,72,97,236] and the increase in loads experienced by facet joints during the combination of axial rotation and extension movements has

also been reported [262]. On the other hand, although change in mean flexion extension moments was significantly greater during passive flexion and extension movements in comparison to passive left axial rotation, it was even greater during manual SMT. This is likely related to the presence of preload phase during SMT application and its resultant loads on PJ structures. Preload phase characteristics (e.g. phase duration and preload force magnitude) have been described to influence Electromyographic (EMG) as well as muscle spindle responses to SMT [57,141]. Therefore, the observations of the current study that PJ structures experienced significantly greater mean flexion extension moments than during passive lumbar movements, but the same was not observed in peak flexion extension moments suggests that preload phase also significantly influence extension moments experienced by PJ structures.

Change in peak torsion moment during manual SMT and passive left axial rotation were significantly greater than passive extension and flexion. This was expected not only due to the nature of the applied motions, but also due to the greater axial rotation during the former mentioned motions (Table 7.2). On the other hand, change in mean torsion moment was significantly smaller during passive flexion than during all other applied motions of manual SMT, passive extension and left axial rotation. This was also expected not only because of the smaller axial rotation observed during passive flexion (Table 7.2), but also due to the previous observation that facet joint surfaces move apart from each other during flexion movement [262], minimizing the loads experienced by PJ structures during passive flexion movement.

In summary, despite the smaller magnitude of overall forces and moments experienced by PJ structures in comparison to the ones experienced by IVD structures, PJ structures experienced

greater torsion moments caused by large axial rotations (e.g. manual SMT and passive axial rotation). Additionally, change in forces and moments experienced by PJ structures during manual SMT were generally not greater than during passive lumbar movements. Nevertheless, two exceptions were observed: superior inferior forces and mean extension moments experienced by PJ structures during manual SMT were significantly greater than during passive lumbar movements.

#### *7.4.3.4 Cut 3: Intervertebral disc, anterior and posterior longitudinal ligaments (IVD)*

Overall, significant changes in forces and moments experienced by IVD structures were observed as a function of the applied motion. Although IVD structures generally experienced the greatest overall forces and moments (Table 7.4), specifically the torsion moments and mean anterior posterior forces during manual SMT and passive axial rotation, were greatly experienced by PJ structures. This indicates that apart from the abovementioned exceptions, IVD structures are the structures that generally experienced the greatest loads during manual SMT and the applied passive lumbar movements of flexion, extension and left axial rotation, which is in accordance to previous investigations [24,170,263,264].

Significant changes in peak lateral and superior inferior forces (forces along x- and z-axes, respectively) were observed with a significantly greater change during passive axial rotation in comparison to manual SMT and passive flexion for superior forces, and also in comparison to passive extension for lateral forces. This might be related to the method in which passive axial rotation was applied to the porcine cadaveric model. Specifically, since passive axial rotation was applied by manually stabilizing L3 and rotating the pelvis to the left side, additional movements

besides the coupled motions normally observed may potentially have occurred, increasing the lateral and superior loads experienced by IVD structures. Despite of this, the vertebral motions caused during the applied passive left axial rotation (Table 7.2) in the current study are comparable with the intersegmental ranges of motion previously reported [88,89,96] and, therefore, representative of an *in vivo* axial rotation.

Significant change in peak anterior posterior force (force along y-axis) was observed with a significantly greater change during manual SMT in comparison to during passive extension and left axial rotation. This was expected given the great anterior posterior displacements caused by manual SMT. On the other hand, change in mean anterior posterior forces was significantly greater during passive extension movement, followed by manual SMT in comparison to passive left axial rotation and flexion, which is also likely related to the greater anterior posterior vertebral displacement observed during these applied motions (i.e. passive extension and manual SMT) (Table 7.2).

Interestingly, significant change in peak anterior posterior force (force along y-axis) was also significantly greater during passive flexion in comparison to during passive extension and left axial rotation. Similarly, changes in mean lateral bending moment experienced by IVD structures during passive flexion movement were significantly greater than during the remaining applied motions included in this study. Even though passive flexion movement did not cause great anterior posterior displacements and lateral bending rotations (Table 7.2), facet joint surfaces have been described to move apart from each other during flexion movement [262] and posterior ligaments have been observed to slack in neutral position and rearrange their fibers orientation

during the small degrees of flexion [73]. This suggests that the IVD structures might be the main resistors to the anterior posterior coupled translations and lateral coupled rotations observed during small degrees of flexion.

Significant changes in peak flexion extension moment (moment around x-axis) experienced by IVD structures were observed with significantly smaller changes during passive left axial rotation movement. This was expected given the nature of the applied motion with the primary motion of axial rotation not occurring in the flexion-extension axis.

Interestingly, changes in peak torsion moment (moment around z-axis) experienced by IVD structures were significantly smaller during manual SMT and passive left axial rotation in comparison to passive flexion and extension movements. This indicates that IVD structures not only resist to coupled motions during flexion, but also during extension they resist to torsion coupled rotations. Although this might be counter-intuitive because of the facet joint surface contact during extension movement [72,236], Table 7.2 shows that with extension, a significant anterior displacement of the inferior vertebra was observed potentially reducing the contact between facet joint surfaces. This anterior displacement is greater than the coupled anterior translations previously reported [88,89,96] and is likely related to the passive application of the extension movement as well as the use of cadaveric model, where no muscle activity is present. Therefore, given the great anterior displacement potentially reducing the facet joint surface contact, the IVD structures become more susceptible to loads arising from coupled motions during extension, experiencing greater torsion moments.

In summary, despite the greater magnitude of overall forces and moments experienced by IVD structures in comparison to the ones experienced by SL and PJ structures, PJ structures were the structures that experienced the greatest torsion moments caused by large degrees of axial rotations in comparison to IVD and SL structures. Additionally, change in forces and moments experienced by IVD structures during manual SMT were not significantly greater than the ones experienced during passive lumbar movements.

#### *7.4.3.5 General discussion*

This study not only quantified but also compared the forces and moments arising from manual SMT with the ones arising from passive lumbar movements. Generally, loads created by manual SMT were not significantly greater than the ones created by applied passive lumbar movements of flexion extension and left axial rotation, with exceptions of particular forces and moments. Specifically, manual SMT created significantly greater anterior posterior forces on the intact specimen, superior inferior forces on both SL and PJ structures and greater flexion extension moments on PJ structures. Although SMT has been observed to produce facet joint capsule strain magnitudes within the range observed during physiological movements [202], unique patterns in facet joint capsule strain were observed during high loading rate SMT in comparison to physiological axial rotation [145]. Therefore, it is possible that, similar to facet joint capsule strain, the loading rate (or other SMT characteristic, such as resulting vertebral motion, force magnitude, etc) creates unique forces, moments and potentially biomechanical stimulus, on spinal structures that differ from the ones arising from passive lumbar movements, eliciting SMT's physiological responses.



Although vertebral motions here observed during the application of manual SMT were within the range of physiological movements, previous investigations using finite element models have described that due to the viscoelastic behavior of spinal structures, high loading rates increase the risk of spinal structures injury [265–267]. Specifically, Wang et al. (2000) [266] assessed slow (0.6N/ms and 0.003°/ms) and fast loading rates (6.6N/ms and 0.03°/ms) of combined compression and flexion movements and found that high loading rates increased intradiscal pressure as well as forces and moments experienced by spinal structures. El-Rich et al. (2009) [265] investigated flexion extension using three loading rates (0.05°/ms, 0.5°/ms and 5°/ms) and found that spinal injuries, such as bone fracture and ligament failure, can occur in loading rates higher than 0.5°/ms. Wagnac and colleagues (2012) [267] applied flexion, extension, anterior and posterior shear at low (0.1m/s) and high rates (1.0m/s for compression and 4.0m/s for flexion and extension) and observed that loading rate significantly influenced spinal injury site. In the current study, manual SMT was applied with a loading rate of 2.38 N/ms (0.04m/s and 0.014°/ms), which is usually close or below the lower loading rates used in the abovementioned studies. This indicates that given the SMT parameters of this study, manual SMT is unlikely to cause injury on spinal structures.

Additionally, the estimated stiffness of the L3/L4 spinal segment during the manual SMT application here observed was also smaller than the stiffness observed right before spinal injury previously described in the literature [174,233,268,269]. Specifically, this study estimated that the L3/L4 spinal stiffness during manual SMT was 2.18 N/mm in anterior shear, 0.33 Nm/deg in extension and 1.51 Nm/deg in axial rotation, which are smaller than the anterior shear stiffness described by Schmidt and colleagues (2013) [233] and Lu et al. (2005) [174] of approximately

550 N/mm, extension stiffness described by Garges et al. (2008) [268] of 10 Nm/deg and torsion stiffness described by Bisschop and colleagues (2013) [269] of 5.7 Nm/deg. This indicates that not only the loading rate of SMT is very unlikely to cause any spinal injury, but also the spinal segmental stiffness caused by manual SMT loading is also smaller than the values attained in injurious conditions.

Noteworthy, despite the greater anterior posterior forces on the intact specimen, superior inferior forces on both SL and PJ structures and extension moments on PJ structures during SMT, the magnitudes of forces and moments experienced by these structures during manual SMT is still considerably smaller than the ones reported in previous research investigating porcine spinal structural failure reporting failure shear forces ranging from 800N to 8700N [173,229,230]. Although the comparison between anterior posterior forces between the current study and previous investigations described in the literature is limited due to methodological differences, anterior posterior forces created by manual SMT did not exceed 40N, which suggests that manual SMT is very unlikely to cause any serious adverse events, such as bone fracture. However, future studies addressing this specific question should be conducted in order to appropriately verify the forces created by manual SMT in comparison to the ones for vertebral injury and failure.

On the other hand, no studies have investigated and specified values of forces and moments experienced by the spinal segment and its composite structures to elicit physiological responses. Consequently, even though the forces and moments experienced by the intact specimen and by the spinal structures were considerably below the values previously described to cause vertebral

injury, it remains unknown if they are large enough to reach the physiological response threshold. Therefore, future studies should be conducted to investigate the minimum force and moment experienced by spinal structures to observe a physiological

Importantly, the results of this study described how the manual SMT load distribution within spinal structures compares to that of passive lumbar movements. For example, in comparison to passive lumbar movements, manual SMT created anterior posterior forces significantly greater on the intact specimen (Figure 7.9). While the IVD structures were the structures that experienced most of these forces, the magnitude of anterior posterior forces experienced by IVD structures were comparable to the ones experienced during extension movement (Figure 7.15). Similarly, although the mean extension moments experienced by the intact specimen during manual SMT was comparable to the ones experienced during passive lumbar movements (Figure 7.9), the moments experienced by PJ structures (responsible for most of these moments) were significantly greater (Figure 7.12). This highlights the difference in load distribution within spinal tissues during the application of different motions. Additionally, these observations indicate that different SMT techniques might potentially change the load distribution within spinal structures, which may (or may not) be greater than the ones created by physiological movements.

Of note, while the intact specimen did not experience greater superior inferior forces during manual SMT than during passive lumbar movements, the superior inferior forces experienced by SL and PJ structures were significantly greater. Nevertheless, it is important to emphasize that manual SMT superior inferior forces were here compared to passive lumbar movements of

cadaveric porcine models, where no forces arising from weight-bearing or muscular tonus were present. This way, it is possible that the comparison of these superior inferior forces with active physiological movements in living models might provide different results.

Interestingly, in Figures 7.8 to 7.15 it is possible to notice that the torsion moments experienced by the intact specimen during manual SMT was significantly greater than the ones experienced during passive flexion and extension, but not during axial rotation. While that same pattern is also observed on PJ structures, it gets reversed on IVD structures, with passive extension and flexion creating greater torsion moments than manual SMT and axial rotation. This demonstrates that PJ structures shield IVD structures not only from extension moments [83,85], but also from torsion moments.

Of note, given the findings of the first study of this dissertation (Chapter 3), the results of the current study is limited to the order in which structures were removed from the specimen during biomechanical testing. By changing the order of structure removal, the loading characteristics experienced by spinal structures during SMT and passive lumbar movements would also be changed. Given the composition and biomechanical function of spinal structures investigated here, it is possible to speculate that structure removal order will not significantly impact the loading characteristics of spinal structures. Nevertheless, future studies are needed to quantify the load difference when different orders of structure removal are used.

#### *7.4.3.6 Clinical implications*

Based on the results of this study, a manual posterior to anterior SMT thrust application loads the spinal segment and its structures differently than passive lumbar movement. Although the majority of forces and moments created during manual SMT were comparable to the ones experienced during passive lumbar movements, the exceptions in which manual SMT created greater forces and moments might be responsible for eliciting the therapeutic effects observed following a SMT application. In this study, vertebral motions caused by manual SMT were also comparable to the ones caused by passive lumbar movement.

Specifically, in comparison to passive lumbar movements of flexion, extension and left axial rotation, a SMT applied at the L3/L4 FJ only created greater anterior posterior force on the intact specimen, superior inferior forces on SL and PJ structures, and extension moments on PJ structures. Manual SMT did not create greater forces or moments on IVD structures. Figure 7.17 summarizes the clinical implications of this study. Noteworthy, given that the current study was conducted using porcine cadaveric models, the clinical implications described here are speculative and further clinical studies are needed to verify their application to human spines.




Forces and moments created during SMT are generally <b>similar</b> to the ones created during passive physiological movements. The <b>only exceptions</b> are:	
SMT creates ↑ anterior posterior forces on:	 Intact Segment
SMT creates ↑ superior inferior forces on:	 Posterior Ligaments
SMT creates ↑ superior inferior forces on: SMT creates ↑ extension moments on:	 Facet complex + Lig. Flavum

Figure 7.17 Summary of clinical implications of the current study.

#### 7.4.4 Limitations

First, even though porcine lumbar spine models have been described to be suitable models to investigate the human spine [93,95,146], anatomical and biomechanical differences have been reported and limits the extrapolation of these results to human living subjects. Second, by using cadaveric models not only limitations related to the kinematics of passive lumbar movement (e.g. muscular tonus), but also limitations associated with differences between *in vivo* and *in vitro* conditions such as muscular effects, and potential differences in repeated loading testing are also present. Third, given the limited number of robotic replications associated with the degradation of cadaveric specimens, this study included only 3 movements and lateral bending was not applied and should be included in future studies. Additionally, given the results of the first study of this dissertation [217], the loads here observed are specific to the order in which

spinal structures were removed from the specimen. Finally, since SMT was provided by a single clinician in this study, these results cannot be generalized to other clinicians.

## **7.5 Conclusion**

Based on the findings of this study, the loads created during manual SMT and its distribution within spinal tissues did not always significantly differ from the ones of passive lumbar movements. The majority of forces and moments created during manual SMT were not significantly greater than the ones created during passive lumbar movements however some exceptions were observed with manual SMT creating significantly greater anterior posterior forces in the intact specimen, superior inferior forces in SL and PJ structures and extension moments in PJ structures only. These unique forces and moments observed during SMT but not during passive lumbar movements may be what confers the unique therapeutic effects elicited following a SMT application, in comparison to the ones following passive lumbar movements.

## **Chapter 8.**

### **General discussion and conclusion**

#### **8.1 Introduction**

This doctoral work consisted of a series of biomechanical experiments with the following objectives: 1) to verify if the superposition principle could be observed in specimens composed of identical structures having identical time-dependent, non-linear behavior, 2) to investigate if SMT load distribution within spinal tissues caused by SMT could be changed by SMT input parameters, and 3) to compare loading in spinal structures between SMT and passive physiological movements.

#### **8.2 Summary of experimental findings**

Given the specific objectives of this dissertation, five experiments were conducted focusing on the loading characteristics experienced by an intact intervertebral motion segment and its constituent subcomponents from the application of SMT with varied input parameters and passive lumbar movements. While figure 8.1 presents a detailed summary of the results of each experiment conducted in the current dissertation, figure 8.2 presents an overview of the findings presented in this dissertation.



## 1. Superposition Principle

Structure:	Is loading independent of connector removal order?
Connector 1	✗
Connectors 2	✗
Connector 3	✗

## 2. SMT Input Parameters – Peak force magnitude and application site

SMT Input Parameter		Spinal Structure			
		Intact Segment	SL Structures	PJ Structures	IVD Structures
Interaction	500N at L3/L4 FJ	↑ Extension moments			
	300N and 500N at L4 TVP				
Peak force magnitude main effect	100N		↑ Lateral forces ↑ Lateral bending moments		
	300N				
	500N	↑ Overall forces and moments		↑ Torsion moments	
Application site main effect	L3/L4 FJ	↑ Sup-inf forces		↑ Lateral forces	
	L4 TVP	↑ Lateral bending and torsion moments		↑ Lateral bending moments	

### 3. SMT Input Parameters – Application site

SMT Input Parameter		Spinal Structure							
		Intact Segment		SL Structures		PJ Structures		IVD Structures	
		General	Specific	General	Specific	General	Specific	General	Specific
Application site	L2/L3 FJ	Ant-post, lateral forces and torsion moments in opposite direction to when applied at L3/L4 FJ and L4 TVP			↑ Sup-inf forces	Ant-post forces in opposite direction to when applied at L3/L4 FJ and L4 TVP	↑ Lateral forces	↑ Ext. moments when SMT applied at FJ and ↑ Lateral forces, lateral bending and torsion moments when SMT applied at TVP	↑ Sup-inf forces
	L3 TVP				↑ Lateral bending moments				↑ Lateral forces
	Btw FJ						↑ Overall forces		
	Btw TVP		↓ Ant-post forces ↓ Torsion moments						↓ Torsion moments
	L3/L4 FJ		↑ Ext. moments		↑ Torsion moments		↑ Ext. moments		↑ Ext. moments
	L4 TVP		↑ Torsion moments			Ant-post forces in opposite direction to when applied at L2/L3 FJ, L3 TVP and Btw FJ and TVP	↑ Torsion moments		↑ Sup-inf forces

### 4. SMT Input Parameters – Method of SMT application

SMT Input Parameter		Spinal Structure			
		Intact Segment	SL Structures	PJ Structures	IVD Structures
Method of SMT application	Activator	↓ Ant-post and lateral forces ↓ Overall moments		↓ Sup-inf forces ↓ Extension moments	↓ Extension moments
	Manual SMT		↑ Sup-inf forces	↑ Ant-post and sup-inf forces ↑ Torsion moments	↑ Ant-post forces
	Linear-actuator motor	↑ Extension moments		↑ Extension moments	↑ Lateral and sup-inf forces ↑ Lateral bending and torsion moments

## 5. SMT and Passive Physiological Movement Load Comparison

Applied Motion	Spinal Structure			
	Intact Segment	SL Structures	PJ Structures	IVD Structures
Manual SMT	↑ Ant-post forces ↑ Torsion moments	↑ Sup-inf forces	↑ Lateral and sup-inf forces ↑ Extension and torsion moments	↓ Torsion moments
Flexion		↑ Lateral forces	↓ Torsion moments	↑ Torsion moments
Extension		↑ Torsion moments	↑ Ant-post and lateral forces ↑ Extension moments	↑ Torsion moments
Left Axial Rotation	↑ Torsion moments		↑ Torsion moments	↑ Lateral forces ↓ Ant-post forces ↓ Extension moments

Figure 8.1 Summary of experimental results. SMT=spinal manipulative therapy; FJ=facet joint; TVP=transverse process; Btw= between; SL structures=supra- and interspinous ligaments; PJ structures=bilateral facet joints, capsules and ligamentum flavum; IVD structures=intervertebral disc, anterior and posterior longitudinal ligaments.

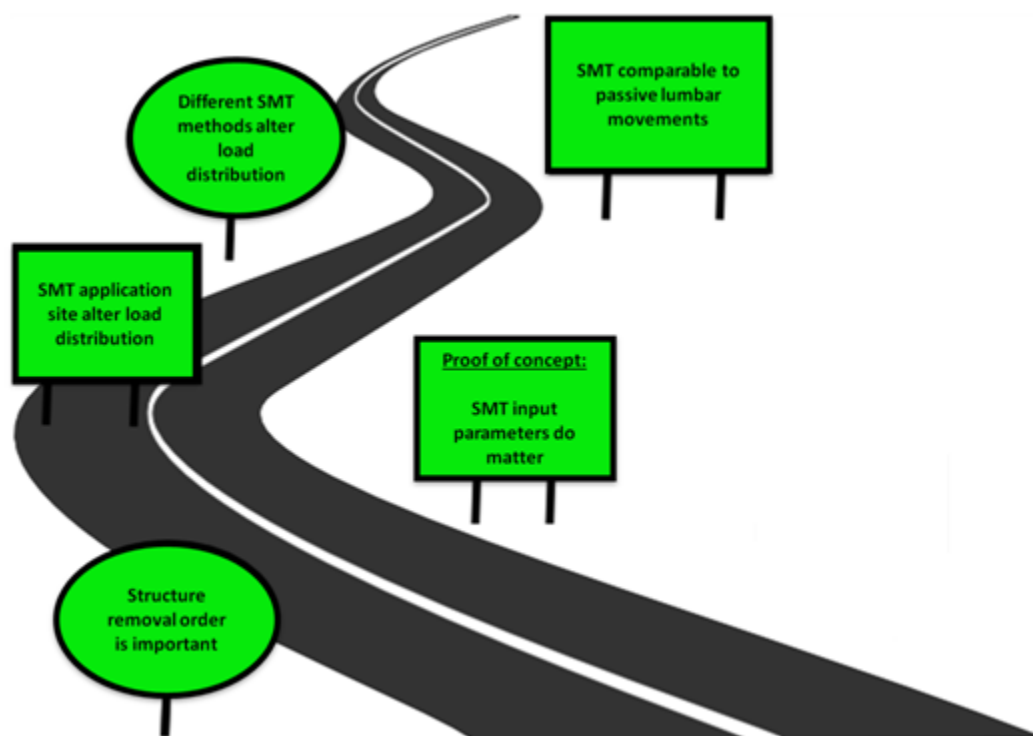


Figure 8.2 Overview of experimental findings.

### ***8.2.1 The principle of superposition***

This experiment investigated the principle of superposition on testing objects presenting identical time-dependent, non-linear behavior. The results revealed that the order in which structures are removed from the testing object affected the loading characteristics they experience. Given this finding, it would not be appropriate for future experiments to remove tissues in a random order. Consequently, a single, consistent sequence was used when removing spinal structures in all subsequent experiments in this dissertation in order to allow appropriate comparisons between specimens.

### ***8.2.2 Spinal manipulative therapy input parameters - Peak force magnitude and application site***

#### ***8.2.2.1 Interaction***

The interaction between SMT peak force magnitude and application site was significant in two circumstances: 1) in the intact specimen between 300 N and 500 N SMT application forces and the L4 transverse process (TVP) application site, and 2) in the intact specimen between 500 N applied force and the L4 facet joint (FJ) application site. In each circumstance, peak and mean extension moments (moments around x-axis) were significantly greater than the other possible interactions, respectively.

#### ***8.2.2.2 Peak force magnitude***

The SMT peak force magnitude main effect was observed to significantly influence SMT load distribution within spinal structures. While a smaller peak force magnitude (100 N) loaded the supra- and interspinous ligaments (SL structures; removed in cut 1) in a significantly greater extent, larger peak force magnitudes (300 N and 500 N) mainly loaded bilateral facet joints,

capsules and ligamentum flavum (PJ structures; removed in cut 2) and intervertebral disc, anterior and posterior longitudinal ligaments (IVD structures; removed in cut 3). These differences in load distribution within spinal structures when different SMT peak force magnitudes are used are likely related to the resulting vertebral motion as well as the specific function of the structures. These data suggest that by controlling SMT peak force magnitude, it is possible to change the loading characteristics experienced by spinal structures.

#### *8.2.2.3 Application site*

The SMT application site main effect was observed to significantly affect the loading characteristics of the intact specimen and PJ structures. In general, while the SMT application at L3/L4 FJ mainly influenced specific forces experienced by the spinal segment, SMT application at L4 TVP influenced the experienced moments. These differences in load distribution within spinal structures when SMT is applied at distinct application sites indicate that it is possible to change the spinal structures loading characteristics by altering the location in which SMT is applied.

#### ***8.2.3 Spinal manipulative therapy input parameters - Application site***

Similar to the above results, chapter 5 of the current dissertation demonstrated that the SMT application site significantly influenced the SMT load distribution within spinal structures. Furthermore, SMT application at adjacent spinal levels created specific forces and moments in opposite direction relatively to each other. While specific forces and moments experienced by the intact specimen and spinal structures significantly changed as a function of the SMT application site, in general, SMT application at FJs created greater extension moments and SMT application at

TVPs created greater torsion moments experienced by the intact specimen and specific spinal structures.

#### ***8.2.4 Spinal manipulative therapy input parameters - Method of SMT application***

The Chapter 6 of this dissertation demonstrated that the method in which SMT is applied influenced the loading characteristics of spinal structures and the distribution of SMT loads within the same spinal structures. While Activator created smaller forces and moments in the intact spinal segment, Manual SMT and SMT application with Motor mainly loaded PJ and IVD structures. Specifically, Manual SMT significantly influenced the overall moments experienced by PJ structures, whereas SMT application with Motor significantly affected the overall moments experienced by IVD structures. These differences are likely related to the difference in SMT force-time profile, including peak force magnitude, loading rate and contact surface area.

#### ***8.2.5 Spinal manipulative therapy and passive physiological movement load comparison***

The loading characteristics of the intact specimens and spinal structures during the application of a manual SMT were comparable to the ones created by passive physiological movements with the exception of specific forces and moments in particular axes. Specifically, manual SMT created significantly greater anterior posterior forces (forces along y-axis) in the intact specimen, superior inferior forces (forces along z-axis) in SL and PJ structures and extension moments (moments around x-axis) in PJ structures only. Given that all other forces and moments arising from SMT were comparable to those arising from physiological movements with the exception of those abovementioned forces and moments, it is possible that these exceptions are associated with the unique therapeutic effects elicited by SMT.

### 8.3 Pilot studies and measurement errors

Pilot testing was conducted in an additional porcine L3-L4 lumbar segment (not included in any of the experiments of the current dissertation) to verify how loading characteristics of intact specimens changed with repeated testing. Based on the loading responses to the repeated applied motion observed in this pilot testing, the measurement errors calculated were noticeably small and used for all experiments of this dissertation (Table 8.1). Importantly, all significant comparisons reported in this dissertation presented load differences above the calculated measurement errors.

<b>Table 8.1 Measurement errors calculated from pilot testing</b>			
	X	Y	Z
Peak Force	0.02	0.13	-0.009
Mean Force	0.08	0.41	-0.009
Peak Moment	0.12	0.004	-0.081
Mean Moment	0.17	0.000	-0.011

### 8.4 Synthesis of experimental data

#### *8.4.1 Principle of Superposition*

Previous biomechanical studies have assumed that the principle of superposition could be applied to biomechanical test of biological structures [24,178]. Nevertheless, the principle of superposition, by definition, is applied to linear systems, which is fundamentally different than biological structures that present non-linear and viscoelastic behavior. Given this fundamental distinction in system behavior, it is not appropriate to assume the application of the principle of superposition to biomechanical tests of biological structures. In support of this, Chapter 3 of the current dissertation demonstrated that the order in which structures are removed from the testing

object during a biomechanical test significantly influence the loading characteristics experienced by the structures.

#### ***8.4.2 Changing SMT input parameters can preferentially increase specific characteristics of spinal structure loading***

The experiments described throughout this dissertation analyzed the forces and moments experienced by spinal structures along and around all 3 axes of movement caused by SMT applications with varied characteristics. As a result, it was demonstrated, for the first time, that specific forces and moments experienced by particular spinal structures can be altered when unique combinations of SMT input parameters are used. As such, particular combinations of SMT input parameters were identified to preferentially target specific spinal structures. As an example, a manual SMT application with greater force magnitude (500N) created greater peak torsion moments in PJ structures while the same moment was preferentially greater in IVD structures when SMT was applied using the linear actuator motor with a 300N force magnitude.

Additionally, the experimental chapters of this dissertation (chapters 4-7) suggest that it possible to alter SMT input parameters not only to preferentially target specific spinal structures, but also to increase specific forces and moments. Specifically, the application of SMT with greater peak force magnitudes (300-524N) at the skin overlying FJs (in comparison to TVP) was observed to generally increase the anterior posterior forces in the intact specimen, superior-inferior forces in SL and PJ structures and extension moments in the PJ structures. Given that these specific loads were observed during manual SMT, and not during passive physiological movements, this



specific characteristic of SMT application (with greater peak force magnitude applied at FJ) may potentially optimize the therapeutic effects elicited by SMT.

#### ***8.4.3 Changing SMT input parameters alter specific spinal loads***

In addition to the possibility of altering SMT input parameters to preferentially target specific spinal structures and specific forces/moments, observations from chapters 4, 5 and 6 of this dissertation revealed that the forces and moments that were more frequently observed to change as a result of perturbing SMT input parameters were: torsion moments, extension moments and superior-inferior forces. More specifically, when changing SMT input parameters, torsion and extension moments created at the intact specimen were observed to be frequently influenced. With respect to individual spinal structures, superior inferior force responses and extension moment responses were also observed to be influenced most frequently by changes in SMT input parameters. Interestingly, superior-inferior forces and extension moments are two of the unique loading characteristics observed during SMT, but not during passive physiological movements. This suggests that SMT not only creates unique loading in spinal segments in comparison to passive physiological movements, but also that these unique loads are the ones that are most influenced by the characteristics of SMT (input parameters).

### **8.5 Implications**

Although this dissertation is comprised of basic biomechanical experiments using cadaveric porcine models, these novel findings provide implications for both biomechanical scientific research and SMT clinical practice.

### ***8.5.1 Implications for biomechanical scientific research***

#### *8.5.1.1 Biomechanical testing*

The study investigating the principle of superposition provided important implications for *in vitro* biomechanical investigations. In contrast to assumptions made to date by other investigators [24,164,178,181,270], this study demonstrated that the moments experienced by time-dependent, non-linear structures are dependent on the order in which they are removed from the testing object. These findings indicate that the mechanical function of spinal structures are cooperative and, as such, the removal of one structure will alter the loads experienced by the remaining structures and significantly affect their mechanical function. Importantly, this finding imposes a significant limitation on previous biomechanical studies as their results are now specific to the order in which spinal tissues were removed from the testing specimen. By using a different order of tissue removal, the results of biomechanical tests based on the combination of kinematic replication and sequential dissection will likely also be altered. Therefore, the determination of the mechanical contribution of specific spinal structures to particular motions becomes more complex as it changes not only with the movements that are being performed (both primary and associated coupled motions), but also with the order of structural removal.

#### *8.5.1.2 Underlying mechanism of SMT*

Contributing to the understanding of the underlying mechanisms of SMT, the current dissertation observed that PJ and IVD structures were the structures in which changes in forces and moments during SMT application were more frequently observed. For this reason, alterations in these structures (such as facet joint or intervertebral disc degeneration) may potentially reduce their

responses to mechanical stimuli limiting the physiological effects elicited by SMT. Indeed, the recent work from Wong (2015) [271] has observed that patients who did not respond to SMT intervention presented a higher frequency of more severe facet joint degeneration. This finding suggests a relation between the SMT therapeutic effects and the mechanical stimulus of facet joint structures. Interestingly, the current dissertation showed that among PJ and IVD structures, only PJ structures were observed to present unique loading characteristics during manual SMT application in comparison to passive physiological movements. Therefore, it is possible that PJ structures might be the main contributors to creating the therapeutic effects of SMT.

#### ***8.5.2 Implications for clinicians***

The spinal structure loading characteristics described in this dissertation can be used by clinicians to guide their choice of SMT input parameters that best fits with the treatment objectives. Based on individual clinical presentations, clinicians now have an foundation to design patient-specific SMT interventions and alter SMT input parameters of force magnitude, application site and method of SMT application to preferentially increase or reduce specific loads experienced by particular spinal structures. As an example, in the absence of specific pathological findings (e.g. spinal degeneration), a SMT application using a mechanical force manually assisted instrument with peak force magnitude of approximately 100 N could be used in patients presenting with facet joint pain as this specific SMT was observed to create smaller changes in superior inferior forces experienced by PJ structures. Alternatively, if an increase in anterior posterior forces in PJ structures is desired, a SMT application with greater force magnitude (500 N) at the skin overlying the space between FJs (Btw FJ) could be used.

On the other hand, for patients presenting intervertebral disc pain, a SMT application using the mechanical force manually assisted instrument at the skin overlying the FJ of the upper vertebra (relatively to the target spinal function unit) could be used as these characteristics were shown to create smaller peak extension moments in IVD structures. Alternatively, to increase peak superior inferior forces in IVD structures, a SMT using the linear actuator motor at the same location (skin overlying the FJ of the upper vertebral of the target spinal segment) could be applied.

## **8.6 Future research**

The findings described on Chapter 3 of this dissertation impose important limitations on previous biomechanical investigations combining kinematic replication with serial dissection, as previous findings are now specific to the order in which structures were removed from the testing specimen. Consequently, additional biomechanical studies quantifying the differences in forces and moments experienced by biological structures when different order of structure removal is used should be conducted. By quantifying the difference of loading characteristics with varied sequence of tissue removal, it may be potentially possible to estimate the loads experienced by each spinal tissue based on the structures that are intact/injured, contributing to the full elucidation of the mechanical contribution of each spinal structure.

While the experiments that comprise Chapters 4, 5 and 6 have pioneered the investigation of loading characteristics of spinal structures with different SMT input parameters, Chapter 7 conducted the first investigation comparing the forces and moments experienced by spinal structures during the SMT application with the ones experienced during passive physiological

movements. Therefore, the findings described in the current doctoral work can be used as an underlying foundation for future research investigating the underlying mechanisms of SMT. Specifically, the structural response of SL and PJ structures to the specific SMT loads could be investigated to delineate the link between SMT application, SMT input parameters and the physiological benefits elicited by SMT.

Based on the observation that unique loads observed during SMT may be responsible for SMT's therapeutic effects, the investigation of these specific loads on pathological spine models (e.g. models presenting induced facet joint degeneration and intervertebral disc degeneration) and the response of pathological spine structures may provide important evidence regarding the differential therapeutic mechanisms of SMT. Given that spinal degeneration alters the biomechanics of adjacent spinal segments [272] and that higher frequency of facet joint degeneration was observed in patients who did not respond to SMT [271], SMT load distribution within degenerated spinal structures may potentially differ from the ones observed in healthy spines and as a function of the degenerated spinal structure. Additionally, the elucidation of loading characteristics during SMT application having different input parameters could also provide additional empirical guidance for clinicians to tailor SMT characteristics to the individual presentation of patients with these clinical alterations and specifically avoid loads on the facet joints of patients presenting with facet joint osteoarthritis or on the intervertebral disc of patients with intervertebral disc degeneration.

This dissertation quantified the loading responses of spinal structures arising from SMT. This response varied with peak force magnitude, application site and method of SMT application.

Given the comparable SMT peak force magnitudes used in distinct experiments of this dissertation (chapters 4 and 6) and the unique loading characteristics observed in each of these experiments, additional SMT characteristics are likely important contributors to modulating spinal structure loading and should be investigated. Specifically, SMT loading rate may potentially influence not only the spinal tissues response given their viscoelastic behavior [266], but also the spinal mechanoreceptors that modulate the sensory input to the central nervous system. Therefore, by clarifying the influence of SMT loading rate on spinal structure loading and response could contribute to elucidating the underlying therapeutic mechanisms of SMT.

This dissertation provided important evidence regarding the influence of SMT input parameters on SMT loading distribution within spinal structures. Nevertheless, these experiments were conducted on porcine cadaveric models, which have been described to be suitable models for human spine investigation [93,95,146], but still present anatomical and biomechanical differences and consequent limitations. Therefore, the study of finite element models are invaluable to verify if similar results presented in the current dissertation could also be observed in validated spine models. One step further, investigations combining 3-dimensional motion capture system with robotic replication are also needed in cadaveric human spines including other SMT techniques frequently observed in the clinical treatment of low back pain, such as side-posture manipulation. In addition to providing evidence with reduced limitations by using human spines, elucidating the SMT load distribution within spinal structures during the application of SMT with distinct techniques may provide further empirical evidence to guide clinicians' choice on the SMT technique in addition to adjusting specific input parameters to tailor SMT application to each individual clinical presentation.

## **8.7 Conclusion**

The current doctoral work provides novel evidence on biomechanical testing and SMT load distribution within spinal structures. Biomechanically, it was demonstrated that for specimens presenting time-dependent, non-linear properties, the structural loading characteristics are specific to the order in which they were removed from the testing object. Additionally, targeting specific spinal structures may be possible by adjusting SMT input parameters as vertebral motion and spinal structure loading during SMT application were shown to be influenced by SMT input parameters of peak force magnitude, application site and method of SMT application. Finally, forces and moments created by manual SMT were shown to be comparable to those created during passive physiological movements. Spinal manipulative therapy has been demonstrated to present loading rates and created forces and moments within values below the established injury values. The unique loading profile created by SMT may be the mechanism that confers SMT's therapeutic effect in comparison to the loading created during daily activities. This work provides an important foundation for future investigations of SMT biomechanics and underlying therapeutic mechanisms.

## Bibliography

1. Balagué F, Mannion AF, Pellisé F, Cedraschi C. Non-specific low back pain. *Lancet*. 2012 Feb 4;379(9814):482–91.
2. Rubin DI. Epidemiology and Risk Factors for Spine Pain. *Neurol Clin*. 2007;25(2):353–71.
3. Gross DP, Ferrari R, Russell AS, Battié MC, Schopflocher D, Hu RW, et al. A population-based survey of back pain beliefs in Canada. *Spine (Phila Pa 1976)*. 2006;31(18):2142–5.
4. Hoy D, March L, Brooks P, Blyth F, Woolf A, Bain C, et al. The global burden of low back pain : estimates from the Global Burden of Disease 2010 study. *Ann Rheum Dis*. 2014;73:968–74.
5. Gore M, Sadosky A, Stacey BR, Tai K-S, Leslie D. The burden of chronic low back pain: clinical comorbidities, treatment patterns, and health care costs in usual care settings. *Spine (Phila Pa 1976)*. 2012 May 15;37(11):E668–77.
6. Katz J. Lumbar disc disorders and low back pain: socioeconomic factors and consequences. *J Bone Jt Surg Am*. 2006;88A(suppl 2):21–4.
7. Maniadakis N, Gray A. The economic burden of back pain in the UK. *Pain*. 2000;84(1):95–103.
8. Mehra M, Hill K, Nicholl D, Schadrack J. The burden of chronic low back pain with and without a neuropathic component: a healthcare resource use and cost analysis. *J Med Econ*. 2012 Jan;15(2):245–52.
9. Brown a, Angus D, Chen S, Tang Z, Milne S, Pfaff J, et al. Costs and outcomes of chiropractic treatment for low back pain [Technology report no 56]. *Health (San Francisco)*. 2005.
10. Dagenais S, Caro J, Haldeman S. A systematic review of low back pain cost of illness studies in the United States and internationally. *Spine J*. 2008;8(1):8–20.
11. Hoy D, Brooks P, Blyth F, Buchbinder R. The Epidemiology of low back pain. *Best Pract Res Clin Rheumatol*. Elsevier Ltd; 2010 Dec;24(6):769–81.



12. Willems P. Decision making in surgical treatment of chronic low back pain: the performance of prognostic tests to select patients for lumbar spinal fusion. *Acta Orthop Suppl.* 2013;84(349):1–35.
13. Saltychev M, Eskola M, Laimi K. Lumbar fusion compared with conservative treatment in patients with chronic low back pain: a meta-analysis. *Int J Rehabil Res.* 2014;37(1):2–8.
14. Chien JJ, Bajwa ZH. What is mechanical back pain and how best to treat it? *Curr Pain Headache Rep.* 2008 Dec;12(6):406–11.
15. Merepeza A. Effects of spinal manipulation versus therapeutic exercise on adults with chronic low back pain: a literature review. *J Can Chiropr Assoc.* 2014;58(4):456–66.
16. Hidalgo B, Detrembleur C, Hall T, Mahaudens P, Nielens H. The efficacy of manual therapy and exercise for different stages of non-specific low back pain: an update of systematic reviews. *J Man Manip Ther.* 2014;22(2):59–74.
17. Brumitt J, Matheson JW, Meira EP. Core stabilization exercise prescription, part 2: a systematic review of motor control and general (global) exercise rehabilitation approaches for patients with low back pain. *Sports Health.* 2013;5(6):510–3.
18. Chung J, Zeng Y, TK W. Drug therapy for the treatment of chronic nonspecific low back pain: systematic review and meta-analysis. *Pain Physician.* 2013;16(6):685–704.
19. Michaleff Z a., Lin CWC, Maher CG, van Tulder MW. Spinal manipulation epidemiology: Systematic review of cost effectiveness studies. *J Electromyogr Kinesiol.* Elsevier Ltd; 2012;22(5):655–62.
20. Herzog W, Conway P, Kawchuk G, Zhang Y-T, Hasler E. Forces exerted during spinal manipulative therapy. *Spine (Phila Pa 1976).* 1993;18(9):1206–12.
21. Herzog W. The biomechanics of spinal manipulation. *J Bodyw Mov Ther.* Elsevier Ltd; 2010 Jul;14(3):280–6.
22. Pickar JG, Bolton PS. Spinal manipulative therapy and somatosensory activation. *J Electromyogr Kinesiol.* Elsevier Ltd; 2012 Feb 19;22(5):785–94.

23. Kirstukas SJ, Backman J a. Physician-applied contact pressure and table force response during unilateral thoracic manipulation. *J Manipulative Physiol Ther.* 1999;22(5):269–79.
24. Kawchuk GN, Carrasco A, Beecher G, Goertzen D, Prasad N. Identification of spinal tissues loaded by manual therapy: a robot-based serial dissection technique applied in porcine motion segments. *Spine (Phila Pa 1976).* 2010 Oct 15;35(22):1983–90.
25. Triano JJ, McGregor M. Use of chiropractic manipulation in lumbar rehabilitation. *J Rehabil Res Dev.* 1997;34(4):394.
26. Carnes D, Mars TS, Mullinger B, Froud R, Underwood M. Adverse events and manual therapy: A systematic review. *Man Ther. Elsevier Ltd;* 2010;15(4):355–63.
27. Paanalahti K, Holm LW, Nordin M, Asker M, Lyander J, Skillgate E. Adverse events after manual therapy among patients seeking care for neck and/or back pain: a randomized controlled trial. *BMC Musculoskelet Disord. BMC Musculoskeletal Disorders;* 2014;15(1):77.
28. Nougrou F, Dugas C, Deslauriers C, Pagé I, Descarreaux M. Physiological responses to spinal manipulation therapy: investigation of the relationship between electromyographic responses and peak force. *J Manipulative Physiol Ther. National University of Health Sciences;* 2014;36(9):557–63.
29. Vaillant M, Edgecombe T, Long CR, Pickar JG, Kawchuk GN. The effect of duration and amplitude of spinal manipulative therapy (SMT) on spinal stiffness. *Man Ther. Elsevier Ltd;* 2012 Dec;17(6):577–83.
30. Cao D, Reed WR, Long CR, Kawchuk GN, Pickar JG. Effects of thrust amplitude and duration of high-velocity, low-amplitude spinal manipulation on lumbar muscle spindle responses to vertebra position and movement. *J Manipulative Physiol Ther.* 2013;36:68–77.
31. Reed W, Cao D, Long C, Kawchuk GN, Pickar JG. Relationship between biomechanical characteristics of spinal manipulation and neural responses in an animal model: effect of linear control of thrust displacement. *Evid Based Complement Alternat Med.* 2013;2013.
32. Colloca CJ, Keller TS, Harrison DE, Moore RJ, Gunzburg R, Harrison DD. Spinal manipulation force and duration affect vertebral movement and neuromuscular responses. *Clin Biomech (Bristol, Avon).* 2006 Mar;21(3):254–62.

33. Keller TS, Colloca CJ, Moore RJ, Gunzburg R, Harrison DE, Harrison DD. Three-dimensional vertebral motions produced by mechanical force spinal manipulation. *J Manipulative Physiol Ther.* 2006;29(6):425–36.
34. Reed WR, Pickar JG, Sozio RS, Long CR. Effect of spinal manipulation thrust magnitude on trunk mechanical activation thresholds of lateral thalamic neurons. *J Manipulative Physiol Ther.* National University of Health Sciences; 2014;37(5):277–86.
35. Forand D, Drover J, Z S, Symons B, Herzog W. The forces applied by female and male chiropractors during thoracic spinal manipulation. *J Manipulative Physiol Ther.* 2004;27:49–56.
36. Kawchuk GN, Prasad NG, McLeod RC, Liddle T, Li T, Zhu Q. Variability of force magnitude and force duration in manual and instrument-based manipulation techniques. *J Manipulative Physiol Ther.* 2006 Oct;29(8):611–8.
37. Fuhr AW, Menke JM. Activator Methods Chiropractic Technique. 2003;9(3):30–43.
38. Fuhr AW, Menke JM. Status of activator methods chiropractic technique, theory, and practice. *J Manipulative Physiol Ther.* 2005 Feb;28(2):e1–20.
39. Descarreaux M, Nougrou F, Dugas C. Standardization of spinal manipulation therapy in humans: development of a novel device designed to measure dose-response. *J Manipulative Physiol Ther.* 2013 Feb;36(2):78–83.
40. Kilby J, Heneghan NR, Maybury M. Manual palpation of lumbo-pelvic landmarks: a validity study. *Man Ther.* Elsevier Ltd; 2012 Jun;17(3):259–62.
41. Harlick JC, Milosavljevic S, Milburn PD. Palpation identification of spinous processes in the lumbar spine. *Man Ther.* 2007 Feb;12(1):56–62.
42. Kim HW, Ko YJ, Rhee WI, Lee JS, Lim JE, Lee SJ, et al. Interexaminer Reliability and Accuracy of Posterior Superior Iliac Spine and Iliac Crest Palpation for Spinal Level Estimations. *J Manipulative Physiol Ther.* 2007;30(5):386–9.
43. Merz O, Wolf U, Robert M, Gesing V, Rominger M. Validity of palpation techniques for the identification of the spinous process L5. *Man Ther.* 2013 Aug;18(4):333–8.
44. Reed WR, Long CR, Kawchuk GN, Pickar JG. Neural responses to the mechanical

- parameters of a high-velocity, low-amplitude spinal manipulation: Effect of specific contact site. *Man Ther.* Elsevier Ltd; 2015;1–8.
45. Edgecombe TL, Kawchuk GN, Long CR, Pickar JG. The effect of application site of spinal manipulative therapy (SMT) on spinal stiffness. *Spine J.* Elsevier Inc; 2013;
  46. Keller TS, Colloca CJ, Gunzburg R, Keller TS, Gunzburg R. Neuromechanical characterization of in vivo lumbar spinal manipulation. Part II. Neurophysiological response. *J Manipulative Physiol Ther.* 2003;26(9):567–78.
  47. Colloca CJ, Keller TS, Gunzburg R. Biomechanical and neurophysiological responses to spinal manipulation in patients with lumbar radiculopathy. *J Manipulative Physiol Ther.* 2004 Jan;27(1):1–15.
  48. Herzog W, Scheele D, Conway P. Electromyographic responses of back and limb muscles associated with spinal manipulative therapy. *Spine (Phila Pa 1976).* 1999;24(2):146–53.
  49. Colloca CJ, Keller TS. Electromyographic Reflex Responses to Mechanical Force, Manually Assisted Spinal Manipulative Therapy. *Spine (Phila Pa 1976).* 2001 May;26(10):1117–24.
  50. Bible JE, Biswas D, Miller CP, Whang PG, Grauer JN. Normal functional range of motion of the lumbar spine during 15 activities of daily living. *J Spinal Disord Tech.* 2010 Apr;23(2):106–12.
  51. Rohlmann a, Zander T, Rao M, Bergmann G. Realistic loading conditions for upper body bending. *J Biomech.* 2009 May 11;42(7):884–90.
  52. Dreischarf M, Rohlmann A, Bergmann G, Zander T. Optimised loads for the simulation of axial rotation in the lumbar spine. *J Biomech.* Elsevier; 2011;44(12):2323–7.
  53. Sousa V, Claro JCP. Simplified multibody model for dynamic loading analysis of the lumbar human spine. 2015;(February):26–8.
  54. Rohlmann A, Consmüller T, Dreischarf M, Bashkuev M, Disch A, Pries E, et al. Measurement of the number of lumbar spinal movements in the sagittal plane in a 24-hour period. *Eur Spine J.* 2014;23(11):2375–84.
  55. Bakker EWP, Verhagen AP, Lucas C, Koning HJCMF, De Haan RJ, Koes BW. Daily

- spinal mechanical loading as a risk factor for acute non-specific low back pain: A case-control study using the 24-Hour Schedule. *Eur Spine J.* 2007;16(1):107–13.
56. Pagé I, Nougrou F, Dugas C, Descarreau. The effect of spinal manipulation impulse duration on spine neuromechanical responses. 2014;3194(2):141–8.
  57. Nougrou F, Dugas C, Loranger M, Pagé I, Descarreaux M. The role of preload forces in spinal manipulation: experimental investigation of kinematic and electromyographic responses in healthy adults. *J Manipulative Physiol Ther.* National University of Health Sciences; 2014 Jun;37(5):287–93.
  58. Krismer M, van Tulder M. Low back pain (non-specific). *Best Pract Res Clin Rheumatol.* 2007;21(1):77–91.
  59. Vos T, Flaxman AD, Naghavi M, Lozano R, Michaud C, Ezzati M, et al. Years lived with disability ( YLDs ) for 1160 sequelae of 289 diseases and injuries 1990 – 2010 : a systematic analysis for the Global Burden of Disease Study 2010. *Lancet.* 2012;380:2163–96.
  60. Murray CJL, Lopez AD. Measuring the global burden of disease. *N Engl J Med.* 2013 Aug 1;369(5):448–57.
  61. Lim SS, Vos T, Flaxman AD, Danaei G, Shibuya K, Adair-Rohani H, et al. A comparative risk assessment of burden of disease and injury attributable to 67 risk factors and risk factor clusters in 21 regions, 1990-2010: a systematic analysis for the Global Burden of Disease Study 2010. *Lancet.* 2012 Dec 15;380(9859):2224–60.
  62. Hong J, Reed C, Novick D, Happich M. Costs associated with treatment of chronic low back pain: an analysis of the UK General Practice Research Database. *Spine (Phila Pa 1976).* 2013 Jan 1;38(1):75–82.
  63. Ekman M, Jo S, Hunsche E, Jo L. Burden of Illness of Chronic Low Back Pain in Sweden A Cross-Sectional , Retrospective Study in Primary Care Setting. 2005;30(15):1777–85.
  64. Deyo RA, Weinstein JN. Low Back Pain. *N Engl J Med.* 2001;344(5):363–70.
  65. Cuesta-Vargas A, Farasyn A, Gabel CP, Luciano J V. The mechanical and inflammatory low back pain (MIL) index: development and validation. *BMC Musculoskelet Disord.* 2014;15(1):12.

66. Maraschin R, Vieira PS, Leguisamo CP, Dal’Vesco F, Santi JP. Dor lombar crônica e dor nos membros inferiores em idosos: etiologia em revisão. *Fisioter em Mov.* 2010 Dec;23(4):627–39.
67. Coenen P, Kingma I, Boot CRL, Bongers PM, van Dieën JH. Cumulative mechanical low-back load at work is a determinant of low-back pain. *Occup Environ Med.* 2014 May;71(5):332–7.
68. Coenen P, Kingma I, Boot CRL, Twisk JWR, Bongers PM, van Dieën JH. Cumulative low back load at work as a risk factor of low back pain: a prospective cohort study. *J Occup Rehabil.* 2013 Mar;23(1):11–8.
69. Busscher I, van Dieën JH, Kingma I, van der Veen AJ, Verkerke GJ, Veldhuizen AG. Biomechanical characteristics of different regions of the human spine: an in vitro study on multilevel spinal segments. *Spine (Phila Pa 1976).* 2009 Dec 15;34(26):2858–64.
70. Niemeyer F, Wilke H-J, Schmidt H. Geometry strongly influences the response of numerical models of the lumbar spine--a probabilistic finite element analysis. *J Biomech.* Elsevier; 2012 May 11;45(8):1414–23.
71. Adams M a, Hutton WC. The mechanical function of the lumbar apophyseal joints. *Spine.* 1983. p. 327–30.
72. Adams M a, Dolan P. Spine biomechanics. *J Biomech.* 2005 Oct;38(10):1972–83.
73. Adams M a, Bogduk N, Burton K, Dolan P. The biomechanics of back pain. 3rd ed. Elsevier Churchill Livingstone; 2013.
74. Okushima Y, Yamazaki N, Matsumoto M, Chiba K, Nagura T, Toyama Y. Lateral translation of the lumbar spine: In vitro biomechanical study. *J Appl Biomech.* 2006;22(2):83–92.
75. Sharma M, Langrana N a, Rodriguez J. Role of ligaments and facets in lumbar spinal stability. *Spine.* 1995. p. 887–900.
76. Schendel MJ, Wood KB, Buttermann GR, Lewis JJ, Ogilvie JW. Experimental measurement of ligament force, facet force, and segment motion in the human lumbar spine. *J Biomech.* 1993 Apr;26(4-5):427–38.

77. Adams M a, McNally DS, Dolan P. “Stress” distributions inside intervertebral discs. The effects of age and degeneration. *J Bone Joint Surg Br.* 1996;78(6):965–72.
78. Cannella M, Arthur A, Allen S, Keane M, Joshi A, Vresilovic E, et al. The role of the nucleus pulposus in neutral zone human lumbar intervertebral disc mechanics. *J Biomech.* 2008;41(10):2104–11.
79. Hukins D, Kirby M, Sikoryn T, Aspden R, Cox A. Comparison of structure, mechanical properties and functions of lumbar spinal ligaments. *Spine (Phila Pa 1976).* 1990;15(8):787–95.
80. Hindle RJ, Pearcy MJ, Cross a. Mechanical function the human lumbar interspinous and supraspinous ligaments. *J Biomed Eng.* 1990;12:340–4.
81. Chazal J, Tanguy a., Bourges M, Gaurel G, Escande G, Guillot M, et al. Biomechanical properties of spinal ligaments and a histological study of the supraspinal ligament in traction. *J Biomech.* 1985;18(3):167–76.
82. Kilinçer C, Inceoğlu S, Sohn MJ, Ferrara L a., Bakirci N, Benzel EC. Load sharing within a human thoracic vertebral body: An in vitro biomechanical study. *Turk Neurosurg.* 2007;17(3):167–77.
83. Pollintine P, Dolan P, Tobias JH, Adams M a. Intervertebral disc degeneration can lead to “stress-shielding” of the anterior vertebral body: a cause of osteoporotic vertebral fracture? *Spine (Phila Pa 1976).* 2004 Apr 1;29(7):774–82.
84. Adams M a, Pollintine P, Tobias JH, Wakley GK, Dolan P. Intervertebral disc degeneration can predispose to anterior vertebral fractures in the thoracolumbar spine. *J Bone Miner Res.* 2006;21(9):1409–16.
85. Ryan G, Pandit A, Apatsidis D. Stress distribution in the intervertebral disc correlates with strength distribution in subdiscal trabecular bone in the porcine lumbar spine. *Clin Biomech (Bristol, Avon).* 2008 Aug;23(7):859–69.
86. Alapan Y, Sezer S, Demir C, Kaner T, Inceoğlu S. Load sharing in lumbar spinal segment as a function of location of center of rotation. *J Neurosurg Spine.* 2014;20(5):542–9.
87. Cholewicki J, Crisco JJ, Oxland TR, Yamamoto I, Panjabi MM. Effects of posture and

- structure on three-dimensional coupled rotations in the lumbar spine A biomechanical analysis. *Spine (Phila Pa 1976)*. 1996;21(21):2421–8.
88. Li G, Wang S, Passias P, Xia Q, Li G, Wood K. Segmental in vivo vertebral motion during functional human lumbar spine activities. *Eur Spine J*. 2009 Jul;18(7):1013–21.
  89. Passias PG, Wang S, Kozanek M, Xia Q, Li W, Grottkau B, et al. Segmental lumbar rotation in patients with discogenic low back pain during functional weight-bearing activities. *J Bone Joint Surg Am*. 2011 Jan 5;93(1):29–37.
  90. Izzo R, Guarnieri G, Guglielmi G, Muto M. Biomechanics of the spine. Part I: Spinal stability. *Eur J Radiol*. Elsevier Ireland Ltd; 2013;82(1):118–26.
  91. Heuer F, Schmidt H, Claes L, Wilke HJ. Stepwise reduction of functional spinal structures increase vertebral translation and intradiscal pressure. *J Biomech*. 2007;40:795–803.
  92. Freudiger S, Dubois G, Lorrain M. Dynamic neutralisation of the lumbar spine confirmed on a new lumbar spine simulator in vitro. *Arch Orthop Trauma Surg*. 1999;119(3-4):127–32.
  93. Busscher I, van der Veen AJ, van Dieën JH, Kingma I, Verkerke GJ, Veldhuizen AG. In vitro biomechanical characteristics of the spine: a comparison between human and porcine spinal segments. *Spine (Phila Pa 1976)*. 2010 Jan 15;35(2):E35–42.
  94. Xia Q, Wang S, Passias PG, Kozanek M, Li G, Grottkau BE, et al. In vivo range of motion of the lumbar spinous processes. *Eur Spine J*. 2009 Sep;18(9):1355–62.
  95. Wilke H-J, Geppert J, Kienle A. Biomechanical in vitro evaluation of the complete porcine spine in comparison with data of the human spine. *Eur Spine J*. 2011 Nov;20(11):1859–68.
  96. Kozanek M, Wang S, Passias PG, Xia Q, Li G, Bono CM, et al. Range of motion and orientation of the lumbar facet joints in vivo. *Spine (Phila Pa 1976)*. 2009 Sep 1;34(19):E689–96.
  97. Heuer F, Schmidt H, Klezl Z, Claes L, Wilke H-J. Stepwise reduction of functional spinal structures increase range of motion and change lordosis angle. *J Biomech*. 2007 Jan;40(2):271–80.



98. Bisschop A, Kingma I, Bleys RL a W, Paul CPL, van der Veen AJ, van Royen BJ, et al. Effects of repetitive movement on range of motion and stiffness around the neutral orientation of the human lumbar spine. *J Biomech*. 2013;46:187–91.
99. Rubinstein SM, van Middelkoop M, Assendelft WJJ, de Boer MR, van Tulder MW. Spinal manipulative therapy for chronic low-back pain: an update of a Cochrane review. *Spine (Phila Pa 1976)*. 2011 Jun;36(13):E825–46.
100. Roelofs PDDM, Deyo R a, Koes BW, Scholten RJPM, van Tulder MW. Nonsteroidal anti-inflammatory drugs for low back pain: an updated Cochrane review. *Spine (Phila Pa 1976)*. 2008;33(16):1766–74.
101. Ferreira ML, Ferreira PH, Latimer J, Herbert RD, Hodges PW, Jennings MD, et al. Comparison of general exercise, motor control exercise and spinal manipulative therapy for chronic low back pain: A randomized trial. *Pain*. 2007;131(1-2):31–7.
102. Hurwitz EL. Epidemiology: Spinal manipulation utilization. *J Electromyogr Kinesiol*. Elsevier Ltd; 2012 Jan 29;1–7.
103. Hurwitz EL, Coulter ID, Adams a H, Genovese BJ, Shekelle PG. Use of chiropractic services from 1985 through 1991 in the United States and Canada. *Am J Public Heal*. 1998;88(5):771–6.
104. Triano JJ. Biomechanics of spinal manipulative therapy. *Spine J*. 2001;1(2):121–30.
105. Goldby LJ, Moore AP, Doust J, Trew ME. A randomized controlled trial investigating the efficiency of musculoskeletal physiotherapy on chronic low back disorder. *Spine (Phila Pa 1976)*. 2006;31(10):1083–93.
106. Schneider M, Haas M, Glick R, Stevans J, Landsittel D. Comparison of Spinal Manipulation Methods and Usual Medical Care for Acute and Subacute Low Back Pain. *Spine (Phila Pa 1976)*. 2015;40(4):209–17.
107. Vieira-Pellenz F, Oliva-Pascual-Vaca Á, Rodriguez-Blanco C, Heredia-Rizo AM, Ricard F, Almazán-Campos G. Short-Term Effect of Spinal Manipulation on Pain Perception, Spinal Mobility, and Full Height Recovery in Male Subjects With Degenerative Disk Disease: A Randomized Controlled Trial. *Arch Phys Med Rehabil*. 2014;
108. Jüni P, Battaglia M, Nüesch E, Hämmerle G, Eser P, van Beers R, et al. A randomised

- controlled trial of spinal manipulative therapy in acute low back pain. *Ann Rheum Dis*. 2009;68(9):1420–7.
109. Rasmussen J, Lætgaard J, Lindecrona AL, Qvistgaard E, Bliddal H. Manipulation does not add to the effect of extension exercises in chronic low-back pain (LBP). A randomized, controlled, double blind study. *Jt Bone Spine*. Elsevier Masson SAS; 2008;75(6):708–13.
  110. Licciardone JC, Stoll ST, Fulda KG, Russo DP, Siu J, Winn W, et al. Osteopathic Manipulative Treatment for Chronic Low. *Spine J*. 2003;28(13):1355–62.
  111. Wong AY, Parent EC, Dhillon SS, Prasad N, Kawchuk GN. Do participants with low back pain who respond to spinal manipulative therapy differ biomechanically from non-responders, untreated or asymptomatic controls? *Spine*. 2015. 1 p.
  112. Pickar JG. Neurophysiological effects of spinal manipulation. *Spine J*. 2002;2(5):357–71.
  113. Maigne J-Y, Vautravers P. Mechanism of action of spinal manipulative therapy. *Jt Bone Spine*. 2003 Sep;70(5):336–41.
  114. Descarreaux M, Dugas C, Lalanne K, Vincelle M, Normand MC. Learning spinal manipulation: The importance of augmented feedback relating to various kinetic parameters. *Spine J*. 2006;6(2):138–45.
  115. Dewitte V, Cagnie B, Barbe T, Beernaert A, Vanthillo B, Danneels L. Articular dysfunction patterns in patients with mechanical low back pain: {A} clinical algorithm to guide specific mobilization and manipulation techniques. *Man Ther*. Elsevier Ltd; 2015;20(3):499–502.
  116. Evans DW. Why do spinal manipulation techniques take the form they do? Towards a general model of spinal manipulation. *Man Ther*. Elsevier Ltd; 2010 Jun;15(3):212–9.
  117. Triano JJ, Bougie J, Rogers C, Scaringe J, Sorrels K, Skogsbergh D, et al. Procedural skills in spinal manipulation: Do prerequisites matter? *Spine J*. 2004;4(5):557–63.
  118. Descarreaux M, Dugas C. Learning Spinal Manipulation Skills: Assessment of Biomechanical Parameters in a 5-Year Longitudinal Study. *J Manipulative Physiol Ther*. National University of Health Sciences; 2010;33(3):226–30.

119. Cleland J a, Fritz JM, Childs JD, Kulig K. Comparison of the effectiveness of three manual physical therapy techniques in a subgroup of patients with low back pain who satisfy a clinical prediction rule: study protocol of a randomized clinical trial [NCT00257998]. *BMC Musculoskelet Disord*. 2006 Jan;7:11.
120. Cleland J a, Fritz JM, Kulig K, Davenport TE, Eberhart S, Magel J, et al. Comparison of the effectiveness of three manual physical therapy techniques in a subgroup of patients with low back pain who satisfy a clinical prediction rule: a randomized clinical trial. *Spine (Phila Pa 1976)*. 2009 Dec 1;34(25):2720–9.
121. Cramer GD, Tuck NR, Knudsen JT, Fonda SD, Schliesser JS, Fournier JT, et al. Effects of side-posture positioning and side-posture adjusting on the lumbar zygapophysial joints as evaluated by magnetic resonance imaging: a before and after study with randomization. *J Manipulative Physiol Ther*. 2000;23(6):380–94.
122. Gudavalli MR. Instantaneous rate of loading during manual high-velocity, low-amplitude spinal manipulations. *J Manipulative Physiol Ther*. National University of Health Sciences; 2014;37(5):294–9.
123. Cramer GD, Ross K, Pocius J, Cantu J a, Lupton E, Fergus M, et al. Evaluating the relationship among cavitation, zygapophyseal joint gapping, and spinal manipulation: an exploratory case series. *J Manipulative Physiol Ther*. 2011 Jan;34(1):2–14.
124. Cramer GD, Cambron J, Cantu J a., Dexheimer JM, Pocius JD, Gregerson D, et al. Magnetic Resonance Imaging Zygapophyseal Joint Space Changes (Gapping) in Low Back Pain Patients Following Spinal Manipulation and Side-Posture Positioning: A Randomized Controlled Mechanisms Trial With Blinding. *J Manipulative Physiol Ther*. National University of Health Sciences; 2013;36(4):203–17.
125. Keller TS, Colloca CJ, Gunzburg R, Keller TS, Gunzburg R. Neuromechanical characterization of in vivo lumbar spinal manipulation. Part I. Vertebral motion. *J Manipulative Physiol Ther*. 2003;26(9):567–78.
126. Gal J, Herzog W, Kawchuk GN, Conway P, Zhang Y-T. Biomechanical studies of spinal manipulative therapy (SMT): quantifying movement of vertebral bodies during SMT. *J CCA*. 1994;38(1):11–24.
127. Keller TS, Colloca CJ, Moore RJ, Gunzburg R, Harrison DE. Increased multi-axial lumbar motion responses during multiple-impulse mechanical force manually assisted spinal manipulation. *Chiropr Osteopat*. 2006 Jan;14:6.

128. Maigne JY, Guillon F. Highlighting of intervertebral movements and variations of intradiskal pressure during lumbar spine manipulation: a feasibility study. *J Manipulative Physiol Ther.* 2000 Oct;23(8):531–5.
129. Lisi AJ, O'Neill CW, Lindsey DP, Cooperstein R, Cooperstein E, Zucherman JF. Measurement of in vivo lumbar intervertebral disc pressure during spinal manipulation: a feasibility study. *J Appl Biomech.* 2006 Aug;22(3):234–9.
130. Beattie PF, Butts R, Donley JW, Liuzzo DM. The Within-Session Change in Low Back Pain Intensity Following Spinal Manipulative Therapy Is Related to Differences in Diffusion of Water in the Intervertebral Discs of the Upper Lumbar Spine and L5-S1. *J Orthop Sport Phys Ther.* 2014;44(1):19–29.
131. Fritz JM, Koppenhaver SL, Kawchuk GN, Teyhen DS, Hebert JJ, Childs JD. Preliminary Investigation of the Mechanisms Underlying the Effects of Manipulation. *Spine (Phila Pa 1976).* 2011;36(21):1772–81.
132. Pickar JG, Wheeler JD. Response of muscle proprioceptors to spinal manipulative-like loads in the anesthetized cat. *J Manipulative Physiol Ther.* 2001 Jan;24(1):2–11.
133. Pickar JG, Kang Y-M. Paraspinal muscle spindle responses to the duration of a spinal manipulation under force control. *J Manipulative Physiol Ther.* 2006 Jan;29(1):22–31.
134. Dishman JD, Burke J. Spinal reflex excitability changes after cervical and lumbar spinal manipulation: a comparative study. *Spine J.* 2003;3(3):204–12.
135. Herzog W, Conway P, Zhang Y-T, Gal J, Guimaraes A. Reflex responses associated with manipulative treatments on the thoracic spine: a pilot study. *J Manipulative Physiol Ther.* 1995;18(4):233–6.
136. Dishman JD, Dougherty PE, Burke JR. Evaluation of the effect of postural perturbation on motoneuronal activity following various methods of lumbar spinal manipulation. *Spine J.* 2005;5(6):650–9.
137. Indahl A, Kaigle A, Reikeras O, Holm S. Interaction Between the Porcine Lumbar Intervertebral Disc, zygapophysial joints, and paraspinal muscles. *Spine (Phila Pa 1976).* 1997;22(24):2834–940.
138. Pickar JG, McLain RF. Responses of mechanosensitive afferents to manipulation of the

- lumbar facet in the cat. *Spine*. 1995. p. 2379–85.
139. Pickar JG, Sung PS, Kang Y-M, Ge W. Response of lumbar paraspinal muscles spindles is greater to spinal manipulative loading compared with slower loading under length control. *Spine J*. 2007;7(5):583–95.
  140. Sung PS, Kang Y-M, Pickar JG. Effect of spinal manipulation duration on low threshold mechanoreceptors in lumbar paraspinal muscles: a preliminary report. *Spine (Phila Pa 1976)*. 2005 Jan 1;30(1):115–22.
  141. Reed WR, Long CR, Kawchuk GN, Pickar JG. Neural responses to the mechanical parameters of a high-velocity, low-amplitude spinal manipulation: Effect of preload parameters. *J Manipulative Physiol Ther*. National University of Health Sciences; 2014;37(2):68–78.
  142. Herzog W, Kats M, Symons B. The effective forces transmitted by high-speed, low-amplitude thoracic manipulation. *Spine (Phila Pa 1976)*. 2001 Oct 1;26(19):2105–10; discussion 2110–1.
  143. Gal J, Herzog W, Kawchuk G, Conway P, Zhang Y-T. Measurements of vertebral translations using bone pins, surface markers and accelerometers. *Clin Biomech (Bristol, Avon)*. 1997 Jul;12(5):337–40.
  144. Gudavalli MR, Devocht J, Tayh A, Xia T. Effect of sampling rates on the quantification of forces, durations, and rates of loading of simulated side posture high-velocity, low-amplitude lumbar spine manipulation. *J Manipulative Physiol Ther*. National University of Health Sciences; 2013;36(5):261–6.
  145. Ianuzzi A, Khalsa PS. High loading rate during spinal manipulation produces unique facet joint capsule strain patterns compared with axial rotations. *J Manipulative Physiol Ther*. 2005;28(9):673–87.
  146. Sheng S-R, Wang X-Y, Xu H-Z, Zhu G-Q, Zhou Y-F. Anatomy of large animal spines and its comparison to the human spine: a systematic review. *Eur Spine J*. 2010 Jan;19(1):46–56.
  147. Maher TR, O'Brien M, Dryer JW, Nucci R, Zipnick R, Leone DJ. The role of the lumbar facet joints in spinal stability. Identification of alternative paths of loading. *Spine (Phila Pa 1976)*. 1994;19(23):2667–71.

148. Gardner-Morse MG, Stokes I a. F. Structural behavior of human lumbar spinal motion segments. *J Biomech.* 2004 Feb;37(2):205–12.
149. Smit TH. The use of a quadruped as an in vivo model for the study of the spine - biomechanical considerations. *Eur Spine J.* 2002 Apr;11(2):137–44.
150. McLain RF, Yerby S a, Moseley T a. Comparative morphometry of L4 vertebrae: comparison of large animal models for the human lumbar spine. *Spine (Phila Pa 1976).* 2002 Apr 15;27(8):E200–6.
151. Bakkum BW, Henderson CNR, Hong S-P, Cramer GD. Preliminary morphological evidence that vertebral hypomobility induces synaptic plasticity in the spinal cord. *J Manipulative Physiol Ther.* 2007 Jun;30(5):336–42.
152. Henderson CNR, Cramer GD, Zhang Q, DeVocht JW, Fournier JT. Introducing the external link model for studying spine fixation and misalignment: part 1--need, rationale, and applications. *J Manipulative Physiol Ther.* 2007 May;30(3):279–94.
153. Ianuzzi A, Pickar JG, Khalsa PS. Validation of the cat as a model for the human lumbar spine during simulated high-velocity, low-amplitude spinal manipulation. *J Biomech Eng.* 2010 Jul;132(7):071008.
154. Cramer GD, Henderson CNR, Little JW, Daley C, Grieve TJ. Zygapophyseal joint adhesions after induced hypomobility. *J Manipulative Physiol Ther.* National University of Health Sciences; 2010 Sep;33(7):508–18.
155. Ge W, Long CR, Pickar JG. Vertebral position alters paraspinal muscle spindle responsiveness in the feline spine: effect of positioning duration. *J Physiol.* 2005 Dec 1;569(Pt 2):655–65.
156. Cotterill PC, Kostuik JP, D'Angelo G, Fernie GR, Maki BE. An anatomical comparison of the human and bovine thoracolumbar spine. *J Orthop Res.* 1986 Jan;4(3):298–303.
157. Wilke HJ, Kettler a, Wenger KH, Claes LE. Anatomy of the sheep spine and its comparison to the human spine. *Anat Rec.* 1997 Apr;247(4):542–55.
158. Kumar N, Kukreti S, Ishaque M, Mulholland R. Anatomy of deer spine and its comparison to the human spine. *Anat Rec.* 2000 Oct 1;260(2):189–203.

159. Busscher I, Ploegmakers JJW, Verkerke GJ, Veldhuizen AG. Comparative anatomical dimensions of the complete human and porcine spine. *Eur Spine J*. 2010 Jul;19(7):1104–14.
160. Dath R, Ebinesan a D, Porter KM, Miles a W. Anatomical measurements of porcine lumbar vertebrae. *Clin Biomech (Bristol, Avon)*. 2007 Jun;22(5):607–13.
161. Wilke HJ, Krischak S, Claes L. Biomechanical comparison of calf and human spines. *J Orthop Res*. 1996 May;14(3):500–3.
162. Kumar N, Kukreti S, Ishaque M, Sengupta DK, Mulholland RC. Functional Anatomy of the Deer Spine : An Appropriate Biomechanical Model for the Human Spine ? 2002;117(June 2000):108–17.
163. Fujie H, Livesay G a, Woo SL, Kashiwaguchi S, Blomstrom G. The use of a universal force-moment sensor to determine in-situ forces in ligaments: a new methodology. *J Biomech Eng*. 1995 Feb;117(1):1–7.
164. Livesay G a, Fujie H, Kashiwaguchi S, Morrow D a, Fu FH, Woo SL. Determination of the in situ forces and force distribution within the human anterior cruciate ligament. *Ann Biomed Eng*. 1995;23(4):467–74.
165. Fujie H, Mabuchi K, Woo SL, Livesay G a, Arai S, Tsukamoto Y. The use of robotics technology to study human joint kinematics: a new methodology. *J Biomech Eng*. 1993 Aug;115(3):211–7.
166. Woo SL, Debski RE, Wong EK, Yagi M, Tarinelli D. Use of Robotic Technology for Diathrodial Join Research. *J Sci Med Sport*. 1999;2(4):283–97.
167. Gilbertson LG, Doehring TC, Kang JD. New methods to study lumbar spine biomechanics: delineation of in vitro load-displacement characteristics by using a robotic?UFS testing system with hybrid control. *Oper Tech Orthop*. 2000;10(4):246–53.
168. Adams M a. Mechanical testing of the spine An appraisal of methodology, results, and conclusions. *Spine (Phila Pa 1976)*. 1995;20(19):2151–6.
169. Yingling VR, McGill SM. Anterior shear of spinal motion segments. Kinematics, kinetics, and resultant injuries observed in a porcine model. *Spine (Phila Pa 1976)*. 1999;24(18):1882–9.

170. Lee RY, Evans JH. The role of spinal tissues in resisting posteroanterior forces applied to the lumbar spine. *J Manipulative Physiol Ther.* 2000 Oct;23(8):551–6.
171. Crawford NR, Brantley AG, Dickman CA, Koeneman EJ. An apparatus for applying pure nonconstraining movements to spine segments. *Spine (Phila Pa 1976).* 1995;20(19):2097–100.
172. Yingling VR, McGill SM. mechanical properties and failure mechanics of the spine under posterior shear load. Observations from a porcine model. *J Spinal Disord.* 1999;12(6):501–8.
173. van Dieën JH, van der Veen A, van Royen BJ, Kingma I. Fatigue failure in shear loading of porcine lumbar spine segments. *Spine (Phila Pa 1976).* 2006 Jul 1;31(15):E494–8.
174. Lu WW, Luk KDK, Holmes AD, Cheung KMC, Leong JCY. Pure shear properties of lumbar spinal joints and the effect of tissue sectioning on load sharing. *Spine (Phila Pa 1976).* 2005 Apr 15;30(8):E204–9.
175. Tang J a, Scheer JK, Ames CP, Buckley JM. Pure moment testing for spinal biomechanics applications: fixed versus 3D floating ring cable-driven test designs. *J Biomech. Elsevier;* 2012 Mar 23;45(4):706–10.
176. Walker MR, Dickey JP. New methodology for multi-dimensional spinal joint testing with a parallel robot. *Med Biol Eng Comput.* 2007 Mar;45(3):297–304.
177. Dickey JP, Gillespie K a. Representation of passive spinal element contributions to in vitro flexion–extension using a polynomial model: illustration using the porcine lumbar spine. *J Biomech.* 2003 Jun;36(6):883–8.
178. Gillespie K a, Dickey JP. Biomechanical role of lumbar spine ligaments in flexion and extension: determination using a parallel linkage robot and a porcine model. *Spine (Phila Pa 1976).* 2004 Jun 1;29(11):1208–16.
179. Goel VK, Wilder DG, Pope MH, Edwards WT. Controversy biomechanical testing of the spine. Load control Vs displacement control. *Spine (Phila Pa 1976).* 1995;20(21):2354–7.
180. Tian L, Gilbertson LG. The study of control methods for the robotic testing system for human musculoskeletal joints. *Comput Methods Programs Biomed.* 2004 Jun;74(3):211–



181. Bell KM, Hartman R a., Gilbertson LG, Kang JD. In vitro spine testing using a robot-based testing system: Comparison of displacement control and “hybrid control.” J Biomech. Elsevier; 2013;46(10):1663–9.
182. Kelly BP, Bennett CR. Design and validation of a novel Cartesian biomechanical testing system with coordinated 6DOF real-time load control: application to the lumbar spine (L1-S, L4-L5). J Biomech. Elsevier; 2013 Jul 26;46(11):1948–54.
183. Bennett CR, Kelly BP. Robotic application of a dynamic resultant force vector using real-time load-control: Simulation of an ideal follower load on Cadaveric L4-L5 segments. J Biomech. Elsevier; 2013;46(12):2087–92.
184. Charriere E a, Beutler T, Caride M, Mordasini P, Orr TE, Zysset PK. Compliance of the L5-S1 spinal unit: a comparative study between an unconstrained and a partially constrained system. Eur Spine J. 2006 Jan;15(1):74–81.
185. Grassman S, Oxland T, Gerich U, Nolte L. Constrained Testing Conditions Affect the Axial Rotation Response of Lumbar Functional Spinal Units. Spine (Phila Pa 1976). 1998;23(10):1155–62.
186. Goertzen DJ, Kawchuk GN. A novel application of velocity-based force control for use in robotic biomechanical testing. J Biomech. 2009 Feb 9;42(3):366–9.
187. Twomey L, Taylor J. Flexion creep deformation and hysteresis in the lumbar vertebral column. Spine. 1982. p. 116–22.
188. Troyer KL, Estep DJ, Puttlitz CM. Viscoelastic effects during loading play an integral role in soft tissue mechanics. Acta Biomater. Acta Materialia Inc.; 2012 Jan;8(1):234–43.
189. Provenzano P, Lakes R, Keenan T, Vanderby J. R. Nonlinear Ligament Viscoelasticity. Ann Biomed Eng. 2001 Oct;29(10):908–14.
190. Troyer KL, Puttlitz CM. Nonlinear viscoelasticity plays an essential role in the functional behavior of spinal ligaments. J Biomech. Elsevier; 2012 Mar 23;45(4):684–91.
191. Woo SL, An K, Frank CB, Livesay GA, Ma CB, Zeminski J, et al. Anatomy, Biology, and Biomechanics of tendon and ligament. In: Einhorn TA, O’Keefe RJ, Buckwacker JA,

- editors. Orthopaedic Basic Science. 2nd ed. American Academy of Orthopaedic Surgeons; 2001.
192. Busscher I, Van Dieën JH, Van Der Veen AJ, Kingma I, Meijer GJM, Verkerke GJ, et al. The effects of creep and recovery on the in vitro biomechanical characteristics of human multi-level thoracolumbar spinal segments. Clin Biomech. Elsevier Ltd; 2011;26(5):438–44.
  193. Little JS, Khalsa PS. Material properties of the human lumbar facet joint capsule. J Biomech Eng. 2005;127(1):15–24.
  194. Rohlmann A, Neller S, Claes L, Bergmann G, Wilke HJ. Influence of a follower load on intradiscal pressure and intersegmental rotation of the lumbar spine. Spine (Phila Pa 1976). 2001 Dec 15;26(24):E557–61.
  195. Solomonow M, Zhou B-H, Harris M, Lu Y, Baratta R. The ligamento-muscular stabilizing system of the spine. Spine (Phila Pa 1976). 1998;23(23):2552–62.
  196. Gallagher S, Marras WS, Litsky AS, Burr D. Torso flexion loads and the fatigue failure of human lumbosacral motion segments. Spine (Phila Pa 1976). 2005;30(20):2265–73.
  197. Schmidt AL, Paskoff G, Shender BS, Bass CR. Risk of Lumbar Spine Injury from Cyclic Compressive Loading. Spine (Phila Pa 1976). 2012;37(26):1.
  198. Dekutoski MB, Schendel MJ, Ogilvie JW, Olsewski JM, Wallace LJ, Lewis JL. Comparison of In Vivo and In Vitro adjacent segment motion after lumbar fusion. Spine (Phila Pa 1976). 1994;19(15):1745–51.
  199. Dreischarf M, Rohlmann A, Bergmann G, Zander T. Optimised in vitro applicable loads for the simulation of lateral bending in the lumbar spine. Med Eng Phys. Institute of Physics and Engineering in Medicine; 2012;34(6):777–80.
  200. An HS, Masuda K. Relevance of in vitro and in vivo models for intervertebral disc degeneration. J Bone Joint Surg Am. 2006 Apr;88 Suppl 2:88–94.
  201. Gunzburg R, Hutton W, Fraser R. Axial rotation of the lumbar spine and the effect of flexion. An in vivo and in vitro biomechanical study. Spine (Phila Pa 1976). 1991;16(1):22–8.

202. Ianuzzi A, Khalsa PS. Comparison of human lumbar facet joint capsule strains during simulated high-velocity, low-amplitude spinal manipulation versus physiological motions. *Spine J.* 2005;5(3):277–90.
203. Cramer G, Budgell B, Henderson C, Khalsa P, Pickar J. Basic science research related to chiropractic spinal adjusting: the state of the art and recommendations revisited. *J Manipulative Physiol Ther.* 1997;29(9):726–61.
204. Sasso M, Palmieri G, Amodio D. Application of fractional derivative models in linear viscoelastic problems. *Mech Time-Dependent Mater.* 2011 Sep 22;15(4):367–87.
205. Panjabi MM. Three-dimensional mathematical model of the human spine structure. *J Biomech.* 1973;6:671–80.
206. Adams M, Hutton W, Stott J. The resistance to flexion of the lumbar intervertebral joint. *Spine (Phila Pa 1976).* 1980;4(3):245–53.
207. Roland CM. *Viscoelastic Behavior of Rubbery Materials.* Oxford University Press; 2011.
208. Treloar L. Physics of rubber-like materials. *Nature.* 1951;167(4246):425–7.
209. Brandolini N, Cristofolini L, Viceconti M. Experimental Methods for the Biomechanical Investigation of the Human Spine: a Review. *J Mech Med Biol.* 2014 Feb;14(01):1430002.
210. Freutel M, Schmidt H, Dürselen L, Ignatius A, Galbusera F. Finite element modeling of soft tissues: material models, tissue interaction and challenges. *Clin Biomech (Bristol, Avon).* Elsevier Ltd; 2014 Apr;29(4):363–72.
211. Xia Q, Wang S, Kozanek M, Passias P, Wood K, Li G. In-vivo motion characteristics of lumbar vertebrae in sagittal and transverse planes. *J Biomech.* Elsevier; 2010 Jul 20;43(10):1905–9.
212. Colloca CJ, Keller TS, Black P, Normand MC, Harrison DE, Harrison DD. Comparison of mechanical force of manually assisted chiropractic adjusting instruments. *J Manipulative Physiol Ther.* 2005;28(6):414–22.
213. Changoor A, Fereydoonzad L, Yaroshinsky A, Buschmann MD. Effects of refrigeration and freezing on the electromechanical and biomechanical properties of articular cartilage.

J Biomech Eng. 2010 Jun;132(6):064502.

214. Chasse AL, Myers BS. Properties in Cadaveric Test Specimens : Effects of Mechanical Loading , Postmortem Time ,. J Biomech Eng. 2000;122(February):9–14.
215. Bass CR, Planchak CJ, Salzar RS, Lucas SR, Rafaels K a, Shender BS, et al. The temperature-dependent viscoelasticity of porcine lumbar spine ligaments. Spine (Phila Pa 1976). 2007 Jul 15;32(16):E436–42.
216. Goldsmith P, Wynd S, Kawchuk G. Robotic measurement and control for chiropractic research. Appl Bionics Biomech. 2006;3(1):43–8.
217. Funabashi M, El-Rich M, Prasad N, Kawchuk GN. Quantification of loading in biomechanical testing: the influence of dissection sequence. J Biomech. 2015;48(12):3522–6.
218. Perle SM, Kawchuk GN. Pressures generated during spinal manipulation and their association with hand anatomy. J Manipulative Physiol Ther. 2005;28(4):1–7.
219. Stokes I a. F. Mechanical function of facet joints in the lumbar spine. Clin Biomech. 1988;3(2):101–5.
220. Cyron B, Hutton W. Articular tropism and stability of the lumbar spine. Spine (Phila Pa 1976). 1980;5(2):168–73.
221. Gravetter FJ, Wallnau LB. Statistics for the Behavioral Sciences. 7th ed. Gravetter FJ, Wallnau LB, editors. Belmont: Thomson Learning, Inc.; 2007.
222. Panjabi MM. The stabilizing system of the spine. Part II. Neutral zone and instability hypothesis. Journal of spinal disorders. 1992. p. 390–6; discussion 397.
223. Osborne JE, Hutchinson PE. The importance of accurate dosage of topical agents: A method of estimating involved area and application to calcipotriol treatment failures. J Eur Acad Dermatology Venereol. 2002;16(4):367–73.
224. Wallden M. Designing effective corrective exercise programs: The importance of dosage. J Bodyw Mov Ther. 2015;19(2):352–6.

225. Hoffman MD, Stuenkel KJ, Sullivan K, Weiss RH. Exercise-associated hyponatremia with exertional rhabdomyolysis: importance of proper treatment. *Clin Nephrol.* 2014;83(4).
226. Robinson R, Robinson HS, Bjørke G, Kvale A. Reliability and validity of a palpation technique for identifying the spinous processes of C7 and L5. *Man Ther.* 2009 Aug;14(4):409–14.
227. Gharaei H, Imani F, Solaymani-dodaran M. Survey of Sonoanatomic Distances For Lumbar Medial Branch Nerve Blocks in Healthy Volunteers. *Korean J Pain.* 2014;27(2):133–8.
228. Kawchuk GN, Prasad N, Parent E, Chapman S, Custodio M, Manzon M, et al. Spinal landmark depth in relation to body mass index. *Man Ther.* Elsevier Ltd; 2011;16(4):384–7.
229. Baranto A, Ekström L, Hellström M, Lundin O, Holm S, Swärd L. Fracture patterns of the adolescent porcine spine: an experimental loading study in bending-compression. *Spine (Phila Pa 1976).* 2005 Jan 1;30(1):75–82.
230. Thoreson O, Baranto A, Ekström L, Holm S, Hellström M, Swärd L. The immediate effect of repeated loading on the compressive strength of young porcine lumbar spine. *Knee Surg Sports Traumatol Arthrosc.* 2010 May;18(5):694–701.
231. Gallagher S, Marras WS. Tolerance of the lumbar spine to shear: A review and recommended exposure limits. *Clin Biomech.* Elsevier Ltd; 2012;27(10):973–8.
232. Skrzypiec DM, Klein A, Bishop NE, Stahmer F, Püschel K, Seidel H, et al. Shear strength of the human lumbar spine. *Clin Biomech.* Elsevier Ltd; 2012;27(7):646–51.
233. Schmidt H, Bashkuev M, Dreischarf M, Rohlmann A, Duda G, Wilke HJ, et al. Computational biomechanics of a lumbar motion segment in pure and combined shear loads. *J Biomech.* Elsevier; 2013;46(14):2513–21.
234. Homminga J, Lehr AM, Meijer GJM, Janssen MM a., Schlösser TPC, Verkerke GJ, et al. Posteriorly Directed Shear Loads and Disc Degeneration Affect the Torsional Stiffness of Spinal Motion Segments. *Spine (Phila Pa 1976).* 2013;38(21):E1313–9.
235. Panjabi MM, White a a. Basic Biomechanics of the Spine. *Neurosurgery.* 1980;7(1):76–

236. Adams M a, Dolan P, Hutton WC. The lumbar spine in backward bending. *Spine*. 1988. p. 1019–26.
237. Pettman E. A history of manipulative therapy. *J Man Manip Ther*. 2007;15(3):165–74.
238. Colloca CJ, Keller TS. Stiffness and neuromuscular reflex response of the human spine to posteroanterior manipulative thrusts in patients with low back pain. *J Manipulative Physiol Ther*. 2001 Oct;24(8):489–500.
239. Liebschner M a. K, Chun K, Kim N, Ehni B. In Vitro Biomechanical Evaluation of Single Impulse and Repetitive Mechanical Shockwave Devices Utilized for Spinal Manipulative Therapy. *Ann Biomed Eng*. 2014;42(12):2524–36.
240. Descarreaux M, Dugas C, Raymond J, Normand MC. Kinetic analysis of expertise in spinal manipulative therapy using an instrumented manikin. *J Chiropr Med*. 2005;4(2):53–60.
241. Downie AS, Vemulpad S, Bull PW. Quantifying the high-velocity, low-amplitude spinal manipulative thrust: a systematic review. *J Manipulative Physiol Ther*. National University of Health Sciences; 2010 Oct;33(7):542–53.
242. Descarreaux M, Dugas C, Treboz J, Cheron C, Nougrou F. Learning Spinal Manipulation: The Effect of Expertise on Transfer Capability. *J Manipulative Physiol Ther*. National University of Health Sciences; 2015;38(4):269–74.
243. Gal J, Herzog W, Kawchuk G, Conway P, Zhang Y-T. Movements of vertebrae during manipulative thrusts to unembalmed human cadavers. *J Manipulative Physiol Ther*. 1997;20(1):30–40.
244. Tsertsvadze A, Clar C, Court R, Clarke A, Mistry H, Sutcliffe P. Cost-Effectiveness of Manual Therapy for the Management of Musculoskeletal Conditions: A Systematic Review and Narrative Synthesis of Evidence From Randomized Controlled Trials. *J Manipulative Physiol Ther*. National University of Health Sciences; 2014;37(6):343–62.
245. Henderson CNR. The basis for spinal manipulation : Chiropractic perspective of indications and theory. *J Electromyogr Kinesiol*. Elsevier Ltd; 2012;22(5):632–42.

246. Stevinson C, Ernst E. Risks associated with spinal manipulation. *Am J Med.* 2002;112(7):566–71.
247. Ernst E. Adverse effects of spinal manipulation: a systematic review. *J R Soc Med.* 2007;100(7):330–8.
248. Ernst E. Chiropractic: A Critical Evaluation. *J Pain Symptom Manage.* 2008;35(5):544–62.
249. Hebert JJ, Stomski NJ, French SD, Rubinstein SM. Serious Adverse Events and Spinal Manipulative Therapy of the Low Back Region: A Systematic Review of Cases. *J Manipulative Physiol Ther.* National University of Health Sciences; 2013 Jun 17;
250. Gouveia LO, Castanho P, Ferreira JJ. Safety of chiropractic interventions: a systematic review. *Spine (Phila Pa 1976).* 2009;34(11):E405–13.
251. Oliphant D. Safety of spinal manipulation in the treatment of lumbar disk herniations: A systematic review and risk assessment. *J Manipulative Physiol Ther.* 2004;27(3):197–210.
252. Walker BF, Hebert JJ, Stomski NJ, Clarke BR, Bowden RS, Losco B, et al. Outcomes of Usual Chiropractic; Harm (OUCH) randomised controlled trial of adverse events. *Spine (Phila Pa 1976).* 2013;38(20):1723–9.
253. Cagnie B, Vinck E, Beernaert A, Cambier D. How common are side effects of spinal manipulation and can these side effects be predicted? *Man Ther.* 2004;9(3):151–6.
254. Wilke HJ, Rohlmann a, Neller S, Schultheiss M, Bergmann G, Graichen F, et al. Is it possible to simulate physiologic loading conditions by applying pure moments? A comparison of in vivo and in vitro load components in an internal fixator. *Spine (Phila Pa 1976).* 2001 Mar 15;26(6):636–42.
255. Yang G, Marras WS, Best TM. The biochemical response to biomechanical tissue loading on the low back during physical work exposure. *Clin Biomech (Bristol, Avon).* Elsevier B.V.; 2011 Jun;26(5):431–7.
256. Kaigle A, Holm S, Hansson T. Kinematic Behaviour of the Porcine Lumbar Spine: A Chronic Lesion Model. *Spine (Phila Pa 1976).* 1997;22(24):2796–806.
257. Wheeler DJ, Freeman AL, Ellingson AM, Nuckley DJ, Buckley JM, Scheer JK, et al.

- Inter-laboratory variability in in vitro spinal segment flexibility testing. *J Biomech.* Elsevier; 2011 Sep 2;44(13):2383–7.
258. Panjabi MM, Krag MH, Chung TQ. Effects of disc injury on mechanical behavior of the human spine. *Spine.* 1984. p. 707–13.
  259. Van Solinge GB, Van Der Veen AJ, Van Dieën JH, Kingma I, Van Royen BJ. Anterior shear strength of the porcine lumbar spine after laminectomy and partial facetectomy. *Eur Spine J.* 2010;19(12):2130–6.
  260. Macintosh JE, Bogduk N, Pearcy MJ. The effects of flexion on the geometry and actions of the lumbar erector spinae. *Spine.* 1993. p. 884–93.
  261. Kim HJ, Chun HJ, Lee HM, Kang KT, Lee CK, Chang BS, et al. The biomechanical influence of the facet joint orientation and the facet tropism in the lumbar spine. *Spine J.* Elsevier Inc; 2013;13(10):1301–8.
  262. Schmidt H, Heuer F, Wilke H-J. Interaction between finite helical axes and facet joint forces under combined loading. *Spine (Phila Pa 1976).* 2008;33(25):2741–8.
  263. Nagel TM, Zitnay JL, Barocas VH, Nuckley DJ. Quantification of continuous in vivo flexion-extension kinematics and intervertebral strains. *Eur Spine J.* 2014;23(4):754–61.
  264. Schmidt H, Kettler A, Heuer F, Simon U, Claes L, Wilke H-J. Intradiscal pressure, shear strain, and fiber strain in the intervertebral disc under combined loading. *Spine (Phila Pa 1976).* 2007;32(7):748–55.
  265. El-Rich M, Arnoux PJ, Wagnac E, Brunet C, Aubin CE. Finite element investigation of the loading rate effect on the spinal load-sharing changes under impact conditions. *J Biomech.* 2009;42(9):1252–62.
  266. Wang JL, Parnianpour M, Shirazi-Adl a, Engin a E. Viscoelastic finite-element analysis of a lumbar motion segment in combined compression and sagittal flexion. Effect of loading rate. *Spine (Phila Pa 1976).* 2000;25(3):310–8.
  267. Wagnac E, Arnoux P-J, Garo A, Aubin C-E. Finite element analysis of the influence of loading rate on a model of the full lumbar spine under dynamic loading conditions. *Med Biol Eng Comput.* 2012;50(9):903–15.



268. Garges KJ, Nourbakhsh A, Morris R, Yang J, Mody M, Patterson R. A Comparison of the Torsional Stiffness of the Lumbar Spine in Flexion and Extension. *J Manipulative Physiol Ther.* 2008;31(8):563–9.
269. Bisschop A, Van Dieën JH, Kingma I, Van Der Veen AJ, Jiya TU, Mullender MG, et al. Torsion biomechanics of the spine following lumbar laminectomy: A human cadaver study. *Eur Spine J.* 2013;22(8):1785–93.
270. Debski RE, Wong EK, Woo SL, Sakane M, Fu FH, Warner JJ. In situ force distribution in the glenohumeral joint capsule during anterior-posterior loading. *J Orthop Res.* 1999 Sep;17(5):769–76.
271. Wong AY. The mechanisms underlying differential biomechanical and clinical responses in patients with low back pain following spinal manipulative therapy (Doctoral thesis). University of Alberta, Edmonton, Canada. 2015.
272. Ruberté LM, Natarajan RN, Andersson GB. Influence of single-level lumbar degenerative disc disease on the behavior of the adjacent segments—A finite element model study. *J Biomech.* 2009;42(3):341–8.

**Appendix I. Linear Mixed Model ANOVA tables for relative mean and peak moments, and area between curves of the moment-displacement graph of Chapter 3**

**Linear Mixed Model ANOVA table for Mean Moment**

Source	Numerator df	Denominator df	F	Sig.
Intercept	1	84	29.989	<.001
Movement	5	84	963.618	<.001
Connector	2	84	70.094	<.001
Order	2	84	11.938	<.001
Movement*Connector*Order	30	84	282.868	<.001
Order(Connector)	4	84	10.685	<.001
Order(Movement)	15	84	99.061	<.001

**Linear Mixed Model ANOVA table for Peak Moment**

Source	Numerator df	Denominator df	F	Sig.
Intercept	1	84	33.858	<.001
Movement	5	84	1554.933	<.001
Connector	2	84	79.13	<.001
Order	2	84	8.87	<.001
Movement*Connector*Order	30	84	318.488	<.001
Order(Connector)	4	84	8.365	<.001
Order(Movement)	15	84	179.974	<.001

**Linear Mixed Model ANOVA table for area between curves of the moment-displacement graph**

Source	Numerator df	Denominator df	F	Sig.
Intercept	1	84	33.217	<.001
Movement	5	84	236.511	<.001
Connector	2	84	2739.819	<.001
Order	2	84	12.578	<.001
Movement*Connector*Order	30	84	49.445	<.001
Order(Connector)	4	84	7.206	<.001
Order(Movement)	15	84	24.752	<.001

## Appendix II. Detailed description of spinal manipulative therapy simulator

Spinal manipulative therapy was applied by a servo-controlled linear actuator motor (Descarreaux et al., 2013) (Figure A). The linear motor (Linear Motor Series P01- 48x360; LinMot Inc, Zurich, Switzerland) applies the SMT force while a microcontroller continuously compares the pre-determined target force to the one measured by a load cell (LCF450 FSH00132; Futek Inc, ON, Canada).

In order to assess the precision and repeatability of this newly developed SMT simulator, Descarreaux and colleagues (2013) applied SMT with 4 different peak force magnitudes (80 N, 130 N, 180 N, 255 N) at the T7 transverse process of 14 healthy participants. They reported that the SMT simulator applied precise (average differences in peak force of less than 3N) and repeatable SMT (coefficient of multiple correlation values  $> 0.98$  for all SMT force-time profiles).

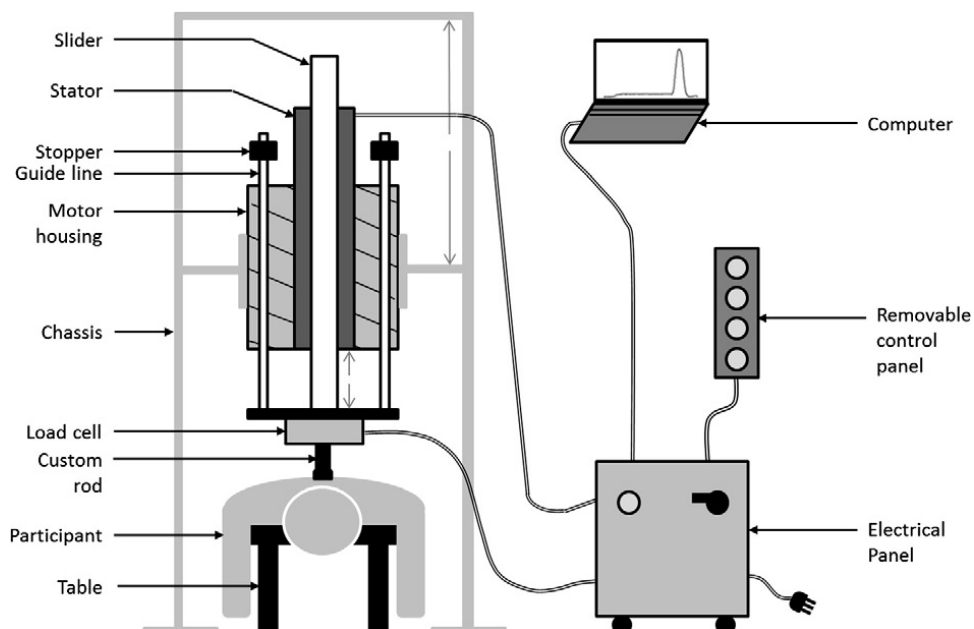


Figure A. Main components of the servo-controlled linear actuator motor [From Descarreaux et al., 2013].

### Appendix III. Detailed description of optical tracking system

The optical tracking system (NDI, Waterloo, Canada) is composed of infrared light-emitting diodes markers (Figure A), which in the current study were combined to compose two rigid bodies (rectangular sensor flags) with 4 markers each. The system also includes one position sensor with 3 lenses (Figure B) that detects the markers and identifies its spatial position, and a system control unit (Figure C), that operates the position sensor and the markers. This system has an accuracy and a resolution of 0.01 mm and a maximum marker frequency of 4600 Hz.

By using this system, the position sensor detected, tracked and recorded the 3-dimensional motion of each of the 4-marker sensor flag (attached to the bone pins which were drilled into the L3 and L4 vertebral bodies) during the SMT application.



Figure A. Rectangular sensor flag with 4-markers



Figure B. Position sensor with 3 lenses



Figure C. System control unit

#### **Appendix IV. Detailed description of calibration process**

Although the 4-markers rigid bodies were removed after the SMT vertebral motions were recorded, the bone pins with a locking system locked at a specified position were kept drilled in the vertebral body during spinal removal and dissection, specimen transportation and potting procedure. This way, it was ensured that the 4-marker rigid body would be at the same place when re-attached back to the bone pin prior to robotic testing.

This calibration process was developed [216] and executed in order to transpose the recorded SMT vertebral motions into the robotic frame of reference. Firstly, following potting procedure, the specimen was bolted to the load cell on the robotic platform. The 4-marker rigid bodies were then re-attached to the bone pins and fixed in the same position as during vertebral motion optical tracking procedure. Following that, the robotic platform was moved through a series of known translations and rotations and the resulting change in markers spatial location recorded. By using previously described algorithms [216], the location of the robot frames relative to the markers attached to the specimen relative to the position sensor was calculated. The SMT vertebral motions previously recorded were then translated into a file with a series of commands composing robotic trajectories.

This calibration process has been reported to produce adequate accuracy in relation to repeatability errors [216]. Prior to biomechanical testing, all resulting robotic trajectories were carefully verified to ensure that all SMT trajectory commands were within the robot's limits